

SOFT SOIL STABILISATION USING A NOVEL BLENDED
CEMENTITIOUS BINDER PRODUCED FROM WASTE FLY ASHES

HASSNEN MOSA JAFER

A thesis submitted in partial fulfilment of the
requirements of Liverpool John Moores University
for the degree of Doctor of Philosophy

July 2017

DECLARATION

The research reported in this thesis was conducted at Liverpool John Moores University, Civil Engineering Department, between February 2014 and July 2017. I declare that the work is my own and has not been submitted for a degree at another university.

Hassnen Mosa Jafer

Liverpool John Moores University

July 2017

ABSTRACT

Soil stabilisation is one of the most common techniques used to mitigate the undesirable properties of soft soils such as low compressive strength and high compressibility. Cement is the most commonly used binder for soil improvement applications in the UK and worldwide due to its high strength performance. However, its manufacture is energy intensive and expensive, contributing approximately 7% of global carbon dioxide (CO₂) emissions. Therefore, the search for alternative raw materials, such as waste and by-products, is becoming critical in order to develop cost effective and more environmentally friendly binders to replace cement and reduce its negative environmental impact.

Blended waste material fly ashes have been identified as promising alternatives to traditional binders (cement CEM-I) in different construction industries including ground improvement. The reuse of waste material fly ashes such as waste paper sludge ash (WPSA), palm oil fuel ash (POFA) and rice husk ash (RHA) has many advantages, specifically in terms of eliminating the cost of their transportation and eventual landfill, their continuous supply and the negligible, or zero, cost of production.

This research project details the process of the development of a new cementitious binder, produced by blending cement-free WPSA, POFA and RHA under physico-chemical activation using flue gas desulphurisation (FGD) gypsum, for use in soft soil stabilisation. The effects of different binders produced from unary (WPSA), binary (WPSA and POFA) and ternary (WPSA, POFA and RHA) blended mixtures, along with ground and FGD gypsum activated ternary mixtures, on the geotechnical properties of soft soils, were extensively investigated.

Comparisons of Atterberg limits, strength (unconfined compressive strength (UCS)), compressibility characteristics and durability (wetting-drying cycles effect) of untreated soil and soil stabilised with the optimum unary, binary, ternary and activated ternary mixtures and a reference cement treated soil, have been carried out. An investigation of the microstructural and mineralogical composition of the newly

developed binder, in comparison to those of the reference cement, was also carried out using X-ray diffraction (XRD) analysis, scanning electron microscopy (SEM) imaging and energy dispersive X-ray (EDX) spectroscopy analysis.

The results indicate that the soil stabilised with the ternary mixture activated by FGD gypsum (T+FGD), had the greatest compressive strength, compressibility and durability improvement; the performance of the newly developed cementitious binder was comparable to that of the reference cement. This binder comprises 8% WPSA + 2% POFA + 2% RHA activated with 5% of FGD, by the total mass of binder. The addition of FGD gypsum has been observed to enhance the pozzolanic reaction, leading to improved geotechnical properties; mainly UCS which increased over time of curing and exceeded that for the soil treated with reference cement, after 180 days. The results obtained from XRD analysis, SEM testing and EDX analysis revealed the formation of hydrated cementitious products represented by calcium silicate hydrates (C-S-H), Portlandite (CH) and ettringite. The formation of these hydrates reveals the developments gained in the geotechnical properties of the treated soil. A solid, coherent and compacted soil structure was achieved after using T+FGD, as confirmed by the formation of C-S-H, CH and ettringite. Therefore, a new, Cost effect, eco-friendly and sustainable cementitious binder has been successfully developed and can be used with confidence for soft soil stabilisation, as a 100% replacement of conventional cement.

ACKNOWLEDGEMENTS

This research could not have been completed without the support, guidance and help of many people. I can safely say that I would not have been successful without their precious support. First of all, I would like to thank my country, Iraq, and the Ministry of Higher Education and Scientific Research as well as University of Babylon in Iraq for funding this scholarship. In addition, I would like to express my sincere gratitude and appreciation to the following persons; if any have been forgotten, please accept my sincerest of apologies:

- I owe my deepest gratitude to my supervisor, Dr. William Atherton, for his excellent supervision, guidance and encouragement throughout this study without which this project would never have been completed.
- I would like to express my sincere thanks to my second supervisor, Mrs Felicite Ruddock, and my third supervisor, Dr. Edward Loffill, for their expert advice and support.
- I am also grateful to Dr Monower Sadique and Dr Anmar Dulaimi for insightful advice, discussions and continual help throughout this research.
- A big thank you goes to Aylesford Newsprint, Sg. Tengli Palm Oil Factory at Kuala Kubu Bharu, Selangor, Malaysia and Dr. Monower Sadique for the supply of materials, free of charge, during the course of the research. Their support is kindly acknowledged.
- I also would like to acknowledge the assistance and friendship of all current and past lecturers, researchers, technicians and administrative staff in the

Department of Civil Engineering, Faculty of Engineering and Technology, Liverpool John Moores University, especially those involved with this research. Their enthusiasm and encouragement have made my research enjoyable and memorable. The author appreciates the efforts of Dr Nicola Dempster, Mrs Elizabeth Hoare, Miss Laura Bellinger, Mr Mal Feegan, Mr Gary Lamb, Mr Paul Gibbons, Mrs Hazel Clark, Mr David Williams, for their assistance.

- The author has had numerous productive discussions and many enjoyable times with past and present fellow students in the Research Hub. The author would like to thank them for their kindness and friendship: Khalid Hashim, Alaa Abbas, Ali Alzeyadi, Hayder Shanbara, Ali Al-Attabi, Muhammad Abdulredha, Salah Zubaidi and Layth Kraidi.
- I would like to thank my friends and colleagues in the University of Babylon: Dr. Zaid Majeed, Dr. Haider Owaid and Dr. Ibtehaj Jawad for continuous support and helpful communications.
- The author would like to express his extreme gratitude to his mother for her unending support, unstinting sacrifice and great love throughout the research duration.
- Last but not least, I am particularly grateful to my wife Mrs Zainab Al-Eqabi and my children, Ali, Ruqayah and Mohammed and my brothers and sisters, for providing tremendous and continuous support and encouragement and for their unconditional patience throughout the research period.

DEDICATION

This thesis is dedicated specially to:

Allah, the most Gracious and the most Merciful.

Prophet Mohammed and his household.

My Mother, the most precious person in my life. You have sacrificed so much for us and I hope that this work will be of benefit for humanity; the reward will be for you. I hope you are proud of me.

In loving memory of my Father, whose death prevented him from seeing this work coming to a fruitful conclusion.

My lovely wife Mrs Zainab Al-Eqabi and beloved children Ali, Ruqayah, Mohammed and my newborn baby Haider.

LIST OF CONTENTS

DECLARATION	I
ABSTRACT.....	II
ACKNOWLEDGEMENTS	IV
DEDICATION	VI
LIST OF CONTENTS	VII
LIST OF FIGURES	XV
LIST OF TABLES	XXII
LIST OF ACRONYMS AND ABBREVIATIONS.....	XXIV
GLOSSARY OF SYMBOLS (UNITS)	XXV
CHAPTER 1	1
INTRODUCTION	1
1.1 GENERAL	1
1.2 AIM AND NOVELTY STATEMENT.....	2
1.3 OBJECTIVES	3
1.4 THE SELECTION OF CANDIDATE MATERIALS	4
1.5 SCOPE OF THE STUDY	4
1.6 THESIS STRUCTURE	5
1.7 SUMMARY	7
CHAPTER 2	8
LITERATURE REVIEW.....	8
2.1 INTRODUCTION.....	8
2.2 SOILS IDENTIFICATION AND CLASSIFICATION	8
2.3 PROBLEMATIC SOILS.....	9
2.3.1 Collapsible Soils	10

2.3.2	Dispersive Soils.....	10
2.3.3	Expansive Soils	11
2.4	SOIL MINERALS	11
2.5	SOIL IMPROVEMENT	17
2.5.1	General	17
2.5.2	Soil Stabilisation	17
2.6	CEMENT-SOIL STABILISATION	18
2.6.1	Chemical Composition of Ordinary Portland Cement.....	19
2.6.2	Chemical Reaction of Soil-Cement Hydration	20
2.6.3	Effects of Cement Stabilisation.....	21
2.6.3.1	Compaction Parameters	21
2.6.3.2	Atterberg Limits.....	25
2.6.3.3	Soil Strength.....	26
2.6.3.4	Compressibility and Volume Change	28
2.6.3.5	Durability	29
2.6.4	Drawbacks of Using Cement in Soil Stabilisation.....	31
2.6.4.1	Environmental Impact.....	32
2.6.4.2	Consumption of Energy	34
2.6.4.3	Cement Carbonation and Sulphate Attack.....	34
2.6.4.4	Effect of Organic Matter	36
2.7	ASHES OF WASTE MATERIALS AS A CEMENT REPLACEMENT ..	37
2.7.1	General	37
2.7.2	Potential of Waste and By-Product Materials for Cement Replacement	38
2.7.3	WASTE PAPER SLUDGE ASH (WPSA).....	40
2.7.3.1	WPSA Production.....	40

2.7.3.2	Characterisation of WPSA	41
2.7.3.3	Application of WPSA in Construction Field	43
2.7.4	Other Waste Fly Ashes as Pozzolanic and Chemical Activators.....	44
2.7.4.1	Pulverised Fuel Ash (PFA)	44
2.7.4.2	Ground Granulated Blast Furnace Slag (GGBS)	45
2.7.4.3	Silica Fume (SF)	46
2.7.4.4	Rice Husk Ash (RHA)	47
2.7.4.5	Palm Oil Fuel Ash (POFA)	47
2.7.4.6	Flue Gas Desulfurization (FGD) Gypsum	48
2.7.5	Methods of Fly Ash Activation.....	49
2.7.5.1	Mechanical Activation	49
2.7.5.2	Chemical Activation	50
2.8	SUMMARY	51
CHAPTER 3	52
MATERIALS AND RESEARCH METHODOLOGY	52
3.1	INTRODUCTION.....	52
3.2	MATERIALS	54
3.2.1	Soil	54
3.2.2	Added Materials	56
3.3	PROGRAMMEME OF LABORATORY EXPERIMENTS AND TESTING EQUIPMENT.....	57
3.3.1	Natural moisture content %	58
3.3.2	Particle Density (Specific Gravity, Gs).....	58
3.3.3	Particle size distribution (PSD).....	59
3.3.4	Consistency Limits.....	60
3.3.5	Compaction Parameters Test.....	62

3.3.6	Unconfined Compressive Strength Test (UCS)	65
3.3.7	Oedometer Test (Consolidation Test)	70
3.3.8	Loss on Ignition Test (LOI) %	73
3.3.9	pH Measurements.....	74
3.3.10	X-Ray Florescence Spectrometry (XRF) Analysis	74
3.3.11	Tests of Hydration Kinetic Investigation	75
3.3.11.1	Samples preparation.....	76
3.3.11.2	X-Ray diffraction (XRD) analysis	78
3.3.11.3	Scanning Electronic Microscopy (SEM) and Energy Dispersive X-ray Spectroscopy (EDX) Analyses.....	79
3.4	SUMMARY	82
CHAPTER 4		88
RESULTS OF MATERIALS IDENTIFICATION		88
4.1	INTRODUCTION.....	88
4.2	VIRGIN SOIL PROPERTIES AND CLASSIFICATION	88
4.2.1	Physical and Geotechnical Properties.....	88
4.2.2	Chemical Properties and Elemental Structure.....	91
4.2.3	Soil Classification	92
4.3	CANDIDATE MATERIALS CHARACTERISATION.....	93
4.3.1	Reference Cement (OPC).....	93
4.3.2	Waste Paper Sludge Ash (WPSA)	96
4.3.3	Palm Oil Fuel Ash (POFA)	99
4.3.4	Rice Husk Ash (RHA)	102

4.3.5	Pulverised Fuel Ash (PFA)	105
4.3.6	Ground Granulated Blast Furnace Slag (GGBS)	108
4.3.7	Silica Fume (SF)	110
4.3.8	Flue Gas Desulphurisation Gypsum (FGD).....	113
4.4	COMPARATIVE PHYSICAL AND CHEMICAL PROPERTIES OF CANDIDATE MATERIALS	115
4.5	SUMMARY	120
CHAPTER 5	121
	MIXING DESIGN FOR THE NEW BINDER MIXTURES OPTIMISATION.	121
5.1	INTRODUCTION.....	121
5.2	OPTIMISATION OF UNARY MIXTURE	121
5.2.1	Consistency Limits.....	122
5.2.2	Compaction Parameters	125
5.2.3	Stress- Strain Behaviour of the Soil Treated with WPSA	128
5.3	MECHANICAL ACTIVATION OF WPSA	136
5.3.1	Effect of Ground Activation on the PSD of WPSA.....	136
5.3.2	Effect of the Ground Activated WPSA on the UCS	138
5.4	OPTIMISATION OF BINARY BLENDED MIXTURE	140
5.4.1	Effect of Binary Treatment on the Atterberg limits.....	141
5.4.2	Effect of Binary Blending on the Compaction Parameters.....	143
5.4.3	Effect of Binary Blending on UCS	145
5.5	OPTIMISATION OF TERNARY MIXTURE	148

5.5.1	Effect of Ternary Blending Treatment on Atterberg Limits	149
5.5.2	Effect of Ternary Blending Treatment on Compaction Parameters...	152
5.5.3	Effect of Ternary Blending Treatment on UCS	154
5.5.4	Effect of Grinding Activation Using FGD.....	159
5.5.4.1	Particle size distribution (PSD).....	159
5.5.4.2	Atterberg limits	161
5.5.4.3	Compaction parameters.....	162
5.5.4.4	Unconfined compressive strength (UCS).....	164
5.6	SUMMARY	167
5.6.1	Summary of the Optimisation of WPSA Content.....	167
5.6.2	Summary of Mechanical Activation	168
5.6.3	Summary of Binary Blending Optimisation	168
5.6.4	Summary of Ternary Blending Optimisation.....	169
CHAPTER 6	170
THE COMPARATIVE PERFORMANCE OF THE OPTIMUM AND REFERENCE MIXTURES	170
6.1	INTRODUCTION.....	170
6.2	COMPARATIVE ATTERBERG LIMITS	170
6.3	COMPACTION PARAMETERS	171
6.4	UNCONFINED COMPRESSIVE STRENGTH.....	173
6.5	COMPRESSIBILITY CHARACTERISATION	177
6.5.1	Virgin Soil Compressibility	178
6.5.2	Comparative Results of the Oedometer Testing	181
6.6	EFFECT OF WETTING-DRYING CYCLES	190

6.7	SUMMARY	196
CHAPTER 7		199
MINERALOGICAL AND MICROSTRUCTURAL ANALYSIS.....		199
7.1	INTRODUCTION.....	199
7.2	X-RAY DIFFRACTOMETRY ANALYSES	200
7.3	ANALYSIS OF SEM AND SEM/EDX TESTING	205
7.3.1	SEM Analysis of Untreated Soil.....	205
7.3.2	SEM Analysis of Hydrated Soil-Binder.....	206
7.3.3	SEM and SEM/EDX Analyses of Hydrated Binder Paste.....	212
7.4	SUMMARY	223
CHAPTER 8		225
CONCLUSIONS AND RECOMMENDATIONS		225
8.1	LIMITATIONS OF THE STUDY	225
8.2	CONCLUSIONS	225
8.3	RECOMMENDATIONS	228
REFERNCES		230
APPENDICES		245
Appendix A: Results of the soil treated with the coarse grade of WPSA.....		245
Appendix B: Lis of journal and conference publications.....		249
Published journal papers:		249
Accepted journal papers (under production):.....		249
Journal papers under preparation:		249
Conference papers with oral presentation:		249

Poster presentations:.....	250
3 Minutes thesis and elevator pitch:.....	251
Contribution in Master Students Publications as a Co-supervisor:.....	251
Appendix C: Awards and Recognitions	252

LIST OF FIGURES

Figure 2.1 Structural units and minerals sheets (a) Silica tetrahedron and Silica sheet, (b) Aluminium octahedron, and Aluminium sheet.....	13
Figure 2.2 clay minerals structures. (a) Kaolinite, (b) Illite, and (c) Montmorillonite....	14
Figure 2.3 Diffuse double layer of clay particles surface.....	15
Figure 2.4 Effect of cement content on maximum dry densities of three different types of soil.....	22
Figure 2.5 Effect of cement content on optimum moisture contents of three different types of soil.....	22
Figure 2.6 Compaction parameters behaviour with different percentages of cement treatment. Cement is denoted with letter (c).....	23
Figure 2.7 Maximum dry density and optimum moisture content relationship with cement content of different types of clay minerals.....	24
Figure 2.8 Atterberg limits-cement content relationship of cement stabilised soil.....	25
Figure 2.9 Effect of cement content and curing time on UCS. y is the estimated UCS value (MPa), and x is the cement content (%).	26
Figure 2.10 Effect of cement treatment of (a) UCS and (b) Modulus of Elasticity of Aberdeen soft soil.....	27
Figure 2.11 SEM images of 10% cement treated samples subjected to modified Proctor energy of compaction using different water content at age of 7 days.....	28
Figure 2.12 Variation of compression index and pre-consolidation pressure of soft soil treated with different cement contents (7 days cured samples).....	29
Figure 2.13 Relationship between soil-cement loss percentage and water cement ratio (DV is for dielectric value).....	30
Figure 2.14 Changes in moisture, volume and weight of cement stabilised specimens subjected to different numbers of wet-dry cycles.....	31
Figure 2.15 Global cement production structure. (a) 2013 and (b) 2015.....	32
Figure 2.16 Worldwide cement consumption.....	33
Figure 2.17 UCS of cement treated soil at different periods of curing.....	37
Figure 2.18 The chemical composition of principal cementitious materials.....	39
Figure 2.19 Pulp and paper residues disposal trends in Europe.....	41
Figure 2.20 Unconfined compressive strength of soft soils treated with WPSA:Cement ratio 25:75. SS6, SS7 and SS8 are soft soils number 6, 7 and 8 respectively.....	44

Figure 2.21 PFA production between 1999 and 2014 in the UK.	45
Figure 2.22 Effect of OPC/POFA combination on UCS for different binder dosages....	48
Figure 3.1 Test procedure of this research project.	53
Figure 3.2 Satellite image of the soil collection site at Hightown, Liverpool.	54
Figure 3.3 Soil texture map of the soil collection site at Hightown, Liverpool	55
Figure 3.4 Detailed stratigraphic soil logs close to the site of sampling of the Hightown soft soil.	55
Figure 3.5 Particle density test using the Pyknometer.....	59
Figure 3.6 LS 13 320 Particle size analyser.	60
Figure 3.7 Cone penetrometer device used in LL test.	61
Figure 3.8 A sample paste with the cone before penetration.....	61
Figure 3.9 The compaction machine used in the study.	62
Figure 3.10 Sequences of sample preparation and compaction.....	64
Figure 3.11 Computerised triaxial machine used for UCS testing.	65
Figure 3.12 Constant volume mould used for preparation of UCS specimens.	66
Figure 3.13 Procedure of the specimens preparation for UCS testing.	67
Figure 3.14 The humidity cabinet used for specimens curing.	68
Figure 3.15 Wetting-drying procedure.	69
Figure 3.16 Preparation of Oedometer test specimens.	71
Figure 3.17 Set up of Oedometer test cell.	72
Figure 3.18 Equipment used for Oedometer test.	73
Figure 3.19 LOI test for virgin soil and candidate materials.	73
Figure 3.20 pH measurement test (a) Solution preparation, and (b) pH meter calibration.	74
Figure 3.21 Shimadzu’s EDX-720 used for XRF analysis.....	75
Figure 3.22 Common procedure of specimens preparation for hydration kinetics investigation.....	77
Figure 3.23 The instrument used for XRD analysis.	78
Figure 3.24 Steps of sample preparation for XRD analysis.	79
Figure 3.25 The instrument used for SEM/EDX analysis in this study.....	80
Figure 3.26 Steps of SEM/XRD samples set up.....	81
Figure 4.1 Particles size distribution curve of the virgin soil.	89
Figure 4.2 SEM image for the virgin soil used in this study.	89
Figure 4.3 Cone penetration – water content relationship for LL determination.	90

Figure 4.4 Standard Proctor compaction curve of the virgin soil.....	90
Figure 4.5 XRD pattern diagram of the virgin soil. (Q: quartz, K: kaolinite, S: smectite, and I: illite)	92
Figure 4.6 Plasticity chart for the soil used in this study.....	93
Figure 4.7 XRD pattern diagram for the reference OPC. (C: calcite, A: alite, Pc: periclase, B: belite, and F: ferrite)	94
Figure 4.8 Particle size distribution of the reference cement.	95
Figure 4.9 SEM image for powder state of reference cement.	95
Figure 4.10 XRD pattern diagrams for coarse and fine WPSA used in this study. (C: calcite, L: lime, G: gehlenite, M: mayenite, Mr: merwinite, and Q: quartz.	97
Figure 4.11 PSD of WPSA used in this study.	98
Figure 4.12 SEM images for both grades of WPSA.....	99
Figure 4.13 The XRD pattern of treated POFA. (Q: quartz, Cr: cristobalite, and K: potassium aluminium phosphate).....	100
Figure 4.14 The PSD for both the virgin and treated POFA.	101
Figure 4.15 SEM images of POFA, (a) virgin, and (b) treated.	102
Figure 4.16 Diffraction patterns of RHA.....	103
Figure 4.17 PSD of RHA used in this study.....	104
Figure 4.18 SEM images of RHA used in this study.....	105
Figure 4.19 XRD patterns of PFA. (Q: quartz, and Mu: mullite).....	106
Figure 4.20 PSD of both types of PFA.	107
Figure 4.21 SEM images of (a) PFA1, and (b) PFA2	108
Figure 4.22 XRD patterns of GGBS.....	109
Figure 4.23 SEM view of GGBS.....	109
Figure 4.24 PSD of GGBS.	110
Figure 4.25 The XRD patterns of SF.....	111
Figure 4.26 PSD of the silica fume particles.	112
Figure 4.27 SEM view of SF particles.	112
Figure 4.28 XRD patterns of FGD gypsum (Gh: calcium sulphate hemihydrate, Gd: calcium sulphate dehydrates, and Q: quartz).....	113
Figure 4.29 PSD of FGD gypsum.	114
Figure 4.30 SEM images of dry powder of FGD gypsum.....	115
Figure 4.31 Comparative principal oxides of candidate materials.	118
Figure 4.32 Comparative PSD of candidate materials.....	119

Figure 5.1 Atterberg limits of the soil treated with WPSA.	122
Figure 5.2 Atterberg limits of the soil treated with OPC.....	123
Figure 5.3 Dry density-moisture content relationship for the soil treated with WPSA.	125
Figure 5.4 The relationship between WPSA and (a) MDD, and (b) OMC.	126
Figure 5.5 Comparative effects of WPSA and OPC on (a) MDDs and (b) OMCs of the stabilised soil in this study.....	127
Figure 5.6 The effect of WPSA treatment on the solid weight per the unit volume of the treated soil.....	128
Figure 5.7 Stress-axial strain diagram of undisturbed, compacted untreated, and soil treated with WPSA without curing.....	129
Figure 5.8 Stress-axial strain diagrams of the soil treated with WPSA at different curing periods	130
Figure 5.9 The development in UCS of the soil treated with WPSA at different periods of curing.....	131
Figure 5.10 The strain behaviour of the soil treated with WPSA at different times of curing	133
Figure 5.11 Non cured strain behaviour of the soil treated with WPSA compared to that of undisturbed and untreated compacted soil.....	134
Figure 5.12 Strain behaviour of the untreated and soil treated with WPSA after 28 days curing.....	135
Figure 5.13 The grinder used for the mechanical activation in this study.....	136
Figure 5.14 Effect of grinding activation on the PSD of WPSA.....	137
Figure 5.15 Effect of grinding activation of WPSA on the UCS.	139
Figure 5.16 The development of UCS over the curing time of the soil treated with normal and mechanically activated WPSA.....	139
Figure 5.17 Effect of grinding and binary blending treatment on Atterberg limits of the stabilised soil.	142
Figure 5.18 Effect of binary blending treatment on compaction parameters.	144
Figure 5.19 Effect of binary blending treatment on UCS.....	146
Figure 5.20 Stress-axial strain diagrams of the binary mixture optimisation at 7 and 28 days of curing.	147
Figure 5.21 Failure shape of the soil treated with BM2 at 7 and 28 days of curing.....	148
Figure 5.22 Effect of the ternary blending treatment on the Atterberg limits.	151

Figure 5.23 Dry density-moisture content relationship of the soil treated with different ternary mixtures.	153
Figure 5.24 Effect of ternary blending treatment on the MDD and OMC.	153
Figure 5.25 Effect of ternary blending treatment on UCS.....	155
Figure 5.26 Stress-axial strain diagrams after ternary blending treatment.	157
Figure 5.27 Failure shapes over the time of curing for the soil treated with (a) TM3, and (b) TM4.....	158
Figure 5.28 Effect of grinding and FGD activation on PSD of TM3	160
Figure 5.29 Effect of grinding with FGD on Atterberg limits.....	161
Figure 5.30 Effect of grinding with FGD on MDD.....	163
Figure 5.31 Effect of grinding with FGD on the OMC.	163
Figure 5.32 Effect of grinding and FGD on the UCS of the soil treated with TM3 and TM4.	165
Figure 5.33 Influence of grinding and FGD on the development rate of UCS over that for corresponding non-ground TM3 and TM4 mixtures.	166
Figure 6.1 Comparative Atterberg limits of the soil treated with different types of mixtures	171
Figure 6.2 Comparative compaction parameters of the soil treated with different types of mixtures.	172
Figure 6.3 UCS development over the curing time of the soil treated with different binders along with the virgin soil and soil treated with OPC.....	174
Figure 6.4 Axial strain failure for the soil treated with the optimum mixtures.	176
Figure 6.5 Casagrande procedure to derive the pre-consolidation pressure (P_c) of the remoulded virgin soil used in this study.	178
Figure 6.6 Pre-consolidation derivation of the undisturbed soil.....	179
Figure 6.7 Raw compression curves for the soil samples of undisturbed and remoulded soil.	180
Figure 6.8 Comparative raw compression curves of the soil treated with different types of binders at (a) 7 days and (b) 28 days of curing.....	182
Figure 6.9 Initial void ratios (e_o) of the soil treated with different binders and subjected to different curing periods.	183
Figure 6.10 Compression and swelling indices of the soil samples treated with different binders.	185

Figure 6.11 Comparative values of M_v calculated from the Oedometer tests on the stabilised soil after (a) 7 days and (b) 28 days of curing.	187
Figure 6.12 Comparative pre-consolidation pressure for the soil treated with different binder types.	189
Figure 6.13 Summary of consolidation settlement S_c for the soil stabilised with different mixtures.	190
Figure 6.14 Residual UCS of the soil treated with different binders after wetting-drying cycles.	191
Figure 6.15 Crack propagation and sample damage of the soil treated with different binders after wetting-drying testing.	193
Figure 6.16 Volume changes of the soil samples treated with different binders experienced during wetting-drying cycles testing.	194
Figure 6.17 Effect of wetting-drying cycles on the soil-binder weight loss of the soil samples treated with different binders.	195
Figure 7.1 Powder XRD patterns of T and T+FGD binders.	200
Figure 7.2 XRD analysis of T+FGD binder paste subjected to different curing periods; along with the dry powder state.	202
Figure 7.3 XRD analysis of reference cement paste subjected to different curing periods; along with the dry powder state.	203
Figure 7.4 SEM images of compacted virgin soil with different magnifications.	206
Figure 7.5 Hydrated paste of stabilised soil at 3 days curing; (a) 13719x and (b) 5051x.	207
Figure 7.6 Hydrated paste of stabilised soil at 7 days curing; (a) 13589x and (b) 4441x.	208
Figure 7.7 Hydrated paste of stabilised soil at 28 days curing; (a) 12466x and (b) 4394x.	209
Figure 7.8 Hydrated paste of stabilised soil at 180 days curing; (a) 7212x and (b) 4413x.	210
Figure 7.9 Hydrated paste of T+FGD at 3 days curing; (a) 15087x and (b) 4555x.	214
Figure 7.10 Hydrated paste of T+FGD at 7 days curing; (a) 12939x and (b) 6976x. ...	215
Figure 7.11 Hydrated paste of T+FGD at 28 days curing; (a) 12900x and (b) 4915x. .	216
Figure 7.12 Hydrated paste of T+FGD at 180 days curing; (a) 15139x and (b) 4544x.	217
Figure 7.13 EDX spectrum of C-S-H in T+FGD paste at 28 days curing.	218
Figure 7.14 EDX spectrum of C-S-H in T+FGD paste at 180 days curing.	218

Figure 7.15 EDX spectrum of C-S-H in control cement paste at 28 days of curing. 219

Figure 7.16 EDX spectrum of C-S-H in control cement paste at 180 days of curing. .. 219

Figure 7.17 EDX spectrum of C-S-H reported by Peethamparan *et al.* (2008)..... 220

LIST OF TABLES

Table 2.1 Common Minerals in Soils	12
Table 2.2 Typical free swell potential for common clay soils.....	14
Table 2.3 Typical values of cation exchange capacity for different clay minerals.	16
Table 2.4 Description of volume change potential for different ranges of PI	17
Table 2.5 Chemical composition of Ordinary Portland cement	19
Table 2.6 Chemical composition of WPSA according to different researchers.	42
Table 2.7 The effect of calcination degree and period on the chemical composition of WPSA	42
Table 3.1 Sources and description of candidate materials identified in this study.	57
Table 3.2 Soil classification and candidate materials identification test.	83
Table 3.3 Optimisation for WPSA content and reference mixture (OPC-Soil)	84
Table 3.4 Optimisation for Unary, and binary mixtures.....	85
Table 3.5 Optimisation for ternary blending.	86
Table 3.6 Comparison the performance of the optimum mixtures with that of reference mixture.....	87
Table 4.1 Main physical and geotechnical properties of the virgin soil.	91
Table 4.2 The chemical properties and oxides contents of the virgin soil.	91
Table 4.3 The chemical properties and XRF analysis of the reference cement.	94
Table 4.4 The chemical compositions of both grades of WPSA used in this study.	96
Table 4.5 Chemical properties of treated POFA.	100
Table 4.6 Chemical properties of treated RHA.	103
Table 4.7 Chemical properties of PFA.	106
Table 4.8 Chemical properties of GGBS.....	109
Table 4.9 Chemical properties of SF.	111
Table 4.10 Chemical properties of FGD gypsum.....	114
Table 4.11 Comparative chemical properties of candidate materials.....	116
Table 4.12 Comparative chemical properties of candidate materials with the requirements of the British Standard.....	117
Table 4.13 Volume statistics of candidate materials with reference OPC.	119
Table 5.1 Comparative effect of WPSA and OPC treatment on the soil Atterberg limits.	123
Table 5.2 Volume statistics of ground activated WPSA	138

Table 5.3	Mixing proportion of binary blending mixtures	140
Table 5.4	Atterberg limits of the soil treated with different unary and binary mixtures	142
Table 5.5	The values of compaction parameters after binary blending treatment.....	144
Table 5.6	Mixing proportions of the ternary blending treatment.	149
Table 5.7	Atterberg limits values after ternary blending treatment.....	151
Table 5.8	The values of compaction parameters after ternary blending treatment.....	154
Table 5.9	UCS values of curing time after ternary blending treatment.....	156
Table 5.10	Volume statistics of TM3 after grinding activation.....	160
Table 5.11	Atterberg limits values for the soil treated with TM3 and TM4 with effect of grinding and FGD.....	162
Table 5.12	UCS values after grinding with FGD application.	165
Table 6.1	MDD and OMC values obtained from compaction tests of the soil treated with different mixtures.	173
Table 6.2	UCS values of the soil treated with different types of binder over curing time.	174
Table 6.3	Compressibility parameters of the undisturbed and remoulded soil.	181
Table 6.4	Summary of compression and swelling indices recorded for the soil treated with different binders over the time of curing.	184
Table 7.1	EDX analysis of T+FGD paste after different periods of hydration reaction	222
Table 7.2	EDX analysis of the paste of reference cement after different periods of hydration reaction	223

LIST OF ACRONYMS AND ABBREVIATIONS

AASHTO	American Association of State Highways and Transportation Officials
ASTM	American Standard Test Method
BS	British Standard
C-A-H	Calcium-Aluminate-Hydrate
CBR	California Bearing Ratio
CEC	Cation Exchange Capacity
C-K-S-H	Calcium-Potassium-Silicate-Hydrate
C-S-A-H	Calcium-Silicate-Aluminate-Hydrate
C-S-H	Calcium-Silicate-Hydrate
C-WPSA	Coarse Waste Paper Sludge Ash
EDX	Energy Dispersive X-Ray Spectroscopy
EDXRF	Energy Dispersive X-Ray Florescence
FGD	Flue Gas Desulphurisation
F-WPSA	Fine Waste Paper Sludge Ash
GA	Grinding Aid
GGBS	Ground Granulated Blast Furnace Slag
GHGs	Greenhouse Gases
LL	Liquid Limit
LOC	Lower Oxford Clay
LOI	Loss on Ignition
OPC	Ordinary Portland Cement
PFA	Pulverised Fuel Ash
PI	Plasticity Index
PL	Plastic Limit
POFA	Palm Oil Fuel Ash
PSD	Particle Size Distribution
RHA	Rice Husk Ash
SCMs	Supplementary Cementitious Materials
SEM	Scanning Electronic Microscopy
SF	Silica Fume
SSA	Specific Surface Area
UCS	Unconfined Compressive Strength
UKQAA	UK Quality Ash Association
USCS	Unified Soil Classification System
VS	Virgin Soil
WPSA	Waste Paper Sludge Ash
WRB	World Reference Base
XRD	X-Ray Diffraction
XRF	X-Ray Florescence

GLOSSARY OF SYMBOLS (UNITS)

%	Percentage
Δe_c	Change in void ratio
ΔH_o	Change in height
μm	Micrometre, Dimension unit (10^{-6} Metre)
AFm	Alumina-ferric oxide-monosulphate (chemical composition)
AFt	Alumina-ferric oxide-trisulphate (chemical composition)
Al	Al_2O_3 (notation used in cement chemistry)
Al_2O_3	Aluminium oxide (chemical compound)
C_2S	Di-calcium silicate
C_3A	Tri-calcium aluminate
C_3S	Tri-calcium silicate
C_4AF	Tetra-calcium Ferro-aluminate
$\text{Ca}(\text{OH})_2$	Hydrated lime
Ca/Si	Calcium to silica ratio
Ca^{2+}	CaO (notation used in cement chemistry)
CaO	Calcium oxide (chemical compound)
C_c	Compressibility Index
CI	Intermediate plasticity clay (notation used in soil classification)
Cl	Chlorine
$^{\circ}\text{C}$	Celsius, temperature unit
CO_2	Carbon dioxide (chemical compound)
C_p	Collapse potential
C_r	Recompression index
C_s	Swelling index
CuO	Copper (II) oxide (chemical compound)
C_v	Coefficient of consolidation
d_{50}	The median particle size
E'_{Oed}	One-dimension elastic modulus.
e_o	Initial void ratio
F_a	Attractive forces
Fe_2O_3	Iron oxide (chemical compound)
F_r	Repulsive forces
g	Gram, Weight unit (10^{-3} kilogram)
GJ	Gigajoule, Energy unit (10^9 Joules)
Gs	Specific gravity
H_o	Initial height
K	Potassium (chemical element)
K_2O	Potassium oxide (chemical compound)

kg	Kilograms, Weight unit (kilograms)
kPa	Stress unit (kilo Pascal or Newton/ m ²)
kWh	Kilowatts per hour, electricity consumption unit.
mEq	Milli-equivalents
Mg	Magnesium (chemical element)
Mg/m³	Mega-gram per cubic metre, weight density unit.
Mg²⁺	MgO (notation used in cement chemistry)
MgO	Magnesium oxide (chemical compound)
min.	Minute, time unit
mm	Millimetre, Dimension unit (10 ⁻³ metre)
MN	Mega newton, load unit (10 ⁶ Newtons)
MnO	Manganese (II) oxide (chemical compound)
M_v	Coefficient of volume compressibility
Na	Sodium (chemical element)
Na₂O	Sodium oxide (chemical compound)
NaOH	Sodium hydroxide (chemical compound)
nm	Nanometre, Dimension unit (10 ⁻⁹ metre)
OCR	Over consolidation ratio
P₂O₅	Phosphorus pentoxide (chemical compound)
P_c	Pre-consolidation pressure
pH	Measure of acidity or basicity of an aqueous liquid
P_o	In-situ exist pressure
q_umax	Maximum compressive strength
S_c	Consolidation settlement
Si	SiO ₂ (notation used in cement chemistry)
Si/Al	Silica to alumina ratio
SiO₂	Silicon dioxide (chemical compound)
SO₃	Sulphur trioxide (chemical compound)
SrO	Strontium oxide (chemical compound)
TiO₂	Titanium oxide (chemical compound)
Tonne	Weight unit (1000 kilograms)
w/c	Water/cement ratio (notation used in concrete mixtures)
γ_dmax	Maximum dry density (notation for soil density)
σ₃	Minor principle stress

CHAPTER 1

INTRODUCTION

1.1 GENERAL

In many countries such as the UK, civil engineering projects are commonly located in areas of ground surface which are characterised by soft soil including alluvium, peats and organic clays. Given their undesirable low strength, high compressibility and shrink/swell durability characteristics, soft soils present challenging ground conditions for civil engineers. (Bowles, 1997; Hassan, 2009; Consoli *et al.*, 2015). The accepted usual method of soft soil mitigation was to replace the soft soil with stronger materials. Due to the high cost of this method, researchers have been driven to look for alternative methods and one of these methods is the process of the soil stabilisation (Karin Axelsson *et al.*, 2002; Harichane *et al.*, 2011; Cristelo *et al.*, 2013; Sol-Sánchez *et al.*, 2016).

Soil stabilisation was technically introduced many years ago, but it has been established since 4000 or 5000 BC. The main purpose of this technique is to render the soil capable of meeting the requirements of the specific engineering projects (Kolias *et al.*, 2005; Venda Oliveira *et al.*, 2011). More specifically, soil stabilisation is recommended to aid the engineer in being able to employ the natural soil of the site of a project as an engineering material with specific properties, especially strength, volume stability, permeability and durability (Tyrer, 1987; Bowles, 1997).

Stabilisation of subgrade soil has traditionally relied on treatment with either lime and/or cement which react chemically to bond the soil particles to each other resulting in stronger soil structure, or special additives such as Pozzolanic materials. Pozzolanic materials such as fly ash, micro silica (SF), rice husk ash (RHA) ground granulated blast furnace (GGBS), etc. are regarded as waste materials which can be used for soil improvement as indicated in recent research projects (Yoder and Witczak, 1975; Wild *et al.*, 1998; Abd El-Aziz *et al.*, 2006; Rios *et al.*, 2016).

Stabiliser materials are divided mainly into the two following types: traditional (such as Portland cement, cement-fly ash, lime, fly ash with lime, etc.), and non-traditional additives (polymers, fibre, chloride compounds, petroleum resins, etc.). Waste materials, sometimes called by-product materials can be added to non-traditional stabilisers, due to their significant performance in the field of soil stabilisation. In recent years the use of non-traditional additives has been increasing for soil stabilisation purposes due to their low cost, ease of application and short curing time (Tingle *et al.*, 2007; Makusa, 2012; Sol-Sánchez *et al.*, 2016).

1.2 AIM AND NOVELTY STATEMENT

Soft soil stabilisation has traditionally been achieved by treating with calcium-based materials such as lime and cement. There are numerous research projects involving Ordinary Portland Cement (OPC) and lime as preferred binder materials in soil stabilisation (Basha *et al.*, 2005; Zhang and Tao, 2008; Oyediran and Kalejaiye, 2011; Bhuria and Sachan, 2014; Bahmani *et al.*, 2016; Goodarzi *et al.*, 2016). Furthermore, it is proven that the use of lime and OPC as soil stabilisers improves the soil properties significantly. It has been reported that cement treatment for soft soils increasing the workability (less water is needed for compaction with the use of cement), the compressive strength, and the durability (resistance against severe conditions such as wetting-drying cycles), and lead to a reduction in the compressibility and permeability as indicated in Miura *et al.* (2001); Jauberthie *et al.* (2010); Farouk and Shahien (2013); Önal (2014); Modarres and Nosoudy (2015). However, the production of lime and OPC have many drawbacks such as negative environmental impact, high cost of production, and the consumption of natural resources. Therefore, researchers have been motivated to look for alternative materials to replace or reduce the use of OPC.

The aim of this research project is the development of a new cementitious material, produced from cement-free blending of different waste material fly ashes for use in soft soil stabilisation, by examining the effect of various by-product material mixtures; unary, binary and ternary with the physico-chemical activation, on different geotechnical properties of the stabilised soil.

Unlike the ordinary Portland cement (OPC), by-product or waste materials, do not require any energy for incineration or heavy grinding power to be produced, as well as being readily available around the world and not depending on virgin mineral materials. Therefore, the use of by-product materials in the field of soil stabilisation will provide a sustainable stabilising agent and reduce the use of OPC, and this achieves undeniable benefits in cost saving as well as in environmental protection issues.

1.3 OBJECTIVES

The objectives of this research project to achieve the aim above are:

1. To identify the physical and chemical properties of different types of waste materials such as pulverised fuel ash (PFA), ground granulated blast furnace slag (GGBS), waste paper sludge ash (WPSA), silica fume (SF), rice husk ash (RHA), palm oil fly ash (POFA), and flue gas desulphurisation (FGD) gypsum. Further, compare their physical and chemical properties with those for ordinary Portland cement (OPC) to predict their potential for use as cement replacement materials.
2. To carry out the experimental work on mixing design by blending different types of waste materials with different proportions using unary, binary, and ternary blending procedures.
3. To conduct the required experimental works for mechanical and chemical activation for different mixtures of waste materials by using grinding energy and chemical activators respectively.
4. To investigate the effect of different mixtures of waste materials on the improvement of the physical and geotechnical properties of the stabilised soil such as compaction parameters, Atterberg limits, unconfined compressive strength and consolidation.
5. To determine the effect of wetting and drying cycles on the unconfined compressive strength and volume changes of the soil treated with different mixtures of waste materials.

6. To quantify and critically review the improvement of soft soil properties for each stage of the experimental works by conducting a microstructural investigation by undertaking X-ray diffraction (XRD), scanning electron microscopy (SEM) and energy dispersive X-ray spectroscopy (EDX) analyses to best realise the results obtained.

1.4 THE SELECTION OF CANDIDATE MATERIALS

Waste or by-product materials have occupied a major element of research projects in terms of modern cement manufacturing due to the wide range of their chemical properties render them promising in the cement replacement industry (Della *et al.*, 2002; Bujulu *et al.*, 2007; Yilmaz and Degirmenci, 2009; Sun *et al.*, 2015; Van den Heede *et al.*, 2016).

The selection of the above-mentioned waste materials (section 1.3; number 1) was dependant on their availability in the UK and worldwide. Additionally, the wide range of the chemical composition of the selected materials was one of the major factors for selection. Significant performances of WPSA, POFA, RHA, GGBS, SF, PFA and FGD gypsum, as potential cement replacement materials, have been reported in recent research projects (Sadique *et al.*, 2013; Gluth *et al.*, 2014; Pourakbar *et al.*, 2015; Yi *et al.*, 2015; Alex *et al.*, 2016; Goodarzi *et al.*, 2016; Cheshomi *et al.*, 2017).

1.5 SCOPE OF THE STUDY

This study emphasises the changes of the geotechnical properties of an intermediate plasticity silty clay with sand (CI); classified according to EN ISO 14688-2:2004+A2013 (European Committee for Standardization, 2013), stabilised with different mixtures (unary, binary, and ternary) combined from blending the fly ashes of three specific types of waste materials as new cementitious materials. These fly ashes are WPSA, POFA and RHA. However, the mix design and optimisation processes for each type of mixtures were dependent initially on the results obtained from compaction testing, determination of the Atterberg limits and unconfined compressive strength (UCS) tests. Further activation using grinding energy with the

use of FGD gypsum as a grinding agent was also employed for the latter types of ternary mixtures. The effect of the most promising mixtures on the consolidation parameters of the stabilised soil was investigated at the later stages along with the effect of wetting-drying cycles on the strength and volume change. The improvement achieved in the geotechnical properties of the stabilised soil was compared with the properties of the untreated soil and with those for soil stabilised with the same amounts of OPC. A microstructural study was conducted on the soil treated with OPC and with the newly developed binder to understand and elucidate the improvement gained in soil strength by conducting XRD analyses, SEM testing and the EDX analyses.

1.6 THESIS STRUCTURE

The structure of this thesis can be broken down into different chapters. These chapters are organised as follows:

- **Chapter 1** presents a general overview about the soft soil stabilisation, the most common materials used as binders and the motivation to investigate alternative materials. The aim and novelty statement, objectives, the thesis structure and summary are also presented in this chapter.
- **Chapter 2** provides a brief background about methods of soil stabilisation focussing on chemical stabilisation. Then, a comprehensive literature review on the use of OPC as the most common traditional additive in soil stabilisation, with advantages and drawbacks, is presented. Moreover, the literature review on the use of waste materials as cement replacements in soft soil stabilisation is also presented. This includes the methods and techniques employed in past research projects to produce new cementitious materials and the fundamental aspects obtained by the researchers to organise the suitability of waste materials to introduce their new binders is also presented in this chapter. A summary is provided at the end of this chapter to conclude the previous studies and establish the state-of-the-art by evaluating the behaviour of soft soil treated with different mixtures of waste materials.

- **Chapter 3** describes the experimental works examination by giving details of the equipment and apparatus used in this study, the methods and procedures of sample preparation, conditioning and testing and the research methodology followed to achieve the aim of this study.
- **Chapter 4** presents the results and discussion of the experimental works which were conducted for the identification of materials including the soft soil, a group of different waste materials and by-products together with a reference cement. The output of this chapter was represented by the selection of the most promising materials that have the potential to be used in the development of the new binder to replace the cement totally.
- **Chapter 5** addressed the results and discussion of the optimisation phases for the unary, binary and ternary blends in addition to a further activation of the ternary mixtures using mechanical and chemical activation techniques with the aid of grinding agent. The optimising evaluation was dependent on the results obtained from compaction parameters, the Atterberg limits and unconfined compressive strength (UCS) tests. A summary of this chapter presented a group of the optimum mixtures of the waste materials used in this study.
- **Chapter 6**, in this chapter, the results and discussion of the effects of the optimum mixtures treatment on different geotechnical properties of the treated soil were displayed in comparison to the effect of reference binder treatment (OPC). The results of the compressibility test (Consolidation test) and the effect of the wet-dry cycles of specimens of soil treated with OPC as well as with the optimum mixtures are analysed and discussed in this chapter in addition to the results of the Atterberg limits, compaction and UCS tests. A comprehensive summary of the results illustrated is provided at the end of this chapter.
- **Chapter 7** introduces the results of the microstructural investigation through XRD, SEM and EDX analyses for specimens of soil treated with the most promising binder (the newly developed binder) and for its paste without soil. The results and their discussion are illustrated by providing XRD patterns

graphs, SEM images and EDX analysis results for the soil treated with the newly developed binder and the binder paste at different curing periods. The results were compared with those of the samples of OPC-treated soil and OPC paste at the same curing periods.

- **Chapter 8** commences with the limitation of the results presented in this thesis. This chapter also draws and concludes the main findings of this research project and highlights the significant achievements in the improvement of the engineering and geotechnical properties of the stabilised soil in this study. Finally, recommendations for future works are suggested.

1.7 SUMMARY

This chapter provides a general overview of soft soils and their problems along with the most common methods to mitigate the properties of such soils. This chapter also highlights the traditional additives which have been used as binders in soil improvements and the disadvantages regarding their use as construction materials particularly the CO₂ emissions result from their manufacturing. The motivation in this research project is the need of cement and civil engineering industries to develop alternative cementitious binders having less or negligible CO₂ emissions and a lower financial cost in comparison to the traditional binders. The utilising of by-products or waste material fly ashes in the production of cement-free blended cementitious binders can be a valuable and promising approach to address the aforementioned issue. This approach is presented as a novel method in this thesis to study the potential of using binders produce from the blending of the fly ashes of waste materials for the use in soft soil stabilisation as a 100% replacement of OPC. The objectives to achieve the aim of this study, the scope of the study and the thesis structure are also included in this chapter.

CHAPTER 2

LITERATURE REVIEW

2.1 INTRODUCTION

This chapter aims first to present a general overview about the soil classification and the identification of problematic soils. Then, it deals with soil stabilisation and the most common method employed in soil improvement. Additionally, the fundamental concepts and the mechanism of soil stabilisation using cement and the changes in the geotechnical properties of cement-stabilised soils such as compaction parameters, consistency limits, strength, compressibility and durability are critically reviewed. Furthermore, a detailed review about the knowledge and findings of the past research regarding the performance of different waste material fly ashes used in soil stabilisation is presented. Finally, the techniques used for the activation of waste materials fly ashes is highlighted.

2.2 SOILS IDENTIFICATION AND CLASSIFICATION

There are many types of soils which range from hard, dense, rocks with large pieces, gravel, sand, silt and clay to soft organic deposits and peat soil with high compressibility. However, there are many factors affecting the type and the behaviour of soil such as the climate, organisms, landscape, parent materials, and the time of weathering and erosion (Mitchell and Soga, 2005). The existence of a standard language for soil description and identification is essential. The characterisation of the soil material and the soil mass, at the location of the project, should be included in an understandable description (Knappett and Craig, 2012). Mitchell and Soga (2005) stated that the engineering properties of any soil might be attributed to two major groups of factors. These are the compositional factors (mineral types and their amount, types of cations, shape of the soil particles and their size distribution, etc.) and the environmental factors which affect the conditions of soil formation (moisture content, density, confining pressure history, degree of temperature and the water existence

within the soil structure). Dependent on the purposes of the soil use, several systems have been employed for soil classification (Bunga *et al.*, 2011; Budhu, 2011; Hartemink, 2015).

British standard BS-5930:2015 (2015) recommended a method for soil identification and description which can be considered as a code of practice in soil investigation. This method specifies symbol, group and recommended name for each type of soil dependent on the percentages of fines and liquid limit as illustrated in section 6-Table 7 the above-mentioned standard. However, in some cases it may be necessary to develop local rules dependent on particular conditions, but these amendments should be kept to a minimum and all new terms and amendments should be defined clearly (Majeed, 2014).

2.3 PROBLEMATIC SOILS

Large quantities of soil are required in different civil engineering projects which are used in many earth structures such as embankments, base layers of roads and railways and retaining walls. Therefore, it is crucial to estimate the available quantities of soil and evaluate the suitability of the in-situ soil for use as a construction material, especially in terms of strength, volume stability, compressibility, permeability and bearing capacity (Kalkan, 2013; Pourakbar *et al.*, 2015; Moghal *et al.*, 2015). However, it is very common that civil engineering projects are located within sites with a problematic soil; such soils, due to their behaviour, cause damage problems that occur in foundations and structures of many geotechnical projects (Estabragh *et al.*, 2013). Soils can be categorised as problematic when they show swelling or expanding characteristics, collapsing and significant settlement in addition to the distinct lack of strength and or are soluble. The behaviour of such soils may be attributed to their chemical and mineralogical compounds, the nature of soil formation and their fabric and pore fluids condition, however the major factors that affect their behaviour is the change in water content and the level of ground water (Rezaei *et al.*, 2012; Dang *et al.*, 2016).

The most common types of problematic soils can be summarised as follows:

2.3.1 Collapsible Soils

Collapsible soils are soils which apparently possess a relatively high strength with their low natural moisture content but they are very sensitive regarding the moisture in which a significant volume reduction occurs when their water content increases which leads them to collapse (Rezaei *et al.*, 2012; Li *et al.*, 2016). Moreover, the structure of such a soil is called metastable and it experiences a large reduction of strength or a significant increase in settlement due to a relatively small development in stress or deformation (Murthy, 2003).

The following examples represent collapsible soils as stated by Murthy (2003):

- 1- Quick clays which experience excessive sensitivity to the changes in moisture content,
- 2- Loose sands in a saturated state which are liable to liquefaction,
- 3- Unsaturated primarily granular soils which have an apparent cohesion, cohesion associated with clay particles that are located at the inter-granular contacts or cohesion due to the accumulative soluble salts which bind granular particles to each other, and
- 4- Chemically weathered rocks, either above or below the water level with high void ratio which is developed, due to leaching processes causing a network of stress transition points of minerals around key zones.

However, the failure happens when the water content increases causing breaking down to the bond points among the collapsible soil particles and the sudden reduction in voids volume occurs due to the particles rearrangement of the collapsible soil subjected to constant value of stress (Jefferson *et al.*, 2015; Iranpour and Haddad, 2016).

2.3.2 Dispersive Soils

Dispersive soils are fine-grained soils with unstable structure, the dispersion in their structure can easily occur, and therefore, they are easily eroded. Dispersion occurs in soils, in which the repulsive forces (F_r) in the electrical double layer at the charged clay particles exceed the attractive forces (F_a) leading to de-flocculation, so that in the presence of relatively pure and static water the particles detach spontaneously from each other to form colloidal suspensions; such soils are termed dispersive clays (Mitchell and Soga, 2005; Rezaei *et al.*, 2012; Goodarzi and Salimi, 2015).

F_r and F_a are controlled by the change in pH (difference between the pH of suspension and the pH at which the net charge on the colloid surface becomes zero) and the ionic strength of the solution. F_r increases with the increase in the difference of pH thus leading the dispersion to occur. However, there are other factors that affect the colloidal stability such as organic matter content, mineralogical composition of the colloid mixture, types and amount of exchangeable cations, the abundance of iron and alumina oxides (Igwe *et al.*, 1999; Sequaris, 2010; Fujita and Kobayashi, 2016; Huang *et al.*, 2016).

2.3.3 Expansive Soils

These are clay soils, which exhibit huge volume changes when a change in their water content occurs regardless of loading and external stresses. Additionally, expansive soils expand when they become wetted and shrink when dried and they are formed from clay minerals such as montmorillonite and illite. Expansion and shrinkage behaviour of such soils has caused significant damage to the foundations and structures of many engineering projects (Seco *et al.*, 2011; Wang *et al.*, 2014; Dang *et al.*, 2016; Jha and Sivapullaiah, 2016)

Expansive soils can be found in environments associated with high degrees of humidity in which the expansion problems can occur due to the high plasticity index (PI). Additionally, expansive problems can also occur in arid or semi-arid soils in which soils even with moderate potential of expansion can cause significant damage (Johnes and Jefferson, 2012). Therefore, it is very important to understand the mineralogical combination of expansive soils and the effect of their swell-shrinkage behaviour.

2.4 SOIL MINERALS

Soils are basically composed of one or several types of minerals with different proportions dependent on the origin of their mother materials as well as the formation conditions; Table 2.1 illustrates the names of most common minerals along with the chemical formula and the characteristics of each corresponding mineral (Sposito, 2008).

Table 2.1 Common Minerals in Soils

Mineral Name	Chemical Formula	Characteristics
Quartz	SiO ₂	Abundant in sand and silt
Feldspar	(Na,K)AlO ₂ [SiO ₂] ₃	Abundant in soil that is not leached extensively
Mica	CaAl ₂ O ₄ [SiO ₂] ₂ K ₂ Al ₂ O ₅ [Si ₂ O ₅] ₃ Al ₄ (OH) ₄ K ₂ Al ₂ O ₅ [Si ₂ O ₅] ₃ (Mg,Fe) ₆ (OH) ₄	Source of K in most temperate-zone soils
Amphibole	(Ca,Na,K) _{2,3} (Mg,Fe,Al) ₅ (OH) ₂ - [(Si,Al) ₄ O ₁₁] ₂	Easily weathered to clay minerals and oxides
Pyroxene	(Ca,Mg,Fe,Ti,Al)(Si,Al)O ₃	Easily weathered
Olivine	(Mg,Fe) ₂ SiO ₄	Easily weathered
Epidote	Ca ₂ (Al,Fe) ₃ (OH)Si ₃ O ₁₂	Highly resistant to chemical weathering; used as “index mineral” in petrologic studies
Tourmaline	NaMg ₃ Al ₆ B ₃ Si ₆ O ₂₇ (OH,F) ₄	
Zircon	ZrSiO ₄	
Rutile	TiO ₂	
Kaolinite	Si ₄ Al ₄ O ₁₀ (OH) ₈	
Smectite vermiculite, chlorite	M _x (si,Al) ₈ (Al,Fe,Mg) ₄ O ₂₀ (OH) ₄ , Where M = interlayer cation	Abundant in clays as products of weathering; source of exchangeable cations in soils
Allophane	Si ₃ Al ₄ O ₁₂ . nH ₂ O	Abundant in soils deived from volcanic ash deposits
Imogolite	Si ₂ Al ₄ O ₁₂ . 5H ₂ O	
Gibbsite	Al(OH) ₃	Abundant in leached soil
Goethite	FeO(OH)	Most abundant Fe oxide
Hematite	Fe ₂ O ₃	Abundant in warm region
Ferrihydrate	Fe ₁₀ O ₁₅ . 9H ₂ O	Abundant in organic horizons
Birnessite	(Na,Ca)Mn ₇ O ₁₄ . 2.8H ₂ O	Most abundant Mn oxide
Calcite	CaCO ₃	Most abundant carbonate
Gypsum	CaSO ₄ . 2H ₂ O	Abundant in arid regions

Source: Sposito (2008), permission to reproduce this table has been granted by Oxford University Press.

The solids constituent of a soil is made up by crystalline materials which are called minerals. Soft soils are formed from platy mineral particles; composed mainly from silicon and oxygen which are the most abundant elements on earth (Budhu, 2011).

According to Das (2010) and Budhu (2011), there are two main types of mineral sheets produced from the combination of a group of minerals called structural units; these

types of sheets are either silica sheets or alumina sheets. The silica tetrahedron is the structural unit of silicates which is combined from a central ion of silica cation (positive charge) surrounded by four negatively charged of oxygen anion, one at each corner of the tetrahedron resulting in a negative charge of -4 for each single tetrahedron. Therefore, single tetrahedrons need to be linked to each other to achieve a natural charge cation as illustrated in Figure 2.1a which presents silica sheets or laminae, which are thin layers of silica tetrahedrons sharing three oxygen ions among each other. On the other hand, the structural unit of alumina sheets is called alumina octahedron which is produced from the combination of alumina minerals in which an aluminium ion is surrounded by six oxygen or hydroxyl atoms. The alumina octahedron and alumina sheets are shown in Figure 2.1b.

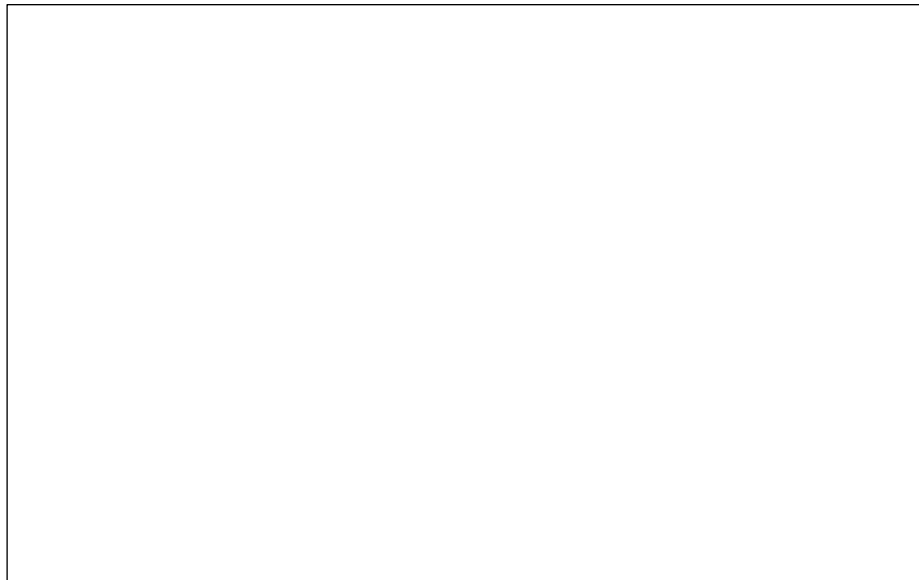


Figure 2.1 Structural units and minerals sheets (a) Silica tetrahedron and Silica sheet, (b) Aluminium octahedron, and Aluminium sheet.

Source: Das (2010). **The diagram originally presented here cannot be made freely available via LJMU Digital Collections because of 'copyright'**

According to Budhu (2011) and Kinuthia (2016), the minerals kaolinite, illite, and montmorillonite are the most common types of crystalline minerals that make up clays. The structure of kaolinite consists of a 0.72 nm thick layer combined from one silica tetrahedral sheet and one alumina octahedral sheet; this layer is stacked repeatedly and the layers are held together by a hydrogen bond as shown in Figure 2.2a. The illite layer is 0.96 nm in thickness consisting of one alumina octahedral sheet inserted between two silica tetrahedral sheets and the repeated layers are held together by potassium ions as shown in Figure 2.2b. With respect to the montmorillonite, the

structure is similar to the illite, but weak van der Waals forces hold the layers together instead of potassium (Figure 2.2c).

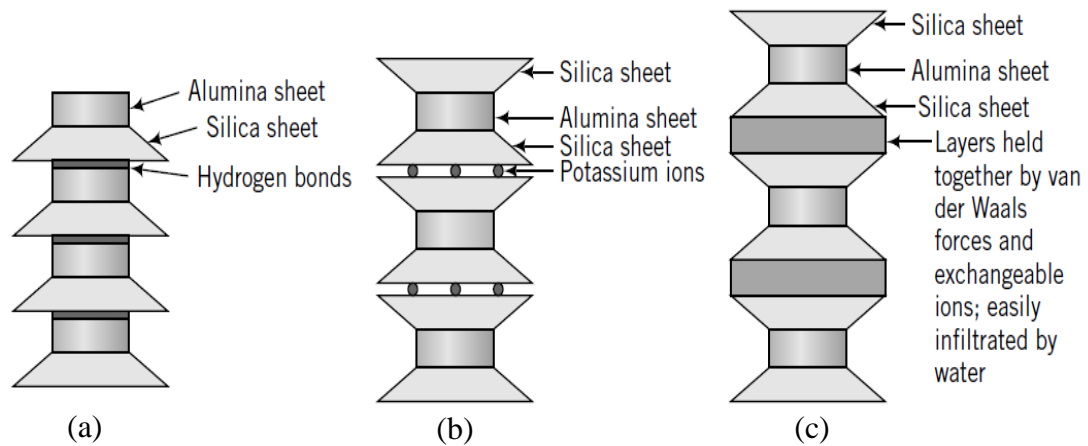


Figure 2.2 clay minerals structures. (a) Kaolinite, (b) Illite, and (c) Montmorillonite.

Source: Budhu (2011), permission to reproduce this figure has been granted by John Wiley and Sons

Montmorillonite belongs to the smectite clay family which has a small amount of Al⁺³ replaced by Mg⁺². This leads to charge disparity which can be balanced by Na⁺ or Ca²⁺ cation exchange and oriented water. Water can enter between the sheets of montmorillonite and makes them split causing significant expansion. Thus, soil which contains a considerable amount of this type of mineral exhibits significant swelling and shrinkage problems (Murthy, 2003; McPhee et al., 2015). Additionally, Kinuthia (2016) explained that there are several types of hydrated cations, such as Mg, Na, K, and Ca, that can be inserted into interlayer spaces of the clay minerals through different mechanisms such as adsorption, diffusion, and osmosis pressure. These cations cause different expansion potentials of different clay soils as illustrated in Table 2.2.

Table 2.2 Typical free swell potential for common clay soils

Clay type	Swell %
Kaolinite	5 – 7
Illinite	15 – 120
Ca-Montmorillonite	45 – 145
Na-Montmorillonite	1400 - 2000

Source: Kinuthia (2016), permission to reproduce this table has been granted by Elsevier.

Surface forces and water adsorption of clay minerals are significantly higher than those for sandy soil because of their high specific surface area and the behaviour of the surface forces of clay minerals is affected by this high surface area. For example, the typical specific surface area of sand is 0.01m^3 per gram, while for montmorillonite is about 1000m^3 per gram (Budhu, 2011). The surface charges of clay sheets are normally negative (anions) as mentioned before, these negative charges attract cations which are positive such as Na^+ and Ca^{2+} and a few anions in addition to the positively charged side of non-axisymmetric water molecules from the added water to float around the clay particles. This configuration is referred to as a diffuse double layer as shown in Figure 2.3a (Das, 2010). In Figure 2.3b, Das (2010) explained that there is an exponential relationship between the concentration of the cations and their distance away from the clay particle surface in which the largest concentration of cations occurs at the clay particle surface.

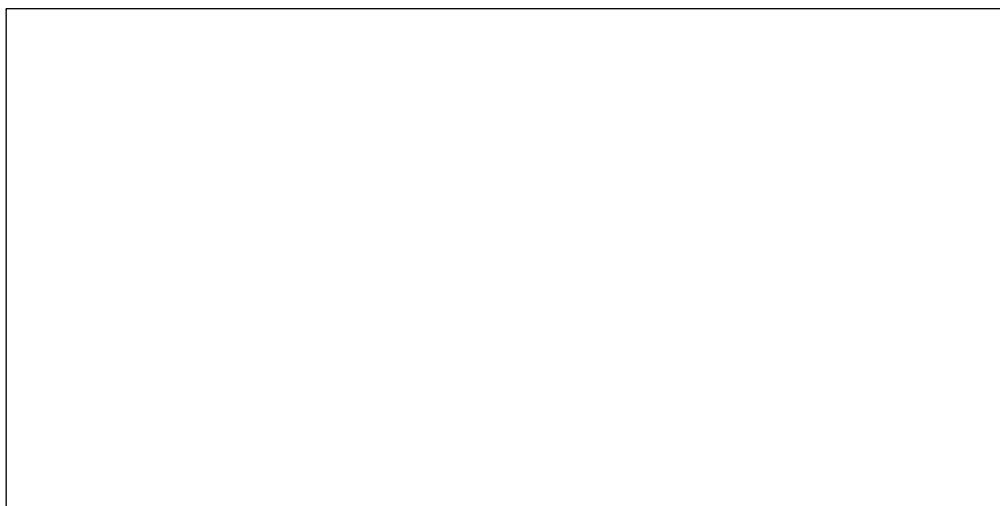


Figure 2.3 Diffuse double layer of clay particles surface.

Source: Das (2010). **The diagram originally presented here cannot be made freely available via LJMU Digital Collections because of 'copyright'**

Cation exchange capacity (CEC) of clay minerals may be defined as a measurement of the availability of exchangeable cations at a given pH value. It is recommended that the pH value has to be specified during the cation exchange reaction. However, the CEC is usually determined at neutral pH ($\text{pH} = 7$) and it is traditionally expressed in milli-equivalents ($\text{mEq}/100\text{g}$) (Bergaya et al., 2013).

Ismadji *et al.* (2015) presented a table that illustrates cation exchange capacity (CEC) values for different types of clay minerals as listed in Table 2.3.

Table 2.3 Typical values of cation exchange capacity for different clay minerals.

Clay mineral type	CEC (mEq/100g)
Kaolinite	3 – 15
Allophane	70
Illinite	10 – 40
Halloysite (2H ₂ O)	5 - 10
Ca-Montmorillonite	40 - 70
Na-Montmorillonite	80 – 130
Hectorite	80 – 130
Palygorskite	30 - 40
Sepiolite	30 – 40
Vermiculite	100 - 150

Source: Ismadji *et al.* (2015), permission to reproduce this table has been granted by Springer.

Regarding the engineering behaviour of expansive soils, the consistency is the most important characteristic which refers to the strength and resistance to penetration of such soil at the site. The parameters that are used to evaluate the response of soft soils to the external stresses or pressure are called consistency or Atterberg limits (shrinkage, plastic and liquid limit) in addition to the plasticity index (Wagner, 2013; Daoudi *et al.*, 2015). Moreover, Johnes and Jefferson (2012) mentioned that there are several laboratory methods to identify the expansive soils in addition to the Atterberg limits such as X-ray diffraction, swell testing using the oedometer consolidation apparatus, and suction measurement. However, most researchers agreed that plasticity index (PI) is the most widely used parameter to determine the potential of swelling and shrinkage of expansive soils. Table 2.4 shows the classification of expansive soils in terms of swelling and shrinkage dependent on several ranges of PI values.

Table 2.4 Description of volume change potential for different ranges of PI

PI	Potential of volume change
> 60	Very high
40 - 60	High
20 - 40	Medium
< 20	Low

Source: Johnes and Jefferson (2012), permission to reproduce this table has been granted by ICE Publishing

2.5 SOIL IMPROVEMENT

2.5.1 General

The most critical criteria for any geotechnical design of a structure which have to be considered for site selection are the function and design load of the structure, the proposed type of foundation, and bearing capacity of the underground soil. However, in the past, bearing capacity had the major effect in making a decision on selection of the site (Makusa, 2012). In a case where the ground surface of the project site had less than the required bearing capacity, the following options were considered to amend the design to be suitable for the site conditions, replace the weak soil of the site with stronger materials, or relinquish the site. The site rejection due to undesirable bearing capacity dramatically increased which led to a lack of suitable land and an increase in demand of natural resources, therefore the use of native soil after improving its geotechnical properties is the most suitable way to solve this problem (Zheng and Qin, 2003; Hassan, 2009; Ornek et al., 2012; Sol-Sánchez et al., 2016).

2.5.2 Soil Stabilisation

Soil stabilisation is a term used for the improvement of the geotechnical properties of the natural soils found on-site to a condition that makes it suitable for re-use as an engineered fill material by improving soil strength and durability, and producing an increased soil resistance against becoming soft in the presence of water (Sherwood, 1993; Prabakar and Sridhar, 2002). It can be done either mechanically, for example by densifying the soil, making soil particles close to each other, this process is known as compaction; or chemically, by altering the chemical composition of soil to be suitable

as an engineering material. Chemical stabilisation can be achieved by adding binder materials, which force soil particles to bind to each other (Veith, 2000; Makusa, 2012; Hashad and El-Mashad, 2014). However, both mechanical and chemical methods are sometimes involved to stabilise soil, and the subsequent results depend on the role of each additive. Mechanical additives are used in order to improve the geotechnical properties mechanically such as the load bearing capacity, while the chemical additives are used to alter the geotechnical properties of soil (Arabani *et al.*, 2012; López-Querol *et al.*, 2014).

Chemical stabilisation involves the use of stabilising agents (binder materials) in weak soils to improve their geotechnical properties such as compressibility, strength, permeability and durability. The components of stabilisation technology include soils and or soil minerals and stabilising agents or binders (cementitious materials). Stabilising agents are hydraulic (primary binders) or non-hydraulic (secondary binders) materials that when in contact with water or in the presence of pozzolanic minerals react with water to form cementitious composite materials. Portland cement, lime, and fly ash are the commonly used additives for soil stabilisation (Zheng and Qin, 2003; Koliass *et al.*, 2005; Horpibulsuk *et al.*, 2010; Cristelo *et al.*, 2013; Consoli *et al.*, 2015; Rios *et al.*, 2016).

2.6 CEMENT-SOIL STABILISATION

Cement is the most commonly used material around the world in all types of construction such as buildings, roads, tunnels, bridges, etc. It has the ability to set and harden independently as well as bind other materials together (Jauberthie *et al.*, 2010; Correia *et al.*, 2013; Dave *et al.*, 2016).

Since the creation of soil stabilisation in the 1930s, cement has been the oldest material of choice in common usage. Several types of cement can be used in soil stabilisation, but ordinary Portland cement (OPC) is the most common type of cement, which is widely used in soil stabilisation around the world. Soil-cement is commonly used to improve the foundations of structures, together with road base stabilisation, airfield pavements, in dams and slope protection, stream bank protection, waterproofing, and

reservoir and channel linings (Ingles and Metcalf, 1972; Tyrer, 1987; Muhunthan and Sariosseiri, 2008; Makusa, 2012; Sol-Sánchez *et al.*, 2016).

2.6.1 Chemical Composition of Ordinary Portland Cement

Ordinary Portland cement (OPC) is one of the cement types and it is a complex product. OPC is simply made from lime and clay minerals mixtures which are heated up to 1500°C to produce clinker. Then, gypsum is added to the clinker and they are ground together into a very fine powder (Montgomery, 1998; Aïtcin, 2016a). The chemical composition of OPC contains several types of mineral oxides with different proportions as illustrated in Table 2.5.

Table 2.5 Chemical composition of Ordinary Portland cement

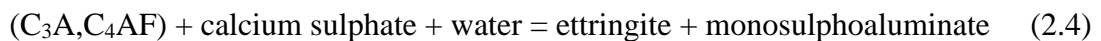
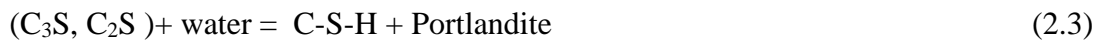
Compound	Percent (%)	Average (%)
Lime (CaO)	59 – 67	64
Silica (SiO ₂)	17 – 25	21
Alumina (Al ₂ O ₃)	3 – 9	7
Iron Oxide (Fe ₂ O ₃)	05 – 6	3
Magnesia (MgO)	0.1 – 4	2
Sulphur trioxide (SO ₃)	1 – 3	2
Sodium potash	0.5 – 1.3	1

Source: Aïtcin (2016a), permission to reproduce this table has been granted by Elsevier

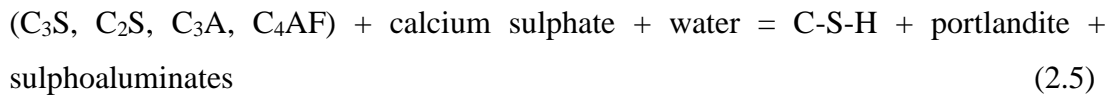
The British standard BS EN 197-1:2000 (European Committee for Standardisation, 2004) specifies that the clinker of Portland cement shall contain calcium silicate (C₃S and C₂S) of at least one third of its mass and the other oxides such as Alumina (Al₂O₃) and Iron Oxide (Fe₂O₃) as the remainder. The standard also states that the ratio of CaO/SiO₂ shall be equal to or not higher than 2, and MgO content shall be not more than 5%. Additionally, the reactive silicon oxides represented by SiO₂, Al₂O₃, and Fe₂O₃ shall be not less than 25% of the mass of OPC (European Committee for Standardisation, 2004).

2.6.2 Chemical Reaction of Soil-Cement Hydration

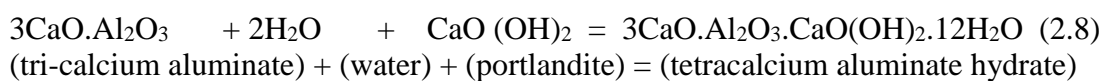
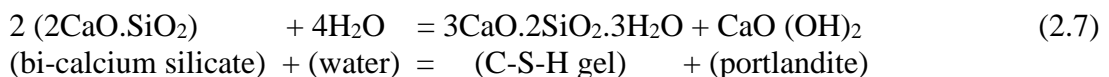
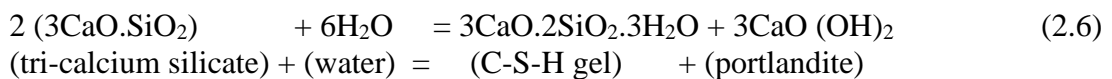
According to Tyrer (1987), Puppala *et al.* (2015), Marchon and Flatt (2016b), and Aïtcin (2016a), the hydration processes of cement treated soil consist of two major phases. The first phase of cement hydration may take a few minutes to a few hours; it is associated in the dissolution and precipitation of the complex chemical system of cement resulting in the formation of different hydrate compounds. The reaction of C₃S and C₂S with water results in the formation of calcium silicate hydrate gel (C-S-H) and calcium hydroxide (hydrated lime Ca(OH)₂) which is called Portlandite. In the existence of calcium sulphate, C₃A and C₄AF are transferred to compounds which are called ettringite and monosulphoaluminate. This stage has the responsibility of the development of early strength of stabilised soil and contributes to change the plasticity index and workability. Aïtcin (2016a) presented the following equations to explain the hydration reaction of cement minerals:



Combining 2.3 and 2.4 produces:



The hydration of tri-calcium silicate produces more portlandite than the hydration of bi-calcium silicate due to the extra calcium oxide (lime) provided by tri-calcium silicate. Schoute (cited in Puppala *et al.*, 2015, p. 298) explained the hydration of cement minerals as follows:



The second phase of the cement treated soil hydration is called the pozzolanic reaction which occurs between the excess hydrated lime (Portlandite) provided from the first phase of cement hydration and the silica and alumina of the clay minerals in treated soil or from other minerals of cement in the presence of water. Pozzolanic reaction is a time dependent activity and it is dependent on the pH value of the environment and the availability of silicate and aluminate compounds (Muhunthan and Sariosseiri, 2008). This reaction leads to form additional C-S-H or calcium aluminate hydrated (C-A-H) compounds (Muhunthan and Sariosseiri, 2008; Puppala *et al.*, 2015).

2.6.3 Effects of Cement Stabilisation

Ordinary Portland cement has been used as the most preferable soil stabiliser for many decades. It can be used for most purposes in soil modification, to improve most of geotechnical properties of treated soils (Miura *et al.*, 2001; Jauberthie *et al.*, 2010; Farouk and Shahien, 2013; Yi *et al.*, 2015; Vakili *et al.*, 2016). A particular review of the effect of cement treatment on the most important physical and geotechnical properties of soft soil can be expressed as follows:

2.6.3.1 Compaction Parameters

Based on the findings of previous researchers, there are two different opinions about the effect of cement treatment on the compaction parameters of the treated soils (maximum dry density (MDD) and optimum moisture content (OMC)). According to Ola (1978); Huat *et al.* (2008); Muhunthan and Sariosseiri (2008); Sariosseiri and Muhunthan (2009); Okyay and Dias (2010); Sarkar *et al.* (2012); Ashango and Patra (2014); Jafer *et al.* (2016), MDD decreases and OMC increases with cement treatment and there is a continuous reduction in MDD and increment in OMC with the increase in the amount of OPC added. Sariosseiri and Muhunthan (2009) conducted their experimental work to investigate the effect of cement treatment on the geotechnical properties of three different types of Washington State soils. They found that the MDDs of all soil types decreased with the increase of cement content until 7.5% then the MDD of Palouse loess soil only increased for higher amounts of cement as shown in Figure 2.4.

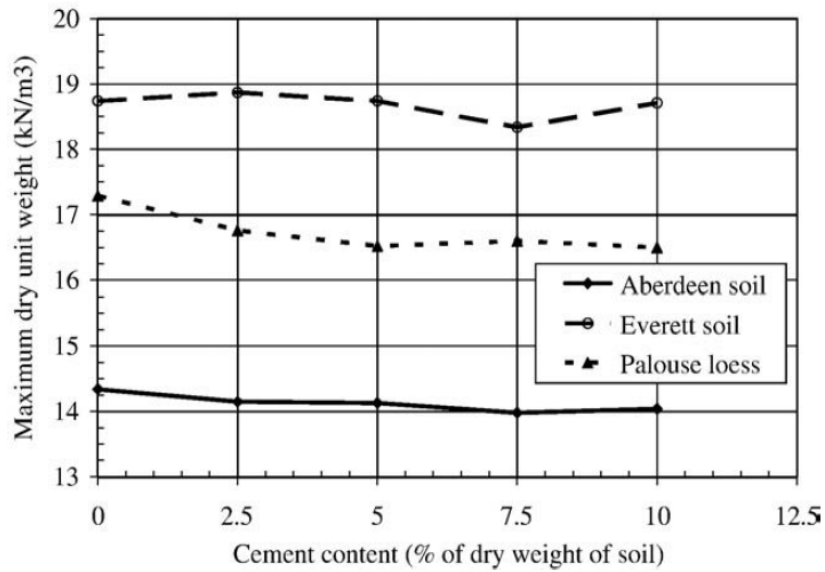


Figure 2.4 Effect of cement content on maximum dry densities of three different types of soil.

Source: Sariosseiri and Muhunthan (2009), permission to reproduce this figure has been granted by Elsevier.

With respect to OMC, there were graduated increments with the increase of cement content except Palouse loess soil again which showed a slight reduction in MDD after 7.5% of added cement (Figure 2.5).

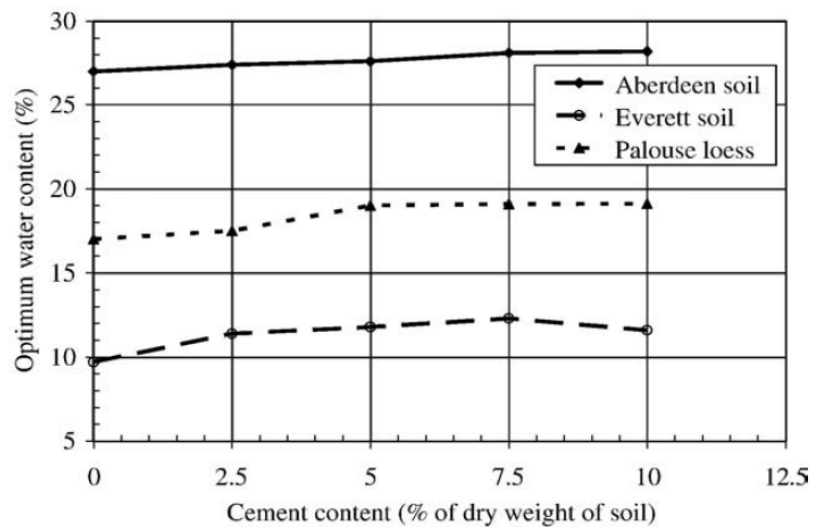


Figure 2.5 Effect of cement content on optimum moisture contents of three different types of soil.

Source: Sariosseiri and Muhunthan (2009), permission to reproduce this figure has been granted by Elsevier.

Other researchers observed an opposite behaviour of maximum dry density-optimum moisture content occurred with cement treatment. Results of many research projects of cement treated soil indicated that when cement dosage increases, MDD increases and OMC decreases (Axelsson *et al.*, 2002; Bhattacharja and Bhattya, 2003; Horpibulsuk *et al.*, 2010; Oyediran and Kalejaiye, 2011; Dhanoa, 2013; Shojaei Baghini *et al.*, 2014).

Shojaei Baghini *et al.* (2014); Baghini *et al.* (2015) attributed the increase in MDD of soil treated with cement to the reduction in void ratio which may occur after mixture compaction due to fine particles of cement occupying to the spaces among the particles of stabilised soil. Moreover, it was revealed that the unit weight of cement soil mixture increased proportionally with cement dosage as well as with the curing period which led to the increase in MDD (Pakbaz and Alipour, 2012). Figure 2.6 shows the effect of cement content on the dry density – moisture content relationship.

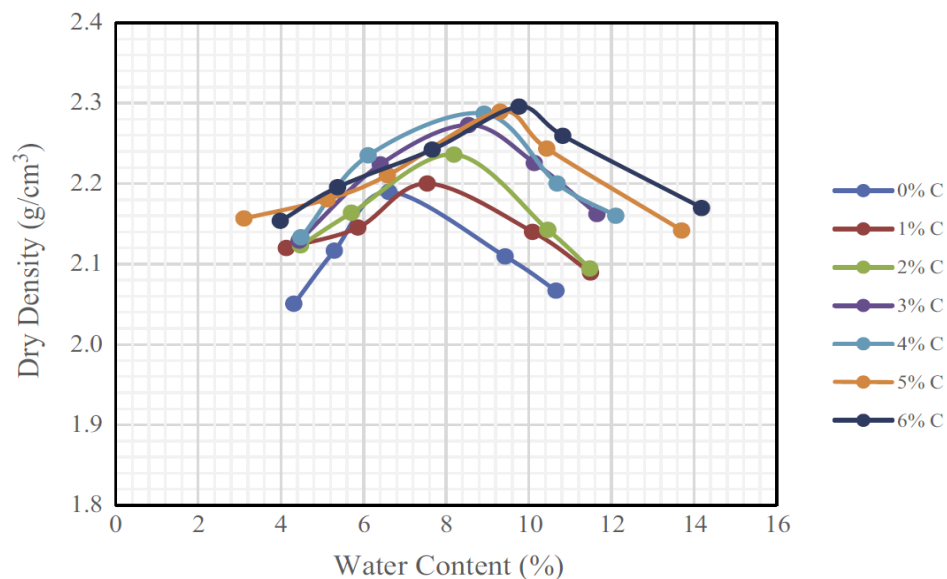


Figure 2.6 Compaction parameters behaviour with different percentages of cement treatment. Cement is denoted with letter (c).

Source: Baghini *et al.* (2015), permission to reproduce this figure has been granted by Elsevier.

Croft (1967) carried out experimental works to investigate the effect of cement treatment on the compaction parameters of several types of clay minerals. The results indicated that overall MDDs increased and OMCs decreased with the increase of cement content for all types of clay minerals except those for montmorillonite which indicated a reversible behaviour as shown in Figure 2.7.

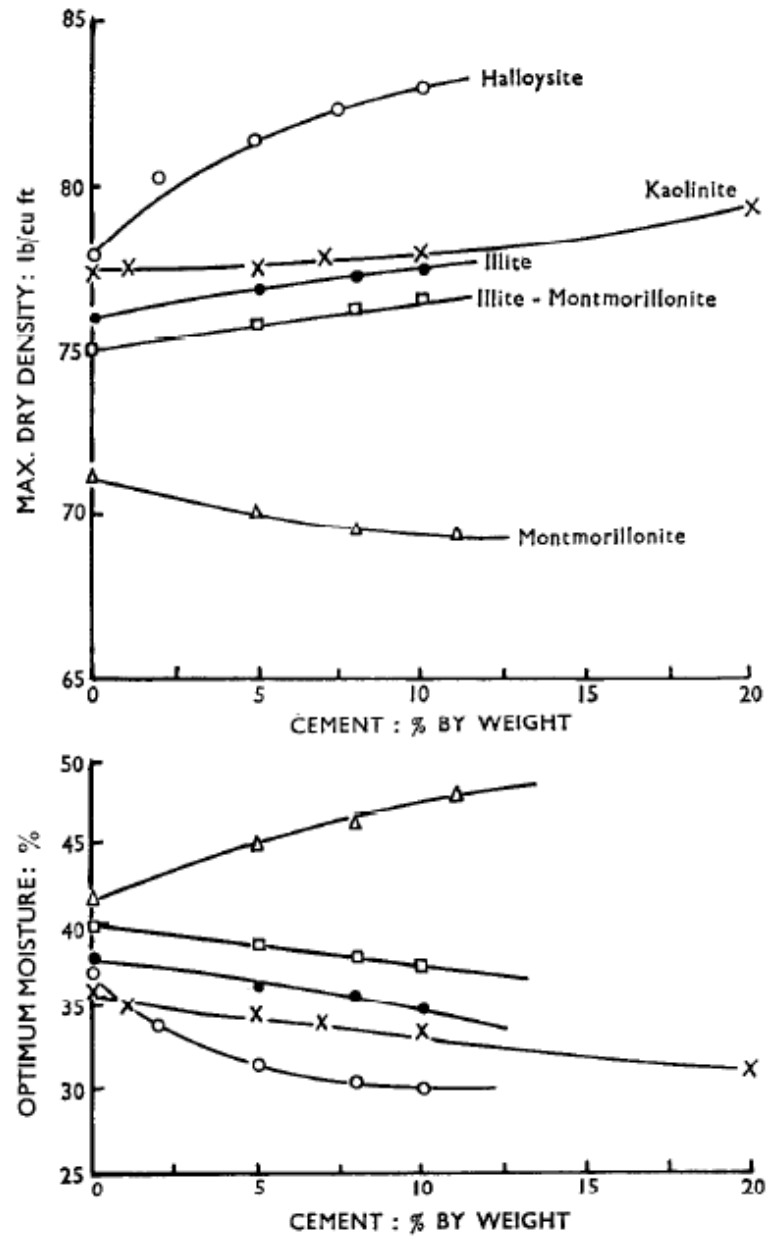


Figure 2.7 Maximum dry density and optimum moisture content relationship with cement content of different types of clay minerals.

Source: Croft (1967), permission to reproduce this figure has been granted by ICE Publication.

In conclusion, it could be stated that the behaviour of the relationship of dry density – moisture content of cement treated soil is dependent on soil type, type of clay minerals, the amount of cement added and the length of the curing period.

2.6.3.2 Atterberg Limits

It was found that liquid limit and plastic limit increased with cement treatment but the increment in plastic limit is greater than that for liquid limit which led to a decrease in the plasticity index. Moreover, the plasticity index of cement treated soil reduces with the increase of cement content and curing period as indicated in Basha *et al.* (2005); Sariosseiri and Muhunthan (2009); Saride *et al.* (2013); Bahmani *et al.* (2014); Goodarzi and Salimi (2015); Bahmani *et al.* (2016). Figure 2.8 (Bahmani *et al.*, 2014) shows the changes of Atterberg limits of a residual soil treated with different percentages of cement. The change in the consistency limits of cement treated soils is attributed to the physico-chemical reaction which occurs between the hydrated lime $\text{Ca}(\text{OH})_2$, resulting from cement hydration, and the clay minerals of stabilised soil (Muhunthan and Sariosseiri, 2008; Pourakbar *et al.*, 2015).

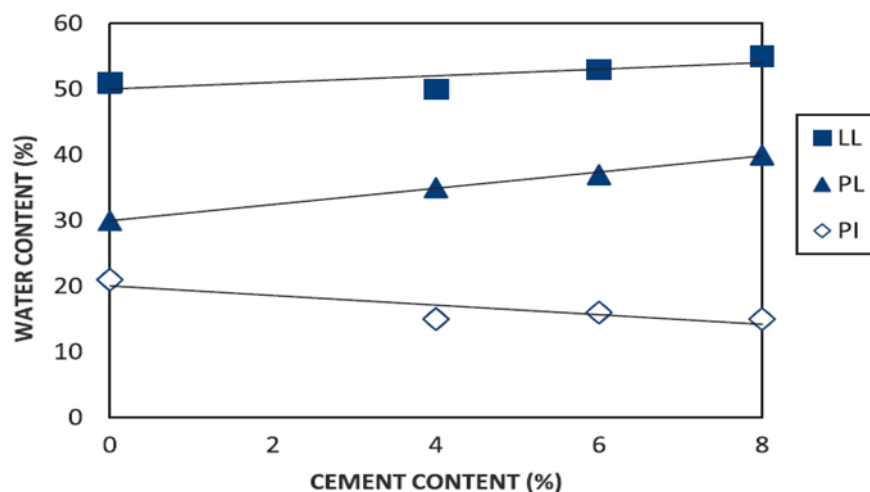


Figure 2.8 Atterberg limits-cement content relationship of cement stabilised soil.

Source: Bahmani *et al.* (2014), permission to reproduce this figure has been granted by Elsevier.

However, many researchers observed that the liquid limit decreases with cement treatment immediately after adding cement to the soil and they attributed this behaviour to the double layer depression resulting from the rising of calcium cations (Ca^{+2}) concentration near the surfaces of clay minerals (Kamruzzaman, 2002; Goodarzi and Salimi, 2015). Sariosseiri and Muhunthan (2009) stated that liquid limit of high plasticity Aberdeen soil increased and the plastic limit decreased with 2.5% of added cement which led to an increase in the plasticity index. However, they observed

that the plasticity index was decreased significantly with the increase of cement content higher than 2.5% up to 10% due to the gradual reduction in the liquid limit along with a noticeable increase in the plastic limit.

2.6.3.3 Soil Strength

The effect of cement treatment and curing time on the geotechnical properties of different types of soils has been intensively investigated by many researchers (Yilmaz and Ozaydin, 2013; Bahmani *et al.*, 2014; Eskisar, 2015; Baghini *et al.*, 2015; Wu *et al.*, 2016; Vakili *et al.*, 2016). It is observed that the unconfined compressive strength (UCS) of soil (fine and coarse grained soils) is increased with the increase of cement content as well as the curing period. Baghini *et al.* (2015) developed two different formulae to estimate the compressive strength of cement stabilised base course soil after curing for 7 and 28 days respectively dependent on the results of laboratory work. They found that there is a relationship between the cement dosage and unconfined compressive strength of stabilised soil with a specific curing period as shown in Figure 2.9.

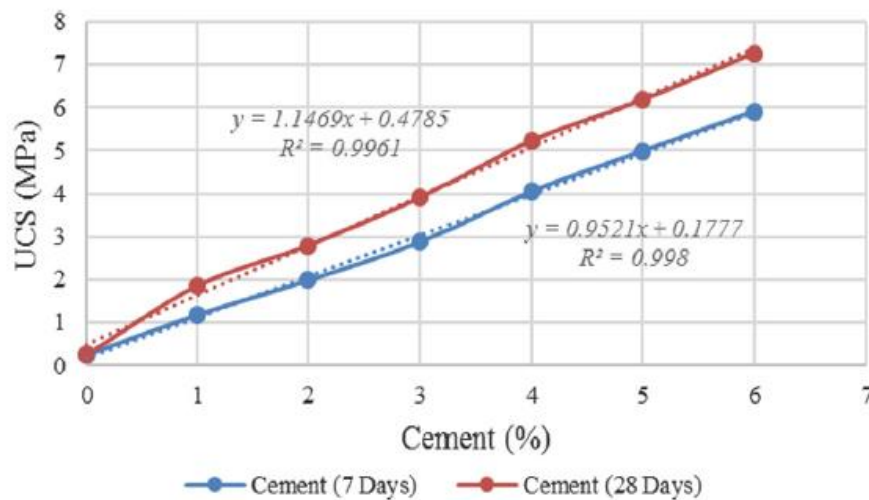


Figure 2.9 Effect of cement content and curing time on UCS. y is the estimated UCS value (MPa), and x is the cement content (%).

Source: Baghini *et al.* (2015), permission to reproduce this figure has been granted by Elsevier.

However, several factors influence the performance of cement in improving the compressive strength of stabilised soils. These factors, but not all, are cement and soil type, grain size distribution of the stabilised soil, curing condition of the cement-soil mixture, compaction effort, water cement ratio, natural moisture content of the treated

soil etc. (Sariosseiri and Muhunthan, 2009; Horpibulsuk *et al.*, 2010; Pakbaz and Alipour, 2012; Kang *et al.*, 2016).

Figure 2.10a shows the UCS values for specimens of Aberdeen soil (high plasticity fine-grained soil) treated with different percentages of cement and provided for two different procedures of curing (soaked and un-soaked). It was observed that the un-soaked specimens possessed higher UCS with cement content not more than 5%, while the soaked specimens treated with more than 5% of cement indicated higher UCS than that for un-soaked specimens. However, the un-soaked specimens had modulus of elasticity values much higher than those for soaked specimens for all cement percentages except when the cement content became 10% as shown in Figure 2.10b (Sariosseiri and Muhunthan, 2009).

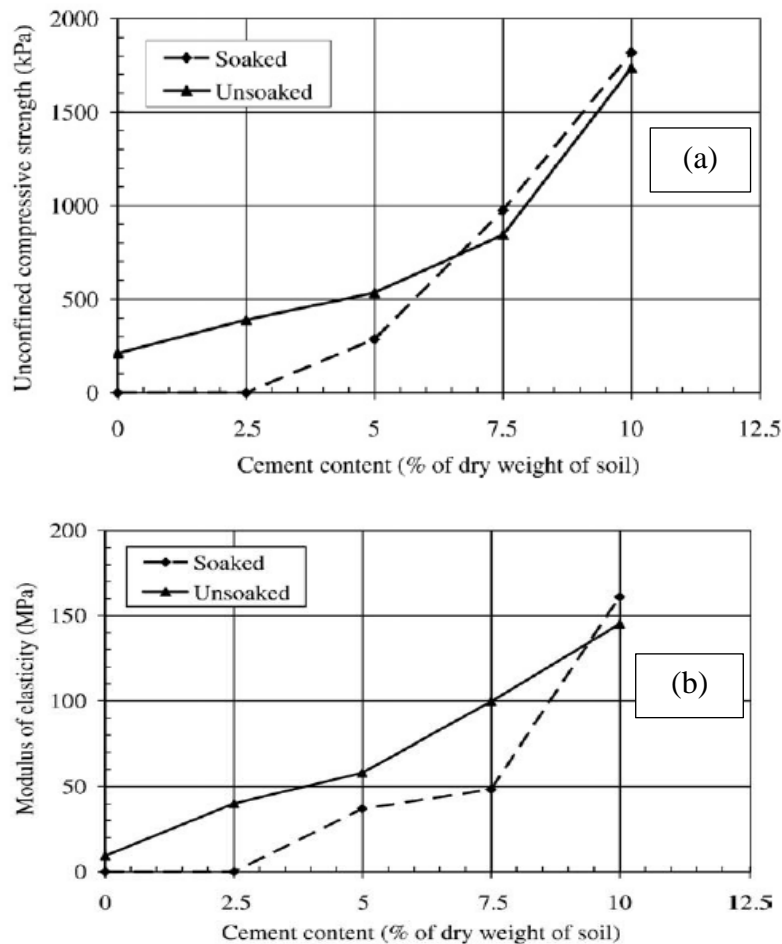


Figure 2.10 Effect of cement treatment of (a) UCS and (b) Modulus of Elasticity of Aberdeen soft soil.

Source: Sariosseiri and Muhunthan (2009), permission to reproduce this figure has been granted by Elsevier.

In terms of the development of the microstructure of soil treated with cement using different moulding water content, Horpibulsuk et al. (2010) stated that the use of 1.2% of optimum water content indicated better results in microstructure development of cement treated soil as well as increased UCS and stiffness as shown in Figure 2.11.

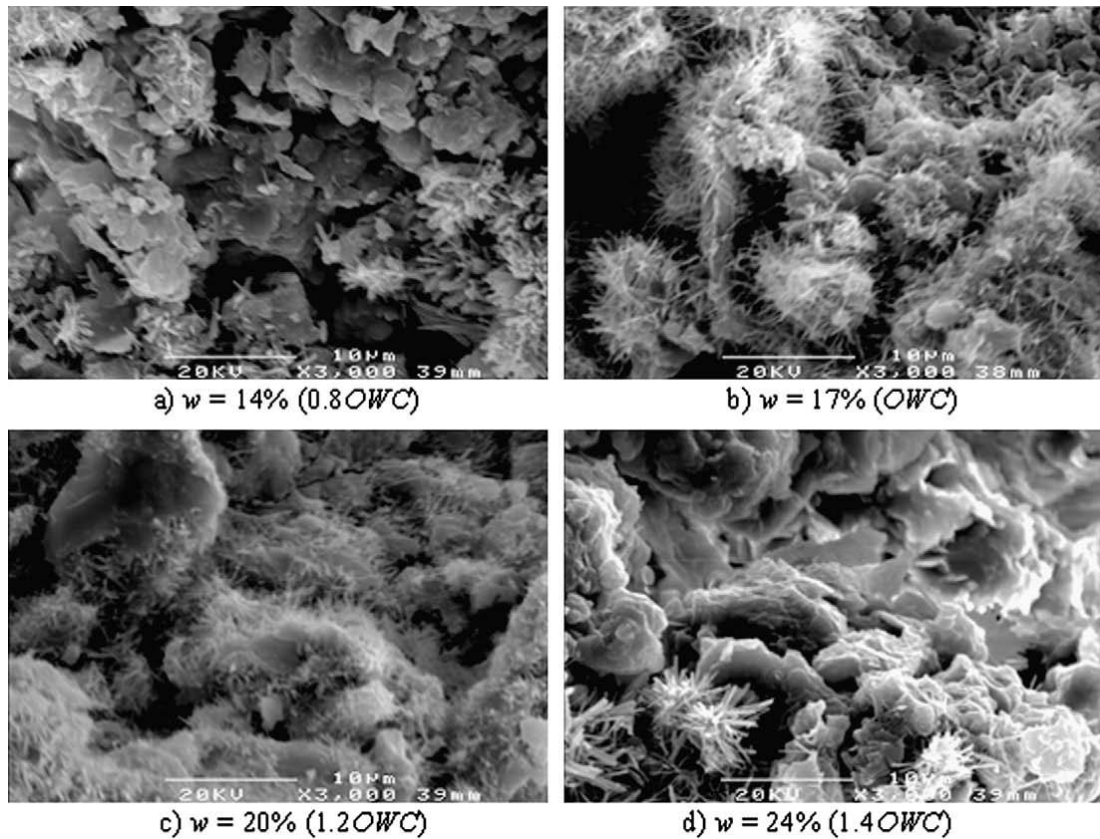


Figure 2.11 SEM images of 10% cement treated samples subjected to modified Proctor energy of compaction using different water content at age of 7 days.

Source: Horpibulsuk *et al.* (2010), permission to reproduce this figure has been granted by Elsevier.

2.6.3.4 Compressibility and Volume Change

One of the objectives of cement stabilisation is to control the volume change (swelling and shrinkage) of potentially expansive soils in addition to decreasing their compressibility (Nicholson, 2015). A study was conducted by Ouhadi *et al.* (2014) to investigate the effect of cement and lime stabilisation on the pozzolanic consolidation and pre-consolidation pressure of soft soils. They demonstrated that the change in void ratio due to increasing the applied load on the stabilised soil was decreased significantly with the increase of cement content and curing time. Moreover, they stated that the compression index (C_c) was decreased while the pre-consolidation

pressure was increased with the increase in cement content. Ouhadi *et al.* (2014) observed that there were significant variations in C_c and pre-consolidation pressure (P_c) when cement content increases up to 6%; after this percentage, slight changes were observed as shown in Figure 2.12.

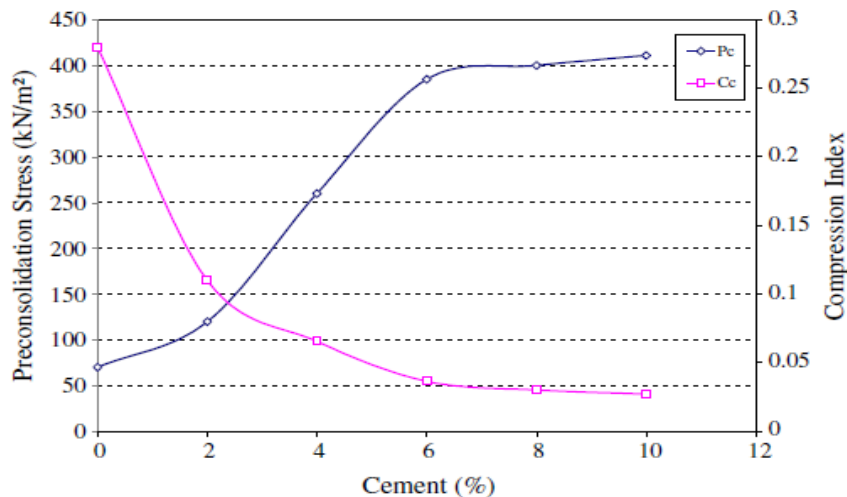


Figure 2.12 Variation of compression index and pre-consolidation pressure of soft soil treated with different cement contents (7 days cured samples).

Source: Ouhadi *et al.* (2014), permission to reproduce this figure has been granted by Elsevier.

With respect to the controlling of the swell potential and volume change of cement treated soft soils, researchers stated that cement treatment led to substantial reduction in swelling index (C_s), swelling pressure and linear shrinkage strain of potential expansive soils (Al-Rawas *et al.*, 2005; Yong and Ouhadi, 2007; Sariosseiri and Muhunthan, 2009; Saride *et al.*, 2013).

2.6.3.5 Durability

Durability is one of the most important criteria to assess the performance of cement-soil mixture as a construction material. It can be defined as the ability of soil to maintain acceptable long-term residual strength as well as to retain its stability and integrity to provide adequate resistance against severe climate conditions. Most results of the research undertaken indicated an acceptable development in soil durability with cement treatment; it is proven that the resistance of stabilised soil against freeze-thaw and wet-dry cycling increases with increasing unconfined compressive strength (Muhunthan and Sariosseiri, 2008; Buttress, 2013; Aldaood *et al.*, 2014; Sargent, 2015; Aldaood *et al.*, 2016).

According to Zhang and Tao (2008); and Tripura and Singh (2015), the durability of cement-stabilised soils can be evaluated by measuring the strength reduction and/or mass losses which occur in specimens of stabilised soils after being subjected to cycles of either wetting-drying or freezing-thawing. Moreover, ASTM (1996) specifies that a minimum of 700kPa of unconfined compressive strength of the cement-stabilised soil is required along with wet-dry or freeze-thaw durability. An experimental study of wetting-drying cycles was conducted by Zhang and Tao (2008) to evaluate the durability of cement-stabilised low plasticity soil using different amounts of cement (2.5, 4.5, 6.5, 8.5, 10.5, and 12.5% of the dry mass of treated soil) with different moisture contents (15.5, 18.5, 21.5, and 24.5%). The results indicated that the water content of cement stabilised soil had a predominant influence on the durability while the relationship between the soil-cement loss percentage and water cement ratio revealed that the higher the water cement ratio, the higher the soil-cement loss percentage as shown in Figure 2.13. Similar findings were presented by Eskişar *et al.* (2015) when they conducted their study to assess freeze-thaw performance of cement-stabilised clay at different moisture contents.

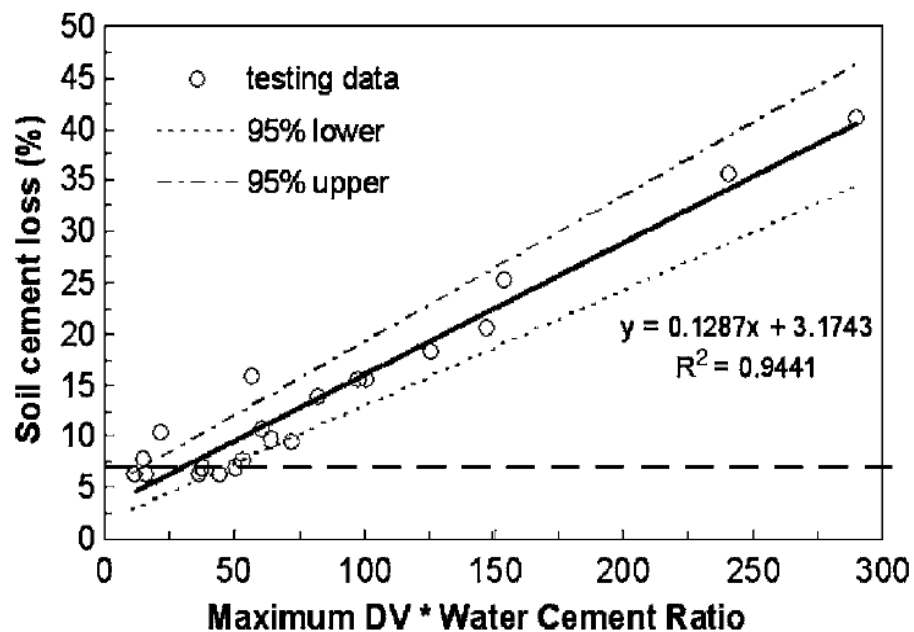


Figure 2.13 Relationship between soil-cement loss percentage and water cement ratio (DV is for dielectric value).

Source: Zhang and Tao (2008), permission to reproduce this figure has been granted by ASCE.

Baghini *et al.* (2015) evaluated the engineering performance of cement-stabilised soil under the effect of wetting and drying cycles. The changes in moisture content, weight and volume of samples of stabilised soil subjected to 12 cycles of wetting and drying were recorded. Significant changes were observed particularly after the second and third cycle. Beyond the third cycle, no noticeable changes were observed as shown in Figure 2.14. These results agree with those of most studies conducted on the durability of stabilised soils in which researchers determined that second or third cycles normally indicate the most significant changes in volume, weight and strength losses (Shibi and Kamei, 2014; Shojaei Baghini *et al.*, 2014; Neramitkornburi *et al.*, 2015; Guney *et al.*, 2007; Yazdandoust and Yasrobi, 2010; Aldaood *et al.*, 2016).

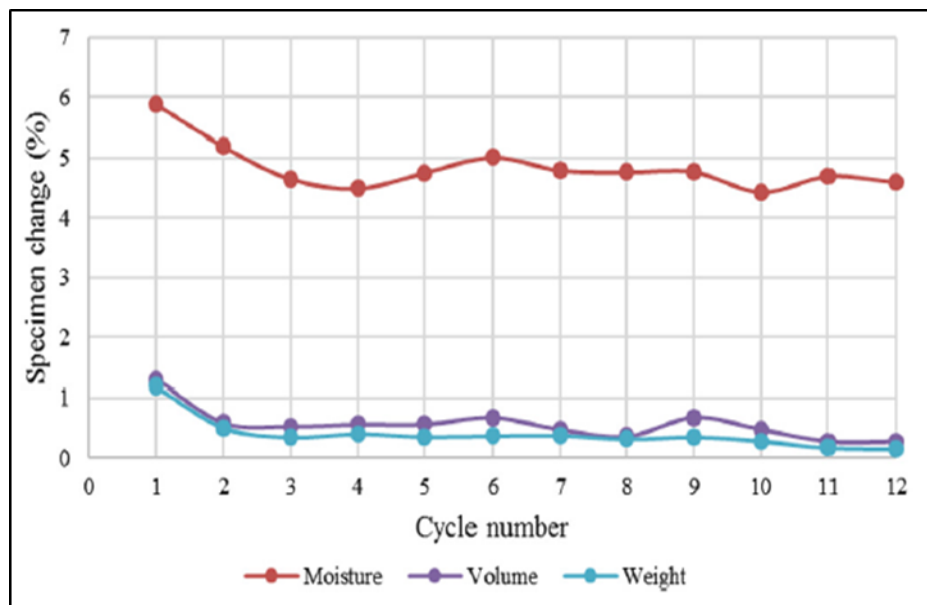


Figure 2.14 Changes in moisture, volume and weight of cement stabilised specimens subjected to different numbers of wet-dry cycles.
Source: Baghini *et al.* (2015), permission to reproduce this figure has been granted by Elsevier.

2.6.4 Drawbacks of Using Cement in Soil Stabilisation

OPC is the second globally consumed material after water and has significant advantages as a construction material in different civil engineering industries and specifically in soil stabilisation. The use of cement has many drawbacks which have become a major concern around the world and raised debates globally about how to reduce cement production. The most critical impacts of cement production can be presented as follows:

2.6.4.1 Environmental Impact

Global warming is linked to the phenomenon of greenhouse gases (GHGs) emissions and one of the gases that contributes most to GHGs is carbon dioxide (CO₂) (Huntzinger and Eatmon, 2009; Hermawan *et al.*, 2015; Anderson *et al.*, 2016; Specht *et al.*, 2016). Cement production has a negative environmental impact due to significant carbon dioxide (CO₂) emissions produced by its manufacturing processes. It was reported that the production of 1 tonne of cement produces between 0.8 and 1 tonne of CO₂ emissions (O'Rourke *et al.*, 2009; García-Gusano *et al.*, 2015; Cao *et al.*, 2016; Mikulčić *et al.*, 2016).

Due to the rapid development in the construction industry around the world, the global production of cement has been continuously increasing. A growth of about 6.95 % annually has been recorded with a highest increase of 9.0 % in 2010, and 2011 with a slowdown to 3.0 % in 2012 to reach 3.7 billion tonnes (MR&CL, 2013). Figure 2.15a and b show the global cement production in 2013 of 4 billion tonnes, and 2015 of 4.6 billion tonnes respectively (CEM-Bureau, 2015). From both figures, it can be observed that China demonstrates the majority of cement production around the world. Overall, the global cement market is predicted to increase at 5% per year. Figure 2.16 shows the quantities of cement consumption globally in the past and current periods along with the future estimation of cement consumption (van Ruijven *et al.*, 2016).

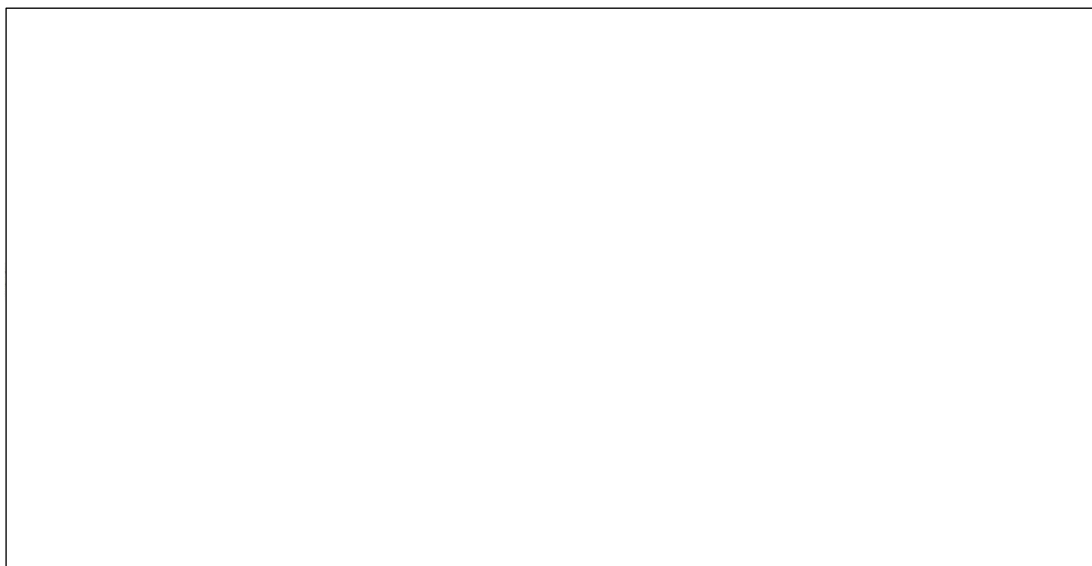


Figure 2.15 Global cement production structure. (a) 2013 and (b) 2015.

Source: CEM-Bureau (2015). **The diagram originally presented here cannot be made freely available via LJMU Digital Collections because of 'copyright'**

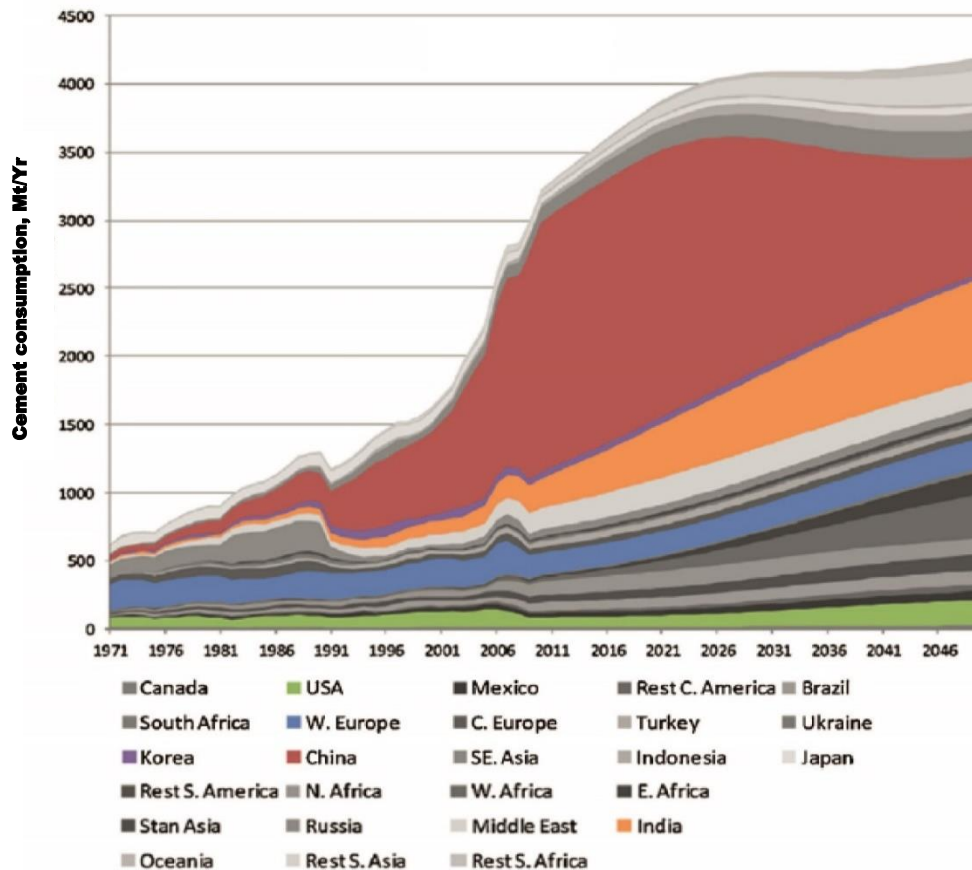


Figure 2.16 Worldwide cement consumption.

Source: van Ruijven *et al.* (2016), permission to reproduce this figure has been granted by Elsevier.

Cement manufacturing contributes to around 6.0% of global CO₂ emissions which represents a critical value as a harmful element for global warming. This issue has motivated the international organisations, politicians, and even the public to think seriously to evaluate and reduce or mitigate cement production (Mikulčić *et al.*, 2016; Song and Chen, 2016; Zhang *et al.*, 2017a).

Another environmental impact of cement production, which plays a principle role in concern for the sustainability of the cement industry, is the consumption of natural resources due to the large quantities of raw materials as well as fuel for power generation that is required in cement manufacturing. The principle component of cement is so called cement clinker. Clinker is produced from raw materials, which are typically limestone and clay or shales of other materials, after being subjected to blending and grinding processes (British Geological survey, 2005; CEMBUREAU, 2009; García-Gusano *et al.*, 2015; Zhang *et al.*, 2017a). According to the British

Geological survey (2005), the production of one tonne of cement requires about 1.5 to 1.8 tonnes of limestone in addition to about 0.4 tonne of clay.

2.6.4.2 Consumption of Energy

One of the important priorities of humans nowadays is to optimise energy consumption due to the shortage of energy resources as well as the environmental considerations (Heravi *et al.*, 2016). Cement production is one of the most energy intensive industries due to the requirement of high temperatures (between 1400°C – 1500°C) for incineration processes to produce the cement clinker (the key component of cement) (O'Rourke *et al.*, 2009; Habert, 2013; Liu *et al.*, 2015; Mikulčić *et al.*, 2016; Horsley *et al.*, 2016). The energy consumed in cement manufacturing accounts for 50% - 60% of its production cost (Liu *et al.*, 2015).

Cement production is the second industry in energy consumption worldwide after the steel industry; it is estimated at around 12% to 15% of the global industrial energy consumption (van Ruijven *et al.*, 2016). It is noted that the production of one tonne of cement clinker requires between 3.0 and 6.5GJ of energy; this energy is required for incineration processes and so called thermal energy (Rahman *et al.*, 2015; Horsley *et al.*, 2016). Another type of required energy in cement manufacturing is the electrical energy which is needed for the grinding stage; this energy is estimated in modern cement plants to be equal to about 110 – 120kWh per tonne of cement (Rahman *et al.*, 2015; Diego *et al.*, 2016).

2.6.4.3 Cement Carbonation and Sulphate Attack

Carbonation reaction occurs when hydrated lime (Ca(OH)₂) reacts with atmospheric carbon dioxide CO₂ as well as CO₂ from rainwater to produce calcium carbonate (CaCO₃) instead of C-S-H and C-A-H compounds (as shown in equation 2.12). CaCO₃ has a detrimental effect when existing in stabilised soil when adjacent to reinforced concrete due to carbonation-induced corrosion (O'Flaherty, 2002; Aitcin, 2016a).



According to Provis *et al.* (2015), cement carbonation causes a reduction in the alkalinity of reinforced concrete which in turns induces a loss in strength and durability. Moreover, the mechanism of carbonation in Portland cement was explained

as the dissolving of atmospheric CO₂ in the pore solution which reacting rapidly with the Portlandite to produce CaCO₃ and water, then with C-S-H and C-A-H gel to form CaCO₃ again and silica alumina gel as shown in the equation 2.13 below (Morandea *et al.*, 2014; Gourley and Greening, 1999):



To avoid the carbonation reaction, it is strongly recommended to evaluate the optimum amount of lime or cement that is added to treated soils to prevent free lime from the reaction with atmospheric CO₂ (Little and Nair, 2009). However, Vakili *et al.* (2016) indicated that the carbonation has a significant role to increase the strength of stabilised soil as well as the bonding rate of soil particles. In contrast, O'Flaherty (2002) mentioned that soil-lime based materials develop lower strength when carbonation occurs because some of the free lime that would normally react with pozzolanic materials during the pozzolanic reaction will be unavailable after being consumed by carbon dioxide.

Another deleterious chemical reaction, that may occur in cement treated soils is sulphate attack which takes place when sulphate salts exist in stabilised soil. Sulphate attack is a well-organised phenomenon which occurs due to the reaction of calcium and alumina produced by C₃A from cement minerals with sulphate compounds, either from cement gypsum or from the stabilised soil and groundwater, to form calcium-sulfoaluminate compound which is so called ettringite (3CaO. Al₂O₃. 3CaSO₄. 32H₂O). The formation of ettringite causes an expansion and degeneration which leads to strength loss and failure (Tasong *et al.*, 1999; Al-Amoudi, 2002; Rozière *et al.*, 2009; Yu *et al.*, 2015).

The mechanism of sulphate attack was explained by Chaibeddra and Kharchi (2014) and Baščarevc (2015) as follows: when the hydrated Portland cement gets in contact with soluble salts such as sulphates, there is diffusion of sulphate ions occurs in the pores and they crystallise inside. Latter, the crystals grow leading to development in internal stresses which cause disintegration. According to Rollings (1999), ettringite forms in two stages during cement hydration: (1) Primary ettringite which is generally formed by the chemical reaction between the alumina and the solution of sulphate ion; and (2) secondary ettringite which is formed from the dissolution of primary ettringite

and redistribution from solution in cracks and voids. Moreover, only the ettringite formed by the chemical reaction is expansive and once generated it is no longer expansive. Therefore, secondary ettringite is not expansive since it is formed due to precipitation from solution only.

2.6.4.4 Effect of Organic Matter

The existence of organic matter in soil has detrimental effects; it may be responsible for increasing the soil plasticity, compressibility and shrinkage and decreasing the hydraulic conductivity and soil strength. The organic matter of soils is complex in both chemical and physical considerations. There are five groups of organic matter which may occur in soils; hydrocarbons, proteins, fats, resins, and waxes (Mitchell and Soga, 2005). However, (Tremblay *et al.*, 2002) divided the organic matters into two different categories: nonhumic, which consists of vegetal, animal, or micro-organism remains, and humic organic matter which results from the weathering and transforming processes of the nonhumic portions of organic matters.

There are three main types of humus combination which are loosely, stably and slightly combined humus. The most detrimental type is the loosely combined humus due to its high susceptibility to combine with other substances and its reaction with hydration products such as portlandite produced from cement hydration; this reaction tends to a decrease in the pH value and retards the hydration and pozzolanic processes (Chen and Wang, 2006; Makusa, 2012).

Sargent (2015) determined that the organic matter has negative surface charges and they attract the positive cations such as the calcium cations produced from the hydrated cement or lime in stabilised soils. Consequently, the formation of cementitious products such as C-S-H and C-A-H is reduced leading to strength losses.

Saride *et al.* (2013) carried out experimental works to investigate the influence of lime and cement stabilisation on the expansion and strength properties of different types of organic clayey soils. The treated soil specimens were cured for different periods of 7, 28, and 56 days. With respect to the cement-treated soil, they observed a reduction in soil strength for most of the specimens subjected to 56 days of curing as shown in Figure 2.17. Moreover, the magnitude of strength loss in soil with high organic content was higher than that for soil with low organic content. This reduction in soil strength

with cement treatment may be attributed to the existence of either black humic acid, which reacts with hydrated calcium produced from cement hydration resulting in the formation of insoluble calcium humic acid, or fulvic acid which tends to combine with minerals containing aluminium leading to the decomposition of the layers of crystal lattice. The absorbed layer generated by the chemical reaction between the fulvic acid and the cement minerals impedes the hydration process of cement (Chen and Wang, 2006; Saride *et al.*, 2013; Ma *et al.*, 2016).

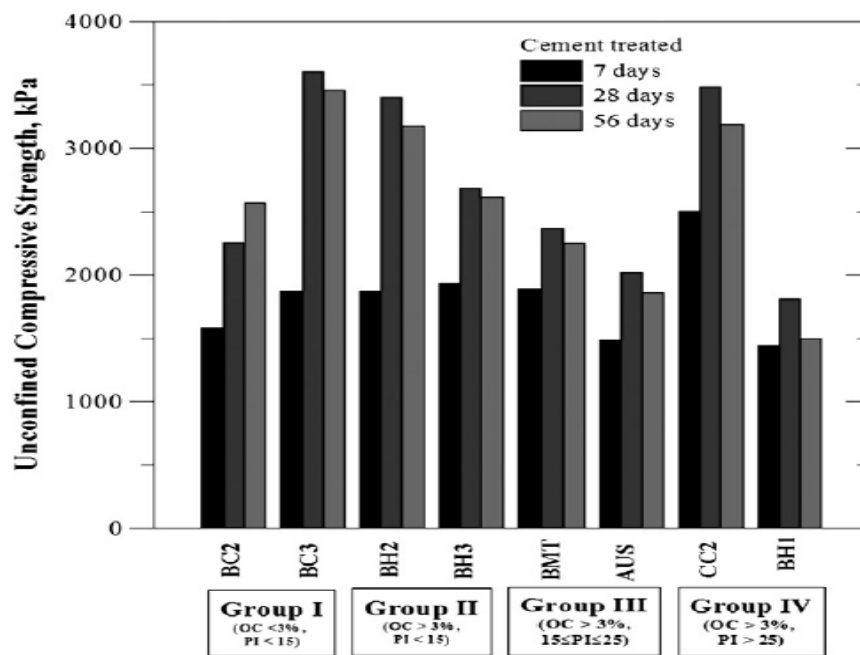


Figure 2.17 UCS of cement treated soil at different periods of curing.
Source: Saride *et al.* (2013), permission to reproduce this figure has been granted by Elsevier.

2.7 ASHES OF WASTE MATERIALS AS A CEMENT REPLACEMENT

2.7.1 General

According to material presented in section 2.6, it is clear that the activities of the construction sector have a huge impact on the environment. Moreover, resources from the natural environment represent the unique provider of the built environment with required substances for construction materials. For instance, the construction industry consumes more than 90% of non-energy materials extracted in the UK, while approximately 50% of CO₂ emissions in the UK are released from the fossil fuel burning to generate the required energy for building construction and operation.

Additionally, it was highlighted that around 6 tonnes of materials are consumed by the construction industry for each person living in Britain annually (Stubbs, 2008; HIE, 2015).

From the aforementioned, the sustainable construction industry is obvious to represent one of the valuable solutions for environmental and economic problems and in turn for the global warming problem. Therefore, looking for alternative materials, such as waste and/or by-products materials, to be used as cement replacement in the construction industry might be an essential attempt as a sustainable solution towards reducing cement production and greenhouse gasses emissions, and achieving an eco-friendly industry.

2.7.2 Potential of Waste and By-Product Materials for Cement Replacement

Recently, the use of waste or by-product materials, as pozzolanic and supplementary cementitious materials (SCMs), have been increasing, especially in blended cement manufacturing and in the development of new cementitious materials (Aïtcin, 2016b). The pozzolanic materials and SCMs are known as rich alumina and/or silica materials. These materials react with the hydrated lime to produce a stronger structure for mortars and concrete by increasing the production of C-S-H and C-A-H compounds (Pontikes and Snellings, 2014; Puppala *et al.*, 2015; Pustovgar *et al.*, 2016; Black, 2016).

The suitability of pozzolanic materials for cement substitution could be evaluated through their ability to provide engineering performance that is either comparable or exceeds those for conventional types of OPC (Malhotra and Mehta, 2012; Sargent, 2015). Aïtcin (2016b) emphasised that it is very interesting to report the chemical characterisations of these materials and compare their compositions to those for OPC using a ternary $\text{SiO}_2 - \text{CaO} - \text{Al}_2\text{O}_3$ to assess their suitability as SCMs, as shown in Figure 2.18.

Waste and by-product materials have been used in diverse types of construction projects, such as concrete for building construction, rigid pavement, and soft soil stabilisation. They either have a high content of amorphous silica which is suitable for pozzolanic reactivity, such as palm oil fly ash (POFA), rice husk ash (RHA), pulverised fuel ash (PFA), silica fume (SF), etc. (Abd El-Aziz *et al.*, 2006; Kumar *et*

al., 2007; Jaturapitakkul *et al.*, 2011; Kanadasan *et al.*, 2015), or have a good amount of calcium oxide (CaO) to perform as cement when mixed with water, such as ground blast furnace slag, sewage sludge ash, Cement Kiln Dust, and Calcium Carbide residue (Fava *et al.*, 2011; Horpibulsuk *et al.*, 2012; Hashad and El-Mashad, 2014; Dave *et al.*, 2016). These materials can react to boost and increase the building of the Calcium Silicate Hydrate compound (C-S-H), which has the ability to strengthen the structure of the stabilised soil.

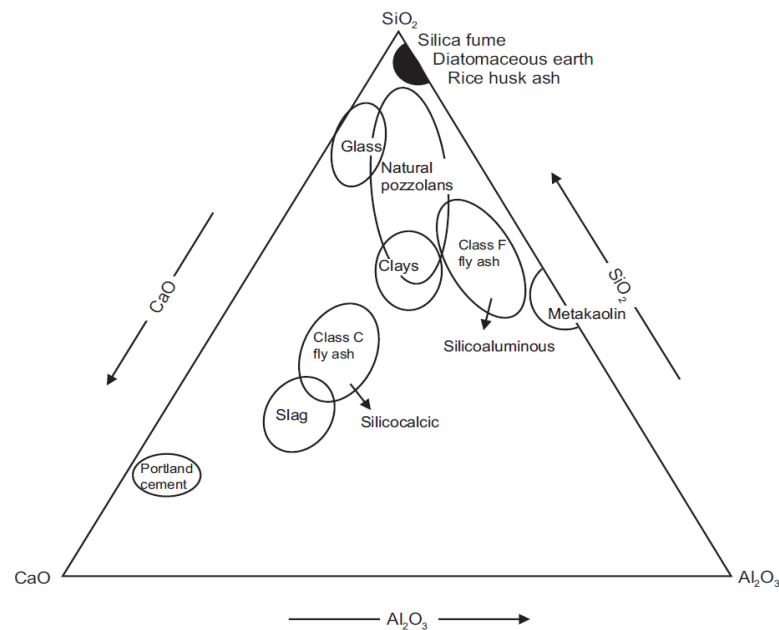


Figure 2.18 The chemical composition of principal cementitious materials.

Source: Aïtcin (2016b), permission to reproduce this figure has been granted by Elsevier.

The aforementioned encouraged researchers to carry out extensive experimental works attempting to produce new sustainable cementitious materials since the mid-1990s (Antiohos *et al.*, 2007). Consequently, many researchers have adopted different mix design procedures to produce their cementitious materials such as binary, ternary and even quaternary blending systems. Moreover, researchers used different techniques of activation such as chemical activation using alkaline additives and mechanical activation using grinding techniques (Blanco *et al.*, 2006; Antiohos *et al.*, 2007; O'Rourke *et al.*, 2009; Sadique *et al.*, 2012b; Sadique *et al.*, 2013; Dave *et al.*, 2016; Soriano *et al.*, 2016).

A group of waste and by-product materials were involved in this research project and then later, three types of these materials were included in the experimental works for additional investigation. The first material that was considered as the calcium-based material was the waste paper sludge ash (WPSA) and the other materials were considered as alkaline and pozzolanic activators. Furthermore, another waste material was employed as a grinder agent in the mechanical activation stage; the latter was flue gas desulfurization gypsum (FGD). Therefore, the literature review in this chapter focuses on this group only.

2.7.3 WASTE PAPER SLUDGE ASH (WPSA)

2.7.3.1 WPSA Production

Waste paper sludge ash (WPSA) is a waste material resulting from the incineration process of waste paper sludge (WPS) in re-pulping factories for energy generation. It has a high content of calcium oxide (CaO) and can be used as lime or cement supplementary material in the concrete industry and soil or sludge stabilisation (ANML, 2015). However, the chemical composition of WPSA varies dependent on the processes and operation at the particular paper mill plant. Mostly, the WPS is burned in combination with other types of waste materials such as waste wood, rejects and other sludge (Marsland and Whiteley, 2015). WPSA is produced in large quantities annually in the industrialised countries. In Trondheim, the source factory produces 800,000 tons annually, which is much more than produced for the entire areas of Norway and Europe. The UK is reported to produce approximately 1 million tonnes of paper sludge each year with main producers represented by UPM - Shotton paper mill - Deeside – North East Wales, and Aylesford Newsprint, Kent (Dunster, 2007).

According to Arena *et al.* (2016), the incineration process of each tonne of pulp sludge produced an average of 5 to 45kg of WPSA, whereas an average of 50kg of residue materials are generated for each tonne of paper produced. Additionally, the global production of paper and paperboard is estimated to be equal to 400 million tonnes annually; however this production is predicted to rise to 550 million tonnes by 2050 (Faubert *et al.*, 2016). The predominant European countries that produce WPSA in large quantities are Germany (1.1 million tonnes) followed by Sweden (about 540,000 tonnes) and Finland (about 530,000 tonnes) (Arena *et al.*, 2016).

With respect to the WPSA production in the UK, The National Archive (2012), reported that 125,000 tonnes of WPSA are generated in the UK annually; this quantity represents serious economic and environmental problems due to the requirement of land for disposing. Figure 2.19 shows the European trend of disposal routes of the residue of waste paper sludge as presented by Monte *et al.* (2009).

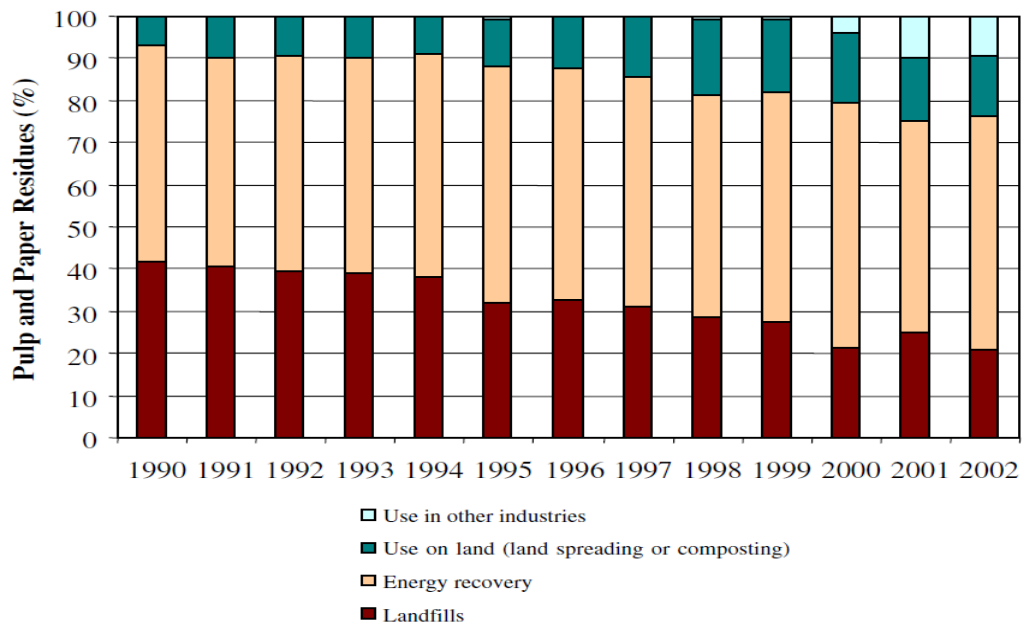


Figure 2.19 Pulp and paper residues disposal trends in Europe.

Source: Monte *et al.* (2009), permission to reproduce this figure has been granted by Elsevier.

2.7.3.2 Characterisation of WPSA

The chemical composition of WPSA varies according to the condition of its generation such as the source materials feeding at the incineration plant, the temperature and degree of combustion along with pollution control measures at the incineration plant (Areprasert *et al.*, 2014). Table 2.6 illustrates a summary of WPSA compositions according to the investigations of different researchers from different countries. At the same time, the change in compositions of WPSA due to the differences in burning temperatures of paper sludge, for two different periods for each temperature, are listed in Table 2.7 (Frías *et al.*, 2008). From these tables, it can be stated that the composition of WPSA differs according to the source of origin and the calcination degree of paper sludge, as the CaO content is increased with the increase of calcination degree as well as the period of combustion.

Table 2.6 Chemical composition of WPSA according to different researchers.

Reference	CaO	SiO ₂	Al ₂ O ₃	Fe ₂ O ₃	K ₂ O	Na ₂ O	SO ₃	Comments	Source
(Segui <i>et al.</i> , 2012)	45.5	28	13.2	1.3	0.7	0.4	1.3	Paper sludge is co-combusted with wood waste at 850°C	France
(Khalid <i>et al.</i> , 2013)	62.4	23.2	5.26	0.77	0.35	0.42	0.58	Paper sludge is combusted at 410 to 515°C	Malaysia
(Vegas <i>et al.</i> , 2014)	47.1	13.9	8.3	0.5	0.3	0.2	0	Thermal activated in lab at 700°C	Spain
	36.5	21.6	14.4	0.5	0.4	0.1	0.3	Thermal activated at industrial scale at 740°C	Exported from a Dutch Company
(Spathi <i>et al.</i> , 2015; Wong <i>et al.</i> , 2015)	61.2	21.2	12.6	0.9	0.4	ND	0.2	Combusted at 850 to 1200°C	UK

Table 2.7 The effect of calcination degree and period on the chemical composition of WPSA

Composition (%)	Raw sludge	600 °C/ 2 h	600 °C/ 5 h	650 °C/ 2 h	650 °C/ 5 h	700 °C/ 2 h
SiO ₂	10.69	20.24	20.65	21.06	21.44	22.32
Al ₂ O ₃	6.74	13.11	13.38	13.58	13.87	14.55
Fe ₂ O ₃	0.41	0.52	0.52	0.54	0.54	0.56
CaO	24.15	36.39	37.20	37.81	38.55	40.21
MgO	0.96	2.15	2.20	2.24	2.30	2.35
SO ₃	0.30	0.28	0.28	0.29	0.29	0.32
K ₂ O	0.22	0.34	0.34	0.35	0.35	0.37
Na ₂ O	0.24	0.08	0.08	0.09	0.09	0.09
TiO ₂	0.21	0.24	0.25	0.25	0.25	0.26
P ₂ O ₅	0.16	0.17	0.17	0.17	0.18	0.18
L.O.I.	55.71	26.24	24.68	23.36	21.93	18.52

Source: Frías *et al.* (2008), permission to reproduce this figure has been granted by Elsevier.

2.7.3.3 Application of WPSA in Construction Field

WPSA has been used as a SCM for different construction fields such as concrete works, mortar, and soil stabilisation; indicating an interesting performance as indicated in Corinaldesi *et al.* (2010); Gluth *et al.* (2014); Fava *et al.* (2011); Martinez-Lage *et al.* (2016). However, it was concluded that due to the high fineness as well as high water absorption of WPSA, the water added to the mixture should be increased with the increase of replacement percentage of WPSA; therefore, not more than 10% as a replacement percentage of WPSA was recommended (Fava *et al.*, 2011; Martinez-Lage *et al.*, 2016).

In the field of soil stabilisation, there are many researchers who have used WPSA as an additive to the weak soil in order to improve the physical and geotechnical properties. WPSA has been used either as a pozzolanic material or as an alternative binder to reduce the cement usage, dependent on its CaO content (Rahmat and Kinuthia, 2011; Khalid *et al.*, 2013; Vieira *et al.*, 2016). However, a small number of researchers carried out their experimental works on soil treated with WPSA and the impact of using WPSA in soft soil stabilisation still requires more investigation.

Lisbona *et al.* (2012) investigated the effect of two different binder mixtures of WPSA:cement; 25:75 and 50:50, on the geotechnical properties of different types of soft soils using 3 and 6% by the weight as binder contents. The study was carried out in the laboratory and on-site involving in-situ stabilisation of a 250m of subgrade using a dry mixing method. The results indicated that the optimal geotechnical behaviour was achieved from the soils stabilised with WPSA:cement ratio of 25:75. Substantial developments were achieved in the unconfined compressive strength of the stabilised soils specifically after 90 days of curing as shown in Figure 2.20.

Khalid *et al.* (2013) investigated the potential of WPSA to be used for fibrous peat soil stabilisation by conducting the unconfined compressive strength tests for peat soil specimens treated with different WPSA contents and subjected to various periods of curing. The results of UCS tests indicated that 7% was the optimum WPSA content to obtain the higher value of soil strength.

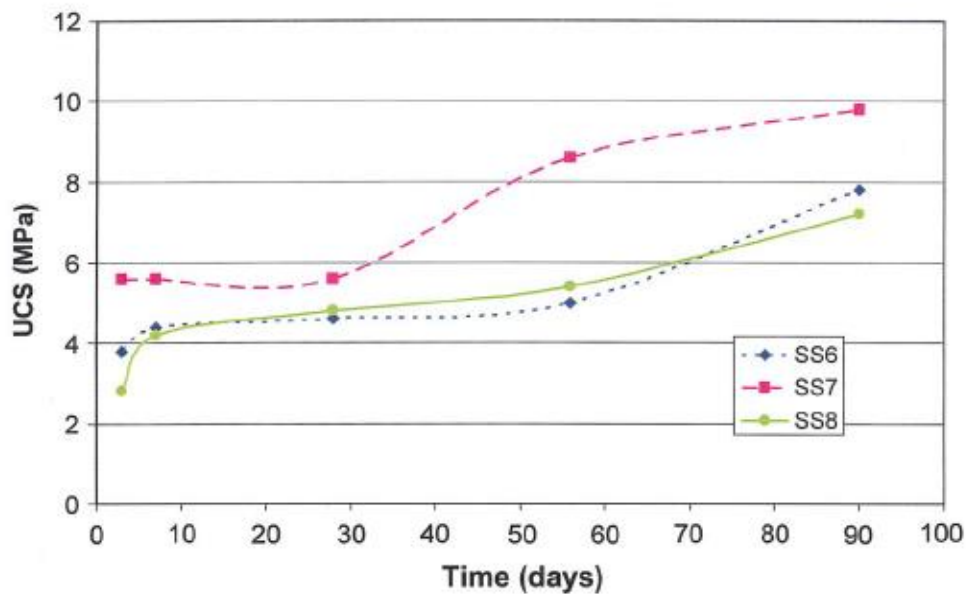


Figure 2.20 Unconfined compressive strength of soft soils treated with WPSA:Cement ratio 25:75. SS6, SS7 and SS8 are soft soils number 6, 7 and 8 respectively.

Source: Lisbona *et al.* (2012), permission to reproduce this figure has been granted by ASCE.

2.7.4 Other Waste Fly Ashes as Pozzolanic and Chemical Activators.

The following are brief literature reviews about the application of waste and by-product materials that were discovered and investigated as further activators for WPSA in this research project.

2.7.4.1 Pulverised Fuel Ash (PFA)

Pulverized fuel ash, sometimes called fly ash, is a by-product material produced from coal combustion in power stations which are found in many parts of the UK as well as around the world (Thomas, 2007). PFA is widely used as SCM in the concrete industry as a pozzolanic material and it has been used in many countries since the 1950s (Gutt and Smith, 1976).

Huge quantities; between four and seven million tonnes of PFA, have been produced annually in the UK and were recorded for the period between 1999 and 2014 reported by UKQAA (2016) (Figure 2.21). It can be seen that despite the reduction which occurred recently in the production of PFA, quantities are still very large and there is huge concern regarding the environmental impact of PFA.

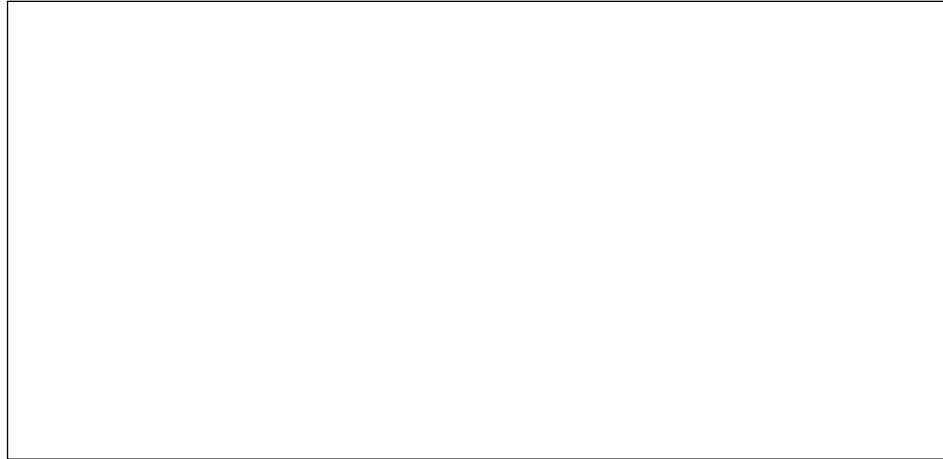


Figure 2.21 PFA production between 1999 and 2014 in the UK.

Source: UKQAA (2016). **The diagram originally presented here cannot be made freely available via LJMU Digital Collections because of 'copyright'**

Indraratna *et al.* (1995) carried out experimental works to study the effect of PFA mixed with cement and lime on the geotechnical properties of a soft clay. They found that UCS could be improved significantly with 18% fly ash and 5% lime treated Bangkok clay, while the compressibility and shear friction angle were improved with 10% PFA with a fixed percentage of cement of 5%. A comparison study was conducted by Lin *et al.* (2007) between sludge ash and fly ash on the improvement of soft soil using five different percentages of both (0, 2, 4, 8, and 16%). The results showed that the pH value increased slightly with increasing curing period for both types, the maximum dry density decreased with the increase of fly ash, while the optimum moisture content increased overall. With respect to the strength of the treated soil, the results showed that using PFA improved the UCS and CBR value significantly, over and above the use of sludge ash.

2.7.4.2 Ground Granulated Blast Furnace Slag (GGBS)

Ground granulated blast furnace slag is a by-product material of iron or steel making from a blast furnace using water or steam, to produce a glassy, granular product that is then dried and ground into a fine powder. The chemical composition of a slag varies considerably depending on the composition of the raw materials in the iron production process. Its pozzolanic properties were discovered in the late 19th century and have been widely used as a partial (20 to 80%) replacement of OPC in concrete (Hanson, 2016).

GGBS has been extensively used in many studies as a cement replacement to produce low carbon emission cement binders for the use in concrete industry (Malagavelli and Rao, 2010; Gadpalliwar *et al.*, 2014; Zhao *et al.*, 2016).

With respect to the field of soil stabilisation, Higgins (2005) carried out an investigation to study the potential of GGBS-lime for use in soil stabilisation in the UK based on research at Glamorgan University and several full-scale site trials. GGBS had no significant effect to improve consistency limits, optimum moisture content for clayey soil or initial lime consumption. GGBS had the potential to increase the compressive strength when mixed with lime, especially after 7 days curing compared to that achieved by lime only. On the other hand, in site trials, Higgins (2005) reported that the results indicated that replacing cement or lime by the same percentages of GGBS gave approximately the same compressive strength before 28 days curing, and exceeded those for cement or lime after 28 days. Yadu and Tripathi (2013) conducted laboratory CBR, and compaction tests on soft soil mixed with granulated blast furnace slag (GBS) and fly ash. 3, 6, and 9% GBS, and 3, 6, 9, and 12% fly ash were used as a soil stabiliser. They found that 3% fly ash + 6% GBS was the optimum contents and gave the best results.

2.7.4.3 Silica Fume (SF)

Silica fume is a by-product material produced from the production processes of silicon metals or ferrosilicon alloys. It is collected as a solid powder from the smoke resulting from electrical furnaces that produce silicon metals or alloys. SF is very widely used in the concrete and soil stabilisation industry because of its chemical and physical properties as well as its high pozzolanic reactivity (SFA, 2016).

Fattah *et al.* (2014) investigated the effect of lime, SF, and lime-SF mixture on the geotechnical properties of compacted soft clay soil, especially the consolidation properties and compression and compressibility characteristics. They found that liquid limit and plasticity index were improved optimally with the increase in stabilizer content. 4-5% of lime and SF were the optimum for the improvement in compressibility index (C_c) as well as for the coefficient of consolidation (C_v).

2.7.4.4 Rice Husk Ash (RHA)

Rice Husk Ash (RHA) is a waste material produced from the burning process of rice husk, which is used as fuel in the boilers for processing of paddy or for power generation. RHA is a super-pozzolanic material due to its high silica content (85% to 90%), thus it can be used as SCM to produce high performance concrete (Singhania, 2004; Rice Husk Ash, 2008). Recently, RHA has been extensively investigated as a potential material to replace cement in different concrete construction projects to produce geopolymer concrete (Soares *et al.*, 2015; Hwang and Huynh, 2015; Alex *et al.*, 2016; Sua-iam *et al.*, 2016).

Roy (2013) investigated the effect of rice husk ash (RHA) used to stabilise clayey soil as a subgrade material. Different contents (5, 10, 15, and 20%) of RHA were mixed with soil, then for further improvement, different contents of lime were used ranging between 1 and 3%. The result showed that adding RHA and lime to soft soil decreased maximum dry density and increased optimum moisture content. The unconfined compressive strength increased with the increase of RHA and lime content of the soil. However, 12.5% RHA, and 4-5% Lime were recommended to be used as additives to improve the geotechnical properties of expansive subgrade soils (Brooks, 2010).

2.7.4.5 Palm Oil Fuel Ash (POFA)

POFA is a type of biomass ashes; it is a waste material resulting from burning palm oil fibre at a temperature ranged between 800 – 1000°C to produce fossil fuel. POFA has a good content of silica oxide, therefore it can be considered as a pozzolanic material. Meanwhile, POFA is an alkali material with a high value of pH, which can be used also as a chemical activator for another pozzolanic or cementitious material in concrete mixtures (Khalid *et al.*, 2014).

In the field of soil stabilisation, Ahmad *et al.* (2011) carried out an experimental study to investigate the possibility of cement replacement by POFA for peat soil stabilisation. They prepared five groups of specimens to conduct UCS tests for untreated, 30% OPC, and for the other the samples replacing the OPC with (1/3, 1/2, 2/3) POFA with 0, 7, and 14 days curing for each group. The highest value of UCS was for samples containing 50% POFA with OPC content, which also gave a strength higher than that for 100% OPC binder. Furthermore, the possibility of using POFA

individually and in combination with OPC in soft soil stabilisation was investigated by Pourakbar *et al.* (2015). The performance of POFA was assessed dependent on the results of Atterberg limits, compaction parameters and UCS tests. The results indicated that there was a significant reduction in the plasticity index of the clayey soil using both POFA alone and mixed with cement. While a slight improvement in soil strength after 28 days of curing with treatment of POFA alone and a sharp increase with treatment of POFA-OPC mixture for selected binder dosages were observed as shown in Figure 2.22.

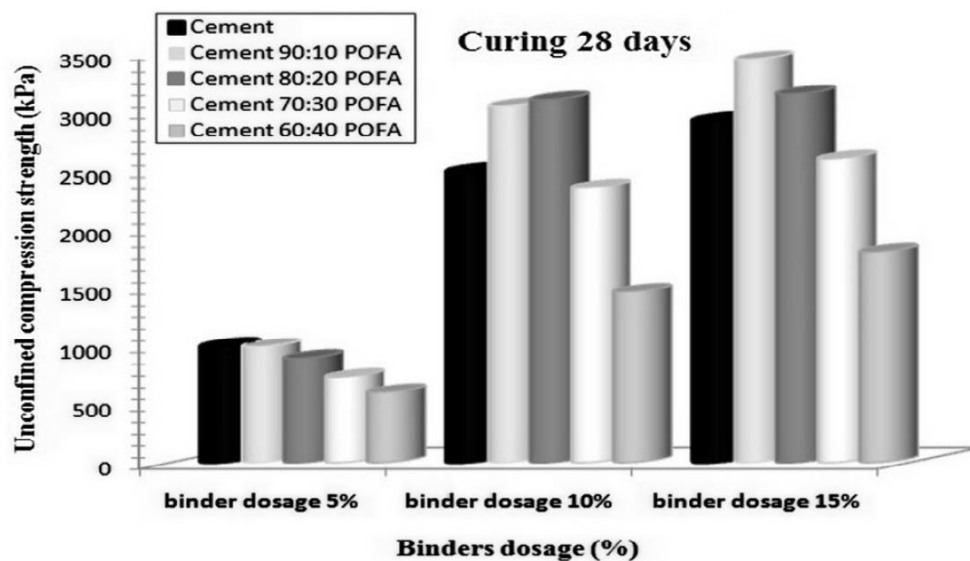


Figure 2.22 Effect of OPC/POFA combination on UCS for different binder dosages

Source: Pourakbar *et al.* (2015), permission to reproduce this figure has been granted by Elsevier.

2.7.4.6 Flue Gas Desulfurization (FGD) Gypsum

Many countries such as Eastern Europe, China and India have been using coal power industry for electrical generation. This industry has been a major source of pollution due to the emission of SO_2 , NO_x and CO_2 resulting from the burning process of fossil fuel (Wright and Khatib, 2016). The aforementioned gases, especially SO_2 , can be controlled and reduced by installing air pollution systems to the power installation using alkaline sorbents such as limestone react with SO_2 gasses resulting in desulphurised wastes (Khatib *et al.*, 2013). The flue gas desulphurisation gypsum (FGD) is a waste or industrial by-product material which is generated from the wet-

type desulphurisation processes used in coal-fired power plants, and its main phase is calcium sulphate dehydrate (Zhang *et al.*, 2016a).

OPC manufacturing requires a small amount of calcium sulphate which is formerly essentially gypsum. This material can be considered as one of the cement ingredients which is normally added to cement clinker as a retarder and grinding agent. However, presently different forms of calcium sulphate are mixed then added to the clinker (Schumacher and Juniper, 2013; Marchon and Flatt, 2016b). Since the major component of FGD is calcium sulphate, it has been used as a grinding aid instead of gypsum as well as to achieve higher early strength in different research projects (Qiao *et al.*, 2006; Sadique *et al.*, 2013; Zhang *et al.*, 2016b).

2.7.5 Methods of Fly Ash Activation

Activation is an essential method to boost the reactivity of fly ashes that are intended to become suitable SCMs for producing blended cement or cement-free binders. According to the literature, there are two main methods for SCMs activation; these methods are mechanical activation and chemical activation. However, a physico-chemical activation technique sometimes is adopted by applying both types of the activation techniques mentioned above. The mechanical activation is normally applied by using grinding energy in order to increase the fineness and specific surface area of the activated materials that in turn increases the capacity of cation exchange and pozzolanic reactivity (Sadique *et al.*, 2013; Aïtcin, 2016b). While the chemical activation could be achieved by using many types of chemical substances (alkaline reagents and alkali salts are widely used) to excite the potential reactivity of SCMs, especially those rich in alumina-silicate based materials (Sargent, 2015). Another technique called thermal activation is mostly used to activate fly ashes that have a high content of incompletely incinerated carbon. This method can be achieved through a calcination and hydrothermal process (Habert, 2014). Brief reviews of the literature regarding the application of the aforementioned methods of activation are as follows:

2.7.5.1 Mechanical Activation

The purpose of mechanical activation is to produce a finer material and increase the surface area of an activated SCM. This type of activation method is normally achieved by applying a grinding energy and/or by separating the ultra-fine particles of fly ashes

by either sieving or using a special system such as air-cyclonic processing (Jones *et al.*, 2006). Mechanical activation or so-called grinding activation was found as a beneficial technique not only in the increase of fineness and specific surface area but also in the improving of electrical and crystalline system of the activated fly ash. Sadique *et al.* (2012b) found that due to comminution that occurs during the grinding activation, the external dynamic forces induce the solid to become an electronically excited structure and disturbs the electronic arrangement of bonding.

A study was conducted by Sinsiri *et al.* (2012) to compare the performance of different biomass fly ashes (RHA and POFA) and the effect of their fineness on the compressive strength of cement-added paste. RHA and POFA were ground into two different grades using an attrition mill with 1000 rpm and 2mm diameter steel balls. The results indicated that the percentages of compressive strength developments increased with the increase of fly ash substitution for both coarse and fine grades to reach approximately 35% of the compressive strength of control pastes. Similar findings were reported by (Chindaprasirt *et al.*, 2014).

However, there is evidence that the long-time grinding could cause agglomeration for the activated materials which has a negative influence on the pozzolanic reactivity and sometimes using grinding aid substances, such as gypsum, is recommended to help to de-agglomerate the particles of the activated materials (Sadique *et al.*, 2012b; Sadique *et al.*, 2013; Sanjuán *et al.*, 2015).

2.7.5.2 Chemical Activation

Chemical activation, sometimes called alkali activation, is widely used as one of the successful processes of SCMs activation in order to produce new environmentally and financially sustainable replacement binders (Sargent, 2015). There is a huge volume of research papers that have been published dealing with the use of alkaline materials, as chemical activators, and their role and performance in cementitious systems. The process of alkali activation has relied on the use of specific alkaline activators which are added and mixed with SCMs, and then the mixture is cured at a certain temperature to achieve hardening. The most preferable SCMs for alkali activation are those which are alumina-silicate based materials such as clays, calcined clays (metakaolin) and fly ashes which contain SiO_2 and Al_2O_3 as the main composition (Pacheco-Torgal *et al.*,

2012; Provis *et al.*, 2015; Zhang *et al.*, 2017b). According to Sargent (2015) the most popular alkali activators in soil stabilisation are lime, sodium hydroxide, sodium silicates and red gypsum (RG), and such materials are secured either synthetically or naturally. However, despite the fact that the sodium silicate is secured synthetically and its production incurs high cost and has negative environmental impacts, it is considered as the most useful alkali activator in comparison to the lime and metakaoline. The latter, in addition to their negative environmental impact, also exhibit poor early strength development and long setting time, and require large volumes of mixing water which decreases a soil stiffness and increases its porosity (Duxson *et al.*, 2006).

Alkali activators are used to maintain an alkaline medium with pH value not less than 10.5 as recommended by Sargent (2015), which promote the glass phases of alumina silicates of activated fly ashes to dissolve and react with the hydrated lime. Many SCMs have high volumes of amorphous silica and/or alumina which either do not react with water or their pozzolanic reaction is too slow. Therefore, when such materials are placed in a high alkali medium, the silicates and aluminates group dissolve and poly-condense into short-range ordered and cross-linked chains performing as a binder that forms a cementitious gel (Habert, 2014).

2.8 SUMMARY

This chapter provided a detailed review about the issues that affect the engineering behaviour of soft soils including soils characterisation, classification, minerals and stabilisation. Additionally, it presented the review of cement-soil stabilisation and its effect on the geotechnical properties of soils along with the potential use of different waste materials as a cement replacement in soft soil stabilisation. It was evident that cement is the preferable binder to improve the geotechnical properties of the stabilised soils significantly. However, the use of cement is characterised with negative environmental impacts specifically the carbon dioxide emissions. Literature revealed that waste materials fly ashes could potentially replace the cement in soil stabilisation. This view can be a motivation for further research in order to develop a novel approach in the production of new cementitious materials that could represent a better utilisation of waste materials fly ashes.

CHAPTER 3

MATERIALS AND RESEARCH METHODOLOGY

3.1 INTRODUCTION

This chapter represents the description of materials and procedures of the testing methods that were employed to achieve the objectives of this research project. The experimental works that were performed in this study can be divided into three main stages dependent on their corresponding aims and type of characterisation. The first stage was performed to classify and identify the virgin soil used in this study along with the identification tests for the waste materials fly ashes which were used as soil binders later on. The second group was represented by conducting the optimisation and experimental works of mix design to investigate the effect of different types and dosages of additives on the physical and geotechnical properties of the stabilised soil. Finally, the last stage was conducted to study the mineralogical and microstructural behaviour of the treated soil as well as of binder pastes produced from the newly developed binder in this study in order to understand and elucidate the hydration kinetics that took place after treatment. Consequently, experiments were conducted to obtain physical properties such as consistency limits, specific gravity, and particle size distribution. Other tests were carried out to determine the geotechnical properties, in particular for the virgin and treated soil, such as compaction parameters, unconfined compressive strength (UCS), and consolidation tests along with the effect of dry-wet cycles on the soil-cement loss to evaluate the durability of treated soil. Chemical tests included loss on ignition (LOI), pH value and X-Ray fluorescence spectrometry (XRF) tests along with the scanning electron microscopy (SEM), energy dispersive X-Ray (EDX) and X-Ray diffraction (XRD) tests.

Moreover, a reference mixture of cement-added soil (OPC mixed with the treated soil) was prepared to compare the performance of the waste materials fly ashes mixtures in each stage of experimental works. The flow chart shown in Figure 3.1 explains the research methodology that was adopted in this study.

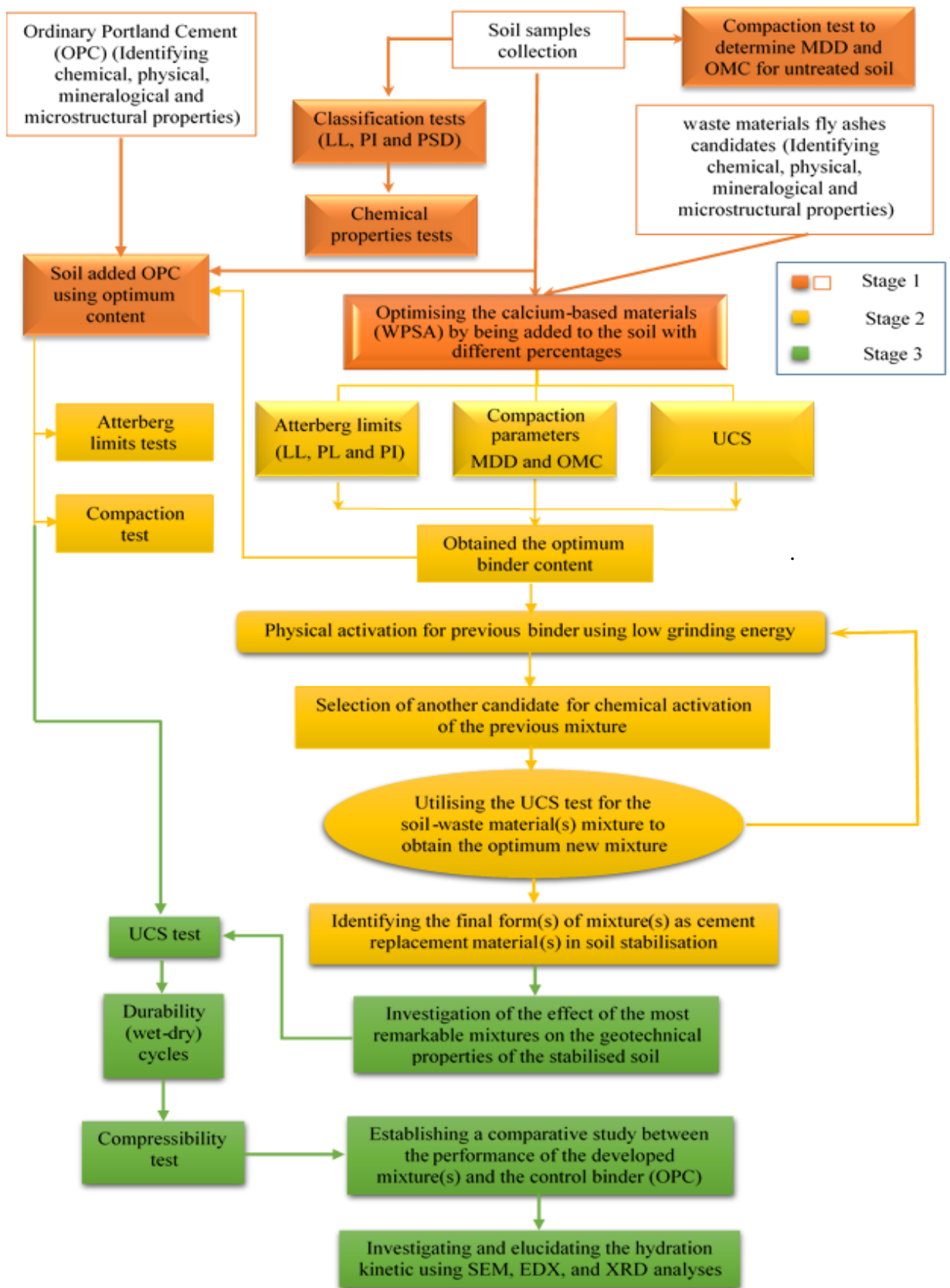


Figure 3.1 Test procedure of this research project.

3.2 MATERIALS

3.2.1 Soil

The soil used in this study was brought from the banks of the River Alt which is located in Hightown to the north of Liverpool city centre in the UK. The soil samples were extracted from the river estuary at a depth ranging between 30 and 50cm below the ground level, then placed in heavy duty plastic bags with approximately 20-25kg in each, then sealed carefully before the transporting to the laboratory. Figure 3.2 shows the site where the soil samples tested in this study were taken along with the boreholes distribution in this area according to the British Geological Survey (NERC, 2017). According to the soil texture map shown in Figure 3.3, the superficial geology of the sampling site characterised by a widespread alluvium deposits ranged from clay > sand to loam along the course of the River Alt which were bounded to the east and northern west by a series of river terrace sand and loam sand deposits (Edina Geology Digimap, 2017). The stratigraphic logs of the soil of the boreholes close to the soil collection point, obtained from the British Geological Survey (NERC, 2017), are shown in Figure 3.4.



Figure 3.2 Satellite image of the soil collection site at Hightown, Liverpool.
Source: NERC (2017)

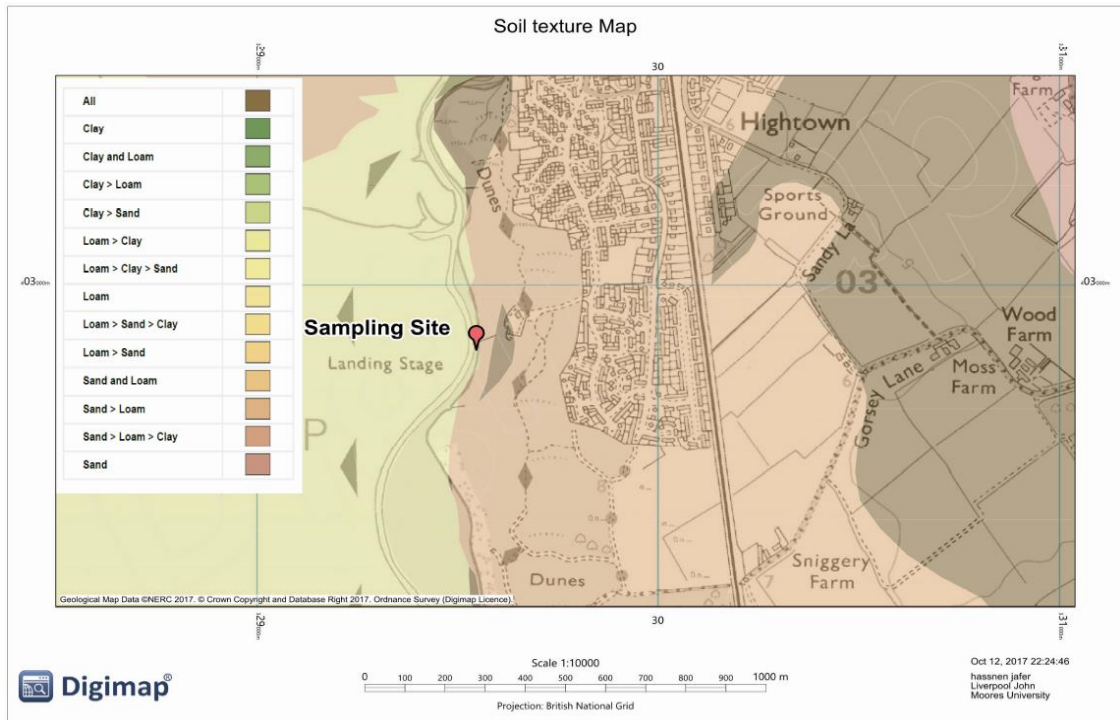


Figure 3.3 Soil texture map of the soil collection site at Hightown, Liverpool
 Source: Edina Geology Digimap (2017)

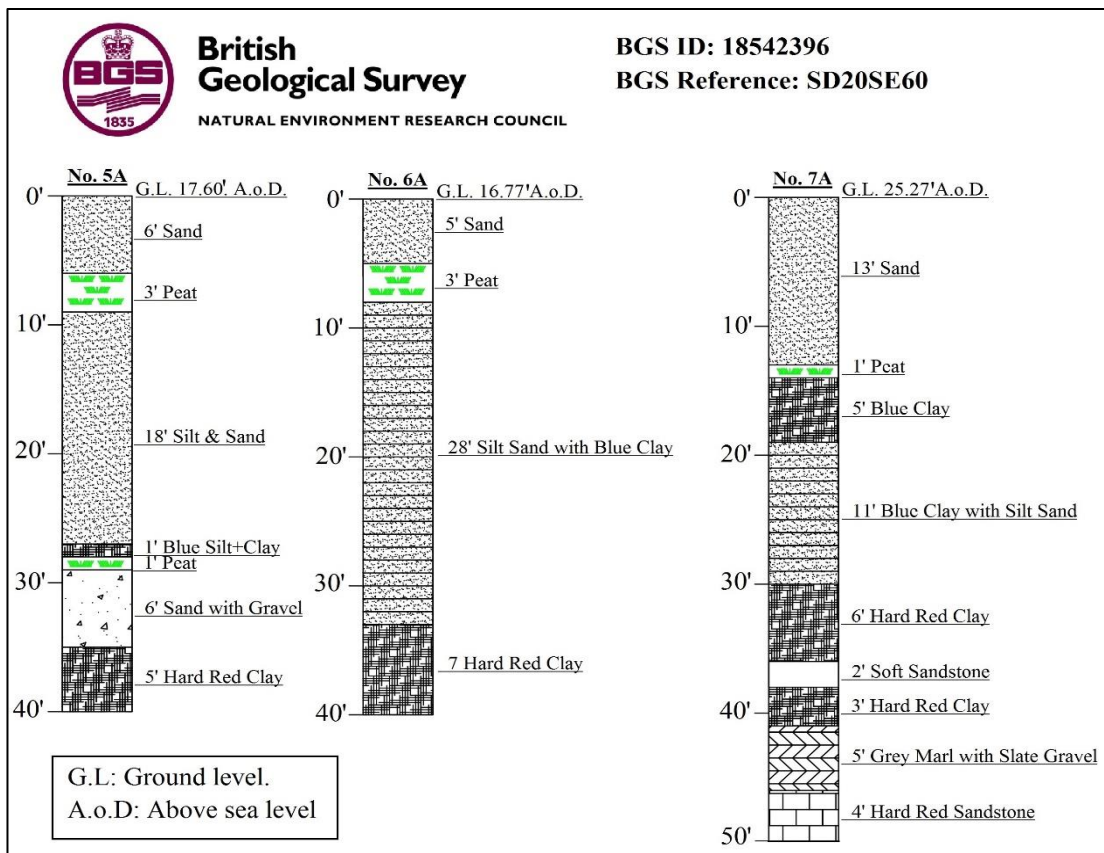


Figure 3.4 Detailed stratigraphic soil logs close to the site of sampling of the Hightown soft soil.
 Source: NERC (2017)

Once the soil samples arrived at the laboratory, representative specimens were taken directly to calculate the soil natural moisture content in accordance to the BS EN ISO 17892-1:2014 (European Committee for Standardization, 2014c). The remaining samples were air dried outside the lab, for one week, to be prepared for the required experimental works at a later stage. Experimental works were conducted to identify physical, chemical, and geotechnical properties of the selected soil.

3.2.2 Added Materials

Seven different waste material fly ashes were identified in this study as SCMs along with OPC which was used for the reference mixture. These materials were waste paper sludge ash (WPSA), palm oil fuel ash (POFA), rice husk ash (RHA), silica fume powder (SF), two different types of pulverised fuel ashes (PFA), and ground granulated blast furnace slag (GGBS). Additionally, another type of waste material was used as a grinding and sulphate activator in this study which was flue gas desulfurization gypsum (FGD). The candidate materials that were identified in this study are waste or by-product materials which are produced from different industrial sectors inside and outside the UK. Table 3.1 illustrates the source and description of each candidate material. Moreover, it should be noted that in addition to the OPC, four of the materials mentioned above were involved in the mixing design to produce the new forms of binder materials. These materials were WPSA, POFA, RHA, and FGD.

Table 3.1 Sources and description of candidate materials identified in this study.

Item	Description and Source
OPC	A commercially available cement type CEM-II/A/LL 32.5-N was brought from Cemex Quality Department, Warwickshire, UK.
WPSA	A sample of waste ash produced from incineration processes of newsprint making residue was supplied by Aylesford newsprint (AN Ltd) Company, Kent, UK.
PFA1	A dark grey sample of PFA was collected from Cemex Ltd company, Warwickshire, UK. The sample is fly ash type 450-S according to the British Standard.
PFA2	Another sample of very dark PFA was provided by SSE.com from the Fiddlers Power Station, Cuerdley, Warrington, UK.
GGBS	Hanson Heidelberg Cement group supplied a sample for trial purposes of GGBS classified under BS EN 15167-1 standard.
POFA	Waste material produced from the incineration processes of palm oil fibres at a temperature ranging between 800 and 1000°C was imported from Sg. Tenggi Palm Oil Factory at Kuala Kubu Bharu, Selangor, Malaysia.
SF	Commercially available grey micro silica fume was identified in this report, supplied by Elkem Materials company, Zuid-Holland, Netherlands.
RHA	A sample of RHA containing micro-silica was imported from NK Enterprises company in India, Jharsuguda, Orissa, INDIA
FGD gypsum	An off-white and semi-dry FGD was collected from a 4000 megawatts coal fired power station. The slurry limestone is used as a sorbent in this station.

3.3 PROGRAMME OF LABORATORY EXPERIMENTS AND TESTING EQUIPMENT

As explained in Figure 3.1, the adopted experimental programme in this study included experiments for soil classification tests such as consistency limits and grain size distribution, and characterisation of geotechnical and chemical properties of the virgin soil such as UCS, compressibility, the effect of wet-dry cycles, pH value, LOI, and

oxides contents. Moreover, the experimental programme was performed for candidate materials identification including physical and chemical properties such as PSD, G_s, pH, LOI, and oxides contents. Then, the experiments for investigating the effect of the selected types of waste materials fly ashes (as mentioned in section 3.2.2) on the physical and geotechnical properties of the stabilised soil were included in the experimental programme. Additionally, the mineralogical and microstructural behaviour experiments were conducted on pastes of the developed mixture as well as soil-binder mixtures to investigate the hydration kinetics that occurred after adding water. However, the adopted sequences of the percentages and blend type of the additives with the corresponding experiments will be illustrated later in this chapter.

The testing methods, the devices and apparatuses used, and the details of samples preparation with the testing procedure for each experiment are explained as follows:

3.3.1 Natural moisture content %

As mentioned in section 3.2.1, the natural moisture content of the virgin soil was determined directly after the soil samples arrived at the soils lab. BS EN ISO 17892-1:2014 standard was adopted in this test (European Committee for Standardization, 2014c) and for all other moisture content determination which is required in most of the experimental works carried out in this research project.

3.3.2 Particle Density (Specific Gravity, G_s)

Specific gravity is mentioned as particle density in the British Standard which means the density of solid material for any substance. Concerning soils, this test is required in the calculations for other geotechnical properties tests particularly the consolidation test in this study. In this study, the G_s was calculated for virgin soil as well as the treated soil samples, and for the dry powder candidates. The British standard BS EN ISO 11508:2014 (European Committee for Standardization, 2014b) was considered using the a Pycnometer method as described in clause 4.1 and shown in Figure 3.5.



Figure 3.5 Particle density test using the Pyknometer.

3.3.3 Particle size distribution (PSD)

Two different testing methods for PSD were adopted in this study. The first method was used for PSD of the virgin soil. A representative sample of dry soil was subjected to both sieve analyses for particles coarser than $63\mu\text{m}$, and the Hydrometer test for the soil passing through sieve size $63\mu\text{m}$ in accordance with BS EN ISO 17892-4:2014 (European Committee for Standardization, 2014a). The wet method procedure was adopted, which includes washing the soil specimen on sieve size $63\mu\text{m}$ to extract the material finer than $63\mu\text{m}$ then oven drying both parts remaining and passing to be ready for sieve and hydrometer testing respectively. On the other hand, the PSD for candidate materials (OPC and waste materials fly ashes) was adopted using Laser Diffraction Particles Analyser brand - Beckman Coulter as shown in Figure 3.6. This device was also used for determining the PSD for mixed and grinding activated mixtures during the optimisation steps in this study. Beckman Coulter LS 13 320 uses reverse Fourier optics incorporated in a patented fibre optic spatial filter system and a binocular lens system. Consequently, the LS 13 320 is enabled to optimize light

scattering measurement across the widest dynamic range, from 40nm to 2000 μ m, in a single scan with no extrapolation (Beckman Coulter, 2009).



Figure 3.6 LS 13 320 Particle size analyser.

3.3.4 Consistency Limits

In this study, the liquid limit (LL), plastic limit (PL), and plasticity index (PI) were determined for each of the following: virgin soil, cement-stabilised soil, and soil stabilised with different percentages and types of the selected waste fly ashes. The consistency limits test was performed in accordance with BS 1377-2:1990 (British Standard, 1998a) using dry samples passed through sieve size 475 μ m. The liquid limits were determined using the cone penetration method (as described in clause 4.3) by the cone penetrometer device shown in Figure 3.7 and 3.8, while the plastic limits were determined by the rolling method as explained in section 5. With respect to the treated soil samples, the consistency limits test was carried out directly after adding distilled water to the soil-binder mixture. Mixtures of soil-binder were prepared by adding a specific percentage of the binder to the soil passed through sieve size 475 μ m then being mixed by a hand mixing process in which the mixing was continued until achieving a homogenous mixture.



Figure 3.7 Cone penetrometer device used in LL test.



Figure 3.8 A sample paste with the cone before penetration.

3.3.5 Compaction Parameters Test

The purpose of this test is to obtain the relationship between the dry density and moisture content which is required to determine the maximum dry density (MDD) and optimum moisture content (OMC) which are called the compaction parameters. Concerning the experimental laboratory work, the compaction parameters are essential to prepare soil specimens for the tests of other geotechnical properties such as UCS, permeability, California bearing ratio (CBR), and consolidation testing. A standard Proctor method test was adopted in this research according to the test procedure described in BS 1377-4:1990 (British Standard, 2002a). An *IMPACT* brand electrical motorised compactor was used for the wet compaction of samples, and the compacted samples were ejected from the mould using a hydraulic manual jack as shown in Figure 3.9.

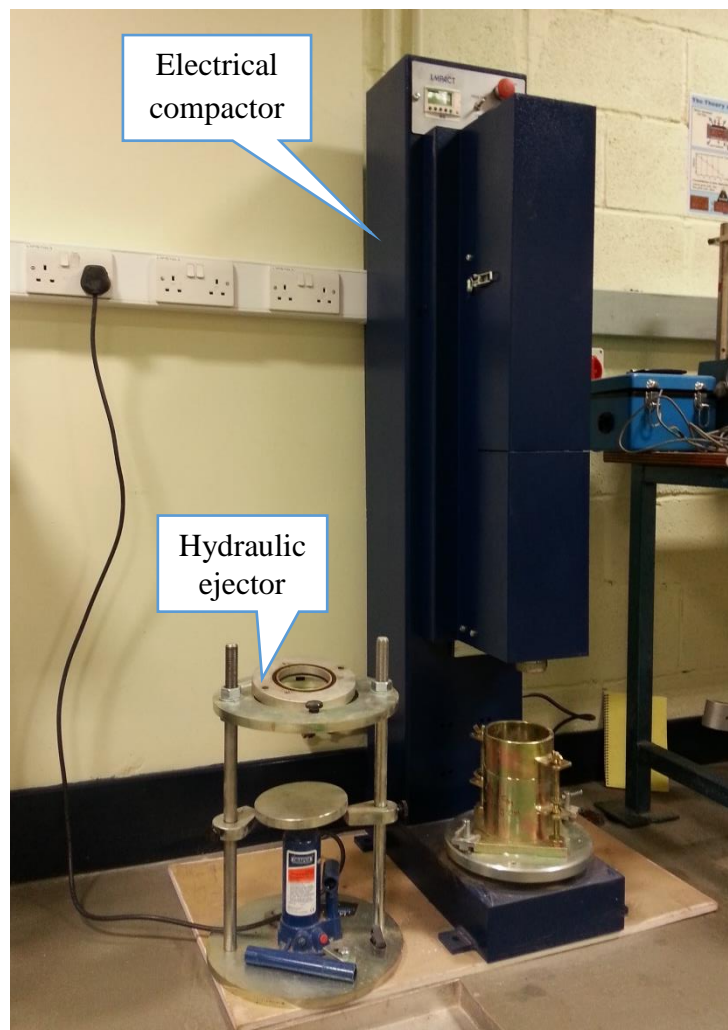


Figure 3.9 The compaction machine used in the study.

The compaction parameters test was performed for the virgin soil as well as for each type of the soil-binder mixture. The samples of soil-binder were prepared by scattering the binder material over the soil then a manual mixing procedure was adopted using mixing tools and hand mixing until achieving a homogenous colour for the mixture. Sequentially, a specific percentage of initial water content was added to the dry mixture of soil-binder to obtain a soil-binder paste which was ready for compaction. Figure 3.10 shows the sequences of soil-binder mixing and preparation for compaction testing.





Figure 3.10 Sequences of sample preparation and compaction.

3.3.6 Unconfined Compressive Strength Test (UCS)

UCS testing was performed to obtain the stress-axial strain diagram, and consequently, the maximum strength at failure ($q_{u_{max}}$) and its corresponding failure strain were determined. This test was conducted in accordance to BS 1377-7 (British Standard, 1999b) using a computerised motorised triaxial machine in which the horizontal stress was maintained to be equal zero by eliminating the horizontal pressure in the triaxial cell ($\sigma_3 = 0$) as shown in Figure 3.11. Based on the British Standard regarding the UCS test, the strain rate (rate of displacement which is responsible for vertical pressure applied on the test specimen) shall be not more than 2.0%/min. from the original height of the specimen (i.e. $0.02 \times 76\text{mm} = 1.52 \text{ mm/min.}$). Thus, a constant rate of vertical displacement was considered in this study which was equal to 1.0mm/min.

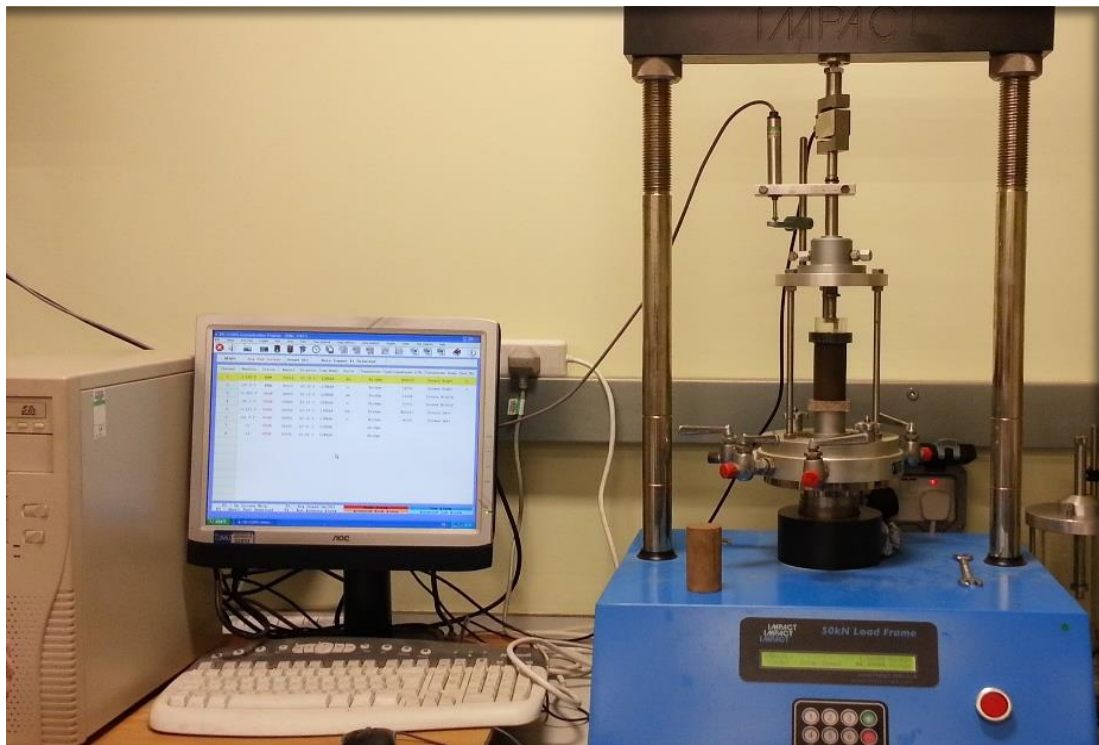


Figure 3.11 Computerised triaxial machine used for UCS testing.

In this study, the UCS test was performed to determine maximum strength ($q_{u_{max}}$) with its strain failure for the virgin soil in both undisturbed and remoulded compacted states. Additionally, this test was also carried out for the treated soil with different types and percentages of binder at different periods of curing (3, 7, 14, 28, 90, 180 and 360 days). Additionally, this test was carried out to evaluate the durability of specimens of virgin

and treated soil regarding the strength losses after being subjected to different numbers of dry-wet cycles. The dry-wet cycles test was conducted according to the procedure explained in ASTM D559-03 (ASTM International, 2003).

The specimens subjected to UCS testing as well as for wet-dry cycles were prepared by adding the specified binder to the dry soil then a dry mixing process was performed using manual mixing until achieving a homogenous colour and mixture. Once a specific amount of water was added to the mix, another manual mixing process was carried out to obtain a wet paste. After that, a fixed volume mould, manufactured in the LJMU workshops shown in Figure 3.12, was used to produce specimens of specific dimensions according to the aforementioned British standard (38mm in diameter and 76mm in height) by pressing the paste directly inside the fixed volume mould using a manual hydraulic jack. As shown in Figure 3.12, the used fixed volume mould can be split into two parts in which the prepared specimens can be easily removed.



Figure 3.12 Constant volume mould used for preparation of UCS specimens.

Consequently, the ejected specimens were weighed, wrapped in cling film, labelled, put in well-sealed plastic bags and stored in a curing room for the required periods of time as shown in Figure 3.13. The specimens in this study were cured in 100% relative humidity under a curing temperature equal to $20\pm 2^{\circ}\text{C}$ using a LEEC humidity cabinet shown in Figure 3.14. This cabinet can provide a temperature of curing with 0.1°C accuracy, and different relative humidities dependent on the salinity degree of the solution used in the base of this cabinet. However, 100% relative humidity could be

obtained when distilled water is used. Three specimens were adopted for each type of binder and age of curing. Specimens were prepared with moisture contents and densities according to the MDDs and OMCs that were obtained from the compaction testing (as mentioned in the previous section) for each corresponding percentage of additives.



Figure 3.13 Procedure of the specimens preparation for UCS testing.



Figure 3.14 The humidity cabinet used for specimens curing.

The same procedure was adopted for the preparation of wet-dry cycles specimens. In this study, the effect of wet-dry cycles on the mass and strength losses was investigated for virgin soil, reference mixture (OPC-soil) and soil treated with different mixtures of waste materials fly ashes which were the most promising mixtures obtained from the optimising stages. Consequently, two specimens were prepared for each type of combination; one was for soil-binder loss in mass, and the second specimen was for strength loss. For each cycle of wetting-drying, the specimens were soaked for five hours in a basin filled with distilled water then taken out and transferred to the oven for drying at 70°C for 48hrs as shown in Figure 3.15.



Figure 3.15 Wetting-drying procedure.

3.3.7 Oedometer Test (Consolidation Test)

Consolidation behaviour is one of the most important geotechnical properties of soils because it gives an indication about the settlement that may occur in the foundation during the construction processes of any engineering project as well as for any time after the completion. Settlement is the control criterion for foundation design when an engineering project is located at a site with soft soils, and stabilisation of such soils could reduce the settlement and make the site soil more suitable (Marto *et al.*, 2014; Moghal *et al.*, 2015). The settlement can be evaluated by measuring different coefficients obtained from the consolidation test such as coefficient of volume change (m_v), compressibility index (C_c) and recompression index (C_r) sometimes called the expansion index (C_v) (Knappett and Craig, 2012). Additionally, the over consolidation ratio (OCR), pre-consolidation pressure (P_c), and one-dimensional elastic modulus (E'_{Oed}) can also be obtained from this test.

In this study, the one-dimensional consolidation test was performed on the virgin soil in both its states, the undisturbed and compacted to the MDD. Moreover, this test was conducted on the soil treated with cement as well as soil treated with the optimum mixtures of the waste materials fly ashes. The treated soils were subjected to this test after 7 and 28 days of curing to investigate the effect of curing on soil compressibility. Specimens for oedometer testing were prepared with densities and moisture contents dependent on the MDDs and OMCs achieved from the compaction parameters testing for each corresponding type of binder using a cylindrical mould with constant volume. The mould was used to produce a compacted specimen with 82mm in diameter and 50mm in height which is larger than the dimension required for the specimens of oedometer test. The prepared specimens were wrapped with cling film, labelled, stored in polythene bags then kept in a humidity cabinet for curing. The same curing condition mentioned in section 3.3.6 was applied in this test. After achieving the required curing period, a stainless steel ring with specific dimension (75mm in diameter and 20mm in height) was driven into the cured specimen using a manual hydraulic jack. Then the extra soil was trimmed using a very sharp tool to get a flat surface of the specimen with top and bottom edges of the ring as shown in Figure 3.16. After that, the specimen was assembled with the cell of oedometer which was a fixed

ring cell in which porous stones were placed at the top and bottom of the samples and only vertical displacement was permitted after pressure application (Figure 3.17).



Figure 3.16 Preparation of Oedometer test specimens.



Figure 3.17 Set up of Oedometer test cell.

The Oedometer testing was carried out according to the British standard BS 1377-5 (British Standard, 1998b). An automatic computerised Oedometer brand ACE manufactured by Controls Ltd was used to conduct this testing. This device consisted of three loading units connected to a lap top computer as shown in Figure 3.18. By using this equipment, the loading and unloading sequences and the test conditions can be set on the computer before running the test, with the test sequences performed automatically. The load sequences applied in this study were 12, 25, 50, 100, 200, 400, 800, 1600, and 3200kPa while the unloading sequences were 800, 200, 50, and 12kPa. After completion of each test, the recorded results were plotted to obtain the e-log pressure diagram which was used to calculate the pre-consolidation pressure and compressibility index (C_c) following the Casagrande procedure described in Knappett and Craig (2012).



Figure 3.18 Equipment used for Oedometer test.

3.3.8 Loss on Ignition Test (LOI) %

This test was conducted to determine the organic matter content of the virgin soil used in this study as well as the total carbon content in the candidate materials which resulted due to the incomplete incineration of raw materials that these candidates were produced from. This test was performed according to British standard 1377-3 (British Standard, 1999a) by adopting a procedure as explained in clause 4. Figure 3.19 shows specimens of soil and candidate materials after being subjected to heating at $440 \pm 25^\circ\text{C}$ for 4 hours.



Figure 3.19 LOI test for virgin soil and candidate materials.

3.3.9 pH Measurements

The pH value is one of the important chemical properties; it helps to select suitable material as a soil stabiliser since the British standard specifies that the pH value should be not less than 8 for materials used in cementitious materials production (British Standard, 1999c). The pH measurements were conducted for the virgin soil and the candidate materials by making a solution of the dry powder (1 part of mass with 10 parts of distilled water) then the solution was stirred for approximately 30 minutes before testing. These tests were conducted according to the British standard BS ISO 10390 (British Standard, 2005) using the pH meter as shown in Figure 3.20.

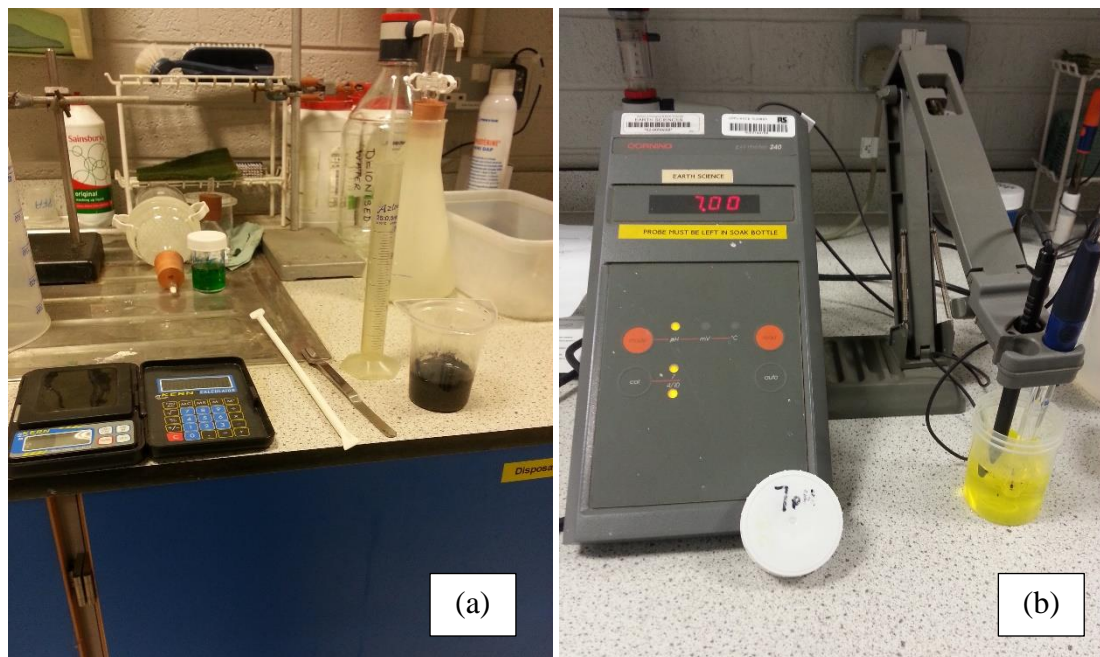


Figure 3.20 pH measurement test (a) Solution preparation, and (b) pH meter calibration.

3.3.10 X-Ray Fluorescence Spectrometry (XRF) Analysis

The elemental compositions (major oxides and trace elements content) of the virgin soil and all candidate materials were analysed using a Shimadzu EDX-720 Energy Dispersive X-Ray Fluorescence Spectrometer shown in Figure 3.21. This high-performance, general-purpose instrument, provides rapid, non-destructive elemental identification and quantification of solid, liquid, and powder samples with no sample preparation required. The analysis is carried out by applying X-rays to the specimen;

then the re-emitted fluorescent X-rays are analysed (Shimadzu, 2016). The preparation of soil specimen for this test was achieved by milling a sample of soil; then the milled soil was passed through sieve size 300 μ m. With respect to the dry powder candidates, they were subjected to this analysis directly without any preparation.



Figure 3.21 Shimadzu's EDX-720 used for XRF analysis.

3.3.11 Tests of Hydration Kinetic Investigation

The mechanism of the hydration process occurring between the soil and binder materials throughout the time of curing was evaluated by investigating the changes in mineralogical structure and compositions, and the microstructure of specimens of soil treated with the optimum mixtures and cured for different periods. Moreover, the same investigation was carried out on pastes of the optimal mixtures (without soil) to elucidate and confirm the development in the strength by monitoring the progression of the pozzolanic reaction and the production of cementitious compounds throughout the time of curing. Three different analyses were performed to investigate the hydration kinetics in this study in which the samples preparation procedures were similar for all analyses. These analyses were XRD, SEM and EDX as they are the most commonly used methods in such investigations (Horpibulsuk *et al.*, 2010; Li *et al.*, 2014; Jha and Sivapullaiah, 2016). However, SEM and XRD tests were also carried out for un-hydrated materials to identify their microstructure and mineralogical phases respectively to be compared with those after mixing and hydration.

3.3.11.1 Samples preparation

The samples for materials identification purposes were in the dry powder state, and they were prepared using the same procedure that was adopted in the preparation of XRF test samples (section 3.3.10). Specimens of compacted untreated soil, cement-treated soil, and soil treated with the optimal developed mixtures were prepared to investigate the subsequent changes in soil microstructure and elementary structure throughout the time of curing. Moreover, a paste of only OPC along with pastes of the optimum mixture; the newly developed binder produced from the ternary blending of WPSA, POFA and RHA activated by FGD gypsum, were prepared to investigate the changes in mineralogical and microstructures after hydration.

The specimens in this investigation were examined at ages of 3, 7, 28, 90 and 180 days. Specimens containing soil, were prepared and cured in a condition similar to that for the UCS specimens as mentioned in section 3.3.6, while the pastes without soil were soaked in a small container filled with distilled water and cured at ambient temperature. After achieving the required curing period, representative fragments were fractured from the cured specimens then left overnight for air drying. An electrical fan providing warm air was used to accelerate the drying process without any deterioration of the entire microstructure of the specimens, as shown in Figure 3.22. Special procedures were adopted to prepare the specimens for each type of the aforementioned analyses (XRD, SEM, and EDX) which will be explained later .

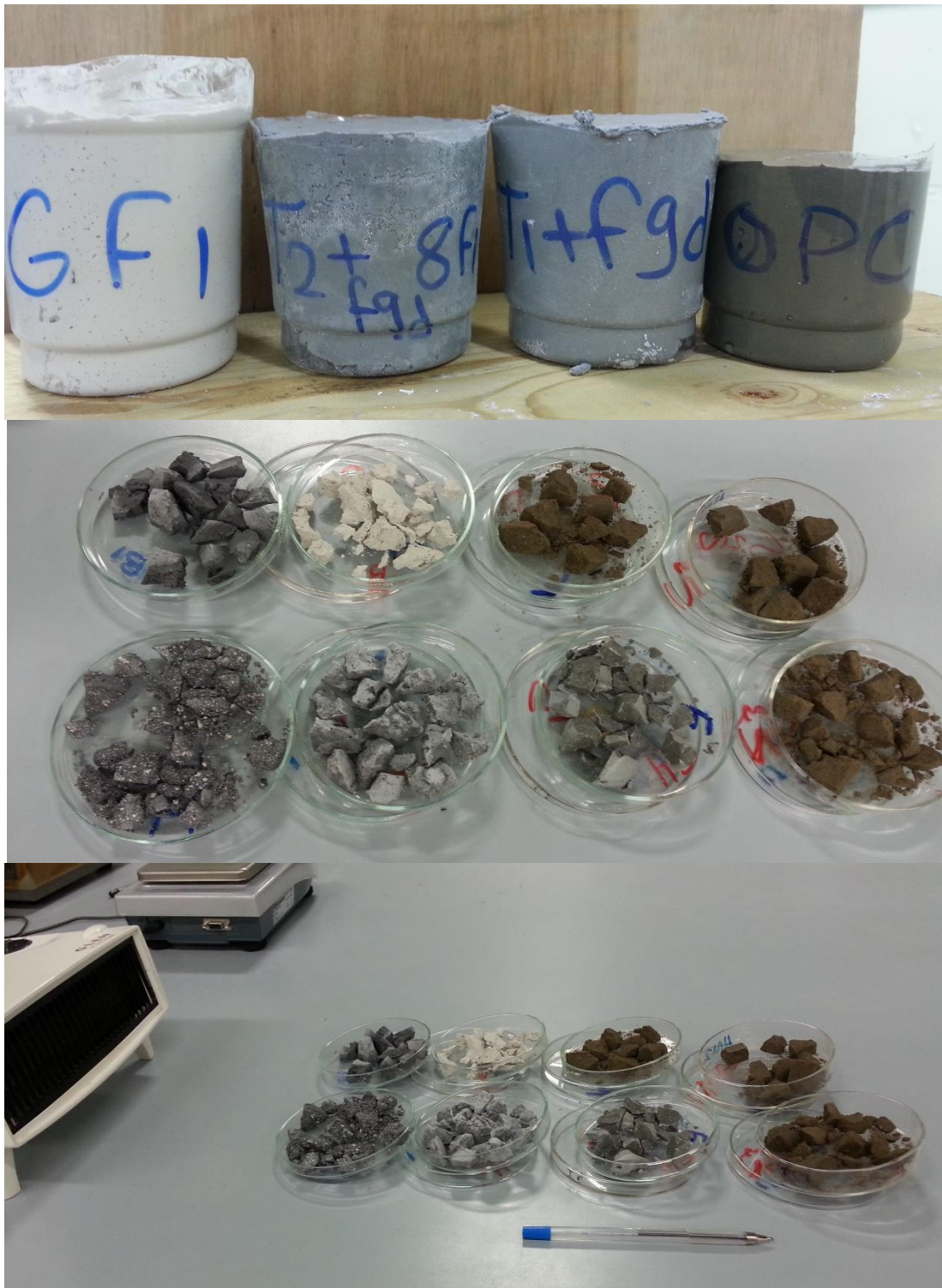


Figure 3.22 Common procedure of specimens preparation for hydration kinetics investigation.

3.3.11.2 X-Ray diffraction (XRD) analysis

This analysis was conducted to study the structural and phase compositions of pastes prepared from different blending of waste materials used in this research project. This type of analysis is represented by using a range of wavelengths of X-rays to penetrate the solid body of the pastes which to probe their internal structure. This technique makes it simple to understand and elucidate the development in the strength of pastes by monitoring the changes in their mineralogical structure and phase composition throughout the time of curing. In this study, the XRD analysis was carried out using a Rigaku Miniflex diffractometer with Cu-K α X-ray radiation, and voltage 30kV as shown in Figure 3.23. A current of 15mA was used with a scanning speed of 2.0 degree/min in continuous scan mode from 5 to 65°.



Figure 3.23 The instrument used for XRD analysis.

After achieving the dry fragments, using the preparation procedure explained in section 3.3.11.1, dry powder samples were prepared by pulverising parts of the pieces to a smaller size using a wooden hammer. Then a small mortar and pestle were used to increase the fineness. The resulting samples were passed through a sieve size 300 μ m to provide fine powders in order to avoid carbonation. Then, the samples were pressed into circular aluminium plates to be ready for analysis. A similar procedure was adopted by (Ramachandran and Beaudoin, 2001; Sadique *et al.*, 2013). Figure 3.24 shows the sequence of XRD samples preparation. The powder diffraction file (PDF)

database was used to compare the achieved patterns with standard patterns of different compounds, so as to identify the unknown compounds.



Figure 3.24 Steps of sample preparation for XRD analysis.

3.3.11.3 Scanning Electronic Microscopy (SEM) and Energy Dispersive X-ray Spectroscopy (EDX) Analyses

SEM is a high-resolution imaging technique which enables the investigation of the microstructure of an object. Energy dispersive X-ray analysis is used to examine the elemental composition of materials. In the modern SEM imaging process, EDX analysis has usually been used in conjunction with scanning electron microscopy testing to examine the morphology of an object as well as to analyse its elemental composition; in this case, such analysis is called SEM/EDX analysis (Cardell and Guerra, 2016). These analyses were carried out on soil treated samples as well as pastes prepared from the optimum mixture of the newly developed binder. Additionally, reference mixtures of a cement-treated soil and cement paste cured at

periods similar to those for other mixes were also analysed. The EDX Oxford Inca x-ray detector and FEI SEM model Inspect S instruments shown in Figure 3.25 were used in this study. Since cement pastes (or pastes prepared from mixing of different cementitious materials) tend to be non-conductive, the samples for these analyses were coated with a thin layer of an electrically conductive material (Zhang *et al.*, 2014; Rêgo *et al.*, 2015). Palladium was used as a coating material in this study, and the sample preparation procedure is illustrated in Figure 3.26.

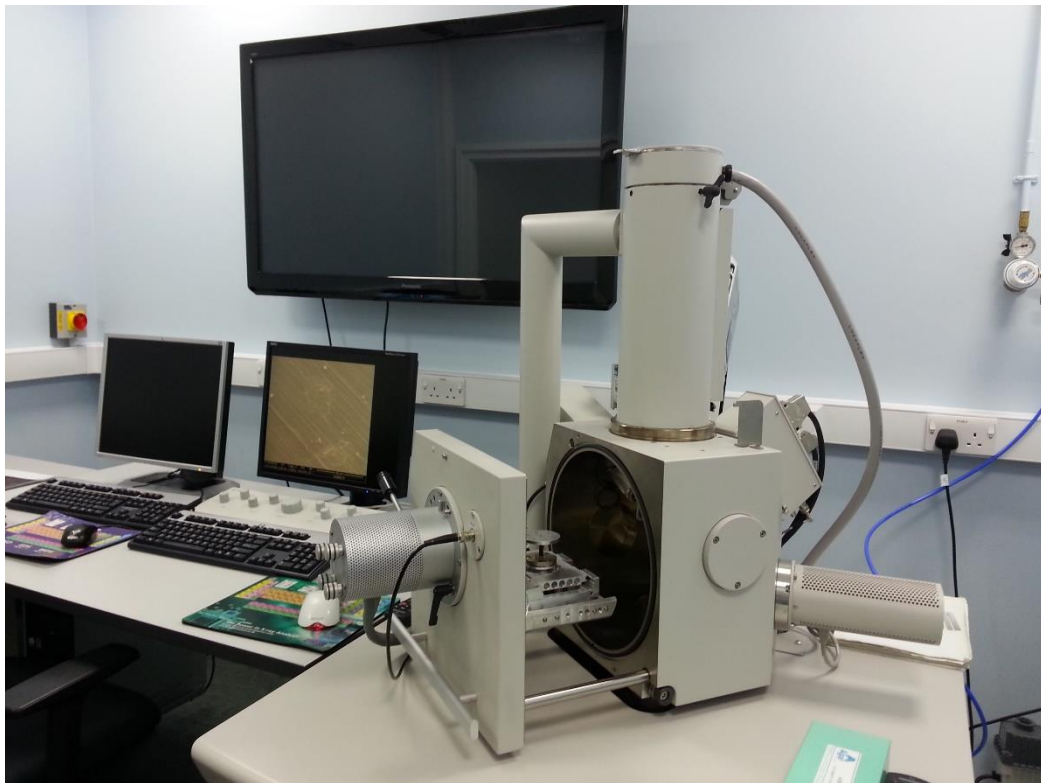


Figure 3.25 The instrument used for SEM/EDX analysis in this study.

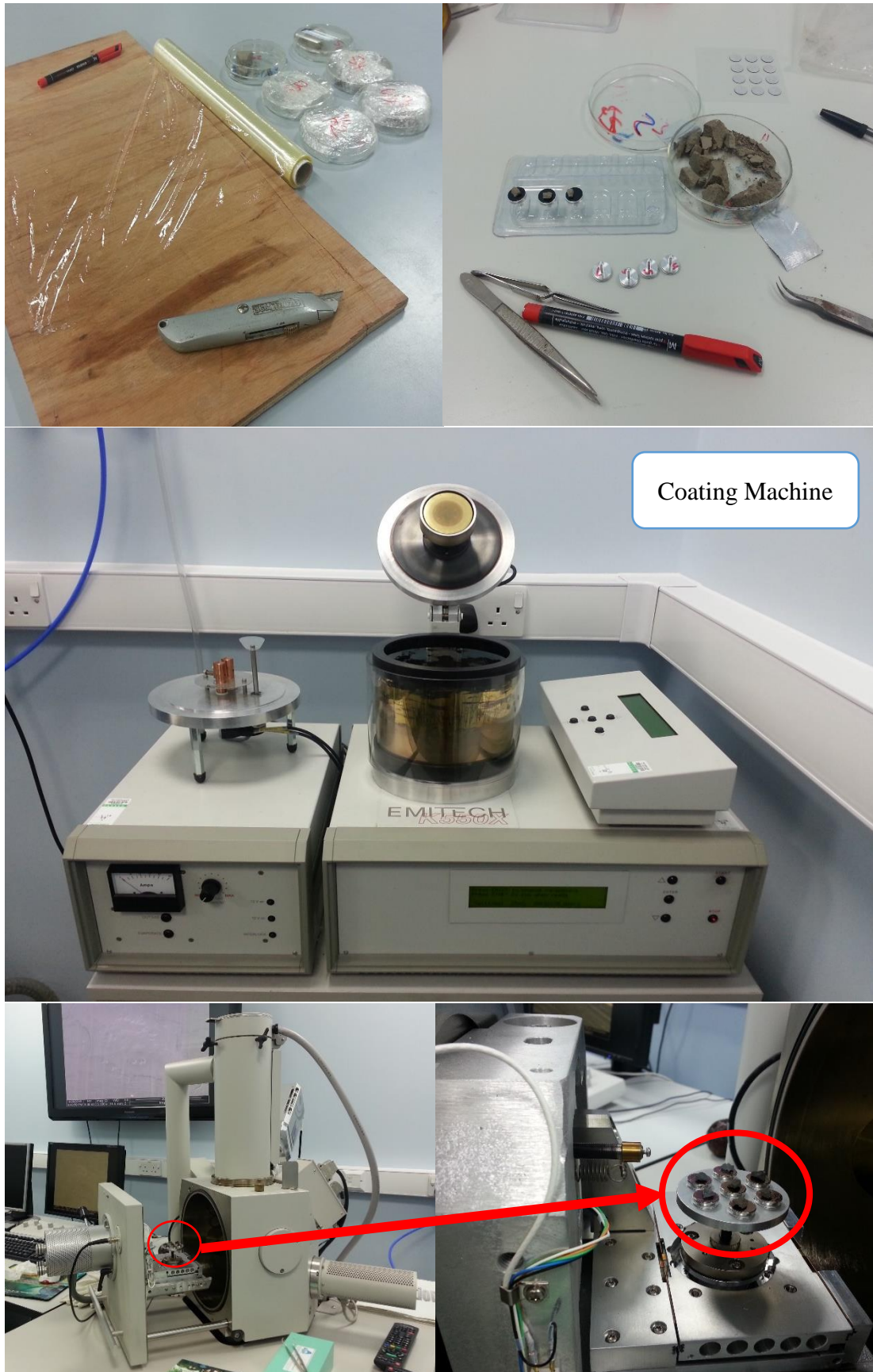


Figure 3.26 Steps of SEM/XRD samples set up.

3.4 SUMMARY

As a summary of the above, the testing programme in this study can be broken down into different stages of experimental works, and these stages are as follows:

- Experiments used for the soil classification and candidate materials identification: The output of this stage was the selection of a group containing four waste materials which were involved in the further experimental works. These waste materials were (WPSA, POFA, RHA, and FGD gypsum), the experiments that were performed in this stage are listed in Table 3.2.
- Optimisation stages: This covers the optimisation for WPSA content to determine optimum binder content, the optimisation for the binary mixture (WPSA and POFA) and ternary blending optimisation (WPSA, POFA, and RHA) along with the investigation of the effects of mechanical activation (using grinding) and FGD as a grinding agent. The output of this stage was the identification of the optimal mixtures (unary, binary, ternary, and activated ternary). Table 3.3, 3.4, and 3.5 illustrate the experiments that were utilised for unary, binary and ternary investigations respectively.
- Experimental works to investigate the influence of the optimal mixtures, developed in the optimisation stages, on the other geotechnical properties of the treated soil such as compressibility and durability: A comparison of the performance of these mixtures added to the soil with that for cement treated soil was carried out at this stage.
- The investigation of hydration kinetics for both treated soil and pastes of binders was conducted by XRD, EDX, and SEM analyses: The output of this stage represented the understanding and elucidation of the achieved development in the strength of treated soil. Table 3.6 shows the experimental program which was adopted for the last two stages in this study.

Table 3.2 Soil classification and candidate materials identification test.

Test/Analysis	VS*	WPSA*	PFA1	PFA2	RHA*	SF	POFA*	FGD*	OPC*
Natural moisture content % (for undried soil sample)	*								
PSD (Sieve and hydrometer analysis)	*								
PSD (laser particle analyser)		*	*	*	*	*	*	*	*
Atterberg limits (LL, PL, PI)	*								
Compaction parameters (MMD and OMC)	*								
Loss on Ignition (%)	*	*	*	*	*	*	*	*	*
Specific gravity (particle density), Gs	*	*	*	*	*	*	*	*	*
UCS for undisturbed soil	*								
pH test	*	*	*	*	*	*	*	*	*
XRF	*	*	*	*	*	*	*	*	*
XRD	*	*	*	*	*	*	*	*	*
SEM	*	*	*	*	*	*	*	*	*

* Materials that were involved in the experimental programme of this study later on.

* Conducted test or analysis.

Table 3.3 Optimisation for WPSA content and reference mixture (OPC-Soil)

Test/Analysis		WPSA (%)					OPC (%)					
		0.0	3.0	6.0	9.0	12.0*	15.0	3.0	6.0	9.0	12.0**	15.0
Compaction parameters test (MDD and OMC)		*	*	*	*	*	*	*	*	*	*	*
Atterberg limits (LL, PL, PI)		*	*	*	*	*	*	*	*	*	*	*
UCS test for specimens cured at different curing periods (days)	0	*	*	*	*	*	*	*	*	*	*	*
	7	*	*	*	*	*	*	*	*	*	*	*
	14	*	*	*	*	*	*	*	*	*	*	*
	28	*	*	*	*	*	*	*	*	*	*	*
	90							*	*		*	
	180							*	*		*	
	360							*	*		*	

* 12.0% of WPSA was the optimum and it was adopted for unary mixture (U) in further experiments.

** 12.0% OPC was considered as the binder content for the reference mixture for comparison purpose.

Table 3.4 Optimisation for Unary, and binary mixtures.

Test/Analysis		Ground activation of U (ground period in minutes)				Binary blending optimisation (WPSA+POFA)=12% binder content			
		10*	20	30	40	10.5+1.5	9+3**	7.5+4.5	6+6
Compaction parameters test (MDD and OMC)						*	*	*	*
Atterberg limits (LL, PL, PI)						*	*	*	*
UCS test for specimens cured at different curing periods (days)	7	*	*	*	*	*	*	*	*
	14					*	*	*	*
	28	*	*	*	*	*	*	*	*

* Best time period of grinding which resulted in ground activated unary mixture (GU) which was the first optimum mixture.

** The optimum binary mixture (BM) which was considered as the optimum binary mixture for the further experiments.

Table 3.5 Optimisation for ternary blending.

Test/Analysis		Ternary blending optimisation (WPSA+POFA+RHA) = 12% binder content					Ground activation; G (15min.) with the effect of 5% FGD by the binder content				
		9+0 +3	9+1.5 +1.5 ^{*1}	7.5+1.5 +3	7.5+3 +1.5	8+2 +2 ^{*2}	6+0 +6	GT1	GT1+FGD ^{**}	GT2	GT2+FGD ^{**}
Compaction parameters test (MDD and OMC)		*	*	*	*	*	*	*	*	*	*
Atterberg limits (LL, PL, PI)		*	*	*	*	*	*	-	*	-	*
UCS test for specimens cured at different curing periods (days)	7	*	*	*	*	*	*	*	*	*	*
	14	*	*	*	*	*	*	*	*	*	*
	28	*	*	*	*	*	*	*	*	*	*

^{*1} The first optimal ternary mixture which was marked as T1.

^{*2} The second optimal ternary mixture which was marked as T2.

^{**} The optimum ternary mixtures (1 and 2) after applying grinding activation with 5 percent of FGD by the binder content.

Table 3.6 Comparison the performance of the optimum mixtures with that of reference mixture.

Test/Analysis	VS	UA		BM		T2		T2+FGD		RE	
		M*	P**	M	P	M	P	M	P	M	P
Atterberg limits Comparison (LL, PL, and PI)	*	*		*		*		*		*	
PSD (laser particle analyser) dry mixtures of the binders only	*		*		*		*		*		*
UCS at different ages (3, 7, 14, 28, 90, and 180 days)		*		*		*		*		*	
Consolidation test (at 7 and 28 days for treated soil)	*	*		*		*		*		*	
Wet-Dry cycles effect (1, 3, 7)	*	*		*		*		*		*	
XRD for dry powder mixtures and pastes cured for 3, 7, 28, and 180 days									*		*
SEM for dry powders, and mixtures and pastes cured for 3, 7, 28, and 180	*							*	*	*	*
EDX for pastes cured for 28 and 180 days									*		*

* M refers to the paste of soil-binder mixture.

** P refers to the binder paste only.

CHAPTER 4

RESULTS OF MATERIALS IDENTIFICATION

4.1 INTRODUCTION

This chapter contains the results and discussion of the experimental works regarding the identification of physical and chemical properties of the soft soil as well as the candidate materials used in this research project. In this chapter, the physical, chemical and geotechnical properties of the soft soil used in this study are initially presented and discussed. The group of the soil used was identified via the unified soil classification system (USCS). After that, the results of experimental works for the identification of the physical and chemical properties of the candidate materials and their potential to be used as cement replacements are presented. Furthermore, a comparison was conducted between the properties of the candidate materials with those of a commercial type of cement (OPC) to select the most suitable materials to be involved in the mix design experiments at a later stage.

4.2 VIRGIN SOIL PROPERTIES AND CLASSIFICATION

4.2.1 Physical and Geotechnical Properties.

The results of particle size distribution of the soil used in this study are shown in Figure 4.1. From this Figure, it was found that the clay, silt and sand contents of the soil used were 43.0, 43.92, and 13.08% respectively. The tested soil was very fine, and there were no particles with gravel size. Moreover, the soil used in this study had a high clay content, and this result was confirmed by the SEM image shown in Figure 4.2. The SEM imaging test demonstrated a high content of flaky shaped particles accumulated on each other which are known as clay minerals.

Figure 4.3 shows the results of the cone penetration tests after conducting three trials as per the British Standard BS 1377-2:1990 (British Standard, 1998a). These tests were used to measure the liquid limit (LL) of the soil used in this study which was obtained

from the water content value for 20mm of penetration, which was 40%. Additionally, the plastic limit of untreated soil was found to be equal to 23.78 %.

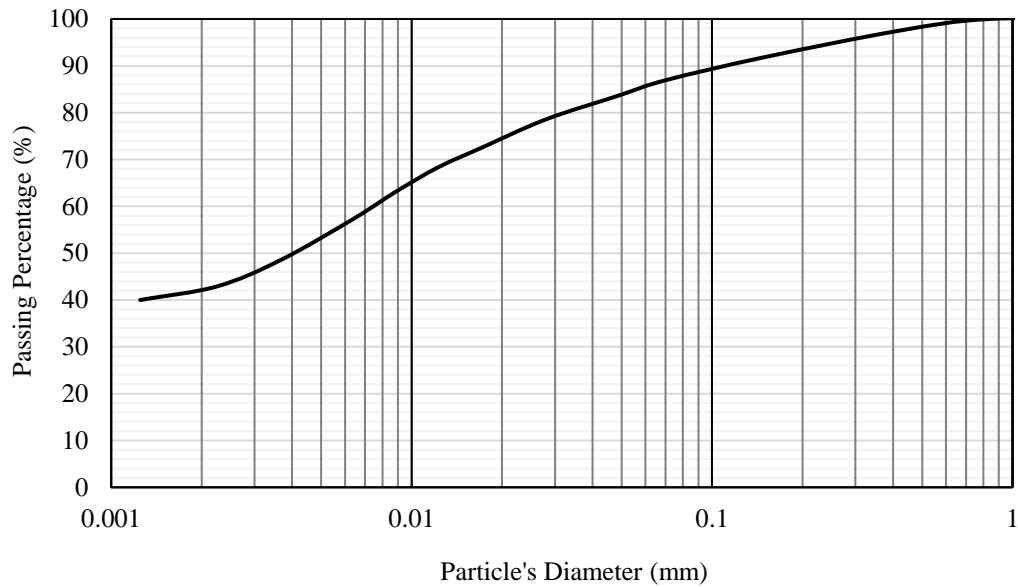


Figure 4.1 Particles size distribution curve of the virgin soil.

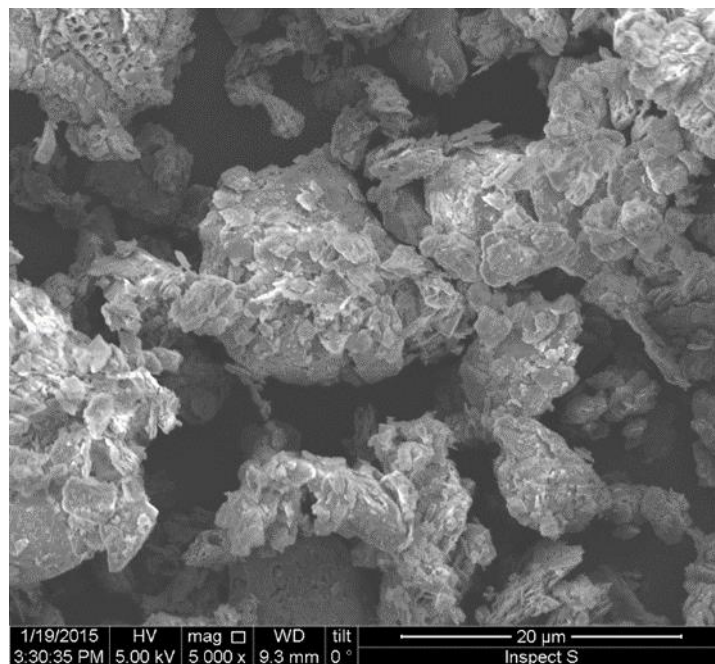


Figure 4.2 SEM image for the virgin soil used in this study.

The dry density – moisture content relationship of the soft soil used in this study achieved from the standard Proctor test is shown in Figure 4.4. This Figure was used to determine the maximum dry density (MDD) and the optimum moisture content (OMC) for untreated compacted soil. The MDD and OMC were found to be equal to

1.57Mg/m³, and 23.0% respectively. However, the natural moisture content of the undisturbed soil was 36.8% which indicated that this soil has a high water holding capacity.

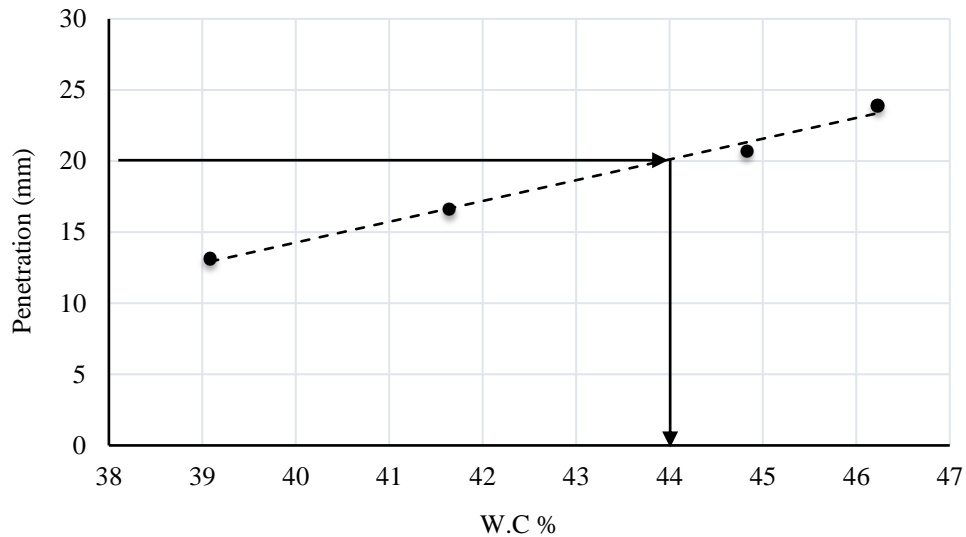


Figure 4.3 Cone penetration – water content relationship for LL determination.

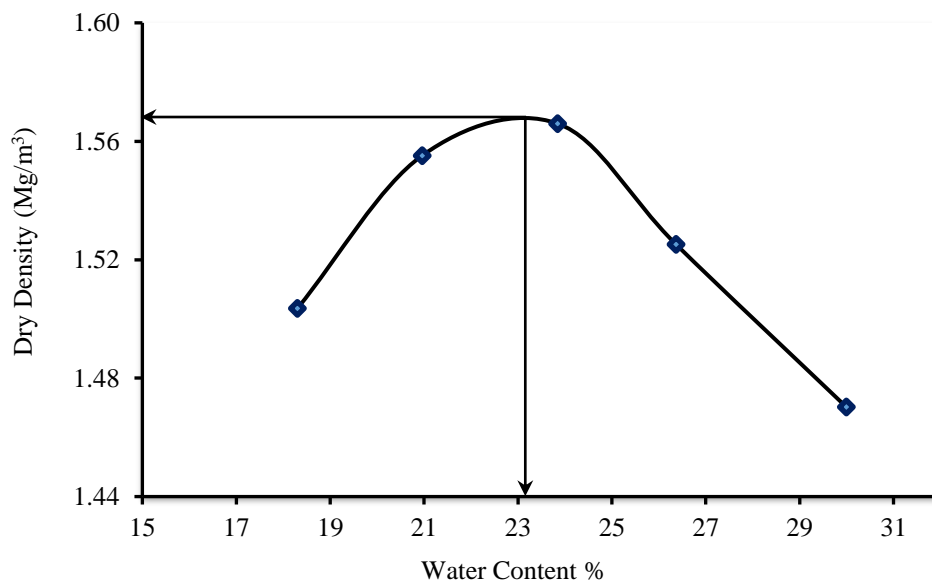


Figure 4.4 Standard Proctor compaction curve of the virgin soil.

The other physical and geotechnical properties of the virgin soil, such as particle density (specific gravity; G_s) and the unconfined compressive strength (UCS) for both the undisturbed and compacted untreated soil, are listed in Table 4.1.

Table 4.1 Main physical and geotechnical properties of the virgin soil.

Property		Value
Natural moisture content %		36.8
LL %		44
IP		20.22
Sand %		13.08
Silt %		43.92
Clay %		43.0
G _s		2.58
MDD (Mg/m ³)		1.57
OMC %		23.0
UCS (kPa)	Undisturbed	66.46
	Compacted untreated	202

4.2.2 Chemical Properties and Elemental Structure

The major oxides contents of the virgin soil which were obtained from the XRF analysis are listed in Table 4.2. This Table also illustrates the values of the soil pH and the organic matter content. The latter is expressed as a percentage of loss on ignition (LOI %). The pH value of the virgin soil was 7.78 while the LOI was 7.95% which indicates that this soil has an intermediate content of organic matter according to British standard BS EN ISO 14688-2:2004+A2013 (European Committee for Standardization, 2013).

Table 4.2 The chemical properties and oxides contents of the virgin soil.

Item	LOI %	pH	SiO ₂ %	Al ₂ O ₃ %	MgO %	CaO %	Fe ₂ O ₃ %	K ₂ O %	TiO ₂ %	SO ₃ %	Na ₂ O %
Value	7.95	7.78	59.88	7.33	2.86	4.49	3.85	2.96	0.75	0.34	1.34

The XRF analysis indicated that silicates were the major components of the soil oxides and the aluminates, magnesium and iron oxides were shown as minors. The diffraction patterns of the powder state of the soil used in this study obtained from the XRD analysis are shown in Figure 4.5. The analysis of the XRD revealed that the major crystals of the virgin soil were quartz (SiO_2) and kaolinite while illite and smectite were indicated as minor crystals.

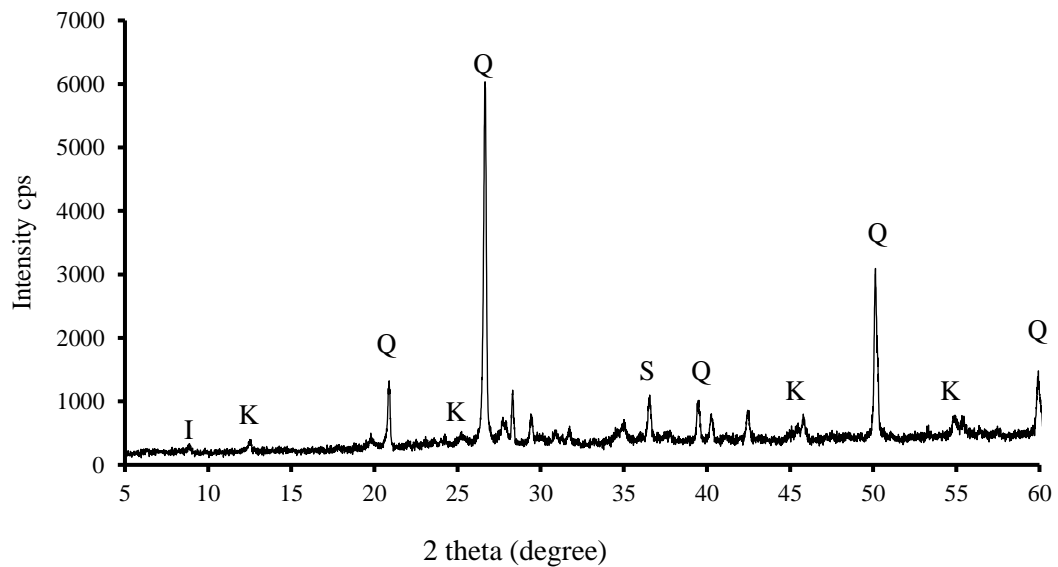


Figure 4.5 XRD pattern diagram of the virgin soil. (Q: quartz, K: kaolinite, S: smectite, and I: illite)

4.2.3 Soil Classification

Figure 4.6 shows the plasticity chart according to the unified soil classification system which was considered to identify the group symbol of the soil used in this study. The highlighted green mark in this Figure refers to the intersection point between the soil LL and PL values. Consequently, according to the location of the soil used in this study on the plasticity chart, and depending on its chemical characteristics, especially the organic matter content, the soil used in this study was classified as an intermediate plasticity silty clay with medium organic content and its symbol was CI. This classification agrees with BS EN ISO 14688-2:2004+A2013 (European Committee for Standardization, 2013).

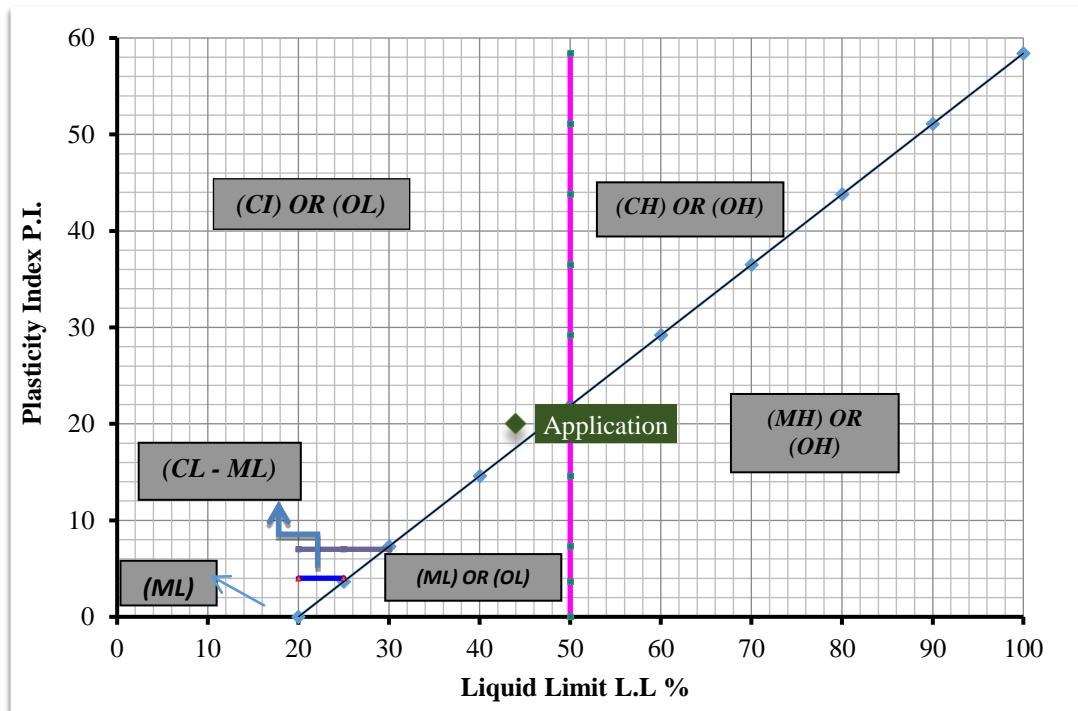


Figure 4.6 Plasticity chart for the soil used in this study.

4.3 CANDIDATE MATERIALS CHARACTERISATION

According to the review of literature and research documentation, and as stated in the methodology of this research study, the WPSA and some of by-products and industrial waste materials along with commercial silica fume and OPC were characterised in this study. The waste materials were collected from different industry sectors from inside and outside the UK, and their most important physical, chemical, mineralogical and morphological properties were identified to explore and assess their potential in cement replacement. The examined properties of the candidate materials used in this study are presented as follows:

4.3.1 Reference Cement (OPC)

As mentioned in the previous chapter of this study, a commercial ordinary Portland Cement CEM-II/A/LL 32.5-N was used as a reference binder. The chemical compositions of this cement along with its pH value and loss on ignition are listed in Table 4.3. The chemical properties of the reference cement used in this study were found to be similar to those of the cement analysed by Sadique *et al.* (2013). The diffraction patterns of the reference OPC, which were obtained from XRD analysis,

are shown in Figure 4.7. The mineralogical analysis revealed that the reference cement was composed of calcite (CaCO_3), alite (3CaOSiO_2), belite (2CaOSiO_2), periclase (MgO), and ferrite ($4\text{CaOAl}_2\text{O}_3 \cdot \text{Fe}_2\text{O}_3$). The particle size distribution (PSD) of the reference cement indicated that the dominant particle sizes are between 10 and 30 μm . Nevertheless, a considerable number of particles were in sub-micron size which might have the effect to reduce the medium particle size of the reference OPC as shown in Figure 4.8. The SEM image of OPC used as a reference binder in this study is shown in Figure 4.9. This Figure revealed that the OPC particles have either crystal or spherical shaped particles along with a small amount of irregular shaped particles.

Table 4.3 The chemical properties and XRF analysis of the reference cement.

Item	LOI %	pH	CaO %	SiO ₂ %	Al ₂ O ₃ %	MgO %	Fe ₂ O ₃ %	K ₂ O %	SO ₃ %	Na ₂ O %
Value	0.28	13.04	65.21	24.56	1.7	1.3	1.64	0.82	2.62	1.34

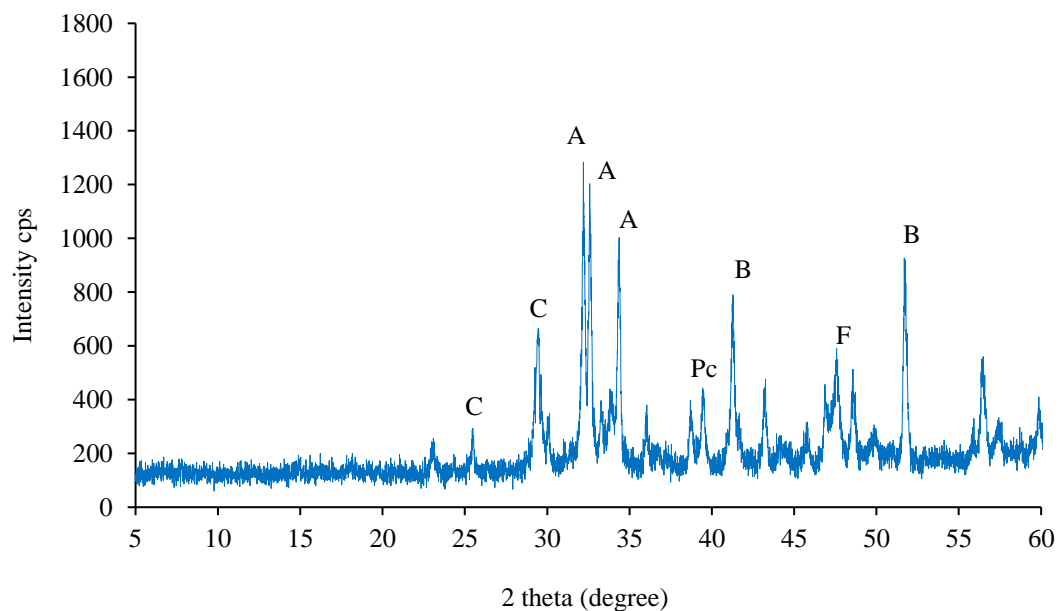


Figure 4.7 XRD pattern diagram for the reference OPC. (C: calcite, A: alite, Pc: periclase, B: belite, and F: ferrite)

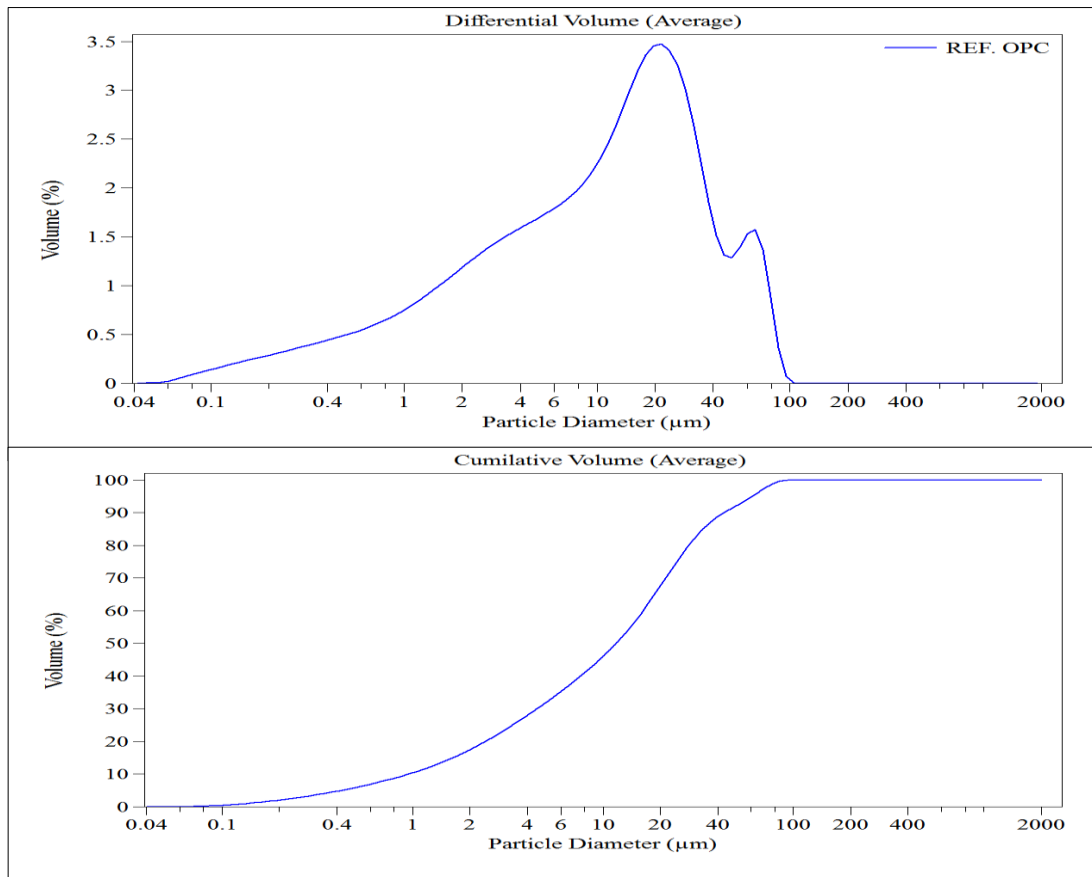


Figure 4.8 Particle size distribution of the reference cement.

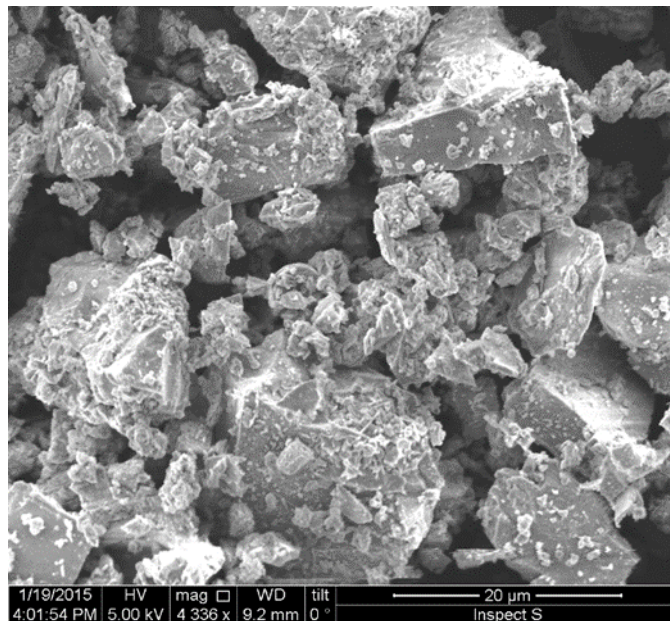


Figure 4.9 SEM image for powder state of reference cement.

4.3.2 Waste Paper Sludge Ash (WPSA)

There were two different grades of WPSA (coarse and fine) which were characterised in this study. These samples were supplied by Aylesford Newsprint Ltd. The WPSA supplied is produced from the combustion of waste paper sludge, which is used as fuel, in power generation plants at AN Ltd. A temperature of 850°C is maintained as the incineration temperature in these plants which are using a fluidised bed combustion (FBC) system to capture sulphur and nitric oxides released during combustion. The measured particle densities of both coarse grade WPSA (C-WPSA) and fine grade WPSA (F-WPSA) were 2.72Mg/m³ and 2.92Mg/m³ respectively. Whereas, 2.85Mg/m³ was reported by Segui (Segui *et al.*, 2012); however, a low value of 1.72Mg/m³ was reported by Fava (Fava *et al.*, 2011). The chemical properties of both types of WPSA along with those reported by Lisbona (Lisbona *et al.*, 2012) are listed in Table 4.4. From this Table, it can be seen that the XRF analysis for both grades of WPSA used in this study revealed an impressive content of calcium and silica oxides in comparison to those reported by Lisbona. However, the XRF analysis results showed that both grades of WPSA have very similar chemical compositions. Moreover, a noticeable amount of alumina was also shown by the XRF analysis. These variations might be due to the differences in the source as well as the combustion conditions.

Table 4.4 The chemical compositions of both grades of WPSA used in this study.

Item	pH	CaO %	SiO ₂ %	Al ₂ O ₃ %	MgO %	Fe ₂ O ₃ %	K ₂ O %	SO ₃ %	Na ₂ O %	TiO ₂ %
C- WPSA	12.28	66.38	24.73	2.11	2.52	0.02	0.33	0.33	1.73	0.67
F- WPSA	12.86	66.76	25.12	2.38	2.57	0.03	0.31	0.26	1.72	0.41
(Lisbona <i>et al.</i> , 2012)	11.9	55.30	11.22	9.62	1.18	0.72	0.21	0.38	0.12	0.49

The XRD analysis of both grades of WPSA revealed that the primary compounds were calcite (CaCO_3), lime (CaO), gehlenite ($\text{CaAl}[\text{AlSiO}_7]$), merwinite ($\text{Ca}_3\text{Mg}[\text{SiO}_4]$), mayenite ($\text{Ca}_{12}\text{Al}_{14}\text{O}_{33}$), and quartz (SiO_2) as shown in Figure 4.10. From this Figure, the differences in mineralogical phases between C-WPSA and F-WPSA can be recognised. Figure 4.11 demonstrates the PSD for both grades of WPSA; the variation in particle sizes was very clear. The PSD tests indicated that there was a significant difference in the median diameter (d_{50}) between the coarse and fine grade of WPSA where it was $275.6\mu\text{m}$ for C-WPSA and $26.14\mu\text{m}$ for F-WPSA. Moreover, most particles of C-WPSA are in the size range from $150\mu\text{m}$ to $600\mu\text{m}$, while they are ranged from $4\mu\text{m}$ to $300\mu\text{m}$ for F-WPSA. SEM images shown in Figure 4.12 indicated that the particles of WPSA were coagulated and had irregular shapes.

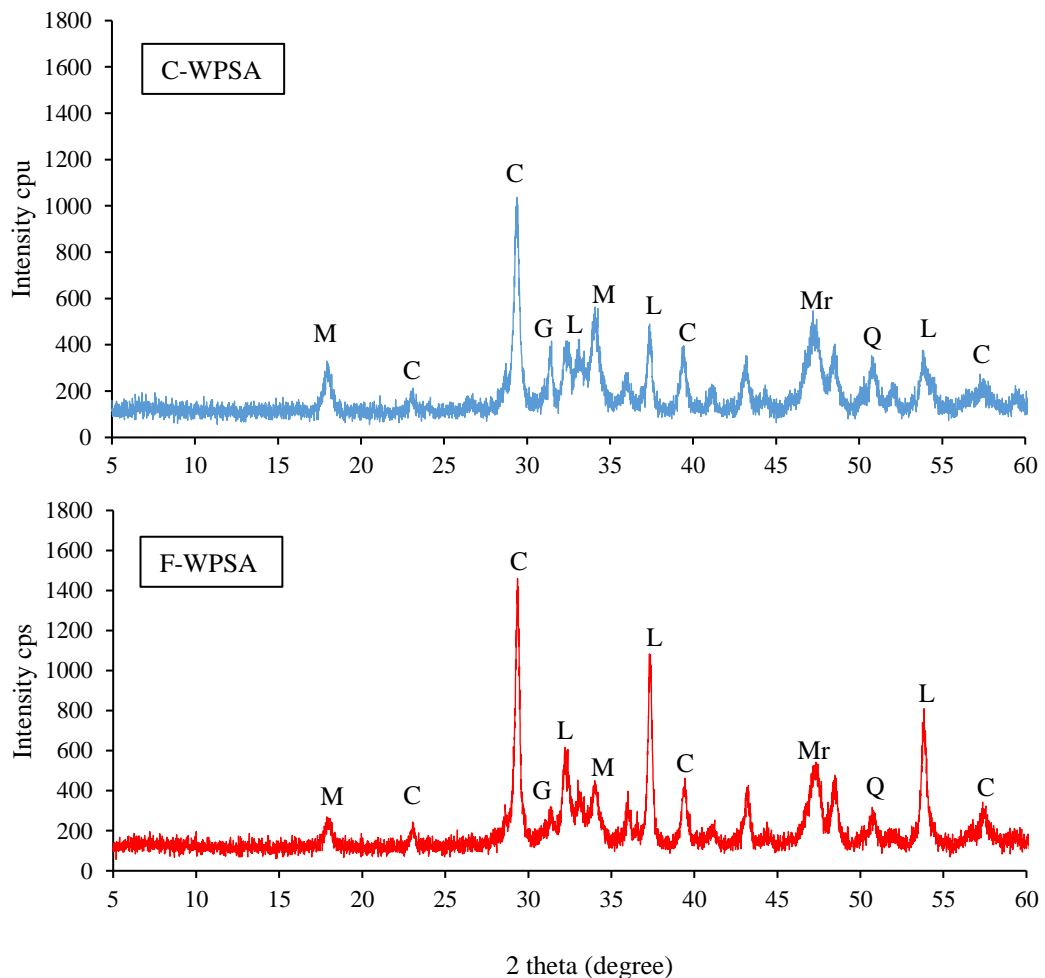


Figure 4.10 XRD pattern diagrams for coarse and fine WPSA used in this study. (C: calcite, L: lime, G: gehlenite, M: mayenite, Mr: merwinite, and Q: quartz).

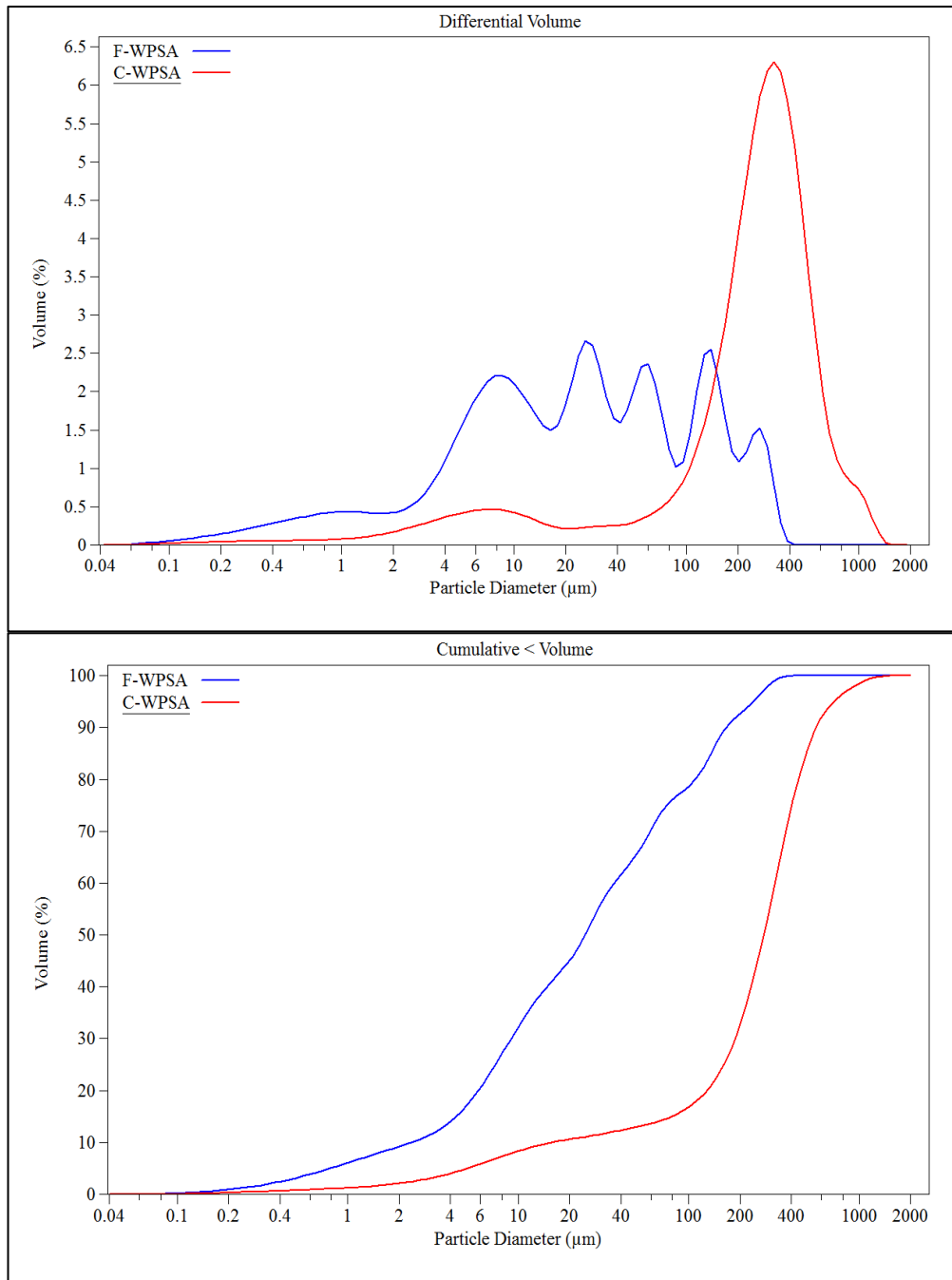


Figure 4.11 PSD of WPSA used in this study.

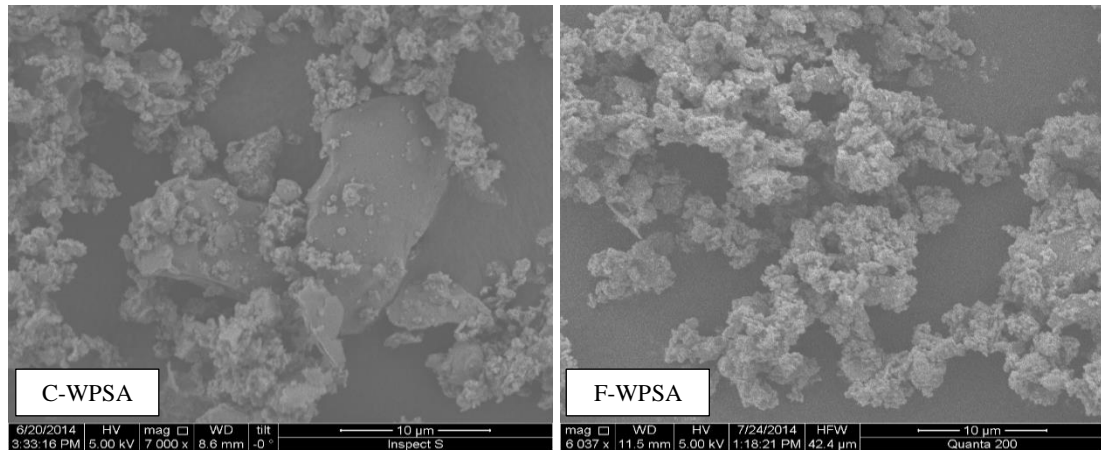


Figure 4.12 SEM images for both grades of WPSA.

4.3.3 Palm Oil Fuel Ash (POFA)

The POFA used in this study was sieved to remove the incompletely combusted materials using sieve size 150 μm . Additionally, POFA was ground using low grinding energy for approximately 15 minutes to increase its fineness and to enhance its pozzolanic reactivity (Aprianti *et al.*, 2015). Awal and Shehu (2013) adopted a similar procedure for their POFA preparation. They prepared the POFA by sieving the ash obtained from the foot of the flue tower using a 150 μm filter then the ash was ground using a modified Los Angeles abrasion machine with ten stainless steel bars instead of steel balls. The particle density of the untreated POFA was measured, and was found to be 2.1Mg/m³ while it was increased after treatment by sieving and grinding to become equal to 2.23Mg/m³. The chemical properties of the treated POFA are listed in Table 4.5. From this Table, a high pH value can be seen for this material which would contribute to maintaining an alkaline environment to the hydration reactivity. Moreover, the results of XRF analysis of POFA revealed that the major oxides were pozzolanic oxides represented by SiO₂, Al₂O₃, and Fe₂O₃ along with a noticeable content of Potassium oxide (K₂O). Similar chemical properties were reported by Chindaprasirt *et al.* (2014) for POFA with slight differences, especially in Potassium and Aluminium oxides (Table 4.5). The X-Ray diffraction analysis, shown in Figure 4.13, revealed that the dominant mineral phase of the treated POFA was quartz (SiO₂), while cristobalite (SiO₂) and potassium aluminium phosphate (K₃Al₂[PO₄]₃) were identified as secondary phases. The XRD results of the POFA in this study agreed with those reported by Ranjbar *et al.* (2014).

Table 4.5 Chemical properties of treated POFA.

Item	LOI %	pH	CaO %	SiO ₂ %	Al ₂ O ₃ %	MgO %	Fe ₂ O ₃ %	K ₂ O %	SO ₃ %	Na ₂ O %
This study (Chindaprasirt <i>et al.</i>, 2014)	2.78	13.04	10.47	61.36	7.51	5.64	1.54	7.53	2.93	1.73
(Chindaprasirt <i>et al.</i>, 2014)	5.2	-	12.5	55.7	0.9	5.1	2.0	11.9	2.9	1.0

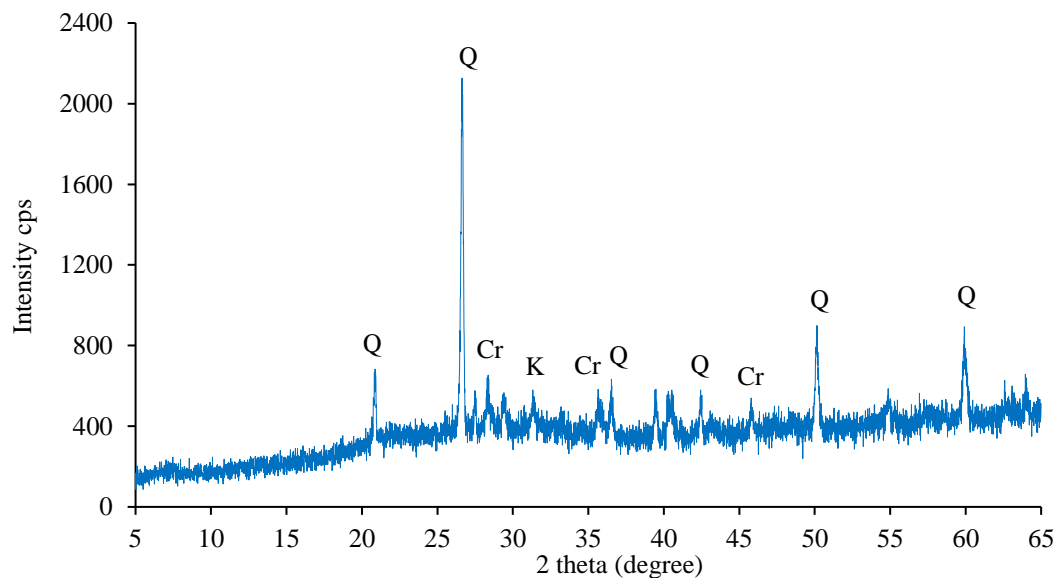


Figure 4.13 The XRD pattern of treated POFA. (Q: quartz, Cr: cristobalite, and K: potassium aluminium phosphate)

The sieving process and grinding treatment showed an apparent reduction in the median particle size (d_{50}) where it was decreased from 57.55 μm for virgin POFA to 29.29 μm for the treated POFA; this reduction would produce a finer grade of POFA and improve its pozzolanic reactivity. The PSD of the virgin as well as the treated POFA, are shown in Figure 4.14. As shown in this Figure, most of the untreated POFA particles are ranged in size between 20 and 200 μm , while the particles of treated POFA are ranged between approximately 15 μm and 100 μm . Moreover, the PSD of the treated

POFA showed a better distribution due to the availability of small numbers of fine particles which are less than $10\mu\text{m}$ in diameter. The SEM imaging test shown in Figure 4.15a and b revealed that the virgin POFA has a coagulated spherical particle shape as shown in Figure 4.15a, while the particle shape of the treated POFA were spherical with a small number of particles that do not have a particular shape (amorphous) as shown in Figure 4.15b.

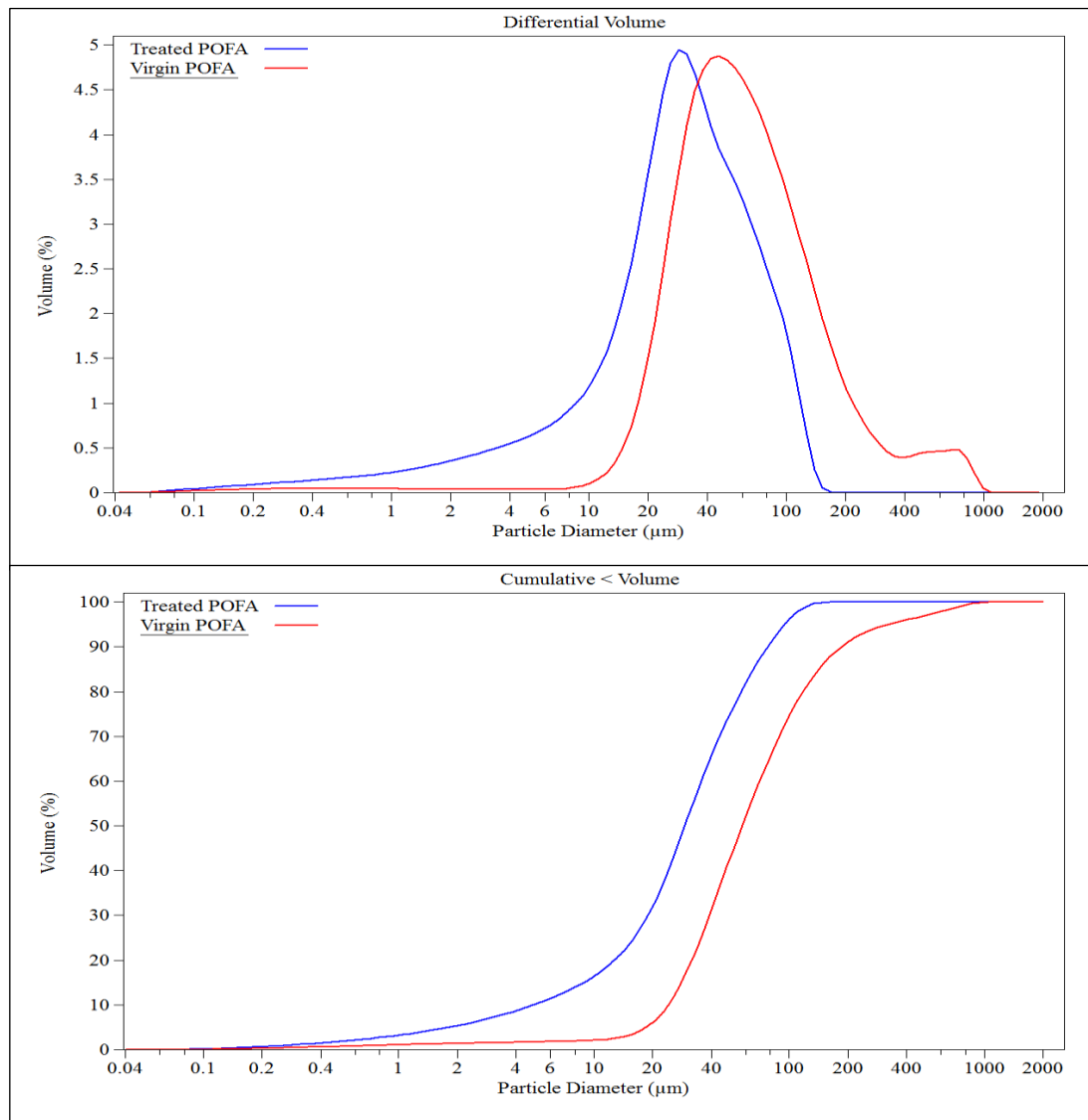


Figure 4.14 The PSD for both the virgin and treated POFA.

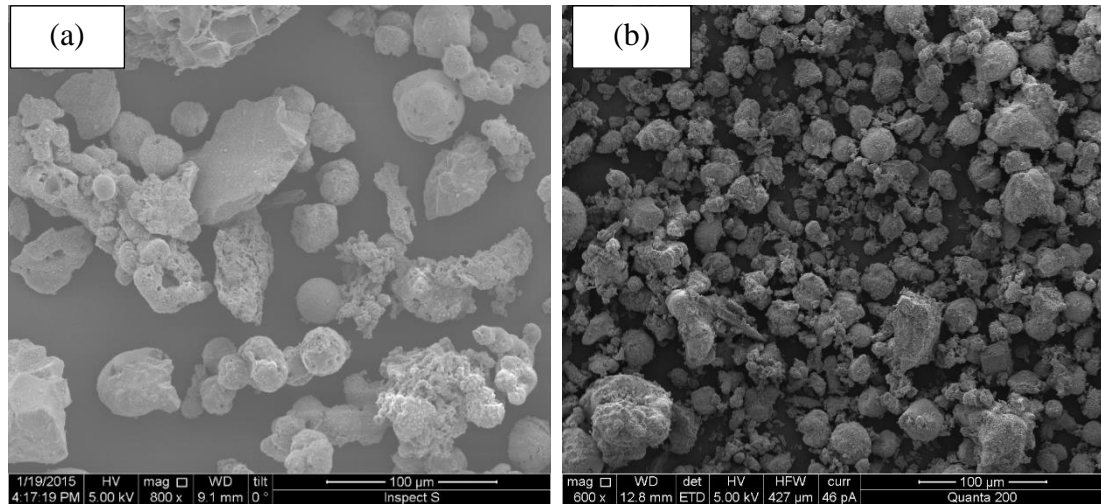


Figure 4.15 SEM images of POFA, (a) virgin, and (b) treated.

4.3.4 Rice Husk Ash (RHA)

The chemical properties of the RHA shown in Table 4.6 indicated that the RHA identified in the present study was composed of silica, which was 90.2%, along with other minor oxides such as aluminium, potassium, and sodium oxides. The pH value was measured, and it was found to be equal to 8.98 which means that the RHA used in this study was alkaline. Similar chemical properties of RHA were reported by Salas *et al.* (2009) as shown in Table 4.6. The results of XRD analysis shown in Figure 4.16 indicated that the RHA was composed of amorphous silica which may cause an increase in water demand. Figure 4.17 shows the PSD analysis of the dry powder of the RHA used in this study; the median particle size was found to be equal to 24.83 μm and the majority of RHA particles were ranged between 10 and 60 μm which gives an indication that the RHA used in this study was very fine. Nevertheless, the peak which appears between the sizes of approximately 29 and 38 μm , as per the PSD curve in Figure 4.17, which may be due to agglomeration occurring for the superfine particles. The SEM view shown in Figure 4.18 indicated that the particle shape of RHA was an angular or irregular which is the reason for the high specific surface area of RHA.

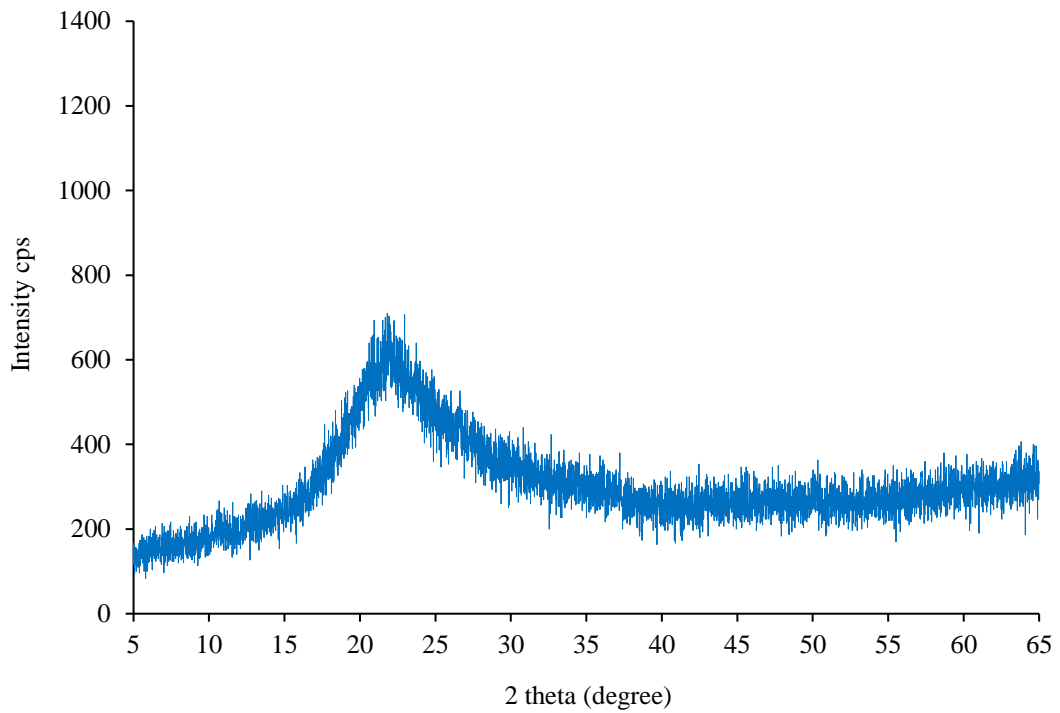


Figure 4.16 Diffraction patterns of RHA.

Table 4.6 Chemical properties of treated RHA.

Item	LOI %	pH	CaO %	SiO ₂ %	Al ₂ O ₃ %	MgO %	Fe ₂ O ₃ %	K ₂ O %	Na ₂ O %
This study	2.05	8.98	0.493	90.203	4.03	0.609	0.183	1.36	0.90
(Salas <i>et al.</i>, 2009)	--	--	1.23	90.0	0.68	0.35	0.42	2.8	0.32

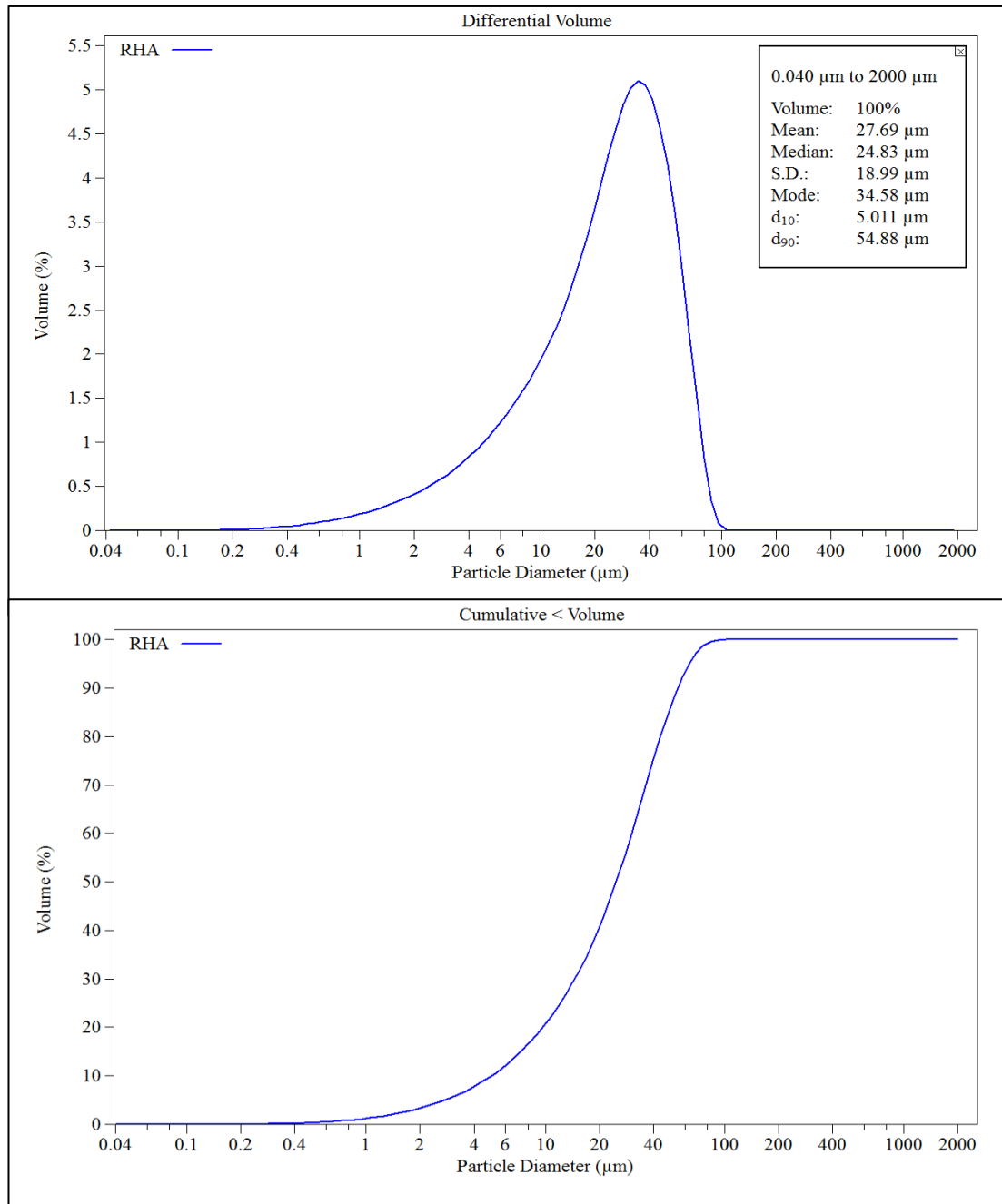


Figure 4.17 PSD of RHA used in this study.

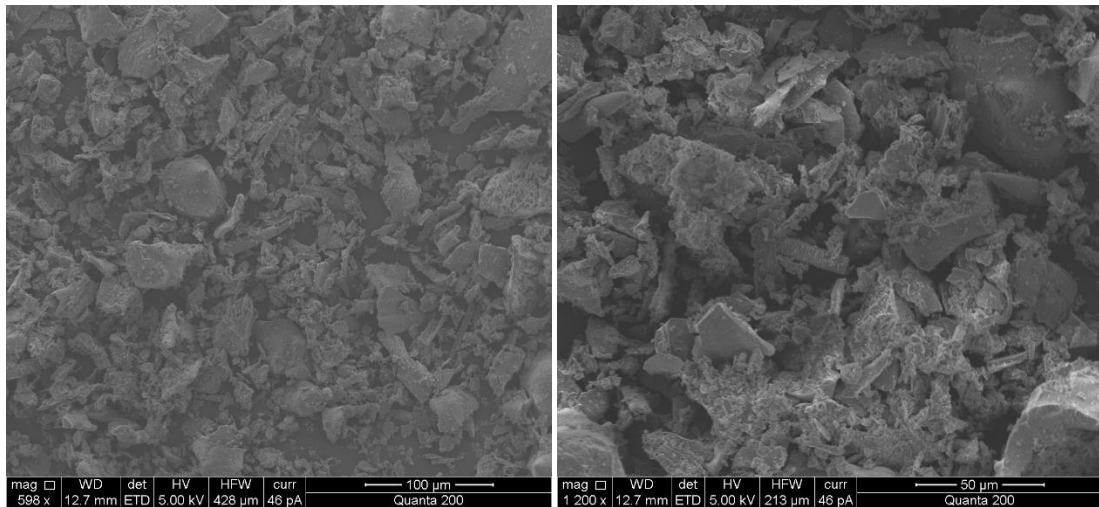


Figure 4.18 SEM images of RHA used in this study.

4.3.5 Pulverised Fuel Ash (PFA)

In this research project, two different types of PFA were characterised regarding their physical and chemical properties. PFA1 was supplied by the CEMEX company which was fly ash for concrete type 450-S according to the British standard BS EN 450-1 (European Committee for Standardization, 2012). While PFA2 was provided by SSE.com from the Fiddlers power station in Cuerdley, Warrington, UK. Table 4.7 shows the chemical properties of both types of PFA. From this Table, it can be seen that both PFA types have similar oxides contents especially the SiO_2 and CaO ; however, other oxides have different contents. Additionally, the loss on ignition test results revealed that LOI% of PFA2 was noticeably higher than that for PFA1 as shown in Table 4.7. The diffraction patterns of both types of PFA were similar with slight differences as shown in Figure 4.19. The XRD analyses revealed that the dominant glassy phase in both PFA types was quartz (SiO_2) in addition to the amorphous silica, while mullite was identified as a minor compound. The PSD shown in Figure 4.20 indicated that the particles of both PFA types have similar sizes and most of the particles are in the size range between $6\mu\text{m}$ and $30\mu\text{m}$. The median diameter (d_{50}) was $22.56\mu\text{m}$ for PFA1, while it was $35.04\mu\text{m}$ for PFA2 which indicated that PFA1 was slightly finer than PFA2. However, the sharp peak at $200\mu\text{m}$ in the PSD of PFA2 may be due to the agglomeration of ultrafine particles which was revealed in the SEM view

of this material as shown in Figure 4.21. The SEM images for both types of PFA revealed that they have almost spherical shape particles (Figure 4.21a and b).

Table 4.7 Chemical properties of PFA.

Item	LOI %	pH	CaO %	SiO ₂ %	Al ₂ O ₃ %	MgO %	Fe ₂ O ₃ %	K ₂ O %	SO ₃ %	Na ₂ O %
PFA1	2.45	10.68	4.47	57.05	9.56	8.25	9.29	3.29	1.14	1.74
PFA2	9.64	6.4	4.31	51.83	15.3	3.34	5.44	2.04	1.06	1.17

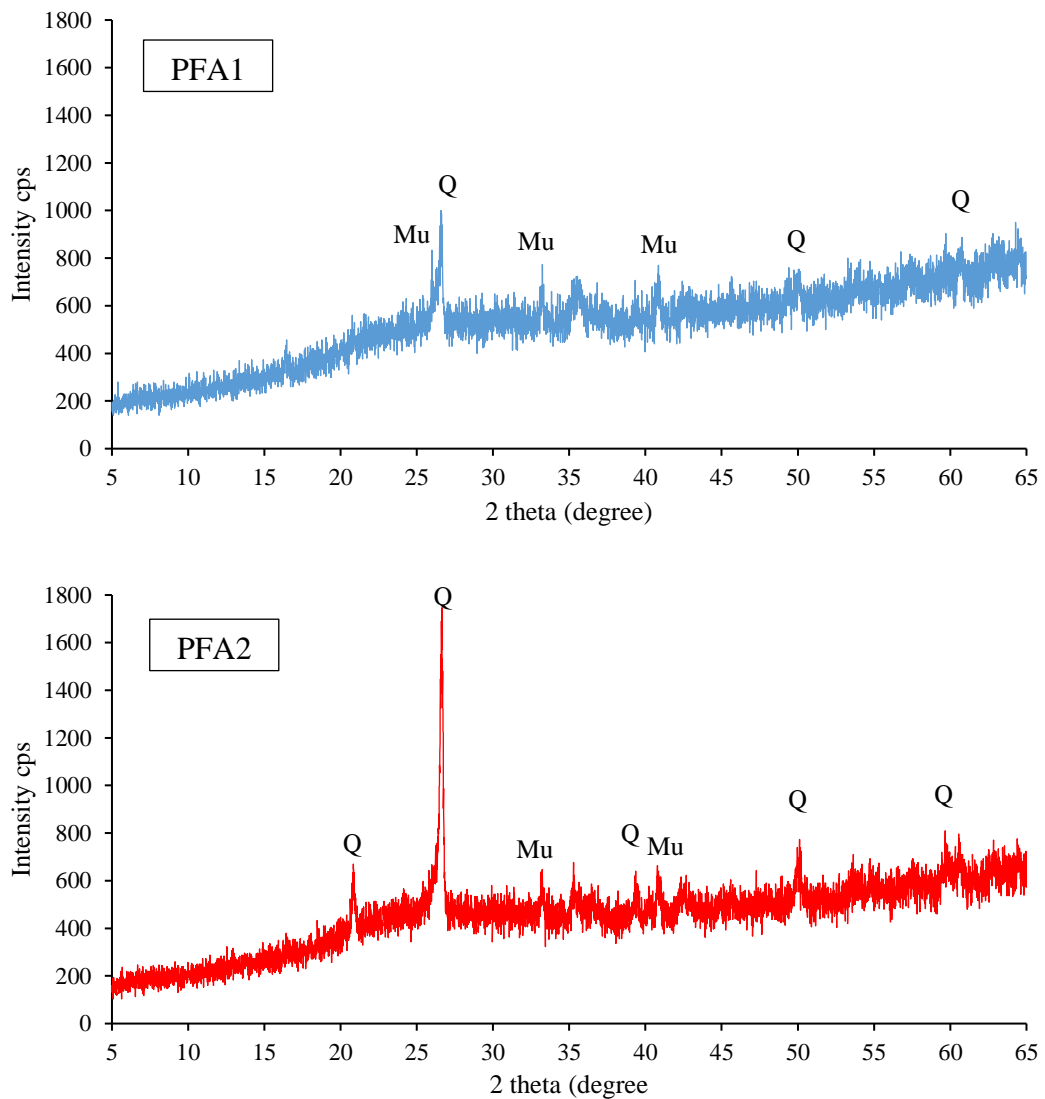


Figure 4.19 XRD patterns of PFA. (Q: quartz, and Mu: mullite)

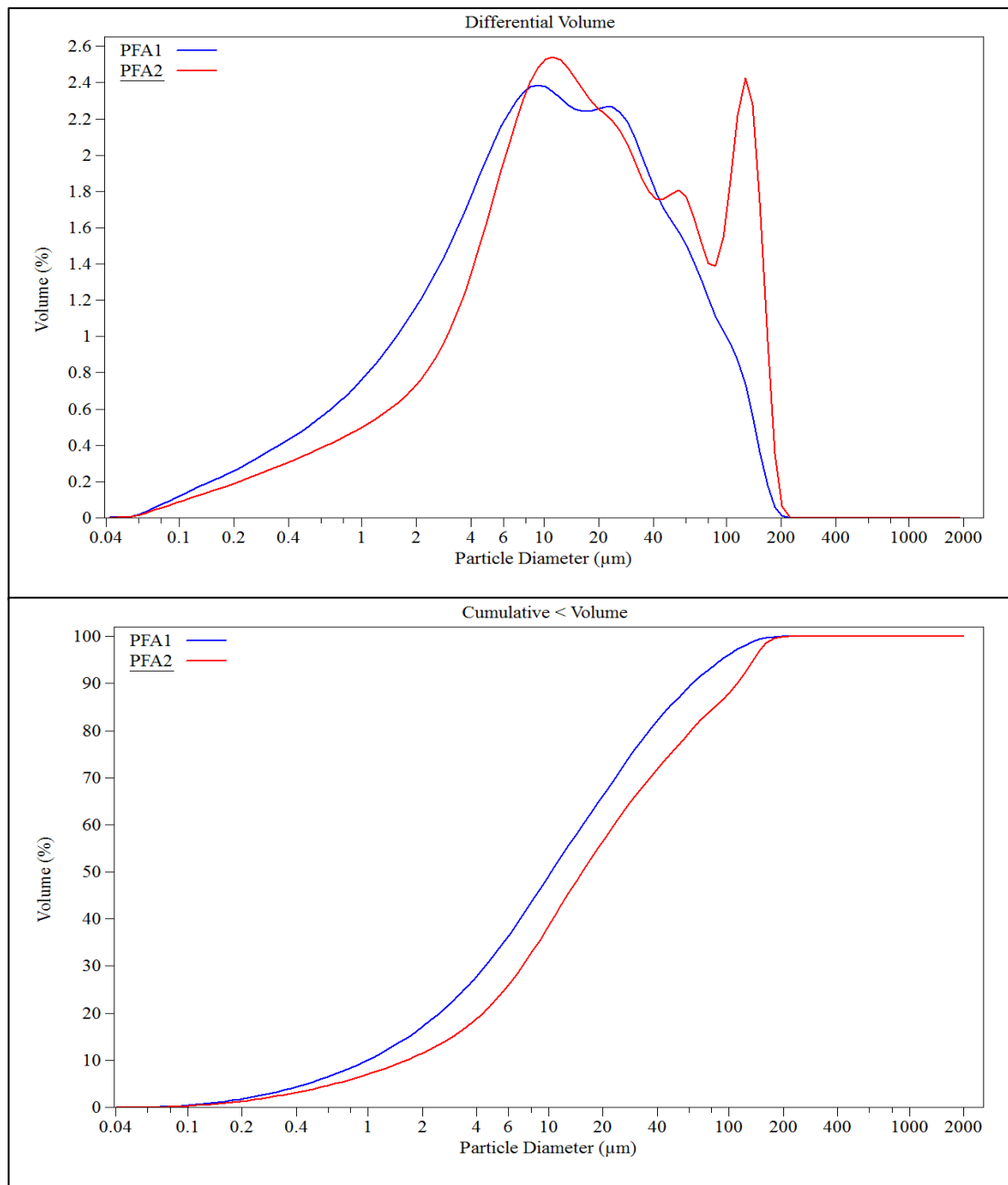


Figure 4.20 PSD of both types of PFA.

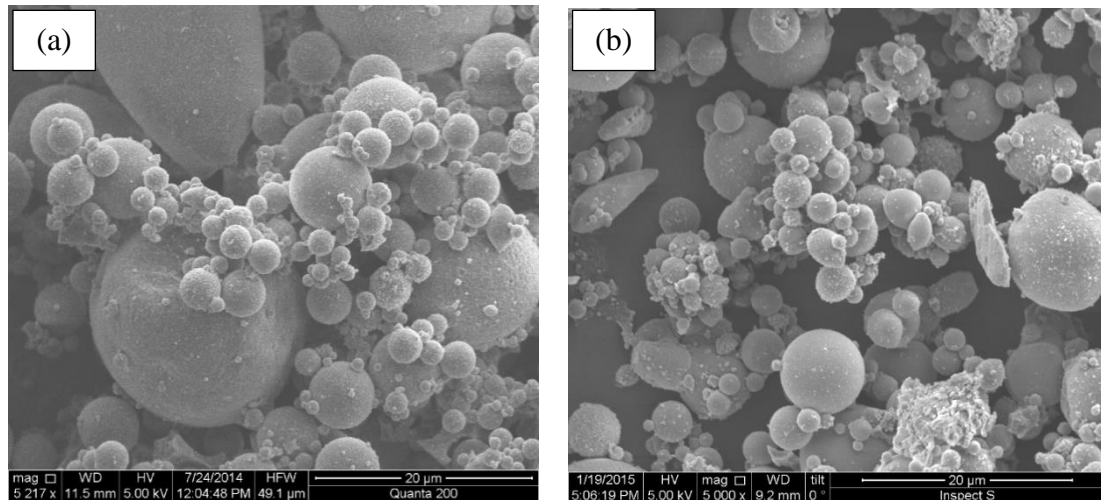


Figure 4.21 SEM images of (a) PFA1, and (b) PFA2

4.3.6 Ground Granulated Blast Furnace Slag (GGBS)

According to the supplier of the GGBS identified in this study (Hanson UK), the GGBS was classified under the British standard BS EN 15167-1. The chemical properties of GGBS listed in Table 4.8 indicated that the major oxides were calcium and silica oxides while lower contents of aluminium, magnesium, and sodium oxides were indicated. Moreover, the LOI% value was found to be equal to 0.373% while the pH value was measured and found to be equal to 11.65. This value of pH agrees with the range of pH values of GGBS specified by Hanson UK (Hanson, 2016). The XRD pattern for GGBS shown in Figure 4.22 indicated that GGBS has an amorphous nature, and therefore, the relation between mineral phases and the efficiency of carbonation could not be investigated (Dri *et al.*, 2014). The PSD of GGBS as shown in Figure 4.24 indicated that most of GGBS particles ranged in size between 5 μm and 25 μm with a median diameter of 7.542 μm . The SEM imaging of GGBS revealed that the particles were either angular or irregular in shape and they were comparable to those of OPC as shown in Figure 4.23.

Table 4.8 Chemical properties of GGBS.

Item	LOI %	pH	CaO %	SiO ₂ %	Al ₂ O ₃ %	MgO %	Fe ₂ O ₃ %	K ₂ O %	SO ₃ %	Na ₂ O %
Value	0.373	11.6	38.67	37.87	4.71	3.73	--	0.63	1.17	2.87

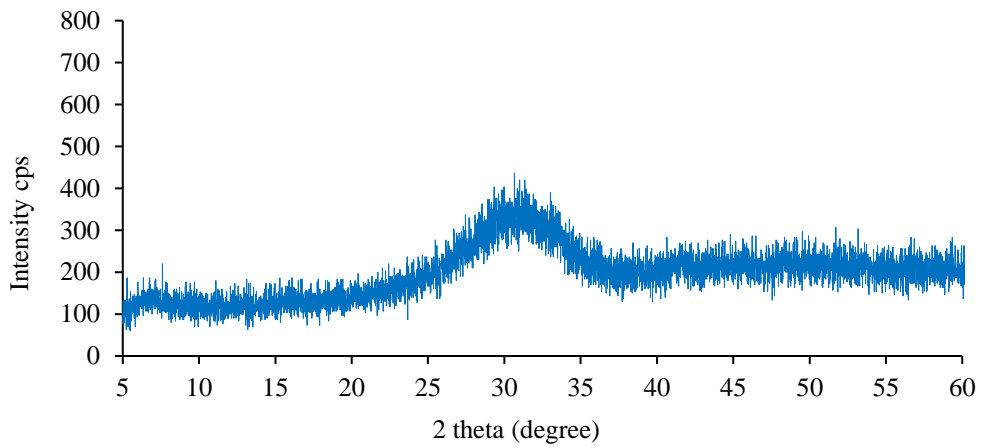


Figure 4.22 XRD patterns of GGBS.

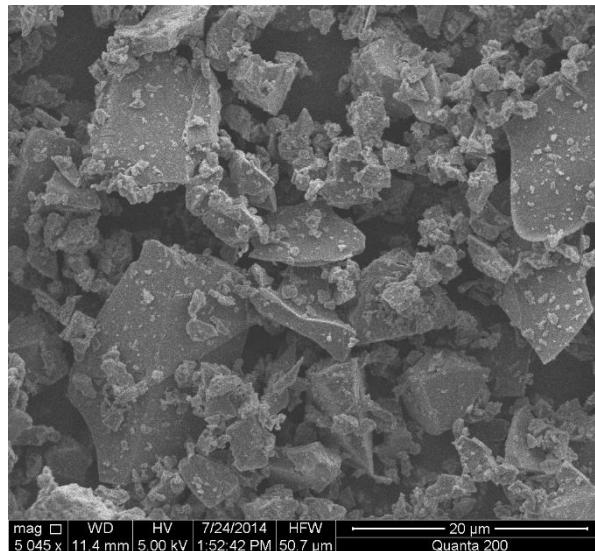


Figure 4.23 SEM view of GGBS.

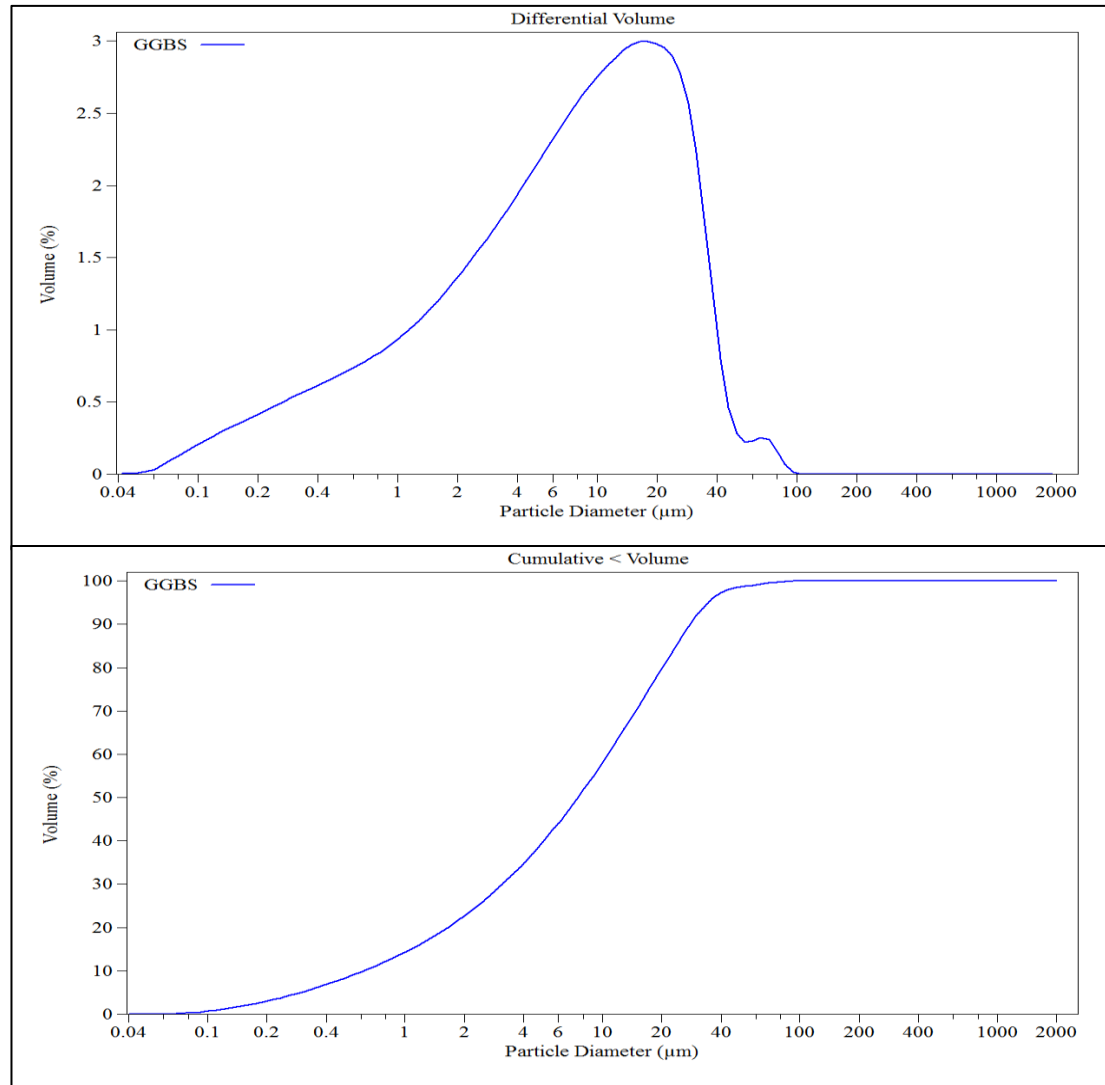


Figure 4.24 PSD of GGBS.

4.3.7 Silica Fume (SF)

The SF identified in this study was a commercially available grey micro silica fume in a powder state, and it was supplied by the Elkem Materials Company, Zuid-Holland, Netherlands. The chemical properties of SF are listed in Table 4.9 which indicated that the SF was mostly composed of silica (approximately 97%). Additionally, the chemical analysis of SF revealed that the LOI was 1.023% and pH was measured as 8.81 (Table 4.9). The XRD patterns of the powder state of SF shown in Figure 4.25, revealed that the amorphous silica was the major mineralogical phase of the SF. The PSD curves of the SF shown in Figure 4.26 indicated a sharp peak at 200 μm sizes and this peak was possibly due to the agglomeration that occurred for superfine particles during the test. However, the PSD analysis revealed that most of SF particles were in

sizes between 170 μm and 270 μm with a median diameter of 214 μm . The agglomeration was revealed noticeably in the SEM imaging test of SF particles as shown in Figure 4.27.

Table 4.9 Chemical properties of SF.

Item	LOI %	pH	SiO ₂ %	Al ₂ O ₃ %	MgO %	Fe ₂ O ₃ %	K ₂ O %	SO ₃ %	Na ₂ O %
Value	1.023	8.81	96.89	0.5	0.51	0.131	0.63	--	0.8

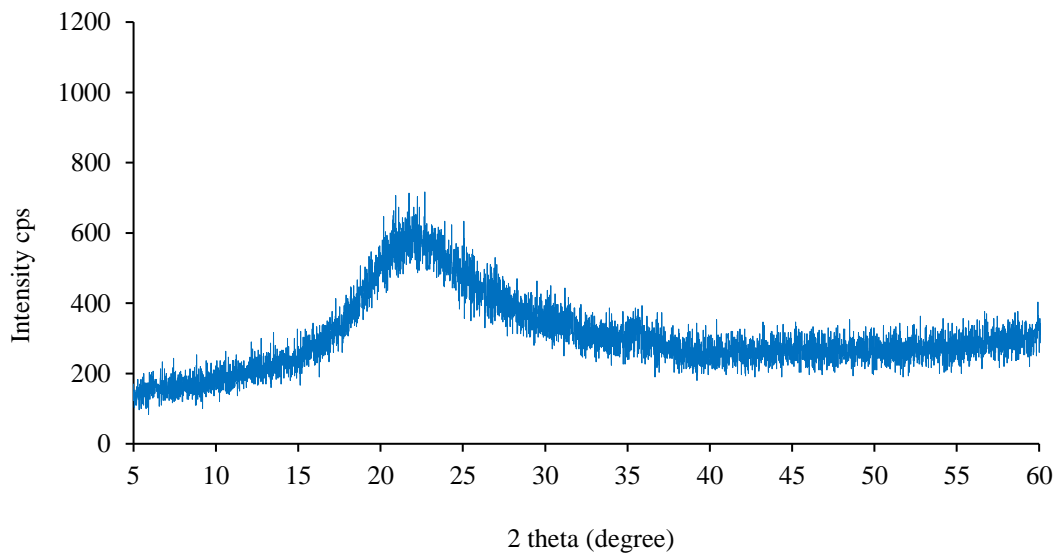


Figure 4.25 The XRD patterns of SF.

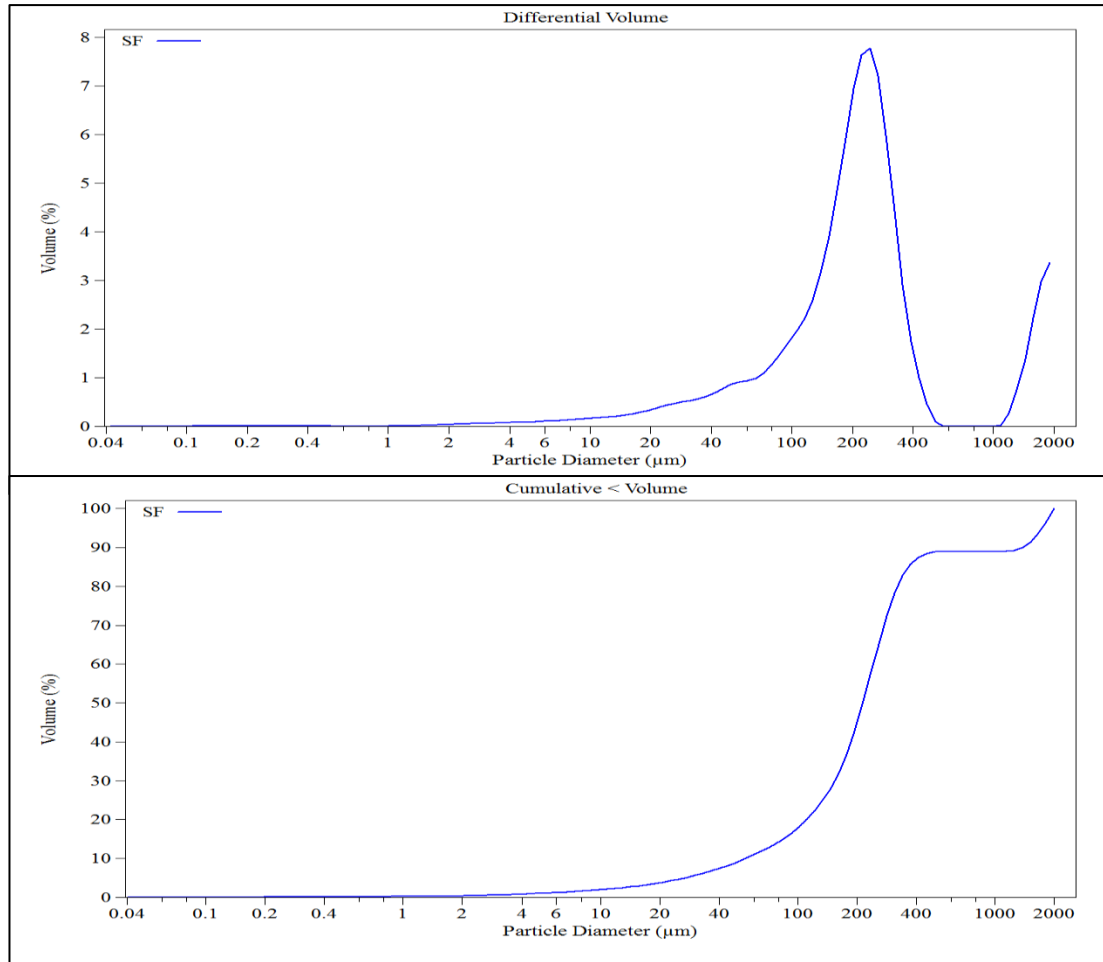


Figure 4.26 PSD of the silica fume particles.

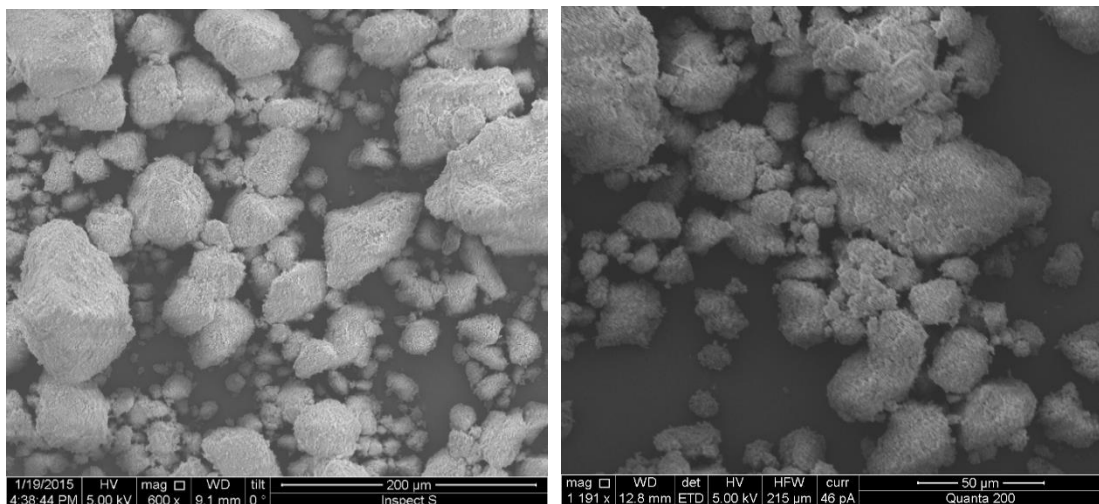


Figure 4.27 SEM view of SF particles.

4.3.8 Flue Gas Desulphurisation Gypsum (FGD)

The FGD identified in this study was received in the semi-dry state. Therefore, it was oven dried at a temperature of $100\pm 5^{\circ}\text{C}$ for 24 hours then the lumps were pulverised gently using a wooden hammer before carrying out the identification experiments. The chemical composition shown in Table 4.10 indicated that the FGD was composed mainly of calcium oxide (CaO) and sulphate (SO_3) with a small amount of silica (SiO_2). The X-ray diffraction patterns of the FGD gypsum indicated that the dominant mineralogical phase of FGD gypsum was composed of calcium sulphate hemihydrate ($\text{CaSO}_4\cdot 0.5\text{H}_2\text{O}$) in addition to the quartz (SiO_2) as shown in Figure 4.28. Similar diffraction patterns of FGD gypsum were reported by Zhang *et al.* (2016a) when they transformed the raw materials of FGD gypsum composed of calcium sulphate dehydrate ($\text{CaSO}_4\cdot 2\text{H}_2\text{O}$) to calcium sulphate hemihydrate ($\text{CaSO}_4\cdot 0.5\text{H}_2\text{O}$) using moderate heating at a temperature of $90\pm 3^{\circ}\text{C}$. The PSD of the FGD gypsum shown in Figure 4.29 indicated that the FGD particles were distributed mainly into two different sizes which were $200\mu\text{m}$ and between $20\mu\text{m}$ and $40\mu\text{m}$ with a median diameter of $28.43\mu\text{m}$. The SEM images shown in Figure 4.30 revealed the large size of FGD particles in comparison to the other candidate materials discussed previously. Moreover, the shape of FGD gypsum particles was flaky with ellipse-like shapes as shown in Figure 4.30.

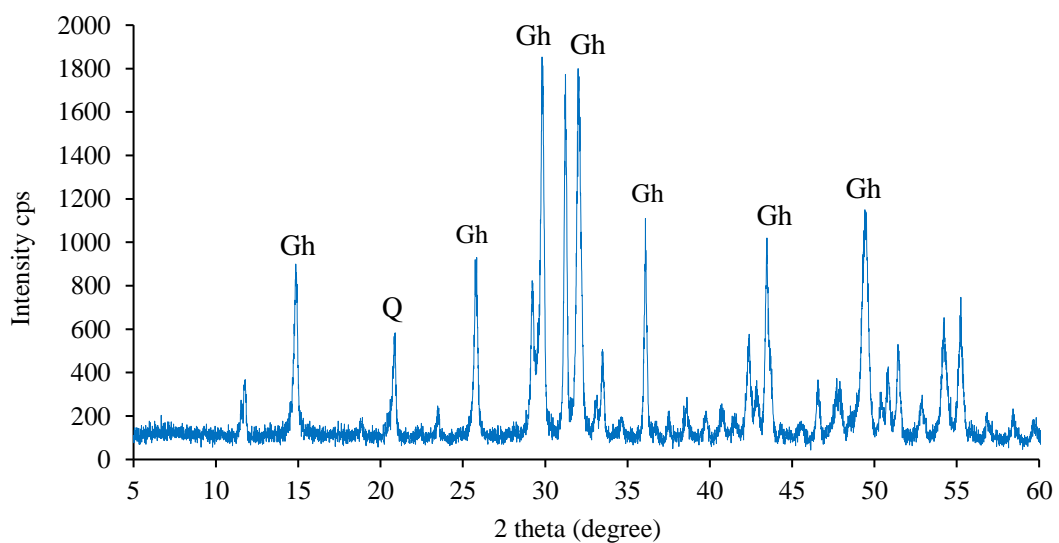


Figure 4.28 XRD patterns of FGD gypsum (Gh: calcium sulphate hemihydrate, Gd: calcium sulphate dehydrates, and Q: quartz)

Table 4.10 Chemical properties of FGD gypsum.

Item	pH	CaO %	SiO ₂ %	MgO %	SO ₃ %	Na ₂ O %
Value	12.3	35.89	14.3	0.54	34.64	1.23

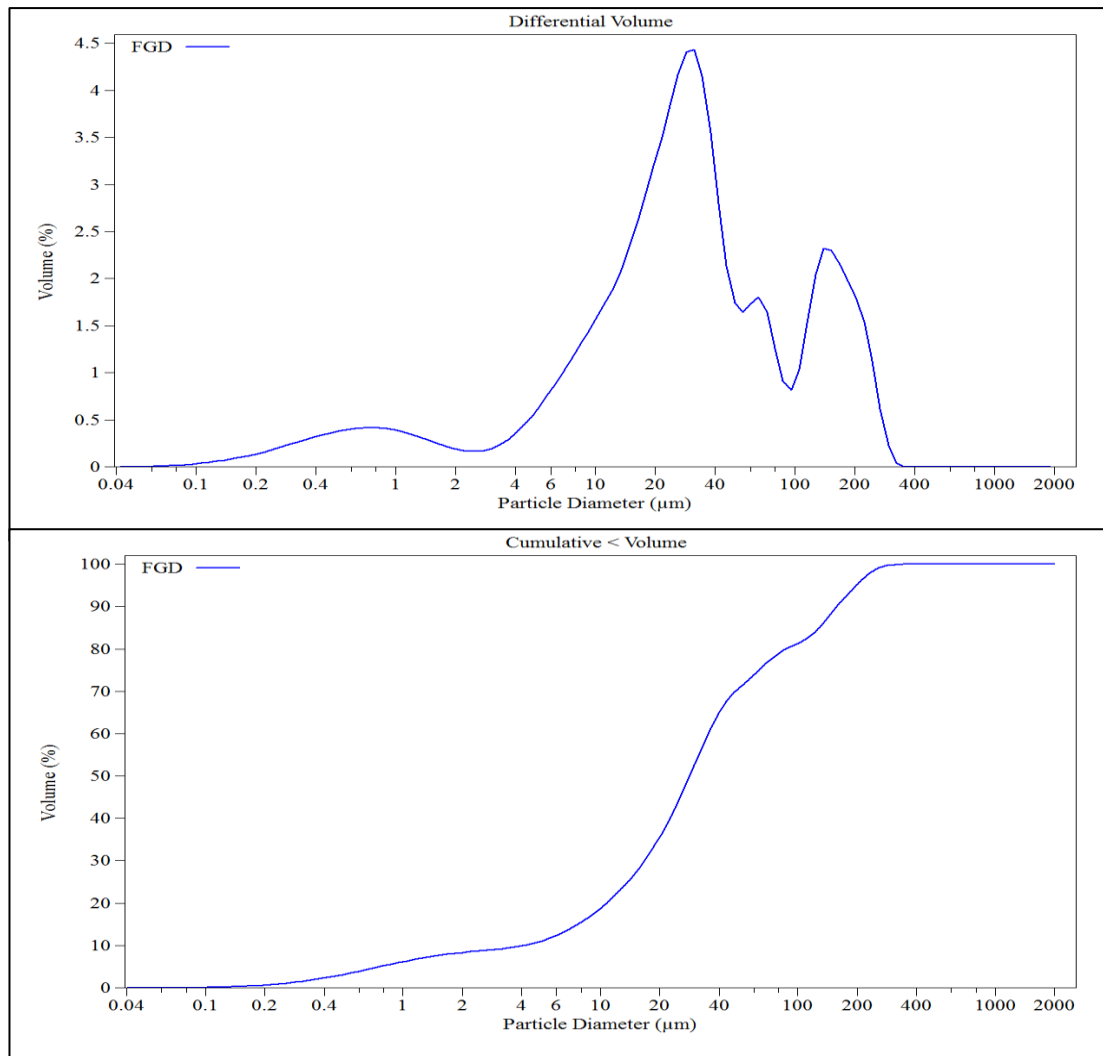


Figure 4.29 PSD of FGD gypsum.

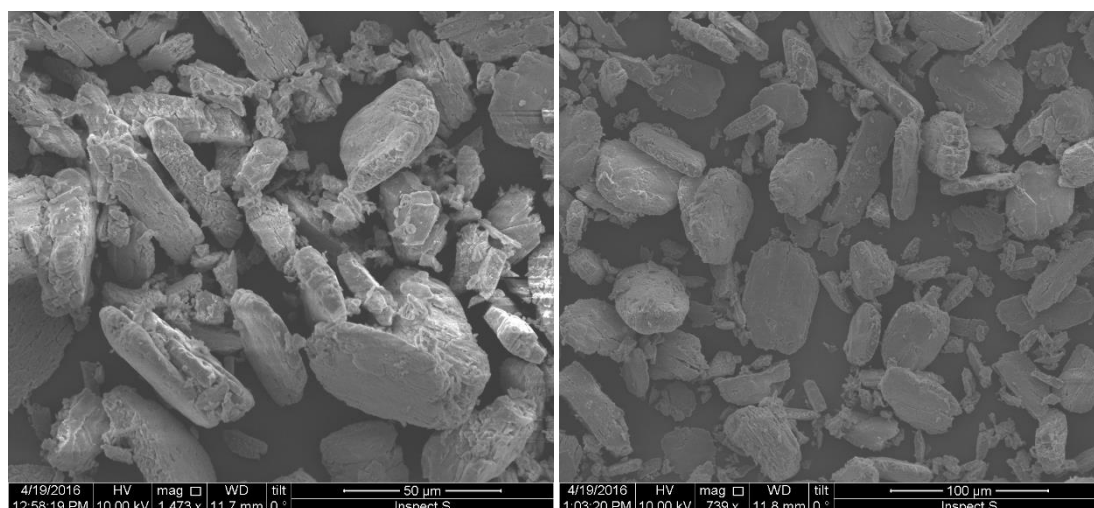


Figure 4.30 SEM images of dry powder of FGD gypsum.

4.4 COMPARATIVE PHYSICAL AND CHEMICAL PROPERTIES OF CANDIDATE MATERIALS

The aim of physicochemical properties identification for the WPSA and the other candidate materials in this research study was to evaluate their suitability and potential for the development of cement-free blends to be used as a fully cement replacement in soft soil stabilisation. Therefore, a comparison was carried out to select the most suitable materials that have the potential to produce the new binder. This comparison was evaluated using chemical properties such as the oxides contents achieved from XRF analyses and pH values measured for each candidate, together with physical properties, such as PSD and LOI of the candidate materials. Since the identified peaks of free lime by XRD analysis for F-WPSA were more than those for C-WPSA in addition to the finer grade of F-WPSA, F-WPSA was considered in the comparison as well as in later experimental works for this research project. The chemical properties of all candidate materials along with those for the reference OPC are summarised in Table 4.11. From this table, it can be seen that the principal oxides of WPSA are very comparable to those for OPC in addition to the free lime that was identified in the XRD patterns of WPSA. This free lime is expected to cause true hydration behaviour. However, the real hydraulic properties of WPSA have not been reported by previous studies as they indicated that the primary mineral content was gehlenite which behaves as an inert material in the presence of water (Segui *et al.*, 2012; Spathi *et al.*, 2015).

Additionally, by the definitions of fly ash for concrete requirements specified in the British standard BS EN 450:1995 (British Standard, 1999c), the value of LOI% should not exceed 5.0% by mass. Therefore, PFA2 was excluded due to its high LOI (9.64%). Table 4.11 also shows that significant silica contents were revealed by the XRF analysis of SF and RHA which could be good pozzolanic activators to boost the pozzolanic reaction. The chemical analysis also showed that a high value of pH (13.04) was indicated for POFA along with an acceptable amount of pozzolanic oxides (SiO_2 , Al_2O_3 , and Fe_2O_3) which reached to 70.41% of the total oxides content of POFA. These chemical properties could be useful for both providing the hydration reaction with the pozzolanic materials and maintaining an adequate level of alkalinity for the hydration environment, which is required for the hydration reaction continuity (Habert, 2014).

Table 4.11 Comparative chemical properties of candidate materials.

Item	pH	CaO %	SiO₂ %	Al₂O₃ %	MgO %	Fe₂O₃ %	K₂O %	SO₃ %	Na₂O %	TiO₂ %
Ref. OPC	13.04	65.21	24.56	1.7	1.3	1.64	0.82	2.62	1.34	--
F-WPSA	12.86	66.76	25.12	2.38	2.57	0.03	0.31	0.26	1.72	0.41
POFA	13.04	10.47	61.36	7.51	1.54	5.64	7.53	2.93	1.73	0.63
RHA	8.98	0.49	90.2	4.03	0.61	0.183	1.36	--	0.897	0.067
PFA1	10.68	4.47	57.05	9.56	8.25	9.29	3.29	1.15	1.74	1.57
GGBS	11.65	38.67	37.87	4.714	3.73	--	0.634	1.176	2.868	0.903
SF	8.81	--	96.89	0.5	0.51	0.131	0.63	--	0.891	0.034
FGD	12.3	35.89	14.3	--	0.54	--	--	34.64	1.23	--

Based on BS EN 197-1:2000 (European Committee for Standardisation, 2004), the clinker in Portland cement shall contain not less than two-thirds by mass calcium silicates ($C_3S: (CaO)_3 \cdot SiO_2$ and $C_2S: (CaO)_2 \cdot SiO_2$). The remainder containing the other oxide compounds like Aluminium oxide (Al_2O_3) and iron oxide (Fe_2O_3). The specification also states that the ratio by mass of (CaO/SiO_2) shall be equal to or be higher than 2.0, and magnesium oxide content (MgO) shall not exceed 5.0%. Concerning the pozzolanicity, the specifications identify that the reactive silicon dioxide shall be not less than 25.0 % by mass as illustrated in Table 4.12. From this table, it can be seen that only WPSA met all the requirement of the aforementioned standard. However, the other materials would not affect the requirements if they were mixed in small portions with WPSA to produce a new cementitious binder. Figure 4.31 shows the percentages of principal oxide components for each of the candidate materials that were to be taken into consideration with those for OPC. From Tables 4.11 and 4.12, and Figure 4.31 indicate the quantitative oxide compositions of all candidate waste materials and revealed that WPSA has comparable principal oxide composition to OPC and encouraging figures in terms of $CaO+SiO_2$, $SiO_2+Al_2O_3+Fe_2O_3$, and CaO/SiO_2 . The other candidates have oxide components more than OPC when excluding CaO, which means silica, aluminium, and iron oxides, which play an important role in the pozzolanic reaction.

Table 4.12 Comparative chemical properties of candidate materials with the requirements of the British Standard

Item	OPC	WPSA	POFA	RHA	PFA1	GGBS	SF
$CaO+SiO_2 \geq 67 \%$	89.77	91.88	71.83	90.69	61.52*	76.54	96.89
$(SiO_2+Al_2O_3+Fe_2O_3) \%$	27.9	27.53	74.51	94.413	75.9	42.584	97.521
$CaO/SiO_2 \geq 2$	2.65	2.66	0.17*	0.01*	0.08*	1.02*	0.01*
MgO %	1.3	2.57	1.54	0.61	8.25*	3.73	0.51

* Do not meet the standard requirements.

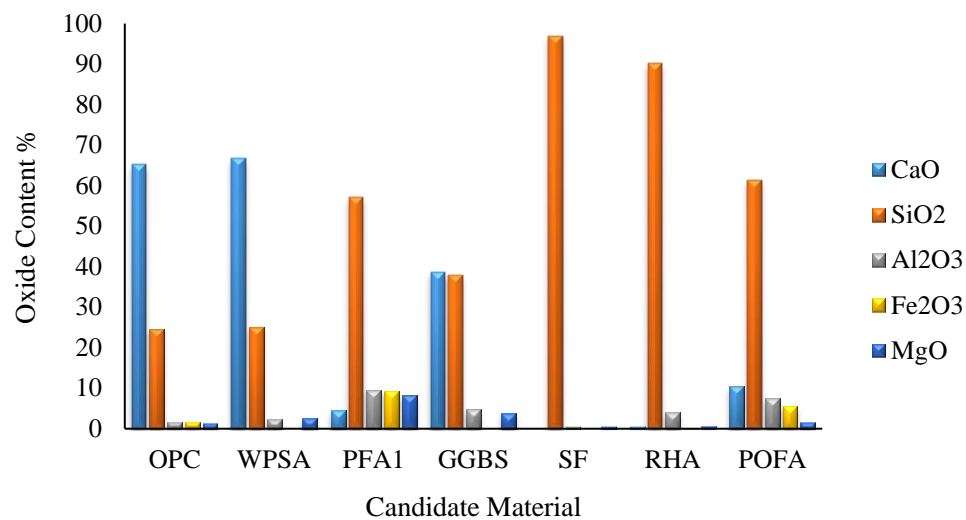


Figure 4.31 Comparative principal oxides of candidate materials.

For the GGBS, most of the principal oxides (Ca, Si, Al, and Mg) were found to have significant proportions. However, a low CaO/SiO₂ ratio was observed (1.02); thus, WPSA has been considered as a more promising material for use as the calcium-base material in the experimental works later on in this study. As per the cement manufacturing, gypsum is added to the cement clinker as a retarder material as well as a grinding agent to prevent the agglomeration of cement particles during the grinding process (Marchon and Flatt, 2016b). Additionally, the gypsum is required to provide the sulphate which reacts with hydrated lime and alumina and forms the calcium sulphoaluminate which is known as ettringite; the ettringite contributes to the development of early age strength (Puppala *et al.*, 2015; Aïtcin, 2016a). Consequently, the FGD identified in this study is composed mainly of gypsum hemihydrate thus, it is promising for use as a sulphate activator along with aiding the grinding activation for WPSA.

The specific surface area and the particle size distribution of OPC, as well as the candidate materials, have an undeniable effect on the compressive strength of stabilised soil. It was found that the finer the particles of fly ashes used in concrete with cement, the higher the compressive strength obtained (Kumar *et al.*, 2008; Zhao *et al.*, 2016). From the overall particle size distribution of all candidate materials as illustrated in Figure 4.32 and their volume statistics as listed in Table 4.13, it can be seen that the finer material is GGBS, while SF is the coarser amongst the candidate

materials. OPC and RHA are nearer to each other with slightly finer results for OPC. POFA and PFA1 have smaller particles than WPSA to some extent. Therefore, a further grinding activation may be essential to increase the pozzolanic reactivity of WPSA. Additionally, a fine material could be produced during the mixing design by mixing portions of POFA and RHA (finer materials) with the ground activated WPSA.

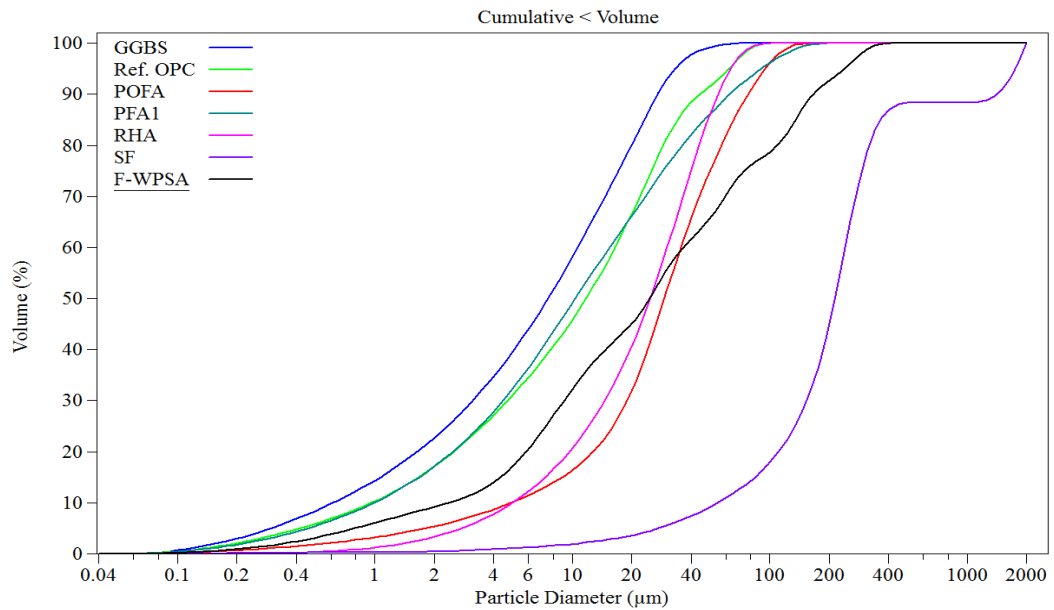


Figure 4.32 Comparative PSD of candidate materials.

Table 4.13 Volume statistics of candidate materials with reference OPC.

Item	OPC	PFA1	WPSA	GGBS	SF	RHA	POFA
d ₁₀ (μm)	0.964	1.012	2.378	0.62	54.29	5.011	4.945
d ₅₀ (μm)	11.78	10.67	24.64	7.565	214.1	24.83	29.29
Median							
d ₉₀ (μm)	44.27	67.45	166.2	27.12	1412	54.88	77.6
Mean (μm)	17.83	23.83	57.87	11.19	364.2	27.69	36.17

4.5 SUMMARY

This chapter presented the identification of the physical, geotechnical and chemical properties of the soft soil used in this study as well as the determination of the physicochemical properties of specific types of waste materials along with the reference binder which was a specific type of OPC. The first aim of this chapter was to classify the virgin soil and characterise its physical and geotechnical properties to be used to evaluate the levels of improvement after treating with different mixtures. Additionally, this chapter aimed to select a group of the most promising waste materials dependent on the comparative chemical and physical properties of the candidate materials. The latter are devoted to be employed in the development of many cement-free mixtures as new binders in soft soil stabilisation. As explained in the previous section, the materials that were adopted in this study were selected after conducting a comparison of physicochemical properties of all candidate materials with those of the reference OPC. The output of this chapter can be summarised as follows.

- The classification experiments revealed that the virgin soil used in this study was an intermediate plasticity silty clay with medium organic content and its symbol was CI.
- Based on the comparative physicochemical properties of the candidate materials, the selected materials used in the mixing design at the later stages were WPSA as the main calcium-based material, POFA as an alkaline activator due to its high pH value in addition to its acceptable pozzolanic compounds, and RHA due to its significant content of amorphous silica and general fineness. Additionally, the FGD gypsum was selected as a grinder as well as sulphate activator to help in the breaking of the glassy phase of non-amorphous silica, and in turn to increase the production of the cementitious gels C-S-H and C-A-H.
- The coarser particles of WPSA as well as the agglomeration could affect and delay its pozzolanic reactivity during the hydration reaction, therefore it would exhibit better reactivity if it was subjected to mechanical activation such as a low energy grinding.

CHAPTER 5

MIXING DESIGN FOR THE NEW BINDER MIXTURES OPTIMISATION

5.1 INTRODUCTION

This chapter presents the results and discussion of a set of laboratory experiments carried out on the soft soil treated with different types of mixtures consisting of cement-free blending of waste materials fly ashes. The mixtures were prepared using the waste materials selected from the previous chapter by mixing them using different proportions to produce unary, binary and ternary mixtures. Therefore, this chapter contains three stages of optimisation to address the most effective mixtures by examining the performance of different blends in soft soil stabilisation. The behaviour of these mixtures was evaluated dependent on the results obtained from the Atterberg limits, compaction parameters and unconfined compressive strength (UCS) tests. The aforementioned results were compared with those for untreated soil only, at this stage of the research project. However, the results of soil treated with the reference binder were referred to on some occasions in this chapter.

5.2 OPTIMISATION OF UNARY MIXTURE

This stage of optimisation was carried out to determine the optimum binder content dependent on the results of the Atterberg limits and UCS tests of the soil treated with different percentages of WPSA (3, 6, 9, 12, and 15% of the dry mass of the treated soil). Similar scenarios of additive ranges were adopted in previous studies in which a fixed value of additive increment was used (Sariosseiri and Muhunthan, 2009; Horpibulsuk *et al.*, 2013; Modarres and Nosoudy, 2015; Wang *et al.*, 2017). However, the increasing in the additive is continued until get a peak value which represents the optimal one. The soil treated with 0% binder refers to the untreated soil (virgin soil). The specimens for the UCS test were cured at different periods of curing (0, 7, 14, and 28 days) to investigate the effect of curing time on the strength development. The behaviour of the soil treated with WPSA is presented as follows:

5.2.1 Consistency Limits

The consistency limits (Atterberg limits) were determined immediately after adding the water to the soil-binder mixtures. The results of the Atterberg limits tests for the soil treated with different percentages of WPSA, obtained from three trials for each percentage, are shown in Figure 5.1. It can be seen that both the liquid limits (LLs) and plastic limits (PLs) increased while the plasticity indices (PIs) decreased continuously with the increase in WPSA content. Additionally, the results of the Atterberg limits tests indicated that the increments that occurred in PL were higher than those for LL, thus the PI decreased. As shown in Figure 5.1, the LL increased gradually with the increase of WPSA, while significant increments were observed in PL for the soil treated with 3 and 6% of WPSA. Then a similar scenario to that which occurred for LL was indicated by PL of the soil treated with more than 6% of WPSA. The PI decreased from 20.22 for the virgin soil to 13.1 for the soil treated with 15% of WPSA. However, a PI of 13.45 was indicated for the soil treated with 12%. A similar behaviour was observed with respect to the Atterberg limits of the soil treated with the reference OPC as shown in Figure 5.2. However, there were slight reductions in both LL and PL when the OPC content increased to higher than 9%, and the PI continued to decrease but then a negligible increase was observed at 15% OPC.

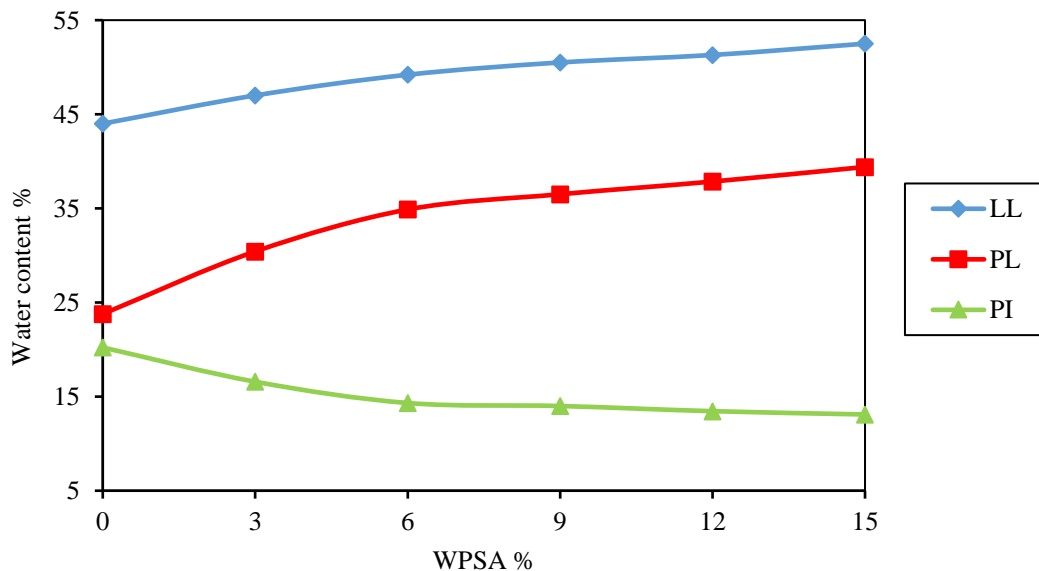


Figure 5.1 Atterberg limits of the soil treated with WPSA.

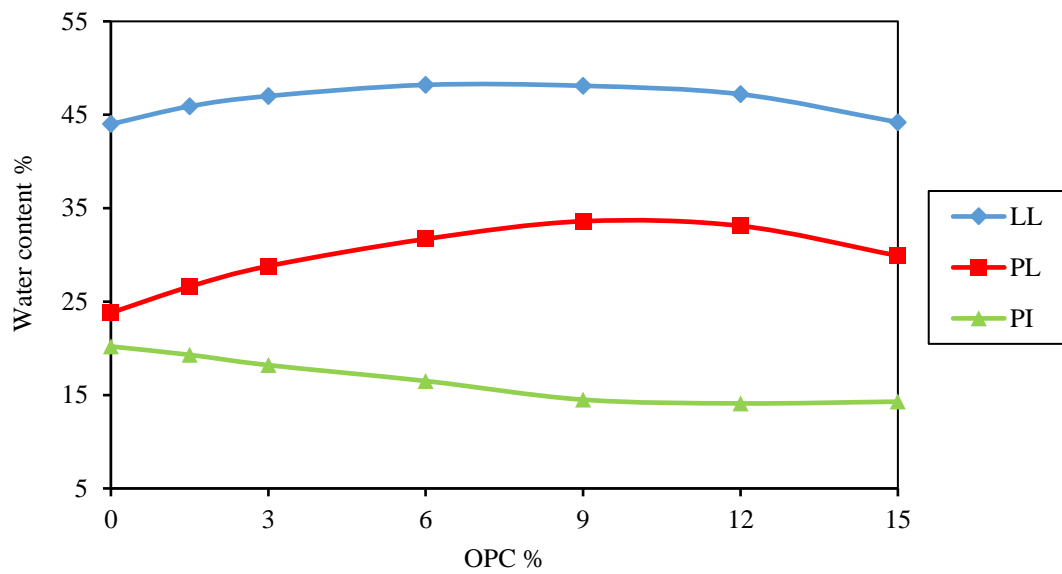


Figure 5.2 Atterberg limits of the soil treated with OPC.

Table 5.1 Comparative effect of WPSA and OPC treatment on the soil Atterberg limits.

Binder	WPSA			OPC		
	LL	PL	PI	LL	PL	PI
0.0	44.00	23.78	20.22	44.00	23.80	20.20
3.0	47.00	30.42	16.58	47.00	28.80	18.20
6.0	49.20	34.88	14.32	48.20	31.70	16.50
9.0	50.50	36.50	14.00	48.10	33.60	14.50
12.0	51.30	37.85	13.45	47.20	33.10	14.10
15.0	52.50	39.40	13.10	44.20	29.91	14.29

Table 5.1 illustrates the comparative effect of WPSA and OPC treatment on the Atterberg limits of the soil used in this study. The values listed in this table represent the average value of three trials for each percentage of additives; the obtained values

are limited to the time of the performing of LL and PL test and the skills and experience of the person who is conducting the test. From this table, it can be observed that the increments in LLs and PLs of the soil treated with WPSA were higher than those for soil treated with OPC for all percentages. Consequently, the reductions in PIs of the soil treated with WPSA were more than those for the soil treated with OPC. In contrast, the PI was reduced from 20.22 for the virgin soil to 13.1 by treating with 15% of WPSA, while it was 14.1 for the soil treated with the same amount of OPC. This indicated that WPSA exhibited better results, in the improvement of the Atterberg limits of the stabilised soil, than that of the reference binder. According to Knappett and Craig (2012), the PI represents the range between the maximum and minimum limits of the water content in which the soft soil exhibits a plastic behaviour. These upper and lower limits of water contents are represented by LL and PL respectively. Thus, decreasing the PI leads to shorten this range and this in turn enhances the comfort of working on site using soils with a particularly high water content. Additionally, the reduction in the PI of soft soils contributes to the increasing workability in addition to the enhancement of the soils resistance against the changes of the water content due to the wetting-drying phenomenon (Baran *et al.*, 2001; Daoudi *et al.*, 2015).

As per the results of the physico-chemical properties identification of WPSA which were presented and discussed in the previous chapter, a high content of calcium was indicated in the mineral compositions of WPSA. Therefore, the increments that occurring in LL and PL of soil-WPSA mixtures might be attributed to the chemical reaction of the hydrated lime provided by WPSA and the clay minerals of the treated soil. Similar scenarios were reported by many researchers when they conducted their studies on soft soils stabilised with calcium-based materials (Saride *et al.*, 2013; Goodarzi and Salimi, 2015; Bahmani *et al.*, 2016). Moreover, the increase in the specific surface area of the soil-WPSA mixture enlarged the thickness of the double layer of the soil particles which in turn increased the water-holding capacity of the stabilised soil, thus the LL increased (Eskisar, 2015). On the other hand, the increase in PL was due to the cation exchange that took place between the positive cation of the calcium of WPSA and water and the negative charges (anions) of the surface of clay minerals of the soft soil (Das, 2010; Budhu, 2011).

5.2.2 Compaction Parameters

Standard Proctor tests were performed to establish the relationship of dry density and moisture content of the soil treated with WPSA, to investigate the effect of WPSA treatment as well as to provide the required data for the maximum dry density (MDD) and optimum moisture content (OMC) for specimens preparation for the unconfined compressive strength (UCS) tests. Different percentages of WPSA (3.0, 6.0, 9.0, 12.0, and 15.0% by the dry mass of the treated soil) were added to the soil then the tests were carried out immediately after the water was added to the soil-binder mixture. The results of the compaction tests shown in Figure 5.3 indicated that the MDD decreased and OMC increased with the increase in WPSA content. Moreover, the MDD dropped from 1.57Mg/m^3 for the virgin soil to 1.48Mg/m^3 after treating with only 3% WPSA, while gradual reductions in MDD were indicated beyond 3% of WPSA up to 12%. However, another significant reduction was observed in MDD for the soil treated with 15% WPSA where it decreased from 1.45Mg/m^3 at 12% WPSA to 1.4Mg/m^3 as shown in Figure 5.4a. The effect of the lower WPSA content (3%) was also recognised on the OMC value in which the OMC increased dramatically from 23% for the virgin soil to 26.5% for the soil-3% WPSA mixture. The WPSA treatment with percentages beyond 3% indicated a gradual increase in the OMC of the stabilised soil as shown in Figure 5.4b.

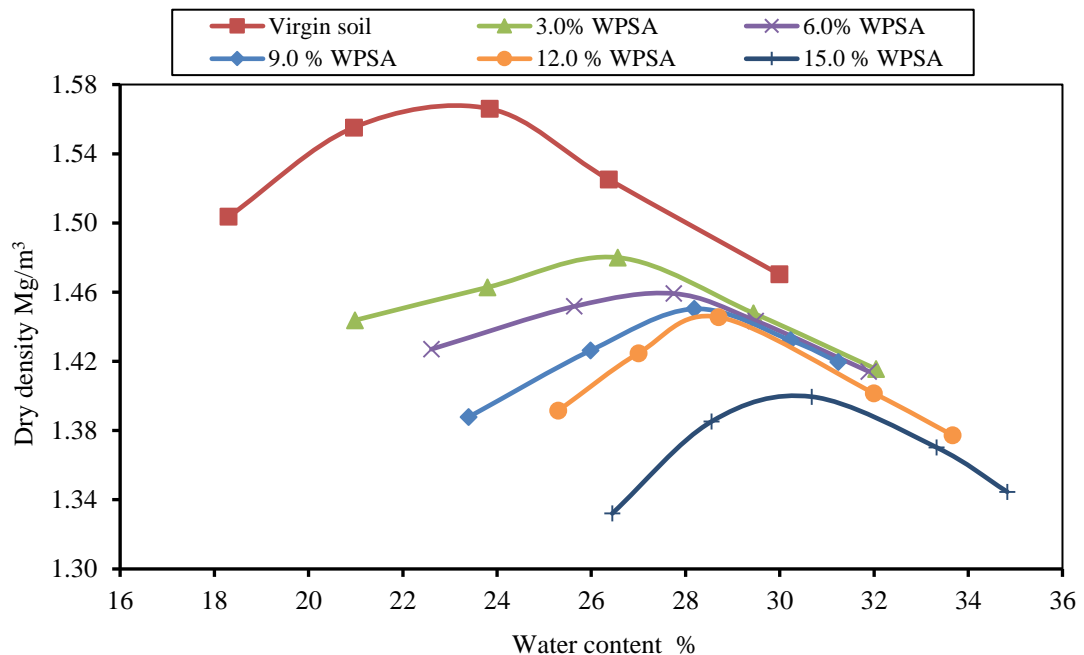


Figure 5.3 Dry density-moisture content relationship for the soil treated with WPSA.

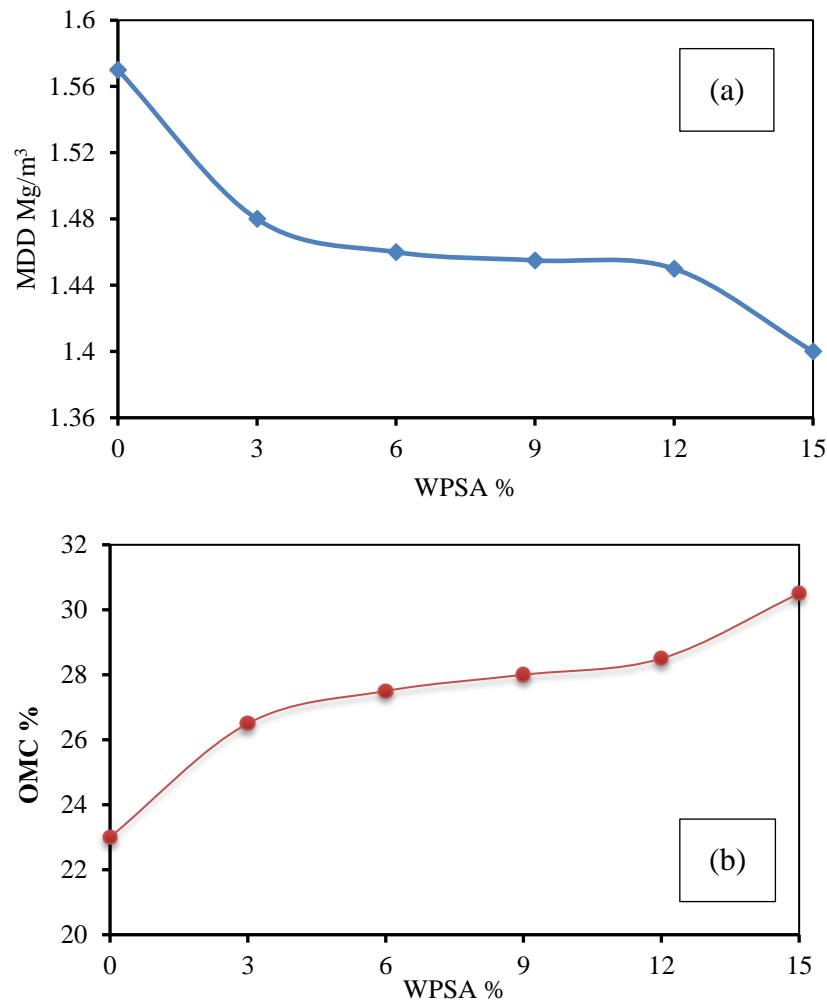


Figure 5.4 The relationship between WPSA and (a) MDD, and (b) OMC.

A similar behaviour of the MDD and OMC was observed for the soil treated with the reference cement but the effect of cement on the compaction parameters was lower than that for WPSA. Figure 5.5a and b show the comparative effect of WPSA and OPC treatment on the MDD and OMC respectively. From these figures, it can be noticed that the reduction in the values of MDD of the soil treated with OPC was gradual and less than those for soil stabilised with WPSA as shown in Figure 5.5a. The increments in the value of OMC for the soil-WPSA mixtures were higher than that for the soil treated with OPC as shown in Figure 5.5b. This behaviour gives an indication about the higher water demand property of WPSA in comparison to that for the reference cement. Additionally, the significant reduction in MDD paired with the corresponding dramatic increase in OMC might be due to this property. Hence, the volumetric ratio

of water/solids was increased after treatment and since the unit weight of water is lighter than that for solids, the weight of total solid per unit volume was decreased; thus, the MDD decreased (see Figure 5.6). Similar behaviours of dry density-moisture content relationships of soft soils treated with calcium-based materials were reported by Huat *et al.* (2008); Okyay and Dias (2010); Sarkar *et al.* (2012); Ashango and Patra (2014); Alrubaye *et al.* (2016). However, many researchers reported that when treating soft soils with calcium-based materials, a chemical reaction between the stabilised soil and the binder may occur immediately after the water is added. Due to the increment in the specific surface area and fineness, the aforementioned chemical reaction causes an agglomeration in the fine particles of the soil which prevents the soil from being compacted properly and this in turn leads to a decrease in the dry density (Ouf, 2001; Muhunthan and Sariosseiri, 2008; Jauberthie *et al.*, 2010; Garzón *et al.*, 2016).

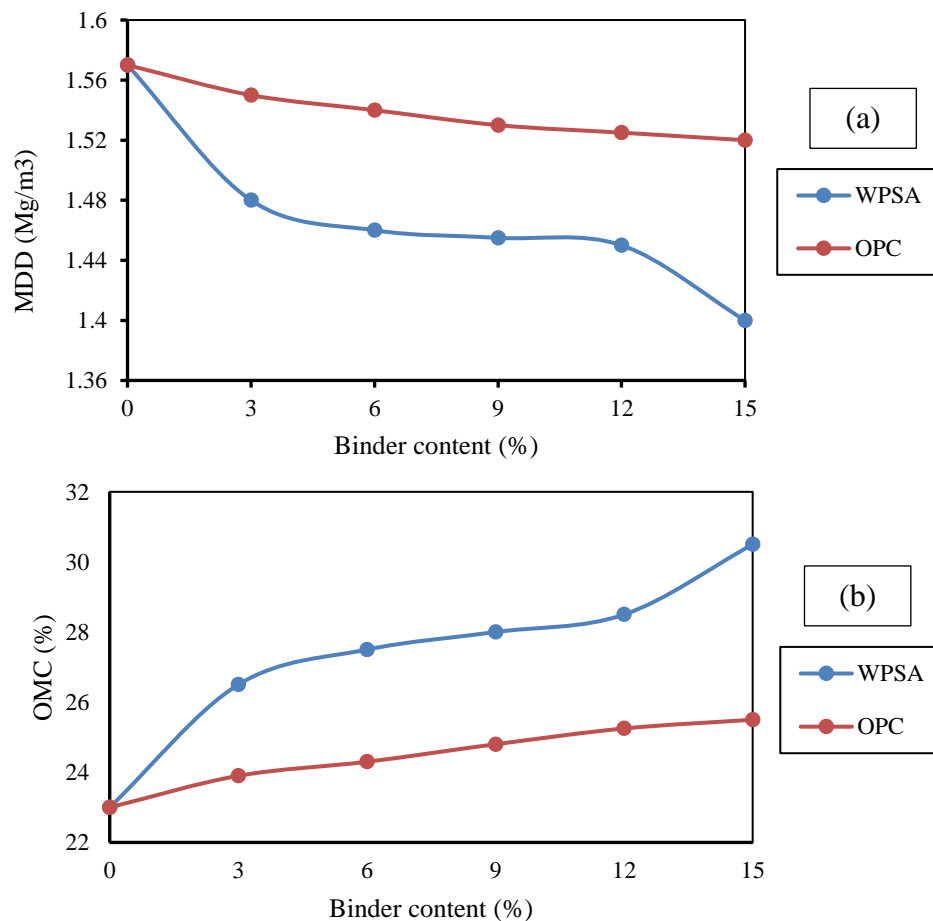


Figure 5.5 Comparative effects of WPSA and OPC on (a) MDDs and (b) OMCs of the stabilised soil in this study.

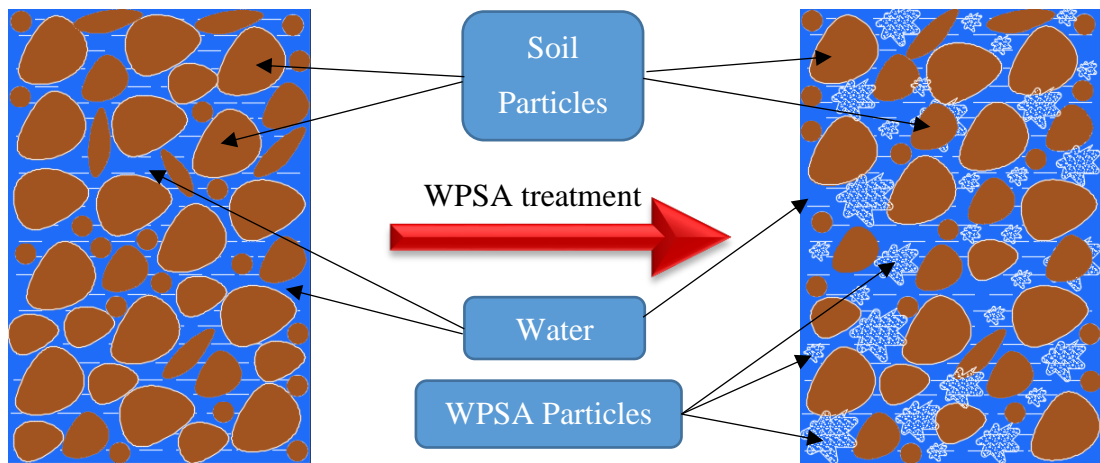


Figure 5.6 The effect of WPSA treatment on the solid weight per the unit volume of the treated soil.

5.2.3 Stress- Strain Behaviour of the Soil Treated with WPSA

The effect of WPSA treatment on the strength characteristics as well as the strain behaviour of the soil stabilised in this research project was studied. The development in the soil strength was assessed dependent on the results of the unconfined compressive strength (UCS) testing. These tests were carried out on specimens of the soil treated with different percentages of WPSA (3, 6, 9, 12, and 15% by the dry mass of the treated soil). Moreover, the specimens were cured at different periods (0, 7, 14, and 28 days) before being subjected to the UCS tests to study the effect of curing time on the development of the soil strength throughout the time of curing. The specimens for the UCS tests were prepared with dimensions of 38mm in diameter and 76mm in height using the constant volume mould mentioned in Chapter 3 of this study (see section 3.3.6). Additionally, the strain behaviour at the failure state of specimens containing different percentages of WPSA and cured for different periods was also evaluated. However, the optimum content of WPSA was determined dependent on the results of the UCS tests in which the percentage of the WPSA by the dry mass of the stabilised soil that exhibited the higher compressive strength ($q_{u \max}$), was considered as the optimum percentage. The maximum compressive strength was taken as the average of the compressive strength of three specimens for each percentage of WPSA.

Figure 5.7 shows the stress-axial strain diagrams obtained from the UCS tests of the soil treated with different percentages of WPSA without curing (i.e. the specimens were tested thoroughly after being ejected from the constant volume mould) along with the same diagrams of the untreated undisturbed and compacted specimens of virgin soil. The undisturbed soil indicated a ductile behaviour with increase of the deviator stress which indicated the super plasticity of the in situ soil. This behaviour is attributed to the natural moisture content which was measured to be equal to 36.8% which was much higher than the plastic limit of this soil (23.78%). However, with only the compaction, a significant improvement was achieved in the compressive strength of the treated soil when it was increased from 66.45kPa for the undisturbed soil to 202kPa for the compacted soil without treatment. The strain behaviour of the compacted soil was also ductile but less plastic in comparison to the behaviour of the undisturbed soil. The results shown in Figure 5.7 also indicated significant increments in the compressive strength of the uncured specimens with WPSA treatment. The compressive strength was found to increase continuously with the continuous increase in WPSA content up to 12% while a slight reduction was indicated beyond 12% (15.0% WPSA) which exhibited a compressive strength approximately equal to that for 9.0% WPSA. However, the behaviour transferred gradually from ductile to semi-brittle with the increase in WPSA content and gradual reductions were observed in the axial strains at failure.

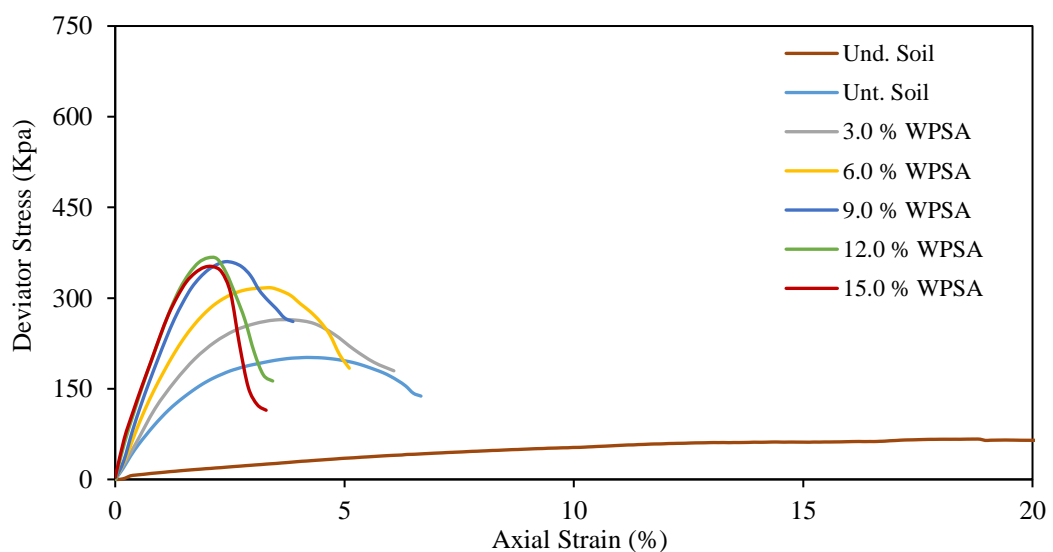


Figure 5.7 Stress-axial strain diagram of undisturbed, compacted untreated, and soil treated with WPSA without curing.

Figure 5.8 shows the stress against axial strain plots of the soil stabilised with WPSA and cured at 7, 14, and 28 days. Figure 5.9 shows the average maximum compressive strength of the soil treated with different WPSA contents compared to the maximum compressive strength of the untreated soil. The results of the UCS testing indicated that the compressive strength increased with the increase in WPSA content as well as with the increase of the curing time. The UCS was increased from 202kPa for untreated soil to 690kPa for the soil treated with 12% WPSA and after 28 days of curing. However, a slight reduction in the UCS was indicated for the soil treated with 15% WPSA for all periods of curing.

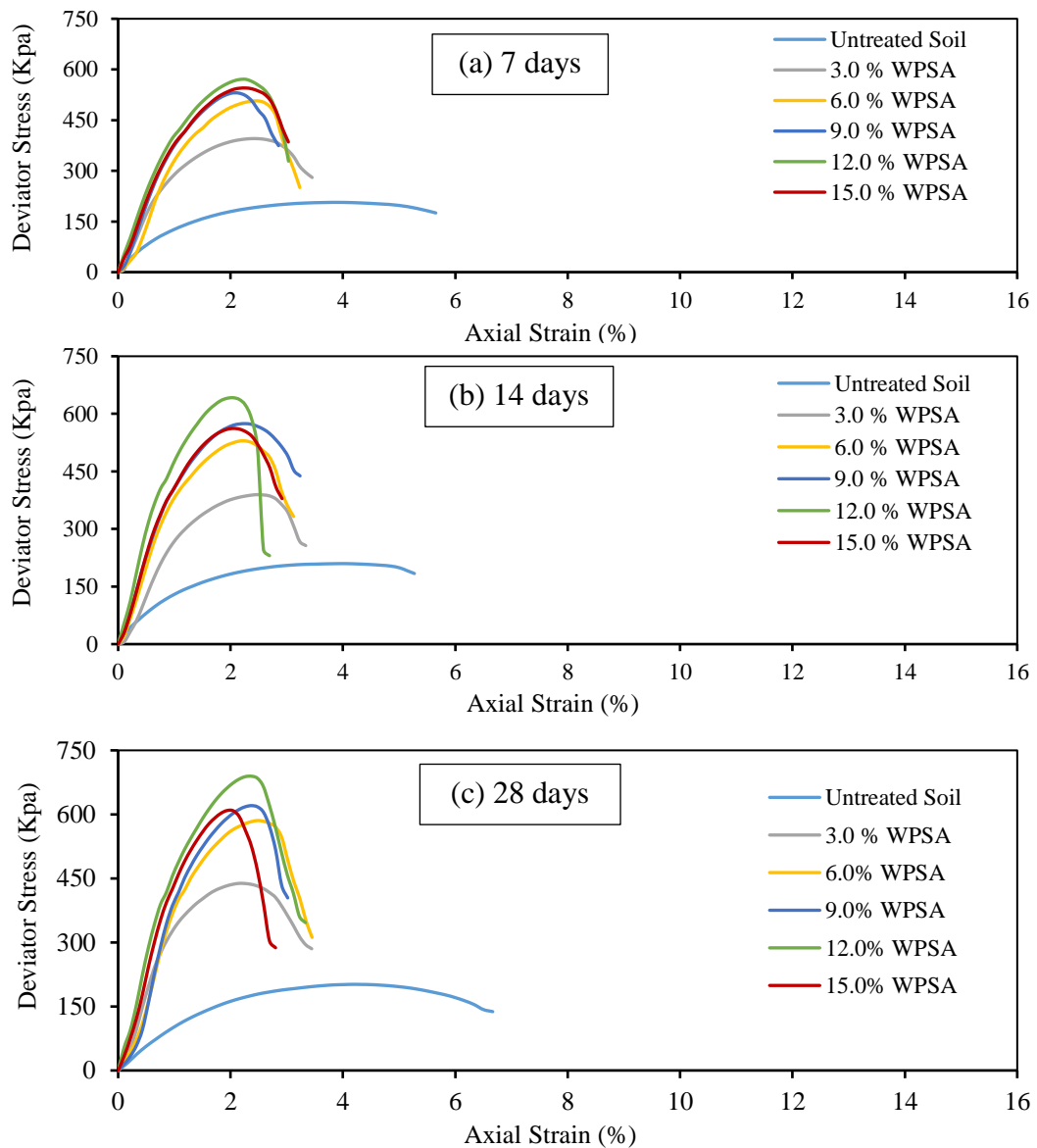


Figure 5.8 Stress-axial strain diagrams of the soil treated with WPSA at different curing periods

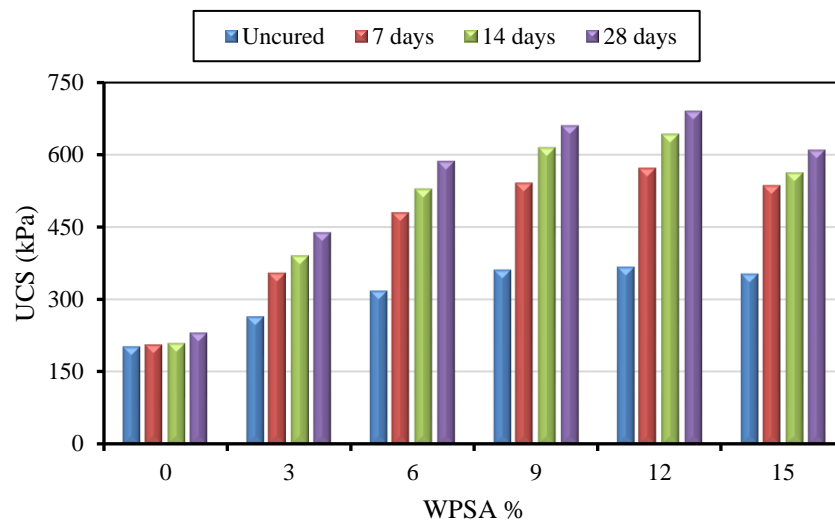


Figure 5.9 The development in UCS of the soil treated with WPSA at different periods of curing

The average maximum compressive strength shown in Figure 5.9 indicated that there was a gradual development in the UCS with time of curing for the specimens treated with lower content of WPSA (3.0%). The specimens treated with percentages beyond 3.0% indicated a noticeable increment just after one week of curing and after that the increment became gradual. According to Sariosseiri and Muhunthan (2009) the soil stabilisation can be considered as an effective treatment when an increase in UCS of 350kPa or more is achieved. Thus, the treatment with WPSA could be considered as an effective treatment since the UCS was increased by 487.5kPa with the use of 12% WPSA and after 28 days of curing. Dependent on the chemical composition of the WPSA and in accordance with the findings of several studies of soft soil treated with calcium-based materials, the behaviour of the compressive strength of the WPSA-treated soil is proven (Kumar *et al.*, 2007; Seco *et al.*, 2011; Horpibulsuk *et al.*, 2013; James and Pandian, 2016; Wu *et al.*, 2016). The development in the UCS achieved from the uncured specimens after WPSA treatment can be attributed to the increase in the soil stiffness due to the reduction in the soil plasticity, as well as to the flocculation-agglomeration reaction (the initial reaction of calcium-based materials by hydration) and cation exchange that takes place between the calcium ions of the WPSA and the clay minerals of the treated soil (Muhunthan and Sariosseiri, 2008; Jha and Sivapullaiah, 2015; Nicholson, 2015). According to James and Pandian (2016) there is an immediate reaction that takes place in lime-stabilised soil which is represented by the ion exchange between the divalent calcium ions of the lime (Ca^{++}) with the

univalent cations of the clay minerals (M^+). Consequently, ions in high concentration will replace those in the lower concentration as explained in Equations 5.1 and 5.2. The improvement in the early compressive strength of lime-treated soils is attributed to the aforementioned reaction.



With respect to the cured samples, the increase in UCS of the treated soil is attributed to the secondary reaction of the reactive calcium oxide of WPSA which reacted with water to produce the hydrated lime (Ca(OH)_2), the so called Portlandite, especially at the age of seven days. While the further development in the soil compressive strength (at 14 and 28 days) can be due to the pozzolanic reaction that occurring between the hydrated lime provided by the WPSA and the soluble silicates and/or aluminates of the stabilised soil which produced the cementitious gel of calcium silicate hydrated (C-S-H) and calcium aluminate hydrated (C-A-H). The latter compounds have the responsibility to bind the soil particles to each other, resulting in a stronger structure (Aïtcin, 2016b; Puppala *et al.*, 2015; Marchon and Flatt, 2016b; James and Pandian, 2016).

Figure 5.10 shows the axial strain values for the corresponding peaks of the stress-axial strain diagrams of the soil treated with WPSA at different periods of curing. It can be seen that the behaviour of the stabilised soil was gradually transferred from ductile to brittle with the increase in WPSA content. Additionally, the brittle behaviour is more pronounced for the cured specimens with the increase in curing time. Moreover, a significant reduction in the failure strain was indicated after 7 days of curing, especially for the specimens treated with WPSA between 3 and 9%. For example, the axial strain decreased from 4.25% for the virgin soil to 3.9% and 2.67% for the soil treated with 3.0% of WPSA without curing and after 28 days curing respectively. While the axial strains at failure were observed to be equal to 2.86% and 2.00% for the soil treated with 15% WPSA after zero and 28 days respectively. However, a noticeable reduction in the soil strain was observed for the uncured specimens after treatment. Once again, this behaviour is attributed to the flocculation and agglomeration with respect to the early ages (less than one day) and to the

hydration reaction resulting in the formation of the cementitious products for the specimens subjected to an extended curing (Seco *et al.*, 2011; James and Pandian, 2016). According to Nicholson (2015) clay soils with a flocculated structure exhibit a higher peak of strength associated with a brittle strain behaviour, and lower compressibility and swell potential.

Figure 5.11 shows the failed shapes of the specimens of the undisturbed and compacted untreated soil along with the specimens of the soil treated with different WPSA contents without curing. While Figure 5.12 shows the failed specimens of the untreated and treated soil after 28 days of curing. From Figure 5.11, the ductile behaviour of the undisturbed soil is very clear while a less ductile behaviour was shown by the untreated soil compacted to MDD. The treated specimens exhibited a behaviour which transferred gradually to the brittle behaviour with the increase in WPSA content even without curing as shown in Figure 5.11. After 28 days of curing, all specimens indicated a brittle behaviour, even the untreated soil, and the failure surfaces can be recognised easily which incline diagonally by approximately 60° as shown in Figure 5.12. The brittle behaviour of the untreated soil after 28 days of curing may be attributed to the decrease in water content due to the drying (Horpibulsuk *et al.*, 2010). Similar findings were reported by many researchers which they conducted their studies on soft soils stabilisation using calcium-based binders, for example calcium carbide residue (Vichan *et al.*, 2013; Neramitkornburi *et al.*, 2015) and alkaline activated GGBS (Sargent, 2015).

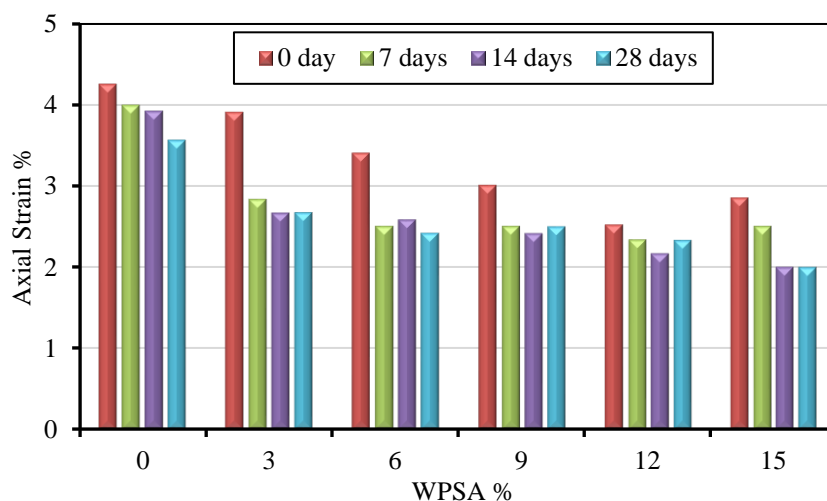


Figure 5.10 The strain behaviour of the soil treated with WPSA at different times of curing

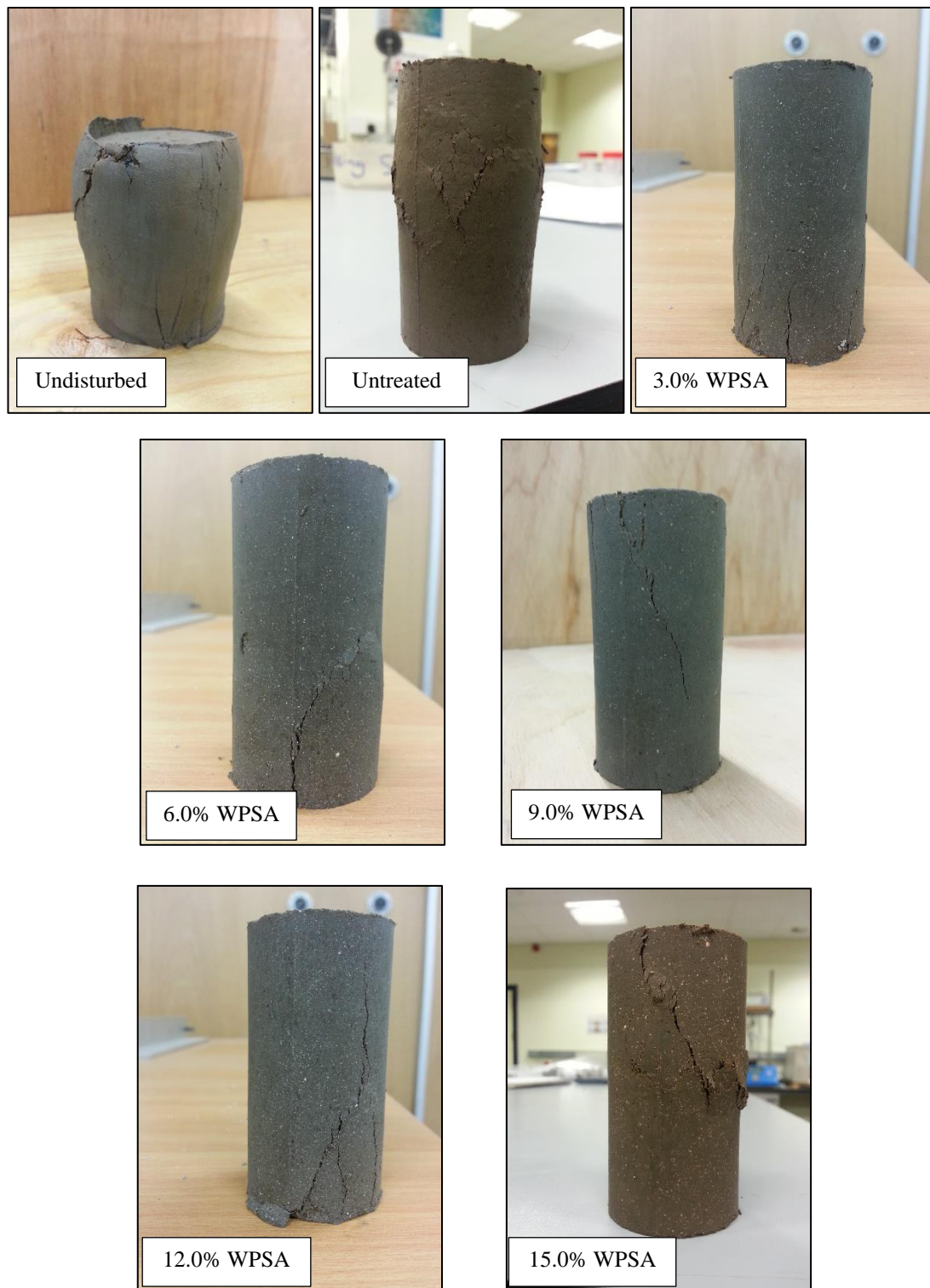


Figure 5.11 Non cured strain behaviour of the soil treated with WPSA compared to that of undisturbed and untreated compacted soil.

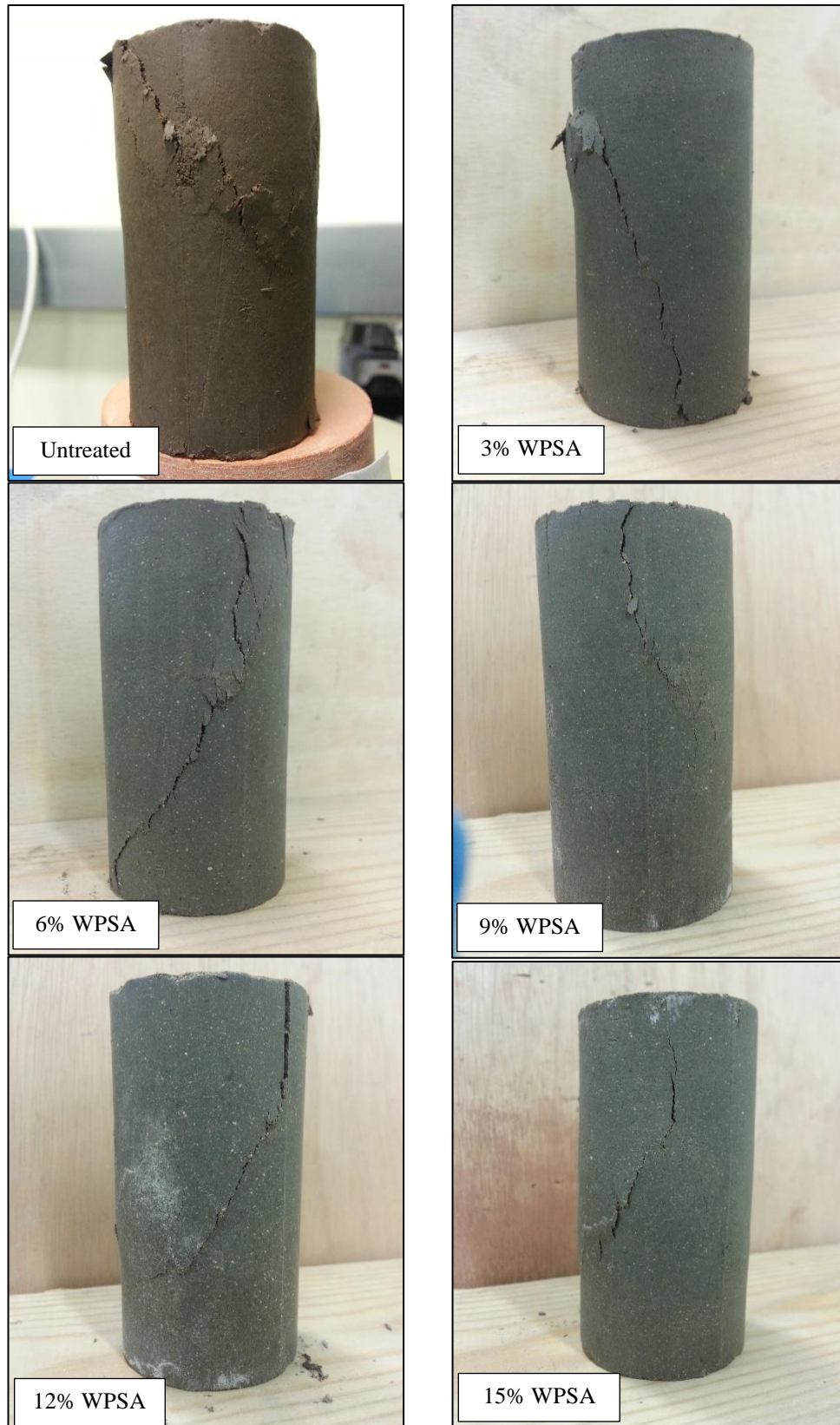


Figure 5.12 Strain behaviour of the untreated and soil treated with WPSA after 28 days curing

5.3 MECHANICAL ACTIVATION OF WPSA

In order to increase the specific surface area (SSA) to enhance the pozzolanic reactivity, the WPSA used in this study was activated mechanically using a grinding technique. A pestle and mortar grinder shown in Figure 5.13 was used to grind the WPSA for four different periods ranged from 10 to 40 minutes with an increment of 10 minutes for each period. The grinder operated with low energy agitation (1 horsepower = 0.75kW), and the capacity of its bowl was 2.5 litres. The effect of grinding activation on the performance of WPSA was evaluated in terms of the particle size distribution (PSD), and the UCS testing of soil specimens treated with the ground activated WPSA.



Figure 5.13 The grinder used for the mechanical activation in this study

5.3.1 Effect of Ground Activation on the PSD of WPSA

The results of PSD for the ground activated WPSA shown in Figure 5.14 indicated that the grinding was an effective technique to improve the PSD of the WPSA. The time of 10 minutes of grinding produced a finer grade, with median particle size of $4.767\mu\text{m}$, with a noticeable difference from that of the untreated WPSA which was $24.64\mu\text{m}$. However, the grade of the ground WPSA transferred toward the coarse side

for grinding periods beyond 10 minutes until it became slightly coarser than the untreated WPSA at 40 minutes of grinding in which the median size was equal to $31.18\mu\text{m}$. Table 5.2 illustrates the statistical information of the ground activated WPSA compared to that for the virgin material. From this Table, the improvement in the SSA can be recognised easily, especially for the grinding periods of 10 and 20 minutes. For example, the SSA of WPSA was increased from $5707\text{cm}^2/\text{g}$ for the non-ground WPSA to $10885\text{cm}^2/\text{g}$ and $9286\text{cm}^2/\text{g}$ for the ground WPSA at 10 and 20 minutes respectively. Wong *et al.* (2015) applied the grinding activation for WPSA to reduce the median particle diameter from approximately $100\mu\text{m}$ to $2\text{-}5\mu\text{m}$. They used a dry ball milling process for 8 hours with the addition of 4% of a grinding agent by the dry mass of the ground material. However, the SSA as well as the fineness of WPSA were found to be decreased at prolonged periods of grinding especially for 40 minutes of grinding which gave a PSD very akin to that for the non-ground WPSA. Since WPSA is comprised of small flocculated particles, the reduction in the median size of particles and SSA for the longer periods of grinding may be due to the agglomeration which occurred in the WPSA particles. It was reported by Sadique *et al.* (2013) that the dynamic force of grinding for long periods causes an electric activation in addition to the mechanical one. This activation may cause the agglomeration of the particles of the activated material directly when they are mixed with water. This phenomenon would decrease the pozzolanic reactivity of the ground materials.

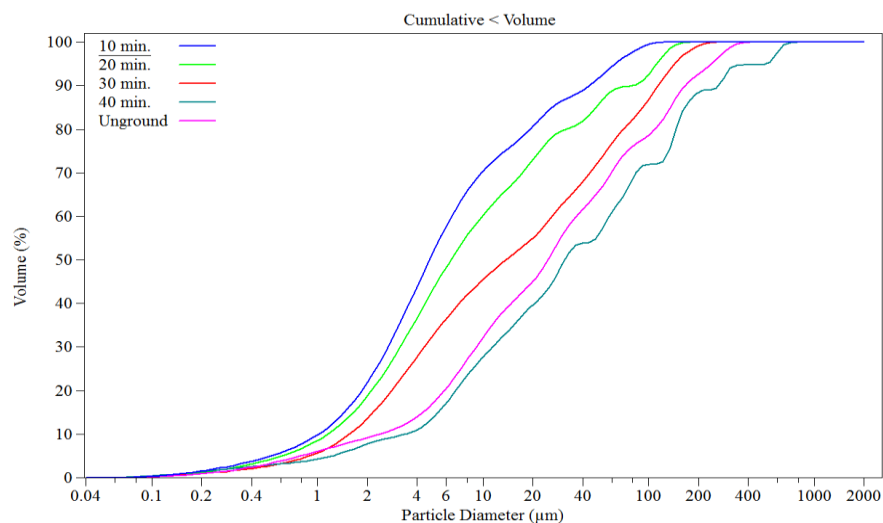


Figure 5.14 Effect of grinding activation on the PSD of WPSA.

Table 5.2 Volume statistics of ground activated WPSA

Time of grinding (min.)	d ₁₀ (µm)	d ₅₀ (µm) Median	d ₉₀ (µm)	Mean (µm)	SSA (cm ² /g)
0	2.38	24.64	166.20	57.87	5707
10	1.02	4.77	44.00	13.36	10885
20	1.16	6.40	77.63	22.04	9286
30	1.57	13.80	114.50	37.61	6825
40	3.39	31.18	263.10	92.52	5763

5.3.2 Effect of the Ground Activated WPSA on the UCS

The time of grinding was optimised dependent on the results of the UCS tests carried out on specimens treated with the optimum content of WPSA subjected to grinding for different periods. The optimisation of the grinding time was evaluated at 7 days curing as shown in Figure 5.15. It can be seen that the UCS of the treated soil was developed effectively using the grinding techniques and 10 minutes of grinding exhibited a higher value of compressive strength than the other periods of grinding. However, the UCS decreased with extended time of grinding (longer than 10 minutes) to reach a value very close to that for the non-activated WPSA with the use of 40 minutes of grinding. The results of the UCS were in a strong agreement with the results obtained from the PSD analysis in which the finer grade of WPSA indicated the highest UCS. Figure 5.16 shows the comparative development of the UCS through the time of curing of the soil treated with the optimum percentage of the normal WPSA (12%) against the soil treated with the mechanically activated WPSA using 10 minutes of grinding. From this figure, it can be seen that the ground WPSA indicated a higher compressive strength than the normal WPSA at all times of curing. Additionally, the UCS increased with the increase in the curing time. In contrast, the grinding technique was found to be an effective method for WPSA activation in which the UCS was increased after 7 days of curing from 570kPa to 622kPa with a rate of development of 9.12%. The rate of the compressive strength enhancement increased with the increase in the curing period to reach approximately 13% and 12.5% after 14 and 28 days of curing respectively.

It was proven that the mechanical activation of additive materials using the grinding technique is an effective method to increase the SSA and to produce finer materials which in turn

enhances the pozzolanic reactivity of the supplementary cementitious materials (SCMs). Moreover, it was also found that increasing the fineness of binder materials would boost the hydration process and increase the production of the cementitious gel, thus the compressive strength increases (Sadique *et al.*, 2012b; Sinsiri *et al.*, 2012; Chindaprasirt *et al.*, 2014; Sanjuán *et al.*, 2015; Sobolev *et al.*, 2016; Velandia *et al.*, 2016). The reduction that occurred in the compressive strength for the specimens treated with WPSA ground for longer than 10 minutes can be attributed to the agglomeration of the WPSA particles which decreased the pozzolanic reaction and disrupted the hydration process (Sadique *et al.*, 2013; Sanjuán *et al.*, 2015).

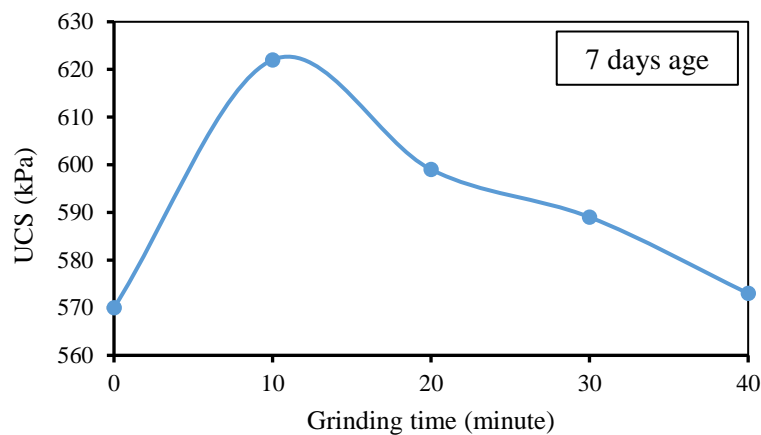


Figure 5.15 Effect of grinding activation of WPSA on the UCS.

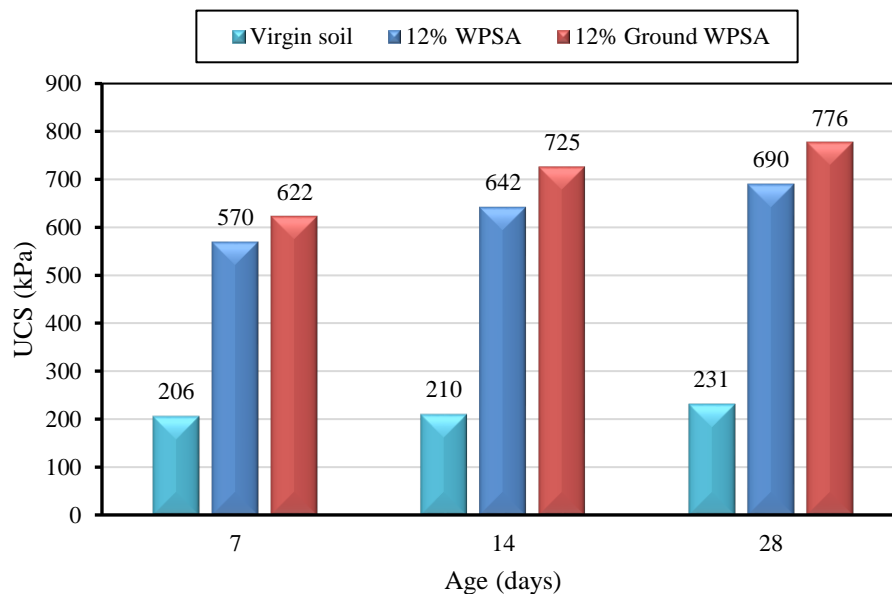


Figure 5.16 The development of UCS over the curing time of the soil treated with normal and mechanically activated WPSA

5.4 OPTIMISATION OF BINARY BLENDED MIXTURE

The binary blending optimisation represented the second stage of mixing design in this research project. This stage was utilised to identify the optimum binary mixture by investigating the effect of different binary blends, produced from a combination of WPSA and POFA with different proportions, on the geotechnical properties of the soil stabilised in this study. The total binder content was fixed at 12% by the dry mass of the treated soil in which different proportions of WPSA and POFA produced different types of binary mixtures as illustrated in Table 5.3. In other words, the WPSA content was substituted up to 50% by POFA in which each increment of POFA was 1.5% by the dry mass of the treated soil (i.e. 12.5% of the total binder content). The evaluation of the performance of the binary mixtures is dependent on the results obtained from the UCS testing. However, the effect of binary blending treatment on the consistency limits and the compaction parameters was also investigated at this stage. The results obtained from binary treatment for each test were compared to those for the soil treated with the mechanically activated unary mixture (GU) and further comparison with the performance of the reference mixture (Soil-12% OPC) were conducted in the next chapter of this study.

Table 5.3 Mixing proportion of binary blending mixtures

Mixture ID	Fly ash content by the dry weight of soil	
	WPSA %	POFA %
U	12.0	0
GU	12.0*	0
BM1	10.5	1.5
BM2	9.0	3.0
BM3	7.5	4.5
BM4	6.0	6.0

* Ground WPSA with the optimum time of grinding
BM is from binary mixture.

5.4.1 Effect of Binary Treatment on the Atterberg limits

Figure 5.17 shows the results of the consistency limits tests for the soil treated with different binary mixtures along with those for the soil treated with optimum WPSA content (12%) and the GU mixture, while Table 5.4 illustrates the values of LL, PL, and PI after binary blending treatment. A slight reduction in the PI was indicated after the mechanical activation, where the PI was decreased from 13.45 to 13.38. This indicates that the effect of grinding activation of the PI was negligible. However, it was found that both the LL and PL were hardly increased after grinding activation but the increment in PL was slightly higher than that for LL which led to this reduction in the PI. On the other hand, the binary treatment was found to be effective for a further improvement in consistency limits of the treated soil when additional reductions in PI were indicated. For example, the PI was decreased from 13.45 for the soil treated with U mixture to 11.73 for the soil treated with BM4. Additionally, the binary mixture treatment indicated that both LL and PL decreased with the increase in the substitution amount of POFA but the reduction in LL was higher than that for PL, thus PI decreased. However, both LL and PL results indicated a gradual reduction with a reasonably constant rate with the binary blending treatment as shown in Figure 5.17. According to the chemical composition of POFA presented in the previous chapter, it has pozzolanic oxides (SiO_2 and Al_2O_3) which are much higher than the content of calcium oxide (CaO) in which the water demand of the pozzolanic compounds is very low in comparison to that for CaO (Aldahdooh *et al.*, 2013; Aprianti *et al.*, 2015; Pourakbar *et al.*, 2015). Therefore, the reduction that occurred in LL and PL after adding POFA in the binary blending treatment could be attributed to the reduction in the water demand due to reducing the WPSA content for the total added binder.

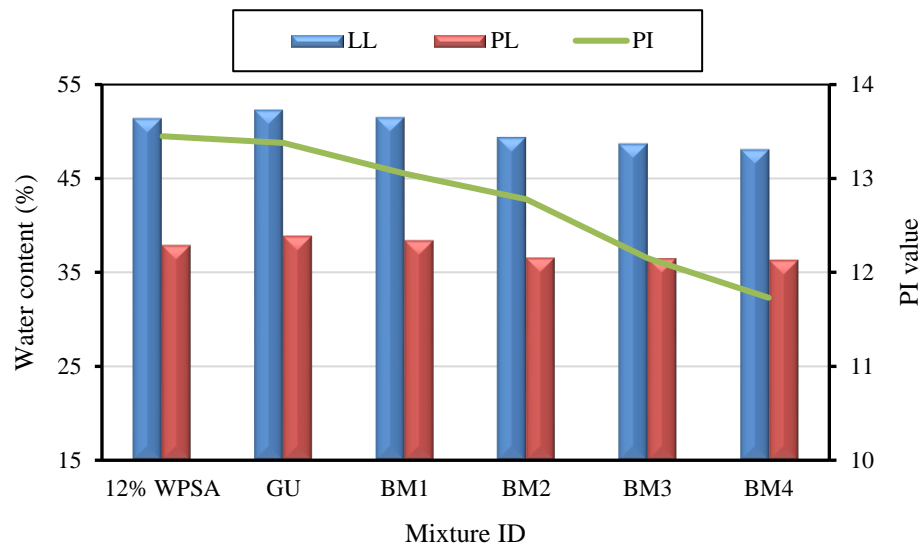


Figure 5.17 Effect of grinding and binary blending treatment on Atterberg limits of the stabilised soil.

Table 5.4 Atterberg limits of the soil treated with different unary and binary mixtures

Mixture ID	LL (%)	PL (%)	PI
U	51.30	37.85	13.45
GU	52.20	38.82	13.38
BM1	51.40	38.35	13.05
BM2	49.30	36.52	12.78
BM3	48.60	36.45	12.15
BM4	48.00	36.27	11.73

The changing trend in Atterberg limits of soils treated with binders produced from the mixing of calcium-based materials such as cement and lime with silica-based materials such as fly ashes, similar to POFA, depends on the type of treated soil and the physico-chemical properties of the additives. A similar reduction trend in LL and PI was reported by Mu'azu (2007) when he studied the effect of bagasse ash on the plasticity of the cement-stabilised lateritic soil. It was found that the increase in the bagasse ash

added to the cement-treated soil reduced the LL and increased the PL, thus the PI decreased. The reduction that occurred in the LL was attributed to the flocculation and aggregation of the clay particles due to the pozzolanic reaction of bagasse ash which turned the clay soil to a salty soil. The last transformation decreased the surface area, thus the LL decreased. Cheshomi *et al.* (2017) also reported a similar behaviour of the Atterberg limits after adding a class F fly ash (FA) to a lime-stabilised sulphate-bearing soil. They observed that the LL decreased first with adding 3% FA to the lime-treated soil then started to increase beyond 3%. The PL was found to increase with the increase in the added FA and this in turn decreased the PI. Overall, and according to James and Pandian (2016), the plasticity of soils treated with lime or calcium-based binder were found to be decreased with combination binders when used with an another pozzolanic additive.

5.4.2 Effect of Binary Blending on the Compaction Parameters

The results of the compaction parameters tests shown in Figure 5.18 and illustrated in Table 5.5 indicated that there was a marginal decrease in the dry density accompanied with a slight increase in OMC after grinding activation. This may be due to the increment that occurred in the specific surface area which increased the water demand of the soil-binder mixture (Edeh *et al.*, 2014). With respect to the binary blending treatment, the results of the compaction tests indicated that the MDD increased slightly while the OMC decreased noticeably with the increase in POFA content in the binary mixtures as shown in Figure 5.18 and Table 5.5. For example, the MDD was increased from 1.44Mg/m^3 for the soil treated with mixture GU to 1.48Mg/m^3 for the soil treated with BM4. The optimum moisture content for the soil treated with both the previous binders decreased from 29 to 24.5%. As the chemical composition of POFA indicated that it has CaO less than WPSA and the major oxides were pozzolanic oxides (section 4.3.3), increasing the POFA:WPSA proportion led to a reduction in the CaO content in the resulting binder. Thus, the water demand of the newly developed mixtures decreased which led to a decrease in the OMC and an increase in the MDD. This agreed with the findings reported by many researchers that they conducted tests using fly ash type F in contrast with studies using fly ash type C, which has high CaO content (Harichane *et al.*, 2011; Sivrikaya *et al.*, 2014; Pourakbar *et al.*, 2015). According to

Pourakbar *et al.* (2015), a proportion of cement:POFA up to 80:20 is enough to increase the MDD of the 10% binder-treated soil by approximately 1.1 times the MDD of the soil treated with OPC only. The same proportion of cement:POFA was found to decrease the OMC by 22.73% of that for soil treated with cement. The reduction that occurred in the optimum moisture content was attributed to the increase in POFA content in the binder which reduced the affinity of treated soil with the water. However, the researchers pointed out that MDD decreased and OMC increased with further increments in the POFA content in the binder. The increase in MDD of the treated soil may contribute to the increase in the soil compressive strength and to the improvement of the other geotechnical properties (Nicholson, 2015).

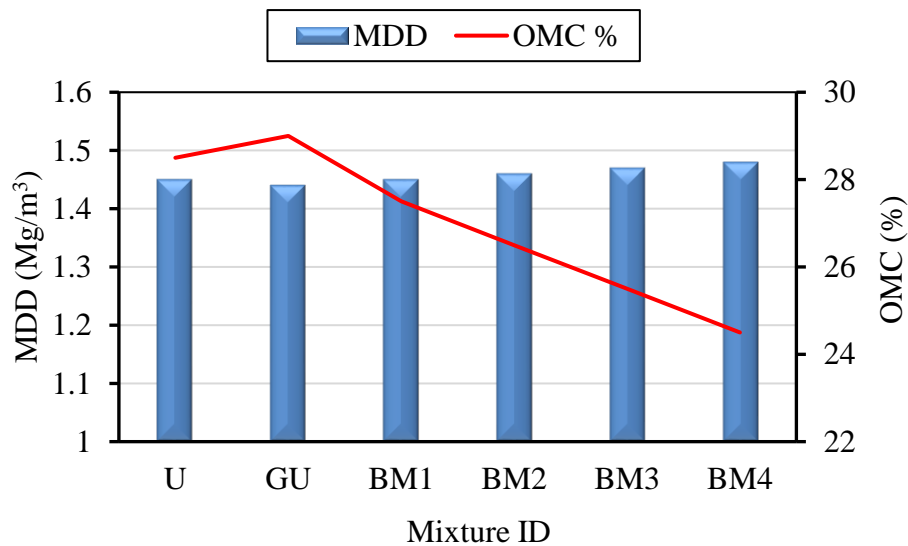


Figure 5.18 Effect of binary blending treatment on compaction parameters.

Table 5.5 The values of compaction parameters after binary blending treatment.

Mixture ID	MMD (Mg/m ³)	OMC %
Virgin soil	1.56	23.5
U	1.45	28.5
GU	1.44	29.0
BM1	1.45	27.5
BM2	1.46	26.5
BM3	1.47	25.5
BM4	1.48	24.5

5.4.3 Effect of Binary Blending on UCS

The average of maximum compressive strength values of soil specimens treated with different binary mixtures along with those of the soil treated with ground activated unary mixture are shown in Figure 5.19. Additionally, this figure shows the effect of the curing time on the compressive strength after binary blending treatment by demonstrating the compressive strengths of the soil specimens subjected to different curing intervals (7, 14, and 28 days). The results obtained indicated that the compressive strength of the treated soil was improved noticeably after binary blending treatment. The UCS increased with the increase in POFA content in the total binder up to a quarter which represents 3% by the dry mass of the treated soil. After that, small reductions were observed in the UCS for further increments in the POFA portion. Similar scenarios occurred for all periods of curing. However, all types of binary mixtures indicated values of compressive strength higher than that for the soil treated with GU which means that the binary blending treatment was found to be useful for the compressive strength enhancement. Moreover, the results of the UCS tests shown in Figure 5.19 indicated that the highest value of UCS was achieved from the specimens of the soil treated with BM2 for all curing times. This mixture contained 9% WPSA with 3% POFA. The latter mixture increased the UCS of the soil significantly, for example, at 28 days of curing; the UCS was increased from 776kPa for the soil treated with GU to 924kPa with BM2 treatment, which means that the UCS was increased by 19.1% after BM2 treatment. Moreover, the compressive strength of the soil treated with BM2 recorded an interesting value for the short term curing (755kPa after 7 days of curing), which was very close to the strength at 28 days curing for the soil treated with GU. Additionally, it was observed that all types of the binary mixtures indicated unconfined compressive strengths, after 14 days of curing, higher than that indicated for the 28 days curing of the soil treated with GU as shown in Figure 5.19.

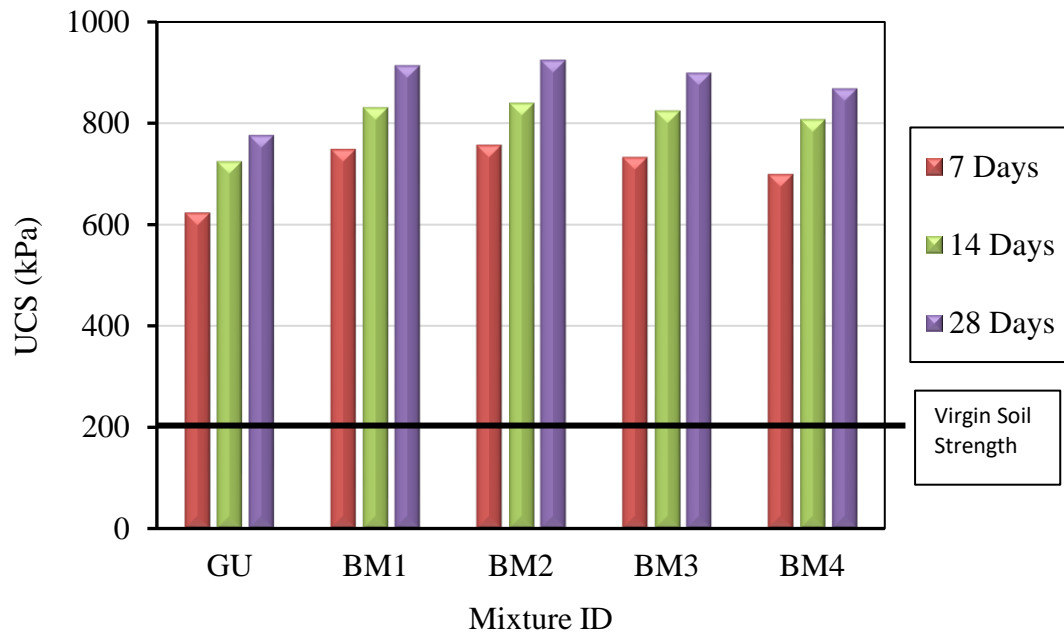


Figure 5.19 Effect of binary blending treatment on UCS.

Figure 5.20 shows the comparative stress-axial strain diagrams, at 7 and 28 days for the untreated soil and the soil stabilised with different binary blends along with the soil treated with GU. It can be seen that the maximum compressive strengths of the soil treated with BM1 and BM2 were very akin to each other. Consequently, the BM2 was considered as the optimum binary mixture in this stage of experimental works because it provided more balance between the two waste materials used in the binary blending technique. As per the chemical composition of the POFA (4.3.3), the existence of the pozzolanic oxides such as the silica (SiO_2) and alumina (Al_2O_3) increased the cementitious gel represented by the calcium-silicate-hydrated (C-S-H) and calcium-aluminate-hydrated (C-A-H). This gel was produced from the hydration reaction took place between these pozzolanic compounds and the hydrated lime ($\text{Ca}(\text{OH})_2$) which was produced from the reaction between the added water and the lime CaO from WPSA (Muhunthan and Sariosseiri, 2008; Puppala *et al.*, 2015; Aïtcin, 2016b). Similar findings were reported by many researchers who conducted their studies to develop the compressive strength of either mortars or stabilised soils (Sadique *et al.*, 2012b; Pourakbar *et al.*, 2015; Arenas-Piedrahita *et al.*, 2016; Matakah *et al.*, 2016). All of them agreed that the increment achieved in the compressive strength was due to the pozzolanic reaction that occurred between the silicates of the supplementary materials and the hydrated lime provided from the calcium-based materials in the

binder used. Pourakbar *et al.* (2015) used an ultrafine POFA to replace a portion of OPC in soft soil stabilisation. It was found that replacing a percentage of 20% of cement by POFA exhibited a significant increase in the soil compressive strength when using a binder dosage of 10%. However, they observed that the proportion of Cement 90:10 POFA indicated the highest UCS after increasing the binder dosage to 15%.

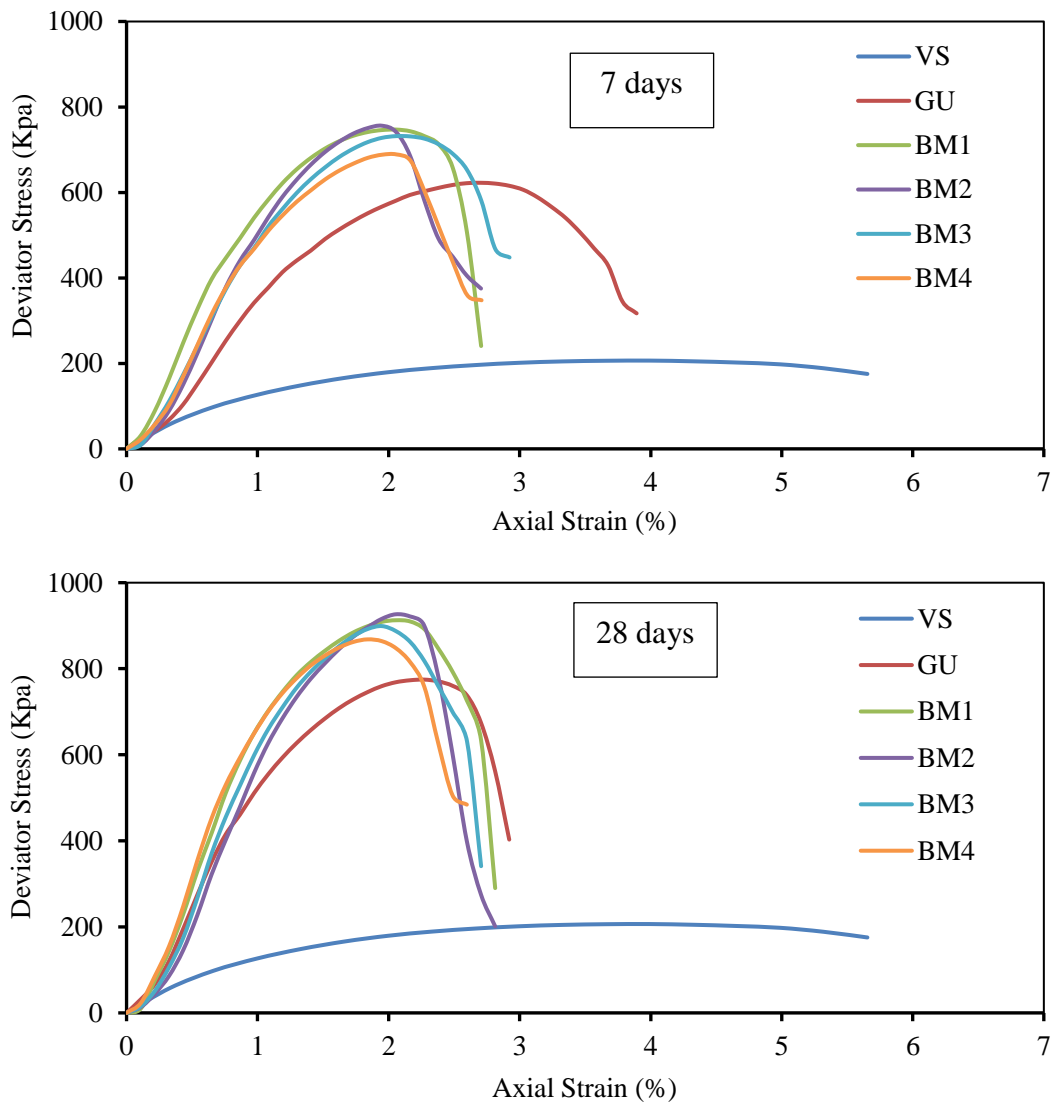


Figure 5.20 Stress-axial strain diagrams of the binary mixture optimisation at 7 and 28 days of curing.

The high pH value of POFA may also have a responsibility in the UCS development gained after binary treatment because it could be considered as an alkaline activator for WPSA. The alkalinity of POFA is essential to boost the dissolution of the solid phases of the aluminosilicate materials which in turn increases the silicates that have

the susceptibility to react with the hydrated lime, thus producing the cementitious gel (Matakah *et al.*, 2016). Moreover, it could play an important role to maintain an alkaline environment which is required to continue the pozzolanic reaction for long periods of curing (Sadique *et al.*, 2012b; Provis *et al.*, 2015; Zhang *et al.*, 2017b). The results shown in Figure 5.20 also indicated that there were reductions in the failure strains of the soil treated with the binary mixtures, which means that the behaviour became more brittle. It was observed that there was no noticeable change in the failure axial strain between 7 and 28 days of curing. Figure 5.21 shows the failure shape at 7 and 28 days for the soil specimens treated with BM2. It can be seen that for both ages of curing, the failure shapes are similar to each other and the failure surface was in a diagonal direction which means that the failure occurred due to the shear failure.



Figure 5.21 Failure shape of the soil treated with BM2 at 7 and 28 days of curing.

5.5 OPTIMISATION OF TERNARY MIXTURE

In order to satisfy an acceptable balance in the waste materials usage in this study, especially to reduce WPSA content in the total binder, rice husk ash (RHA) was used in this stage of the experimental works as a third waste material. Consequently, the optimisation of the ternary mixture was carried out to evaluate the best ternary

mixture(s) that produced higher soil compressive strengths. In this stage, the soft soil was treated with 12% binder of different ternary mixtures produced from mixing the WPSA, POFA and RHA in different proportions. Table 5.6 illustrates the mixing procedure that was considered in the ternary optimisation process in this research project. However, RHA was blended with WPSA only to produce a new binary mixture to evaluate the effect of RHA without the effect of POFA. The performance of the ternary mixtures was evaluated by conducting the UCS testing on specimens cured for different periods of curing (7, 14, and 28 days) along with evaluation of the Atterberg limits and compaction parameters. Moreover, this stage of optimisation included the use of flue gas desulphurisation (FGD) gypsum as grinding aid as well as a retarder for the developed cementitious material. However, FGD was added in a very small amount (5% by the total binder added to the soil) and the grinding was performed for not longer than 15 minutes.

Table 5.6 Mixing proportions of the ternary blending treatment.

Mixture ID	Fly ash content by the dry weight of soil		
	WPSA %	POFA %	RHA %
TM1*	9	0	3
TM2	6	0	6
TM3	9	1.5	1.5
TM4	8	2	2
TM5	6	3	3

* TM is from ternary mixture.

5.5.1 Effect of Ternary Blending Treatment on Atterberg Limits

The results of the Atterberg limits tests after the ternary blending treatment compared with those for the virgin soil and the soil treated with the mixture GU are shown in Figure 5.22. This figure depicts that there were slight changes in LL, PL and PI after the ternary treatment in comparison to the Atterberg limits of the soil treated with GU. Overall, slight reductions in LLs were recognised with the ternary treatment in

comparison with the GU treatment. This behaviour was in contrast to what occurred with binary treatment as presented in section 5.4.1. However, a noticeable reduction in the PI was observed for the soil treated with T5 as shown in Figure 5.22. Moreover, the magnitudes of the Atterberg limits listed in Table 5.7 showed that the values of the liquid limits were almost above 50% for the treated soil, while the plastic limits were around 38. However, the lowest values of the PI were 12.59 and 12.06 which were achieved by using T2 and T5 respectively. It was noticed that the mixtures with a low content of WPSA indicated the better improvement regarding the consistency limits as well as further reductions in PI. The behaviour of the Atterberg limits with ternary blending treatment can be attributed to the same reason that was shown for the behaviour with the binary mixtures (section 5.4.1). The increase in the materials associated with high silica content (POFA and RHA) that replaced the WPSA in the binder reduced the water demand of the soil-binder mixture, thus the LL decreased and caused a reduction in the PI. A study was carried out by Choobbasti *et al.* (2010) to investigate the effect of the rice husk ash (RHA) treatment on the consistency limits and geotechnical properties of the lime-stabilised soft soil. The results revealed that there were gradual increments in the LL of the 6% lime-soil mixture with the increase in RHA content. On the other hand, the PL increased significantly with the increase in RHA which in turn led to a reduction in the PI. Similar findings were reported by James and Sivakumar (2014) during their investigation of the effect of adding RHA to a lime stabilised soft soil on the index properties.

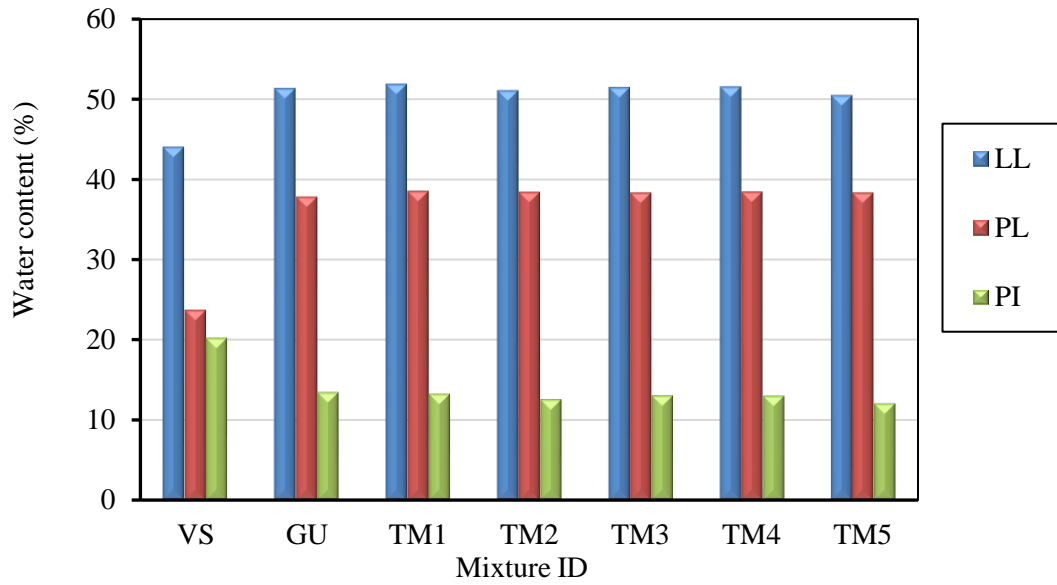


Figure 5.22 Effect of the ternary blending treatment on the Atterberg limits.

Table 5.7 Atterberg limits values after ternary blending treatment.

Mixture ID	LL	PL	PI
VS	44.00	23.78	20.22
GU	51.30	37.85	13.45
TM1	51.80	38.53	13.27
TM2	51.00	38.41	12.59
TM3	51.40	38.34	13.06
TM4	51.50	38.46	13.04
TM5	50.40	38.34	12.06

5.5.2 Effect of Ternary Blending Treatment on Compaction Parameters

Figure 5.23 presents the dry density – moisture content relationships for the soft soil treated with different ternary mixtures compared with those for the virgin soil and soil treated with GU. It can be seen that almost all MDDs increased and OMCs decreased with ternary treatment. This figure shows that there was a clear raise in the dry density of the soil treated with T5 in comparison to that achieved from the soil treated with GU. However, the highest curve of dry density – moisture content was still much lower than that for the virgin soil. The comparative effect of ternary blending treatment and GU mixture on the values of MDD and OMC is shown in Figure 5.24 and illustrated in Table 5.8. From this figure and table, it can be acknowledged that there were slight increments in MDDs accompanied with a noticeable decline in OMCs after ternary treatment. Moreover, and with the reference to the mixing proportions illustrated in Table 6.6, it can be observed that the dominant substance that controlled the behaviour of the compaction parameters was WPSA and its content in the total binder added to the treated soil. In other words, the lower the WPSA content within the binder, the higher MDD and lower OMC were indicated. For example, the higher MDDs were achieved from the soil treated with TM2 and TM5 which contained 50% WPSA of total binder (6% by the dry mass of the soil) which were 1.47Mg/m^3 and 1.48Mg/cm^3 respectively. Furthermore, the results of the compaction tests demonstrated that for the mixtures having the same WPSA content (6% by the dry mass), when they have POFA, indicated a MDD higher than those included RHA as it was observed for TM2 and TM5. The increase that occurred in MDD accompanied with the reduction in OMC could be considered as a beneficial in terms of increasing the compressive strength as well as enhancing the workability of the soil-binder mixture. As explained in the binary blending treatment (section 5.4.2), this behaviour can be attributed to the reduction of CaO in the binder which resulted after ternary blending using POFA and RHA of which their major chemical compounds are silica materials. Consequently, the water demand of the soil-binder mixture decreased and led to a reduction in the OMC and an increase in the MDD (Harichane *et al.*, 2011; Sivrikaya *et al.*, 2014).

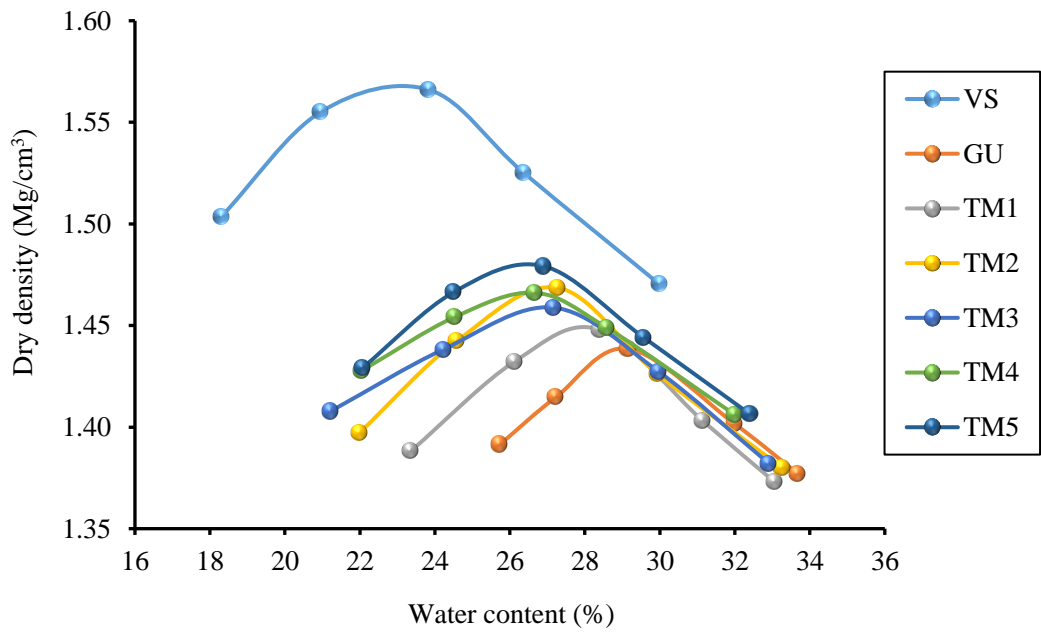


Figure 5.23 Dry density-moisture content relationship of the soil treated with different ternary mixtures.

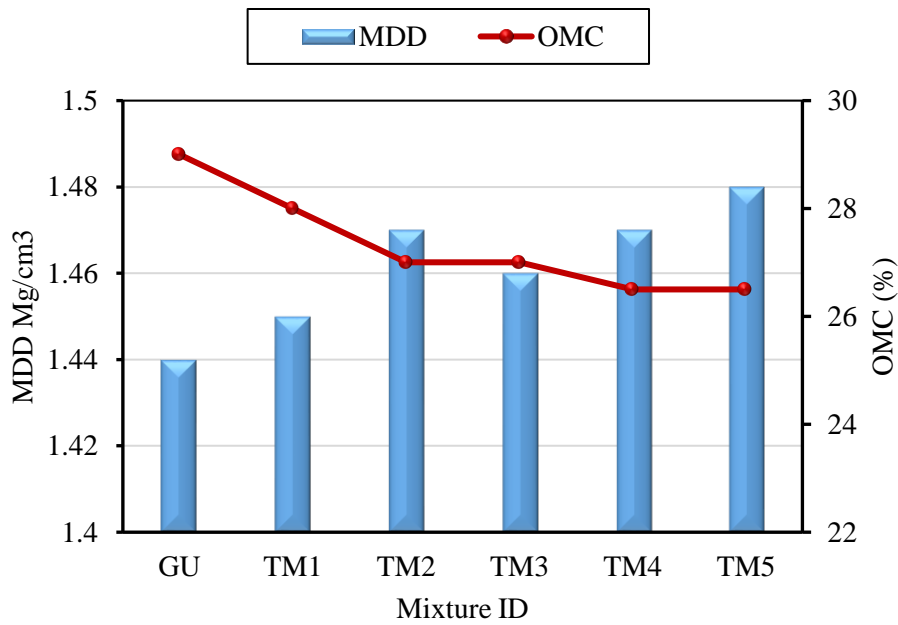


Figure 5.24 Effect of ternary blending treatment on the MDD and OMC.

Table 5.8 The values of compaction parameters after ternary blending treatment.

Mixture ID	MMD (Mg/m ³)	OMC %
Virgin soil	1.56	23.5
GU	1.44	29.0
TM1	1.45	28.0
TM2	1.47	27.0
TM3	1.46	27.0
TM4	1.47	26.5
TM5	1.48	26.5

5.5.3 Effect of Ternary Blending Treatment on UCS

A synopsis of the average maximum compressive strengths after the ternary blending treatment obtained from the unconfined compressive strength tests is presented in Figure 5.25 and Table 5.9, along with those achieved from samples of the virgin soil and the soil treated with the unary mixture (GU) for the comparison purposes. Additionally, the effect of the curing time on the strength development is also shown in this figure. A similar scenario, of the compressive strength development, that occurred in the binary blending treatment, as shown in section 5.4.3. With the exception of the mixture TM2, it is evident that there were increments in specimen strengths over the 28 days curing period for all ternary mixtures. However, the degree of the soil compressive strength development observed within the tested specimens varied according to the WPSA content in the total binder. In general, the mixtures containing between 8% and 9% WPSA by the dry mass of the treated soil, exhibited higher compressive strength. To be more precise, the use of TM3 and TM4 indicated higher compressive strength after 28 days of curing, which were 959kPa and 944kPa respectively. However, it was observed that all ternary mixtures showed a development in the UCS higher than that achieved from the soil specimens treated with GU. Additionally, it was noticed that TM4 indicated a compressive strength higher than that achieved from the use of TM1 despite the fact that TM4 contained a lower amount of WPSA (8% WPSA for TM4 in comparison to 9% WPSA for TM1).

Nevertheless, a reduction in the UCS was observed when the WPSA content became less than 8% by the dry mass of the treated soil. Based on the high amorphous silica content of the RHA (section 4.3.4) along with the chemical composition of the POFA associated with high alkalinity (section 4.3.3), the development in the compressive strength achieved after ternary blending treatment can be attributed to the pozzolanic reaction that occurred between the silicates materials of the aforementioned fly ashes and the hydrated lime produced from WPSA (Sadique *et al.*, 2013; Puppala *et al.*, 2015). The latter reaction led to an increase in the production of the cementitious compounds (C-S-H and C-A-H) which have the responsibility for the strength development. Moreover, the amorphous silica of RHA has susceptibility to dissolve in the alkaline environments (Sargent, 2015). Such an environment could be provided by POFA, since it has a significant value of pH. Thus, the propensity of the RHA silica to dissolve may have occurred, and this in turn caused an acceleration of the hydration process resulting in an early formation of the cementitious gel (Habert, 2014). In summary, the mixtures TM3 and TM4 were considered as optimum ternary mixtures for the further activation experimental work in this study. These experiments involved the investigation of the effect of inter-grinding activation using 5% FGD by the mass of the total binder.

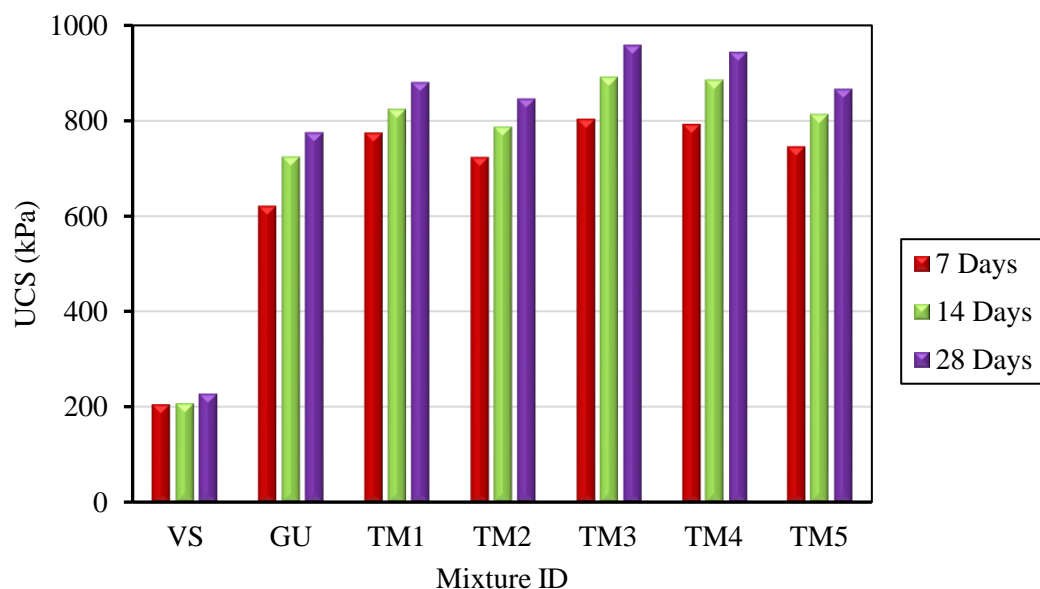


Figure 5.25 Effect of ternary blending treatment on UCS.

Table 5.9 UCS values of curing time after ternary blending treatment.

Mixture ID	Fly ash content by the dry weight of soil			UCS (kPa) at the specific age of curing (days)		
	WPSA %	POFA %	RHA %	7	14	28
	VS	0	0	0	206	209
GU	12	0	0	622	725	776
TM1	9	0	3	775	825	881
TM2	6	0	6	724	788	847
TM3	9	1.5	1.5	804	892	959
TM4	8	2	2	793	886	944
TM5	6	3	3	746	814	867

The stress-axial strain behaviour of the stabilised soil after ternary blending treatment through the various curing times is shown in Figure 5.26. At 7 days of curing, the samples treated with ternary mixtures possessed strain failures less than those for the soil samples treated with GU. However, there were slight differences in the strain failure amongst the soil specimens treated with various ternary mixtures. This behaviour could elucidate the high compressive strength achieved using the ternary mixtures within 7 days of curing, which almost exceeded the 28 days compressive strength of the soil treated with GU as illustrated in Table 5.9. Additionally, the results obtained from the stress-strain diagrams indicated that the samples tested after 28 days of curing generally exhibited failure strains similar to or slightly higher than that for the soil treated with GU. This could be beneficial to decrease the soil brittleness after treating with ternary mixtures. For example, the failure strain of the soil treated with TM4 was 2.48%, while it was 2.271% for the soil treated with GU. Although some engineering projects require high compressive strength as well as stiffness, there are also engineering projects such as the foundations for highways and railways that may require lower stiffness. The latter types of engineering projects normally experience impact or dynamic loads, therefore, a ground characterised with lower stiffness may be desirable to avoid the brittle failure. A range between 300-3000kPa is typically

required for shallow or deep stabilised soils (EuroSoilStab, 2002; Horpibulsuk *et al.*, 2013). In general, all soil samples treated with different ternary mixtures exhibited brittle failure behaviour. Figure 5.27a and b show the failure shapes after 7 and 28 days for selected samples treated with TM3 and TM4 respectively.

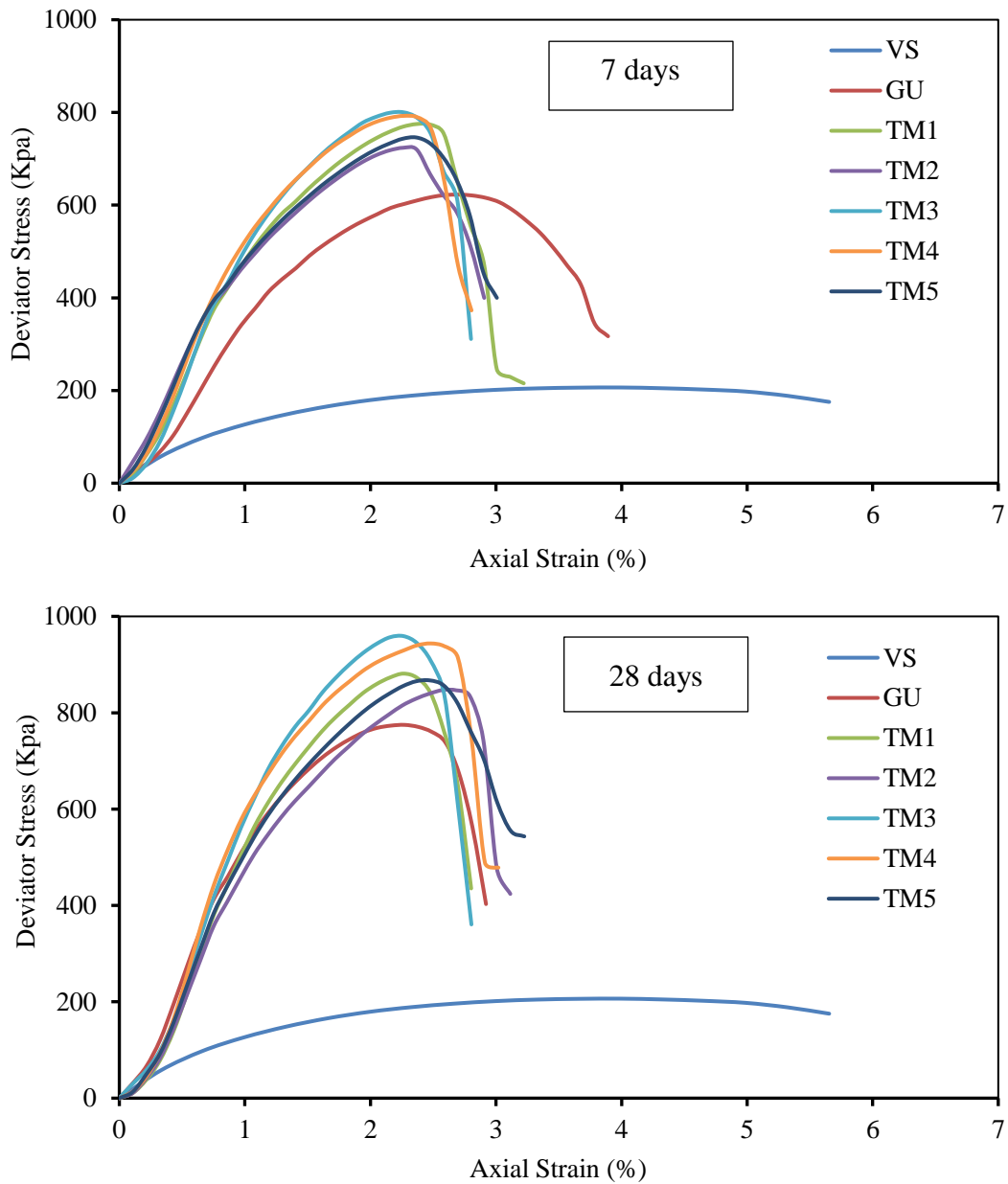


Figure 5.26 Stress-axial strain diagrams after ternary blending treatment.

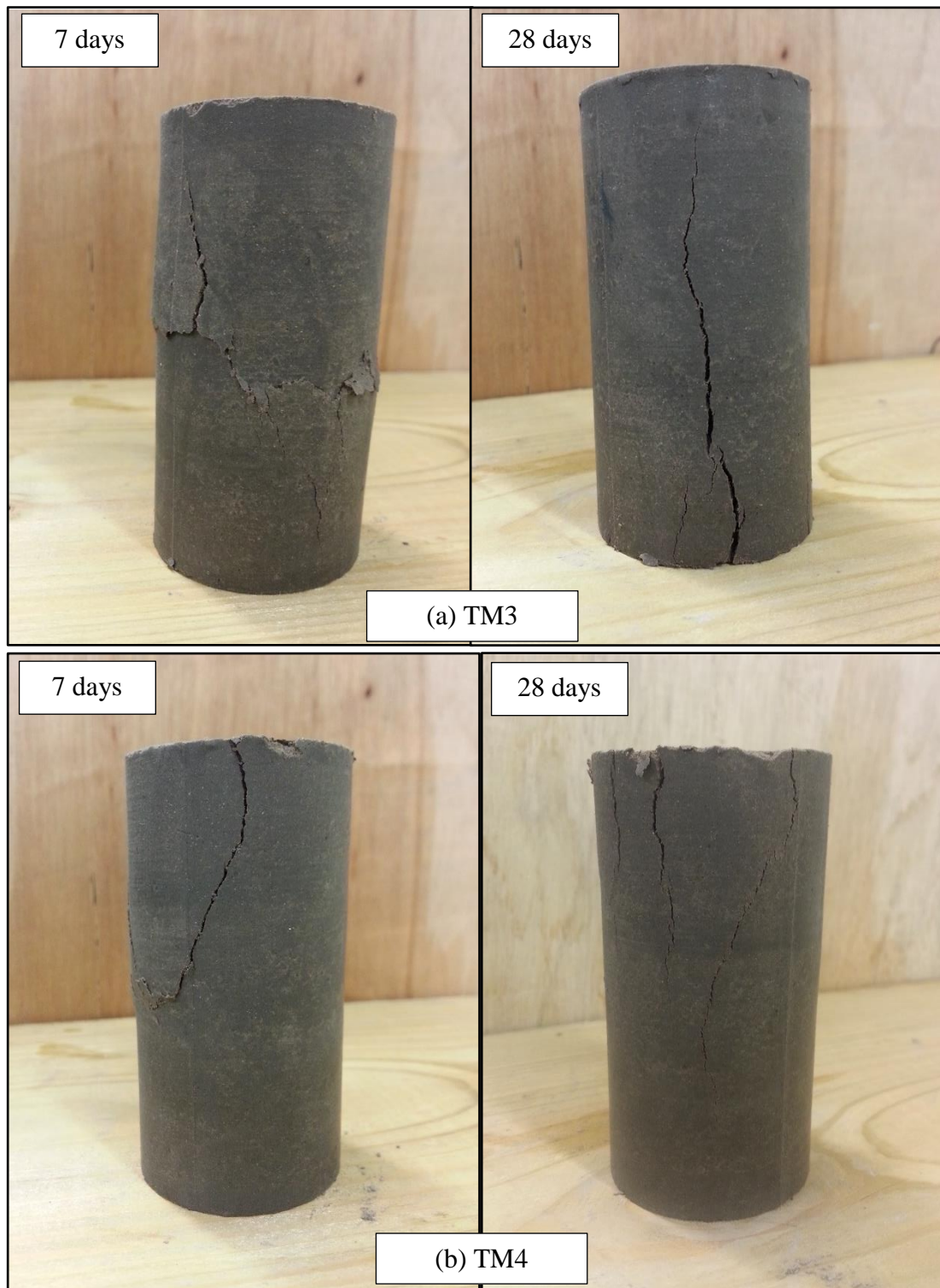


Figure 5.27 Failure shapes over the time of curing for the soil treated with (a) TM3, and (b) TM4.

5.5.4 Effect of Grinding Activation Using FGD

This stage of experimental work included the utilisation of FGD which was used as a grinding agent (GA) and for sulphate activation (as a retarder for the fast setting which is associated with the WPSA) applied to the selected ternary mixtures TM3 and TM4. The effect of grinding activation using FGD was evaluated dependent on the results obtained from the particle size distribution, Atterberg limits, compaction parameters and UCS tests. The same scenario was adopted by Sadique *et al.* (2013) and considered 5% FGD use, by the total mass of the binder. This was mixed with the selected mixtures then subjected to a low grinding energy for no longer than 15 minutes using the grinding machine presented earlier in section 5.3. The period of grinding was selected to be short as to prevent the agglomeration which has a detrimental effect on the pozzolanic property of the ground substances (Juhász and Opoczky, 1990). However, an inter-grinding procedure was applied in this study instead of the individual grinding adopted by Sadique. The performance of the ground activated ternary mixtures is presented as follows.

5.5.4.1 Particle size distribution (PSD)

The effect of the grinding activation along with the effect of using the grinding aid (FGD) on the PSD of TM3 is shown in Figure 5.28. It is evident that the fineness of TM3 was increased slightly when it was subjected to a period of 15mins of grinding without using FGD. However, a significant improvement in PSD was achieved after using the FGD as a GA. The results indicated that the particles of TM3 and ground TM3 without FGD (GTM3) ranged between 4 - 200 μm , while after using FGD, the majority of the particles became ranged between 2 - 45 μm . Moreover, Table 5.10 illustrates the volume statistics of the TM3 after grinding activation and using FGD as a GA. It can be observed that the median diameter size of particles of the TM3 was decreased from 17.69 μm to 10.10 μm and 5.996 μm after the grinding and FGD application respectively and these reductions in the median sizes were accompanied with increments in the specific surface area (SSA). Similar findings were reported by Sadique and Al-Nageim (2012) and the improvement achieved in the PSD was attributed to the high fineness of FGD and to the alteration of grain distribution along with the morphological modification caused by the grinding energy and the FGD.

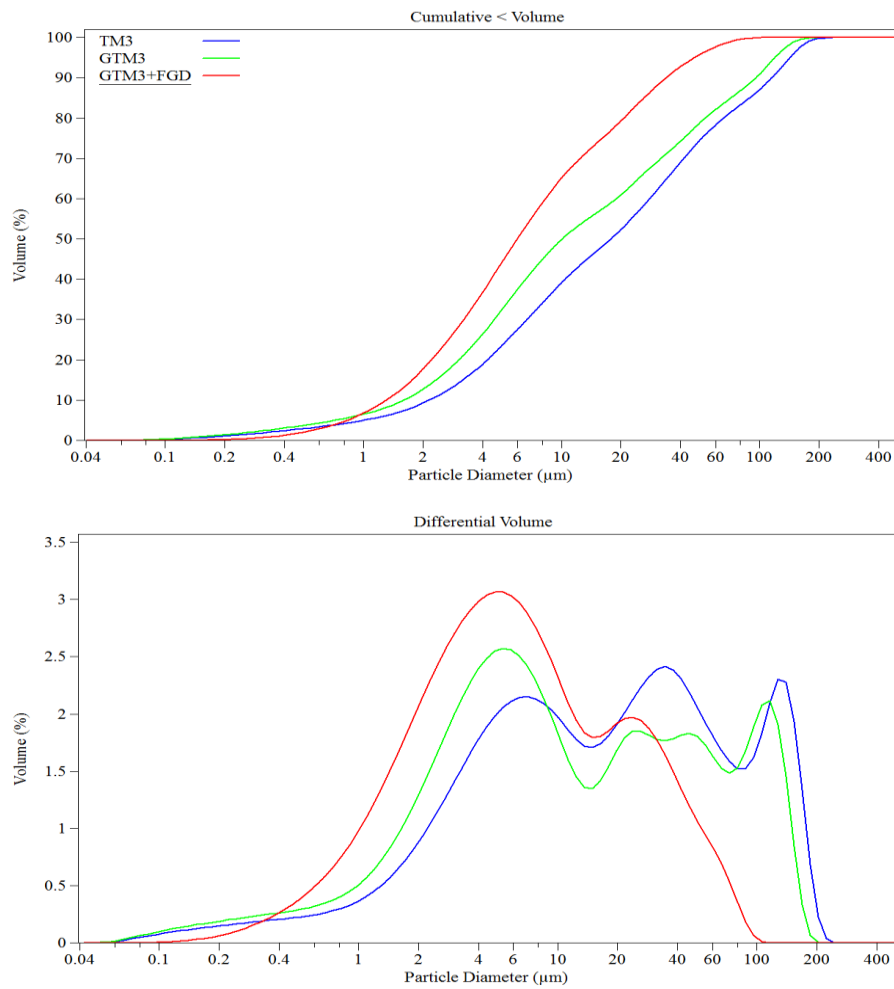


Figure 5.28 Effect of grinding and FGD activation on PSD of TM3

Table 5.10 Volume statistics of TM3 after grinding activation

Time of grinding (min.)	d_{10} (μm)	d_{50} (μm) Median	d_{90} (μm)	Mean (μm)	SSA (cm^2/g)
TM3	2.158	17.69	115.6	37.56	6441.76
GTM3	1.601	10.10	95.40	29.63	10107.5
GTM3+FGD	1.308	5.996	33.72	12.45	11232

5.5.4.2 Atterberg limits

The results of Atterberg limits tests after the grinding activation with the use of FGD shown in Figure 5.29 indicated that there were slight reductions in the LLs of both TM3 and TM4 with no noticeable changes in the PLs. Thus, further reductions in the PI of the soil treated with TM3 and TM4 were achieved after the addition of FGD and the application of the grinding energy. As shown in Table 5.11, the lowest value of PI was obtained from the soil treated with ground TM4 with FGD (GTM4+FGD). The use of the latter mixture decreased the PI significantly, which was reduced from 13.04 for the soil treated with untreated TM4 to 11.74 for the soil treated with GTM4+FGD. The reduction in LL can be attributed to the decrease in the water demand of the binder after using FGD along with the grinding technique. It was evident that the use of grinding with the FGA as GA boosts the dissolving of ground particles of the activated fly ash when it is mixed with water. Thus, the water demand is decreased and this would increase the reactivity of the activated fly ash (Sadique *et al.*, 2012a). Moreover, the FGD assisted in the breaking-up of large plerospheres (i.e. reduction of porous particles) which in turn decreased particle roughness for the grinding process and thus the water demand decreased as argued by Aydın *et al.* (2010). The newly achieved reduction in PI would increase the soil-binder mixture workability as well as increasing the soil resistance against swelling and shrinkage stresses.

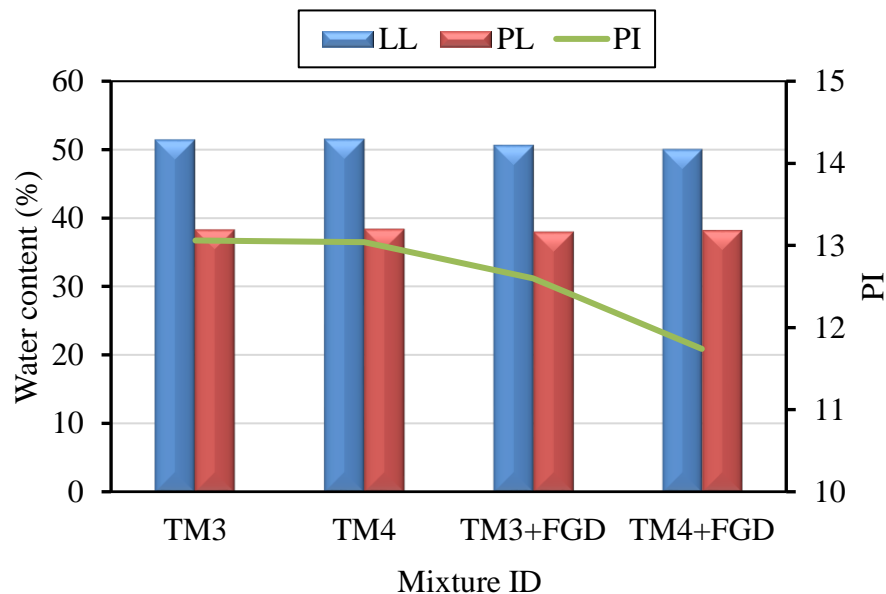


Figure 5.29 Effect of grinding with FGD on Atterberg limits.

Table 5.11 Atterberg limits values for the soil treated with TM3 and TM4 with effect of grinding and FGD.

Mixture ID	LL	PL	PI
TM3	51.40	38.34	13.06
TM4	51.50	38.46	13.04
GTM3+FGD	50.60	38.00	12.60
GTM4+FGD	50.00	38.26	11.74

5.5.4.3 Compaction parameters

The effect of grinding activation along with the effect of using the FGD as a GA on the MDD of the soil treated with TM3 and TM4 is shown in Figure 5.30. Additionally, Figure 5.31 presents the influence of the aforementioned processes on the values of the OMC. The results shown in these figures indicated that there was a gradual increment in MDD of the soil treated with both ternary mixtures after the application of the grinding as well as the FGD as a GA. The MDD increased from 1.47Mg/cm³ to 1.49Mg/cm³ for TM4; while it increased from 1.46Mg/cm³ to 1.48Mg/cm³ for TM3. The increase in MDD was accompanied by a gradual reduction in OMC. This behaviour can be attributed to the same reason presented in the previous section (section 5.5.4.2) in which the reduction in water demand of the binder materials after the grinding and FGD activation led to a reduction in the OMC, thus the workability of the soil-binder paste increased and led to increase the MDD. The results of the compaction parameters testing revealed that the reduction in the OMC of the TM4 after grinding with the aid of FGD was higher than that for TM3. This means that TM4 would exhibit a higher workability than the TM3 and this may lead to an increase in the compressive strength of the stabilised soil.

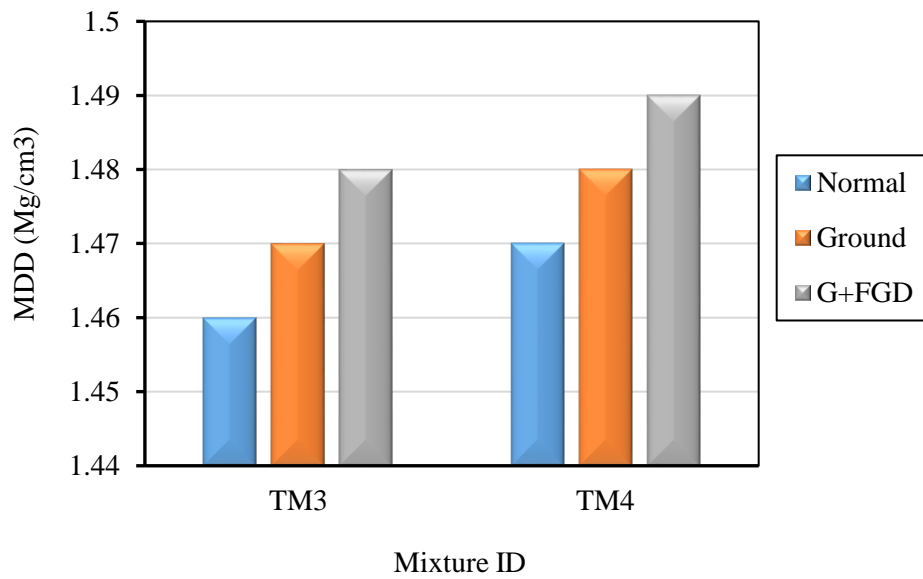


Figure 5.30 Effect of grinding with FGD on MDD.

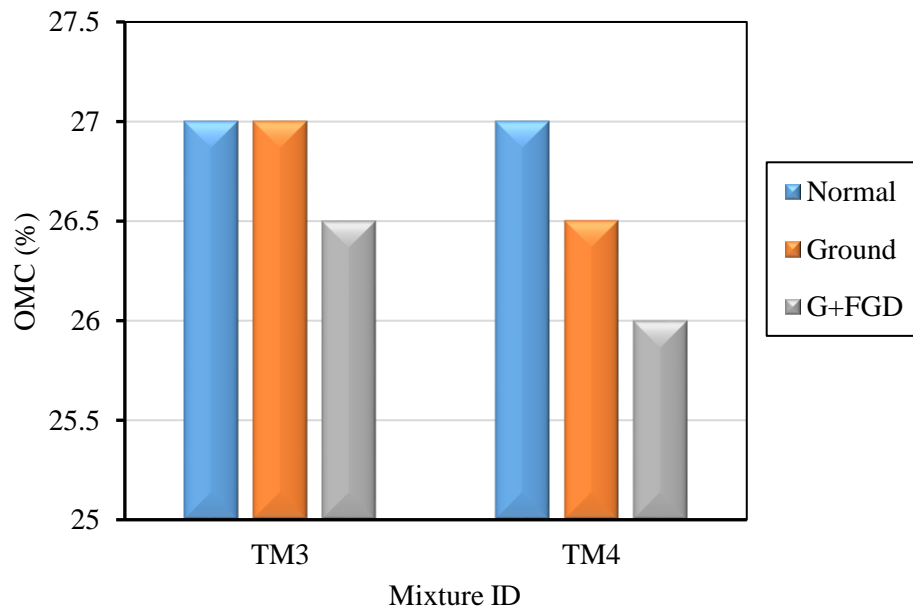


Figure 5.31 Effect of grinding with FGD on the OMC.

5.5.4.4 Unconfined compressive strength (UCS)

Specimens of soil treated with TM3 and TM4 after grinding only and then with the application of FGD were prepared to carry out the UCS testing. The associated compressive strengths of the test specimens were compared with those treated with normal TM3 and TM4 to evaluate the influence of grinding and FGD as a GA on the compressive strength. The average maximum compressive strength achieved from the UCS tests after using the grinding and FGD through the 28 days curing period are presented in Figure 5.32. Both mixtures indicated gradual development in the soil compressive strength through the time of curing and for both methods of activation (grinding only and grinding with GA). However, the rate of compressive strength increment achieved from TM4 was higher than that obtained from TM3. As illustrated in Table 5.12, both of the activated ternary mixtures indicated similar rates of compressive strength increments after grinding over the 28 days of curing. The increments became higher with the use of FGD as a GA, especially for the first and second week of curing. However, and in contrast to what was obtained from the ternary blending optimisation, the highest compressive strength after FGD application was achieved from the specimens treated with TM4. The average UCS values, at 28 days of curing, after grinding with the GA were 1087kPa and 1157kPa for the soil treated with TM3 and TM4 respectively. Moreover, the rates of UCS development shown in Figure 5.33 indicated that the mixture TM4 subjected to the grinding with GA demonstrated a 22.56% increase in the compressive strength over that for untreated TM4 which was the highest value of development achieved by the grinding activation with the use of FGD as a GA. On the other hand, the rate of development indicated from TM3 activation was 13.11% referring to the UCS recorded by untreated TM3. As a summary, FGD was found very effective to increase the compressive strength of the soil treated with ternary mixtures, especially the specimens of the soil treated with TM4 which indicated the highest value of UCS. Moreover, the early strength (within the first week of curing) was improved significantly with the use of FGD along with the grinding technique. For example, the GTM4+FGD revealed a compressive strength of 992kPa after 7 days of curing which was higher than the compressive strength achieved by the untreated TM4 after 28 days of curing (944kPa) as shown in Table 5.12. This would effectively play a good role to enable sites associated with a low

compressive strength soils to have a suitable bearing capacity that is essential for site equipment movement within a short period.

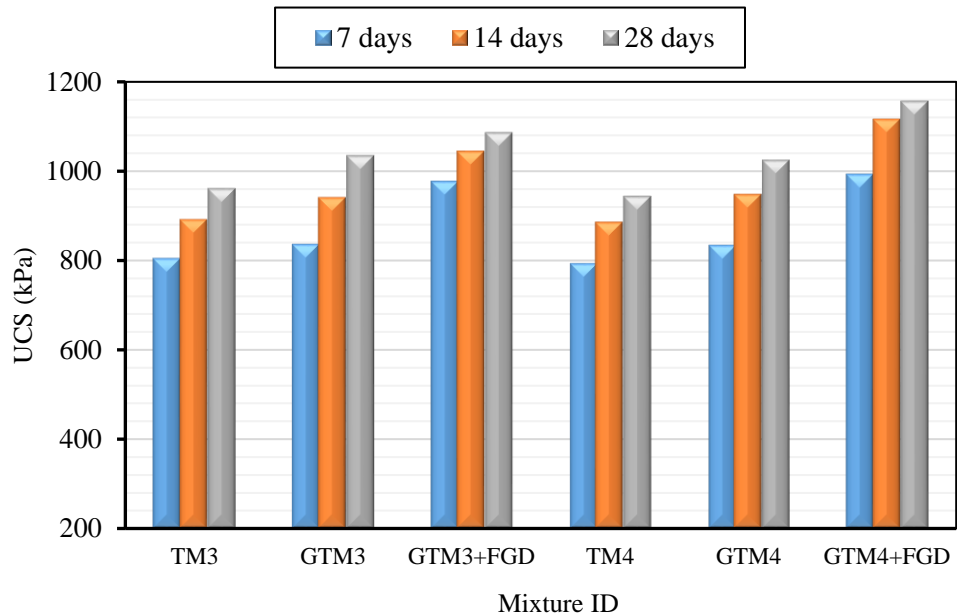


Figure 5.32 Effect of grinding and FGD on the UCS of the soil treated with TM3 and TM4.

Table 5.12 UCS values after grinding with FGD application.

Mixture ID	UCS (kPa) at the specific age of curing (days)		
	7	14	28
TM3	804	892	961
GTM3	836	941	1035
GTM3+FGD	976	1045	1087
TM4	793	886	944
GTM4	834	948	1025
GTM4+FGD	992	1117	1157

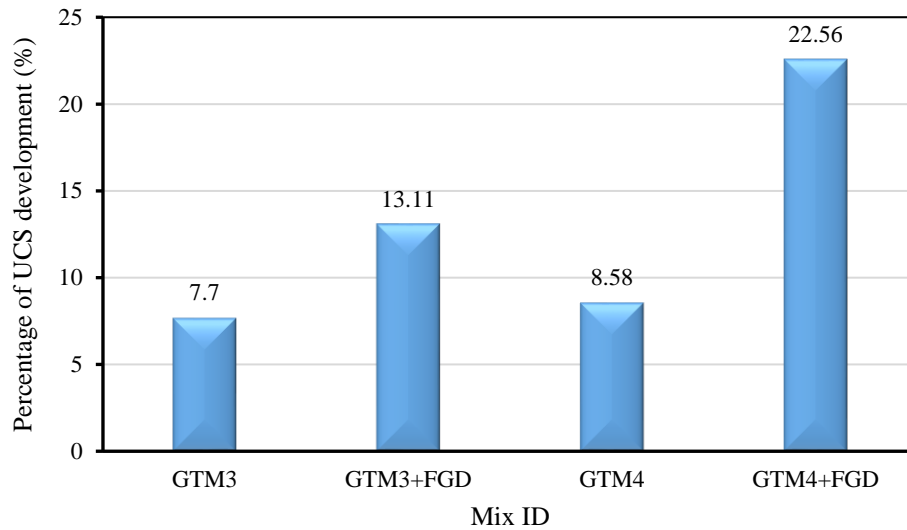


Figure 5.33 Influence of grinding and FGD on the development rate of UCS over that for corresponding non-ground TM3 and TM4 mixtures.

The increments in the soil compressive strength achieved after grinding can be attributed to the increase in fineness of the binder particles as well as to the changes in electronic assembly of binder particles caused by the crashing forces of grinding. These activations played a positive role in the acceleration of the pozzolanic reaction that took place between the hydrated lime produced from the WPSA and the silicates provided by POFA and RHA (Sadique *et al.*, 2013; Li *et al.*, 2014; Zhao *et al.*, 2016). Thus, the UCS increased at a greater rate in comparison to that for soil treated with normal ternary mixtures, and both of the early and moderate curing periods exhibited noticeable increments in the UCS. With respect to the ground ternary mixtures with the GA, it was proven that the use of FGD as a GA contributed not only to the prevention of the agglomeration of the ground products, but also produced a strength above the control value (Sekulić *et al.*, 1999; Sadique *et al.*, 2012a). Additionally, FGD was used recently by Zhang *et al.* (2016b) as a retarder to prolong the initial setting time of mortars containing cement and metakaolin. The results revealed that the initial setting time of the FGD treated samples was longer than that for the reference in which the time interval between the initial and final setting time was shortened. The prolonged curing samples containing FGD exhibited compressive strengths above that for the reference samples prepared using Ordinary Portland Cement (OPC). However, the strength of the FGD-treated mortars at curing periods earlier than 28 days indicated

a strength lower than that for the reference mortars. Nevertheless, the hydration products such as trisulfoaluminoferrite (AFt; a product which comprised of aluminium with variable substitution of iron) and C-A-H were found to exist from the first day of curing until beyond one year. As a summary, the increment in strengths with the use of FGD was attributed to the formation of AFt and C-A-H products since the early ages of curing (Sadique *et al.*, 2013; Zhang *et al.*, 2016b). Based on a previous study carried out by Sadique *et al.* (2012a), the mortars prepared from a ground activated cementitious materials (comprised from high calcium fly ash and silica fume) with the aid of FGD as a GA demonstrated higher compressive strengths than those prepared from unground powders. The achieved development in the compressive strength was credited to the higher solubility and rapid solution of the gypsum produced from FGD which made the concentration of the SO_4^{2-} ions reach the point of saturation almost immediately in the presence of water. This process accelerated the formation of C-S-H, Portlandite, ettringite, etc. by the utilisation of the reactive silica with arcanite for FA2 and the soluble calcium and aluminium in the case of FA1. The aforementioned reason can be considered to elucidate the reason why TM4 indicated UCS higher than that for TM3 after FGD application as TM4 contained higher silicate and aluminate contents which represented more availability of pozzolanic materials when compared with the amount in TM3.

5.6 SUMMARY

As this chapter comprised three main stages of optimisation, the summary can be broken down to the following sub-summaries:

5.6.1 Summary of the Optimisation of WPSA Content.

As a summary of the optimisation of WPSA content the following outputs can be noted:

- A noticeable effect of WPSA on the consistency limits of the stabilised soil was observed in which the liquid limit and plastic limit increased with the increase of WPSA content. However, the increment in PL was higher than that of LL, thus the plasticity index decreased significantly.

- The MDD decreased and the OMC increased with the increase in WPSA content. Moreover, the results of the compaction tests indicated that there was an immediate chemical reaction occurred between the soil minerals and WPSA.
- The results of UCS tests revealed that the optimum percentage of WPSA was 12% which indicated the higher compressive strength at different times of curing. The latter percentage was fixed as a binder content for the further experimental works carried out later in this study.

5.6.2 Summary of Mechanical Activation

The results of mechanical activation indicated that WPSA became agglomerated when the grinding time was increased which revealed a problem in the both pozzolanic and hydration reaction. This behaviour led to a reduction in the compressive strength. Therefore, the elimination of this phenomenon by using grinding aid materials would enhance the performance of the mechanical activation. However, a grinding time for a period between 10 and 15 minutes was found the most effective period for the grinding activation to avoid the agglomeration and to prevent costs increasing. At the end of the grinding activation, the first optimum mixture (GU) was presented which was the mechanically activated unary mixture.

5.6.3 Summary of Binary Blending Optimisation

The results of binary blending treatment demonstrate that the treatment with the mixtures BM1, BM2, and BM3 indicated approximately similar compressive strength. However, the mixture that exhibited the higher value of UCS was selected as the optimum binary mixture. This mixture was BM2 which was achieved from 9% WPSA and 3% POFA by the dry mass of the stabilised soil. The optimum binary mixture indicated further improvement in the soil plasticity where the PI was decreased from 20.22 for the untreated soil to 13.38 and 12.78 for the soil treated with GU and BM2 respectively.

5.6.4 Summary of Ternary Blending Optimisation

The engineering behaviour of the soil treated with different ternary mixtures was compared with that for virgin soil and the soil treated with GU. There was no significant improvement in terms of the consistency limits after ternary treatment. The results of the compaction parameters testing revealed that the dominant material for the water demand, which in turn controls the behaviour of MDD and OMC, was WPSA. However, slight increments were observed in MDDs accompanied by slight reductions in OMCs after ternary blending treatment. Based on the results obtained from the UCS testing, it was revealed that TM3 (9% WPSA + 1.5% POFA + 1.5% RHA) indicated the highest values of compressive strength over the 28 days of curing. However, TM4 (8% WPSA + 2% POFA + 2% RHA) indicated compressive strength close to that obtained from TM3. Therefore, for the balance in the materials usage consideration, both of these ternary mixtures were considered for further activation using the grinding energy along with the assistance of FGD.

According to the results of grinding activation, it was evident that the use of FGD as a GA was very effective in increasing the fineness and improving the Atterberg limits, workability and the compressive strength, specifically for TM4. The optimum ternary mixture showed a higher compressive strength of the treated soil after grinding and FGD activation was TM4 which was composed from 8%, 2% and 2% of WPSA, POFA and RHA respectively, in addition to 5% FGD as a percentage from the total mass of the binder used.

Additionally, the output of this chapter comprised the presentation of the most optimum mixtures which are as follows:

VS: the virgin soil.

GU: the soil treated with 12% of ground activated WPSA.

BM: the soil treated with 12% of BM2.

T: the soil treated with 12% of TM4.

T+FGD: the soil treated with 12% of ground activated TM4 containing 5% FGD.

CHAPTER 6

THE COMPARATIVE PERFORMANCE OF THE OPTIMUM AND REFERENCE MIXTURES

6.1 INTRODUCTION

This chapter comprises the performance evaluation of the optimum mixtures obtained from the previous chapter in the comparison with the performance of the reference mixture which is the soil treated with OPC. Brief discussions of the comparative performance for all mixtures are presented in this chapter in terms of the physical and geotechnical properties of the stabilised soil. Additionally, the durability of the soil treated with the adopted mixtures along with the OPC-stabilised soil is also evaluated by investigating the effect of wet-dry cycles on the volume change, soil-cement loss of mass and the compressive strength of the treated soil. Moreover, the comparative strength for soil specimens subjected to short (3 days) as well as prolonged (up to 180 days) curing periods is discussed in this chapter.

6.2 COMPARATIVE ATTERBERG LIMITS

The behaviour and values of the consistency limits of the soil treated with the optimum mixtures along with the virgin soil and reference mixture are shown in Figure 6.1. It can be seen that the LLs and PLs increased significantly for the treated soil in comparison to the virgin soil, while the PIs decreased with the treatment. The highest value of LL was obtained from the GU treatment. Then slight reductions occurred after employing the blended mixtures. Similar values of PLs were observed for all optimum mixtures which were between 38% and 39%, except for the soil treated with BM which indicated a PL 36.5. Additionally, the results of Atterberg limits tests indicated that the lowest value of PI was obtained from T+FGD which was 11.74. However, all mixtures indicated PIs lower than that for the reference mixtures. Although the PI achieved from the ternary mixture (T) was above the PI obtained from the binary mixture (BM), an additional improvement of the PI was reached after adding the FGD

as a grinding agent (GA) to the T mixture, which indicated a PI even lower than that for BM. The binder containing RHA (T) exhibited a higher consistency than that for BM, which can be attributed to the RHA morphology which is associated with porous and spongy particles. Such microstructure indicates the presence of more voids in the particles, thus the water demand increases (Karim *et al.*, 2013). Moreover, it was reported by Ganesan *et al.* (2008) that gradual increments were observed in the water demand of the RHA-blended paste with the increase in the amount of the added RHA. They concluded that the blended pastes of pozzolanic materials could exhibit greater consistency than those prepared from only OPC.

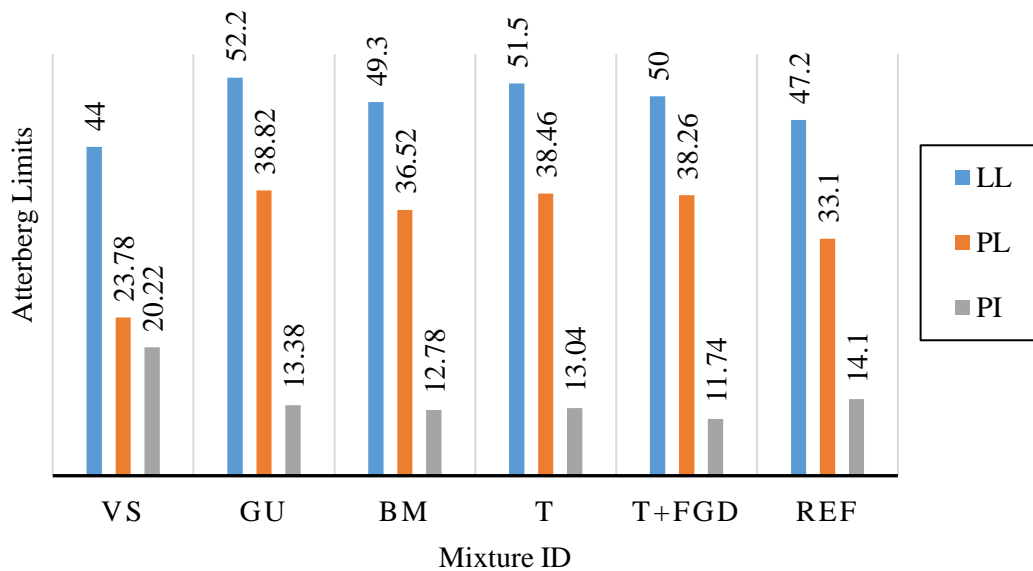


Figure 6.1 Comparative Atterberg limits of the soil treated with different types of mixtures

6.3 COMPACTION PARAMETERS

The results of the compaction parameters testing shown in Figure 6.2 indicated that the MDD decreased and OMC increased for all soil-binder mixtures in comparison to those for the untreated soil. However, there were gradual increments in MDD accompanied in continuous reductions in OMC after blended mixture treatments (BM, T and T+FGD). The higher maximum dry density was achieved from the soil treated with T+FGD binder which was 1.49Mg/m^3 as shown in Table 6.1. However, all mixtures showed MDDs lower than that for the reference mixture. The OMC declined

noticeably from 29% for the soil treated with GU to 26.5% after BM treatment which was remained with slight reductions for the treatment with the other mixtures until it reached its lowest value 26% for the soil treated with the T+FGD mixture. As was mentioned in the previous chapter, the WPSA content had the major effect on the water demand and in turn, it influences the value of both MDD and OMC (see section 5.5.2). Therefore, MDD increased and OMC decreased with the reduction in WPSA content. Additionally, the results of the compaction tests indicated that the mixtures containing RHA exhibited a slight increase in water demand. This may be due to the morphology of the RHA which is associated with high porous and spongy particles, thus the water demand increased (Karim *et al.*, 2013). The use of FGD as a GA (for the soil treated with T+FGD) was found to increase the MDD and decrease the OMC which enhanced the workability of the soil-binder mixture. As was explained in the previous chapter, section 5.5.4.2, that this behaviour was attributed to the reduction of the time required for binder particles dissolving. This behaviour led to a reduction in the water demand, thus the OMC decreased and with the increase in the workability, the MDD increased (Sadique *et al.*, 2013).

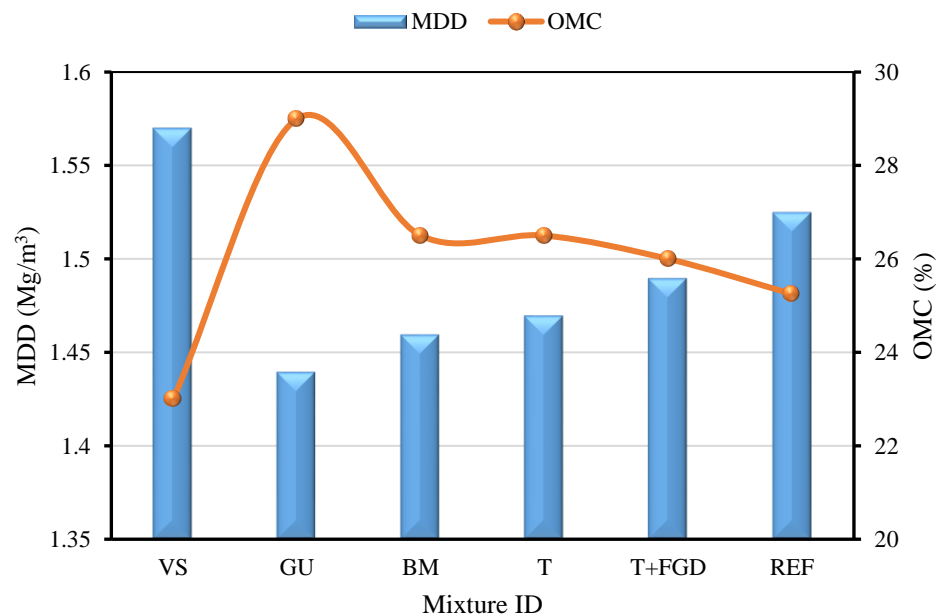


Figure 6.2 Comparative compaction parameters of the soil treated with different types of mixtures.

Table 6.1 MDD and OMC values obtained from compaction tests of the soil treated with different mixtures.

Mixture ID	MMD (Mg/m ³)	OMC %
Virgin soil	1.56	23.5
GU	1.44	29
MB	1.46	26.5
T	1.47	26.5
T+FGD	1.49	26
REF	1.525	25.25

6.4 UNCONFINED COMPRESSIVE STRENGTH

In addition to the curing periods (7, 14, and 28 days) employed in the previous chapter during the optimisation processes, the effect of a short curing period (3 days) as well as prolonged curing periods up to 180 days were investigated. The results obtained were compared with the behaviour of the reference binder (OPC) in terms of UCS. The comparative average unconfined compressive strengths (UCSs) of the soil treated with the optimum mixtures are shown in Figure 6.3, along with those for the virgin soil and the soil treated with the reference binder (OPC). This figure also presents the UCS test results for the soil specimens subjected to short and prolonged periods of curing. Moreover, the values of the maximum compressive strengths over different curing periods are listed in Table 6.2. It was evident that the compressive strength of the samples increased over the 180 days of curing for all types of mixtures investigated. However, the degree of strength development varied significantly amongst binder types. In general, the soil specimens treated with blended binders indicated compressive strengths higher than those achieved from the virgin soil and soil treated with GU for all curing periods. However, all mixtures showed compressive strength lower than that for the soil treated with OPC for curing periods up to 90 days. Nevertheless, at 180 days of curing a very impressive compressive strength was obtained from the soil samples treated with T+FGD mixture (1464kPa) which exceeded that of the soil treated with the reference binder (1450kPa). Moreover, even at short period of curing (3 days) the increase in the compressive strength was evident

for all types of mixtures. Unlike the other binders, T+FGD indicated an impressive compressive strength development when it showed a UCS of 923kPa at 3 days of curing. This value of UCS exceeded the values of UCS for the soil samples treated with the other mixtures even after 28 days of curing. As Figure 6.3 indicates, the rates of compressive strength development over the curing time achieved from the soil samples treated with blended binders (BM, T and T+FGD) were higher than that obtained from samples of the soil treated with GU. Moreover, although the mixture T contained WPSA content lower than that for BM, its recorded strengths over all of the curing periods were noticeably higher than those for BM.

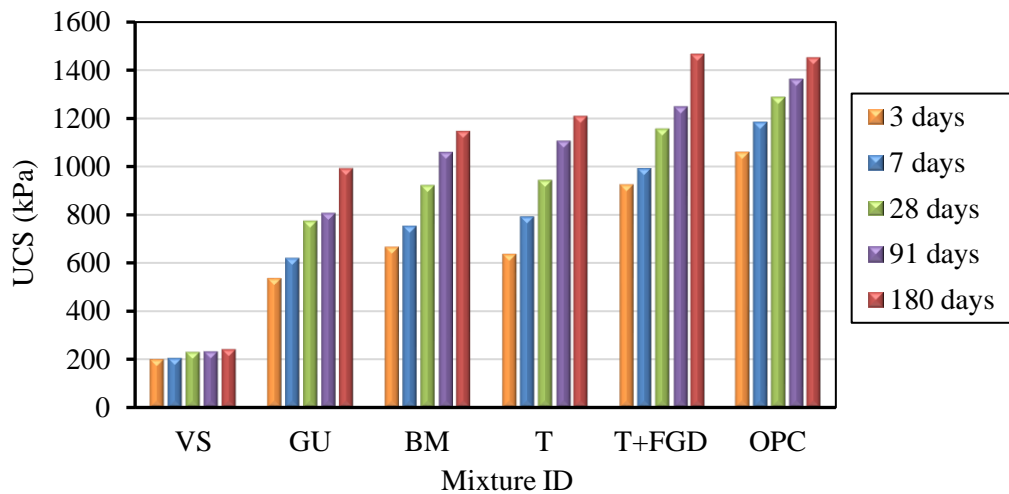


Figure 6.3 UCS development over the curing time of the soil treated with different binders along with the virgin soil and soil treated with OPC

Table 6.2 UCS values of the soil treated with different types of binder over curing time.

Mix ID	UCS (kPa) at the age of curing (days)					
	3	7	14	28	90	180
VS	200	206	210	231	232	242
GU	536	622	725	776	807	866
BM	665	755	840	924	1059	1145
T	636	793	886	944	1106	1208
T+FGD	923	992	1117	1157	1247	1464
OPC	1058	1184	1238	1289	1362	1450

As was explained in the previous chapter (section 5.4.3), the increase in the compressive strength achieved after the treatment with BM was due to the increase in the cementitious products resulting from the superior pozzolanic reaction between the silicates of POFA and the hydrated lime produced from WPSA (Muhunthan and Sariosseiri, 2008; Aïtcin, 2016b). A further increase in the compressive strength achieved with the use of the mixture T, despite it having less WPSA content than that for BM. This increment can be attributed to the high content of pure amorphous silica produced from RHA which has more susceptibility to dissolve and react chemically with the hydrated lime resulting in the increase of cementitious products formation. Additionally, the high alkalinity of POFA contributed in the increase of the dissolution of the amorphous silica. Thus, the providing of a sufficient amount of pozzolanic materials that is required for better pozzolanic reaction with the hydrated lime from WPSA, may be achieved. Puppala *et al.* (2015) reported that the high alkaline environment for the chemical reaction of binders is more preferable to boost the hydration and pozzolanic reactions. Such circumstances accelerate the solution of the glassy phases of silicates and aluminates and thus provide an extra amount of silica that has the ability to react with the hydrated lime, resulting in more cementitious compounds. Similar findings were stated by Al-Hdabi *et al.* (2014) when they developed a new cold bitumen emulsion mixture (CBEM) using supplementary cementitious materials to replace the lime; the conventional filler in such mixtures. The new binder filler (6% of the total aggregates mass) was produced using the ternary blending technique of a high calcium waste ash (FA1) and high alkaline fly ash (FA2) along with the silica fume (SF), which is normally associated with ultra-silica content. The development in the mechanical properties of the developed CBEM, such as the stiffness modulus, creep performance and fatigue resistance, after adding the SF, were notably higher than that with the use of FA1 and FA2.

With respect to the results achieved after the application of grinding along with the use of FGD as GA, it was evident that an impressive increase in the compressive strength was observed after relatively long curing periods (Sadique *et al.*, 2013; Zhang *et al.*, 2016b). Zhang *et al.* (2016b) studied the performance of a composite cementitious system produced from FGD gypsum combined with metakaolin-cement composite. The compressive strengths testing was carried out on cubes prepared using the

aforementioned composites using different proportions after being subjected to short and prolonged curing periods. The results obtained demonstrated that FGD enhanced the workability of both the pastes and mortars. Moreover, the results indicated that the samples containing FGD exhibited compressive strengths that exceeded those for the mortars prepared using pure cement after 120 days of curing.

The axial strain failure of the soil treated with different mixtures are presented in Figure 6.4, along with those for the virgin soil and soil treated with reference binder. The strain behaviour of all samples of the treated soil was becoming brittle after it was ductile and semi-ductile for the untreated soil. However, the samples treated with the optimum mixtures produced axial strain failures slightly higher than that for the sample treated with the reference binder for all curing periods, which were above 2%. This means that the soil treated with binders derived from different blending of the waste materials fly ashes exhibited less brittle behaviour when compared with the samples treated with OPC. Samples treated with the mixture T showed higher axial strain failures than the samples treated with the other mixtures. Slight reductions in the axial strain failure were observed when using FGD, especially in the samples subjected to curing periods of seven days and beyond.

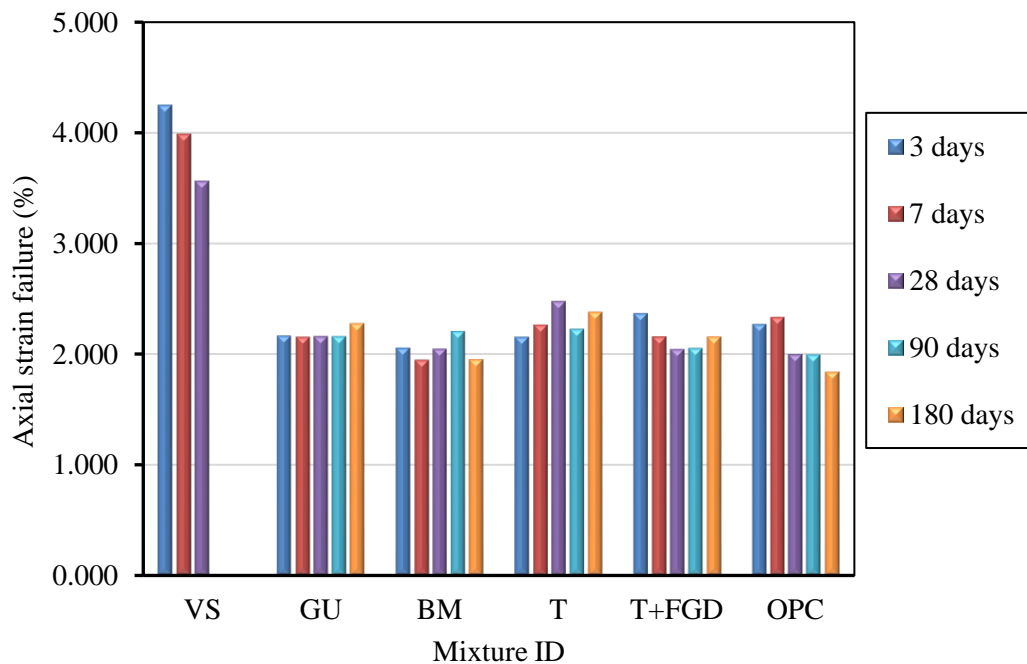


Figure 6.4 Axial strain failure for the soil treated with the optimum mixtures.

6.5 COMPRESSIBILITY CHARACTERISATION

The compressibility characteristics of the undisturbed samples, remoulded compacted soil dependent on MDD and OMC obtained from the compaction test, and the samples of the soil treated with different optimal mixtures, were evaluated by conducting the Oedometer tests, along with the samples of the soil treated with the reference binder (OPC). Oedometer studies were conducted in accordance with the British standard BS 1377-5 (British Standard, 1998b). The test conditions, procedure and the adopted loading sequences were explained earlier in section 3.3.7. Overall, the samples of the treated soil were allowed to cure for 7 and 28 days before they are subjected to the consolidation testing. The Oedometer test loading was initiated by a stress of 5kPa, then the specimens were subjected to different load values by applying the loading sequence of 12, 25, 50, 100, 200 and 400kPa. The loading sequence was continued to higher stresses of 800, 1600, and 3200kPa before being unloaded incrementally back to 5kPa. Each cycle of load increment or reduction was allowed to act for 24hrs before switching to the next cycle of load. The compressibility (C_c) recompression (C_r), and swelling (C_s) indices were then determined from the loading and unloading paths respectively. Casagrande, cited in Knappett and Craig (2012), proposed an empirical procedure to derive, from the void ratio – log effective stress (e-log P) for an over-consolidated soil, the maximum previous vertical stress that has acted on the soil in its past history. This stress is known as the pre-consolidation pressure (P_c). This parameter may be utilised to determine the in-situ over consolidation ratio (OCR) which is the ratio of the maximum past effect stress to the in-situ existing pressure (P_o) as shown in the Equation 6.1.

$$OCR = \frac{P_c}{P_o} \quad (6.1)$$

When $OCR > 1$, then the soil is considered as an over consolidated clay, while it is considered as a normally consolidated clay when its $OCR \leq 1$. The procedure suggested by Casagrande to derive P_c is shown in Figure 6.5, which represents the e-log P diagram for the remoulded soil used in this study.

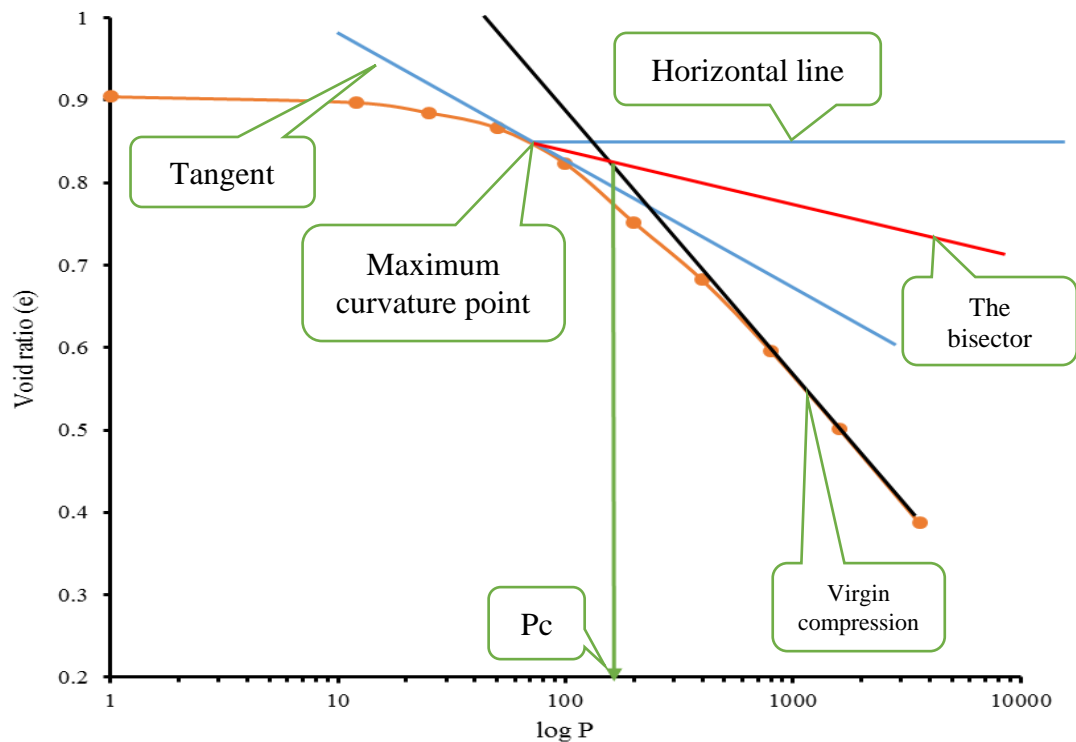


Figure 6.5 Casagrande procedure to derive the pre-consolidation pressure (P_c) of the remoulded virgin soil used in this study.

Source of the procedure: Knappett and Craig (2012)

6.5.1 Virgin Soil Compressibility

Initially, the consolidation testing was conducted on samples of undisturbed soil and compacted remoulded soil to evaluate the effect of compaction with the MDD and OMC on the compressible nature of the Hightown soil used in this study. The virgin soil compressibility was measured by calculating the coefficients of volume compressibility (m_v) which is defined as the ratio of change in the unit volume to the change in the unit effective stress as displayed in Equation 6.2 (Knappett and Craig, 2012). This coefficient can be also derived from e - $\log P$ diagram as shown in Equation 6.3.

$$m_v = \frac{1}{H_o} \left(\frac{H_o - H_1}{P'_1 - P'_o} \right) \quad (6.2)$$

$$m_v = \frac{1}{1 + e_o} \left(\frac{e_o - e_1}{P'_1 - P'_o} \right) \quad (6.3)$$

Additionally, the pre-consolidation pressures (P_c) for both states of the virgin soil were derived after plotting the relationship between the void ratio and log of effective stress for each state. The determination of P_c of the remoulded virgin soil is presented in Figure 6.5, while that for the undisturbed soil is shown in Figure 6.6. The results revealed that the pre-consolidation pressure for the virgin soil was increased after drying and applying compaction for the MDD with OMC, from less than 90kPa for the undisturbed soil with natural moisture content to approximately 155kPa. As the soil samples were collected from a very shallow depth and the soil density is 1.58Mg/m^3 , the in-situ effective stress of the undisturbed soil is much lower than its P_c . This provides an over-consolidation ratio (OCR) higher than 1, thereby confirming that the Hightown soft soil used in this study was an over-consolidated soil. Moreover, Figure 6.7 displays the raw compression curves of the undisturbed and remoulded compacted soil. It can be seen, that the initial void ratio (e_o) decreased significantly after applying the compaction. Consequently, the results indicated that the reduction in the void ratio during the compression for the remoulded soil sample was lower than that for the undisturbed one.

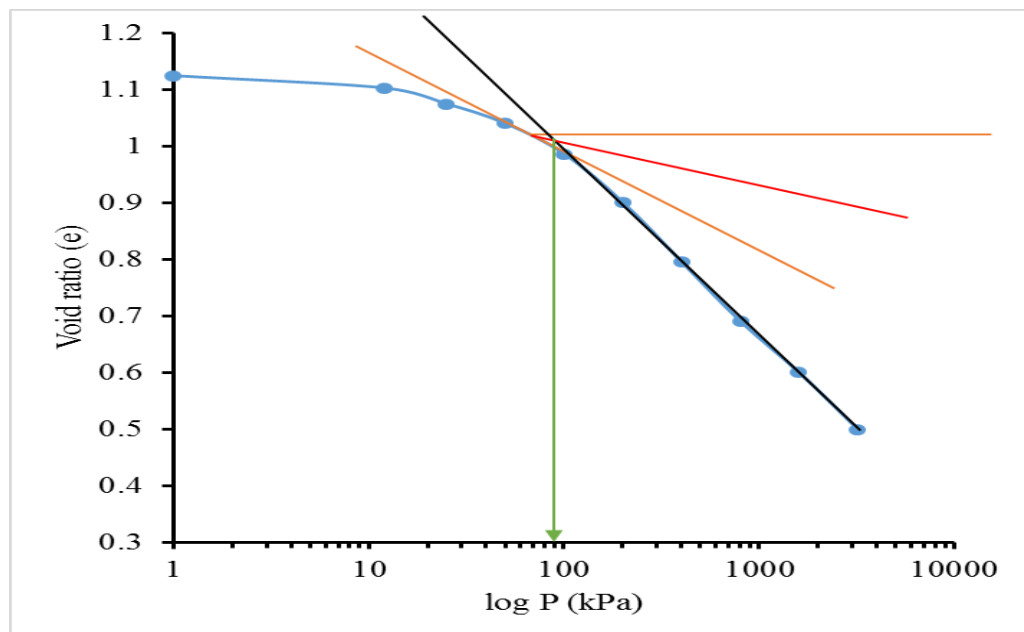


Figure 6.6 Pre-consolidation derivation of the undisturbed soil.

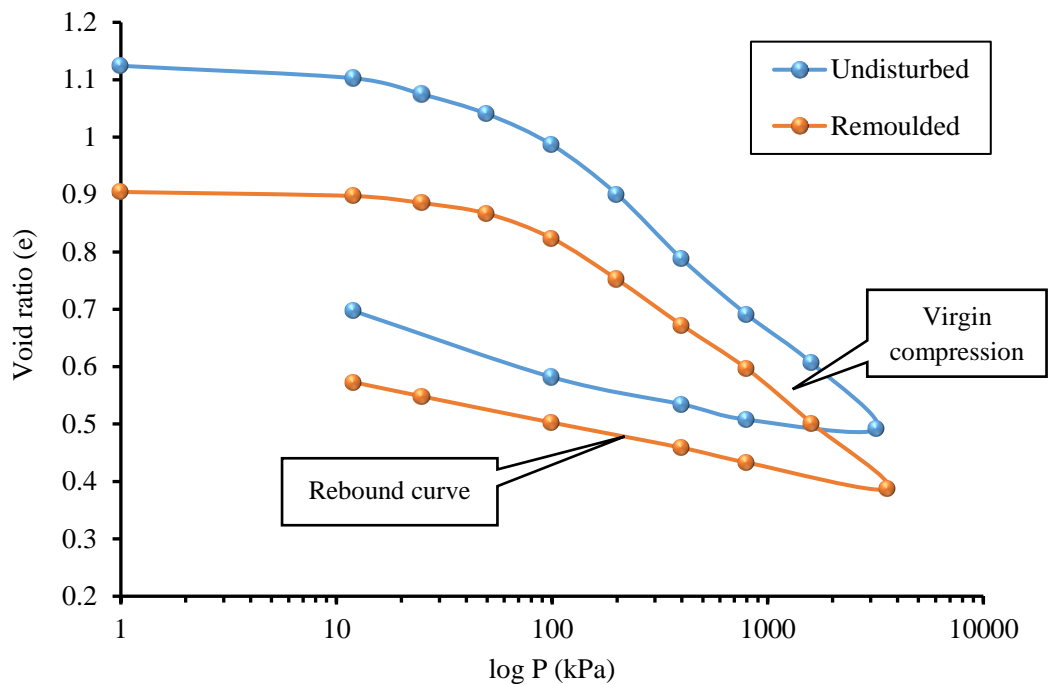


Figure 6.7 Raw compression curves for the soil samples of undisturbed and remoulded soil.

The raw compression curves displayed in Figure 6.7 also indicated that no swelling behaviour was observed from both states of the virgin soil used in this study. This behaviour may give an indication that the main clay minerals of the virgin soil are kaolinite (Moghal et al., 2015). Table 6.3 illustrates the other parameters of compressibility for the virgin soil in both its states. The values of C_c and C_s were considered as the slopes of the virgin compression line and the rebound curve respectively as indicated in Figure 6.7. The value of C_c obtained for the undisturbed sample was 0.310 which indicates a high compressibility behaviour. A noticeable reduction in C_c was achieved from the samples of the remoulded soil in which its C_c was 0.27. However, both states of the soil still give an indication of a significant compressibility, thereby according to the criteria stated by Reeves et al. (2006), they are classified as medium compressibility silts. Skempton (1944) cited in Das (2010), suggested empirical expressions to calculate C_c for undisturbed and remoulded clays as presented in Equations 6.4 and 6.5 respectively. Since the liquid limit of the soil used in this study is 44%, by applying these empirical equations, the calculated C_c will be 0.306 and 0.259 for undisturbed and remoulded soil respectively. These values agree with those actual C_c indices which were 0.31 and 0.27 as derived from the raw compression curve of the undisturbed and remoulded soil respectively.

$$C_c = 0.009(LL - 10) \quad (6.4)$$

$$C_c = 0.007(LL - 7) \quad (6.5)$$

There was no major change in the swelling index (C_s) for both states of the virgin soil except for a slight reduction after the application of compaction effort. The values of C_s were 0.09 and 0.075 for the undisturbed and the remoulded soil samples respectively. Additionally, C_r was decreased from 0.0242, for the undisturbed soil, to 0.0094 for the remoulded soil. The reductions that occurred in C_c , C_s and C_r may be attributed to the reduction in the void ratio achieved after compaction and the sample loading throughout the consolidation testing. The total consolidation settlement (S_c) also decreased after the compaction as shown in Table 6.3.

Table 6.3 Compressibility parameters of the undisturbed and remoulded soil.

Soil state	C_c	C_s	C_r	e_o	S_c (mm)
Undisturbed	0.31	0.09	0.0242	1.124	5.824
Remoulded	0.27	0.075	0.0094	0.904	5.325

6.5.2 Comparative Results of the Oedometer Testing

Figure 6.8 displays the e -log P relationships for the soil samples treated with different mixtures after being subjected to curing periods of 7 and 28 days; along with the remoulded soil and the soil treated with OPC. After 7 days of curing, with the exception of the samples treated with T+FDG and OPC, the consolidation behaviour was approximately the same for all other mixtures as shown in Figure 6.8a and Figure 6.9. At this period of curing, a marginal increment was observed in the initial void ratio (e_o) for the soil treated with the unary mixture. This increase can be attributed to the large reduction in its MDD after treating in comparison to the MDD of the untreated soil (Bushra and Robinson, 2009; Moghal *et al.*, 2015). Moreover, the samples treated with this mixture may not have experienced enough formation of

cementitious products that would fill the voids at this age. However, there were noticeable reductions in e_0 achieved after 7 days curing from the samples treated with the ternary mixtures and OPC which may be due to cementitious products formation.

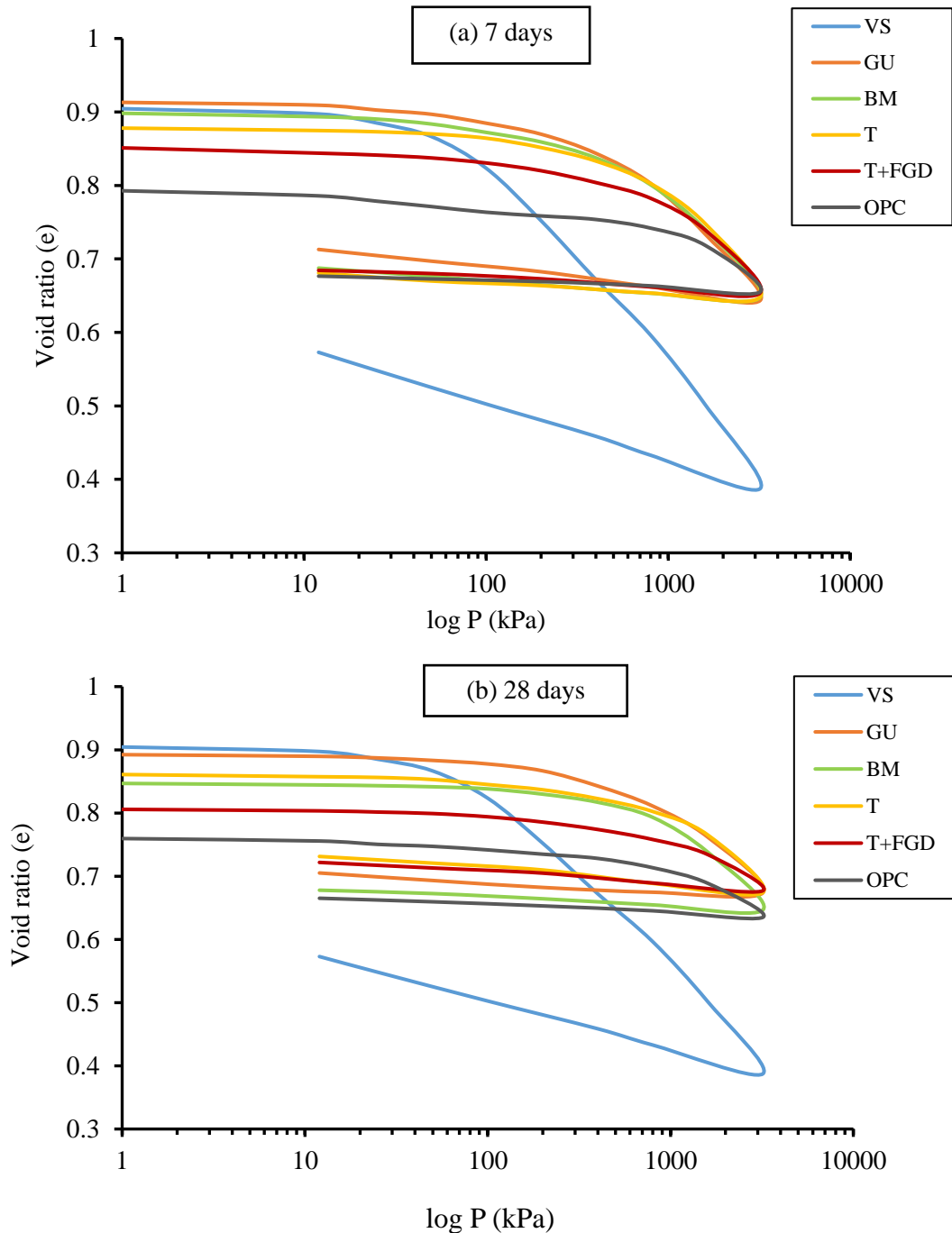


Figure 6.8 Comparative raw compression curves of the soil treated with different types of binders at (a) 7 days and (b) 28 days of curing.

As per Figure 6.8b, the differences in raw compression curves for the samples subjected to 28 days of curing, can be easily recognised. The samples treated with T+FGD exhibited stiffest behaviour under load than the samples treated with the other mixtures. Additionally, a comparable consolidation behaviour to the OPC was achieved using the ternary mixture activated with FGD gypsum (T+FGD) as represented by the red curve shown in Figure 6.8b. Moreover, all binders indicated initial void ratios less than that for the remoulded soil after 28 days of curing as illustrated in Figure 6.9, in which a significant reduction was achieved for the sample treated with T+FGD which recorded a e_o of 0.806. However, the reference samples (soil-OPC) exhibited the lowest void ratios for both periods of curing. This may be due to the higher MDD associated with a lower void ratio in comparison to those for the soil treated with the optimum mixtures. A reduction in the void ratio of lime-stabilised clayey soils was reported by Moghal *et al.* (2015). They concluded that the void ratios of stabilised soft soil decreased when the lime content increased from 2% to 4% with the increase in the period of applied consolidation load. The reduction in the void ratio was attributed to two processes. The first one was due to the flocculation reaction that occurred between the clay cations and calcium ions of the lime and resulting in a dense flocculated structure associated with relatively higher concentrations of crystallised calcium ions. The second contributor was the pozzolanic reaction which formed the cementitious gel which connected the clay particles and increased the resistance against any further compression.

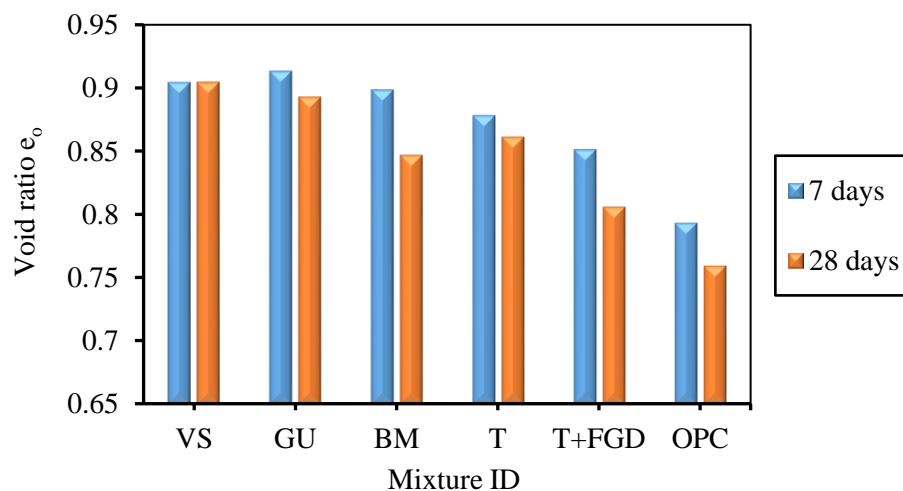


Figure 6.9 Initial void ratios (e_o) of the soil treated with different binders and subjected to different curing periods.

The compression (C_c) and swelling (C_s) indices exhibited by samples treated with different mixtures, along with those for the reference mixture and remoulded soil are summarised in Table 6.4 as well as being displayed in Figure 6.10a and b. All stabilised samples had lower values compared with those recorded for the untreated soft soil which had C_c and C_s of 0.28 and 0.075 respectively. Moreover, it was observed that both indices decreased with time of curing for the same type of binder. The values of C_c and C_s obtained from the samples subjected to 7 days of curing were relatively comparable to those obtained from the samples cured for 28 days. This may be due to the time-dependence nature of the hydration reaction of the samples cured for 7 days that continued during the time of consolidation testing which took about 13 days to be completed. The latter reaction altered the compression characteristics of the soil samples, thus these samples exhibited a stiff behaviour (Bushra and Robinson, 2009). When comparing the C_c and C_s values obtained from the samples treated with the ternary mixtures, the samples stabilised with ternary mixture activated with FGD (T+FGD) have the lowest values of C_c (0.145 and 0.107) and C_s (0.014 and 0.012) after 7 and 28 days of curing respectively; whereas their respective non-activated samples (samples treated with T) had C_c of 0.173 and 0.129 and C_s of 0.017 and 0.014. This indicates that the samples treated with T+FGD binder were much less compressible compared with the soil treated with the other types of binders. Additionally, the results indicated that T+FGD exhibited an improvement in the soil compressibility superior to the samples treated with the OPC, especially at 28 days of curing.

Table 6.4 Summary of compression and swelling indices recorded for the soil treated with different binders over the time of curing.

Mixture ID	Compression index (C_c)		Swelling index (C_s)	
	7 days	28 days	7 days	28 days
VS	0.280		0.075	
GU	0.169	0.153	0.030	0.018
BM	0.164	0.149	0.019	0.014
T	0.173	0.129	0.017	0.014
T+FGD	0.145	0.107	0.014	0.012
OPC	0.129	0.111	0.009	0.011

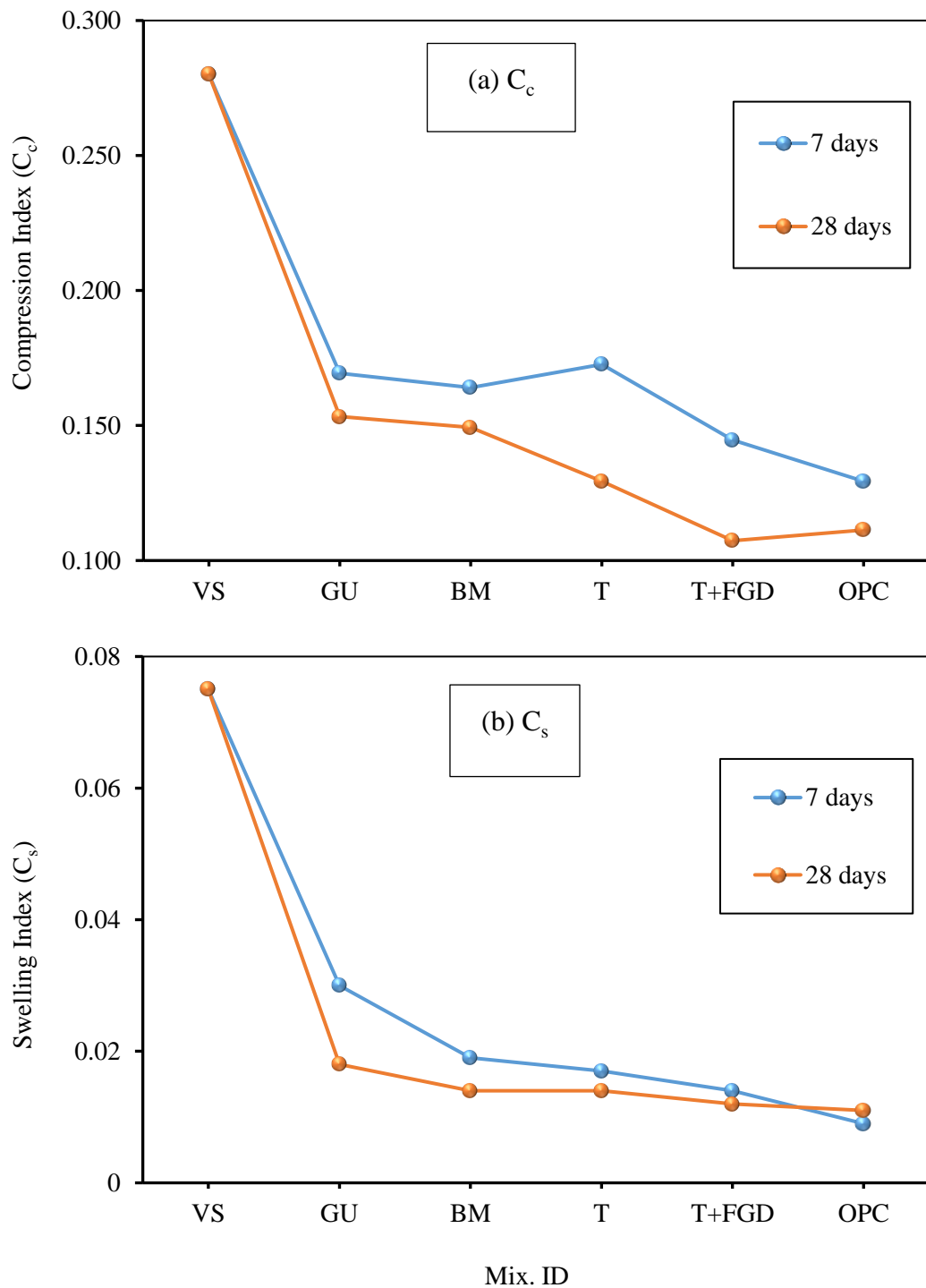


Figure 6.10 Compression and swelling indices of the soil samples treated with different binders.

Figure 6.11a and b show the values of the volume compressibility coefficients (M_v) before and after the treatment with different types of binders for the samples subjected

to 7 and 28 days of curing; along with those treated with the reference binder (OPC). The results of M_v complemented the compression curves in Figure 7.8; whereby all binders significantly reduced the compressibility of the soft soil used in this study after just 7 days. Tomlinson (2001) categorised four ranges of the soil compressibility dependent on the value of M_v , as per Figure 6.11, and these ranges are as follows:

- High compressibility: $M_v > 0.3\text{m}^2/\text{MN}$;
- Medium compressibility: $M_v (0.1 - 0.3\text{m}^2/\text{MN})$;
- Low compressibility: $M_v (0.05 - 0.1\text{m}^2/\text{MN})$ and
- Very low compressibility: $M_v (0 - 0.05\text{m}^2/\text{MN})$.

The calculated initial M_v of the untreated soil for the stresses up to 400kPa were equal to or above $0.4\text{m}^2/\text{MN}$ which means that it is considered as a highly compressible soft soil according to Tomlinson criteria (Tomlinson, 2001). The results indicated that the compressibility dropped significantly for all stabilised samples. The 7 days M_v values for all mixtures ranged between $0.169\text{m}^2/\text{MN}$ and $0.046\text{m}^2/\text{MN}$ for the consolidation effective pressures of 50Kpa and 800kPa respectively (Figure 6.11a). According to Tomlinson (2001) and Reeves *et al.* (2006), all stabilised samples had a medium to very low compressibility. The ternary mixture T exhibited the lowest values of M_v ranging from 0.084 to $0.06\text{m}^2/\text{MN}$ for the consolidation pressures 50 to 400kPa respectively. Consequently, the samples stabilised with T can be considered as a low compressible soils. However, T+FGD indicated the lowest value of M_v ($0.046\text{m}^2/\text{MN}$), after 7 days curing, when the consolidation pressure increased to 800kPa, which transferred the soil to the range of very low compressibility (see Figure 6.11a). The latter value was comparable to that for the soil treated with OPC which had an M_v of $0.036\text{m}^2/\text{MN}$ for the same conditions; subsequently, the soil is considered as very low compressibility (Tomlinson, 2001). For 28 days M_v , for all mixtures had a low to very low compressibility for all values of consolidation pressures as shown in Figure 6.11b. The highest reduction in M_v after 28 days of curing was achieved from the samples treated with T+FGD for the effective pressure of 800kPa, which was equal to that achieved from the reference mixture which was $0.033\text{m}^2/\text{MN}$.

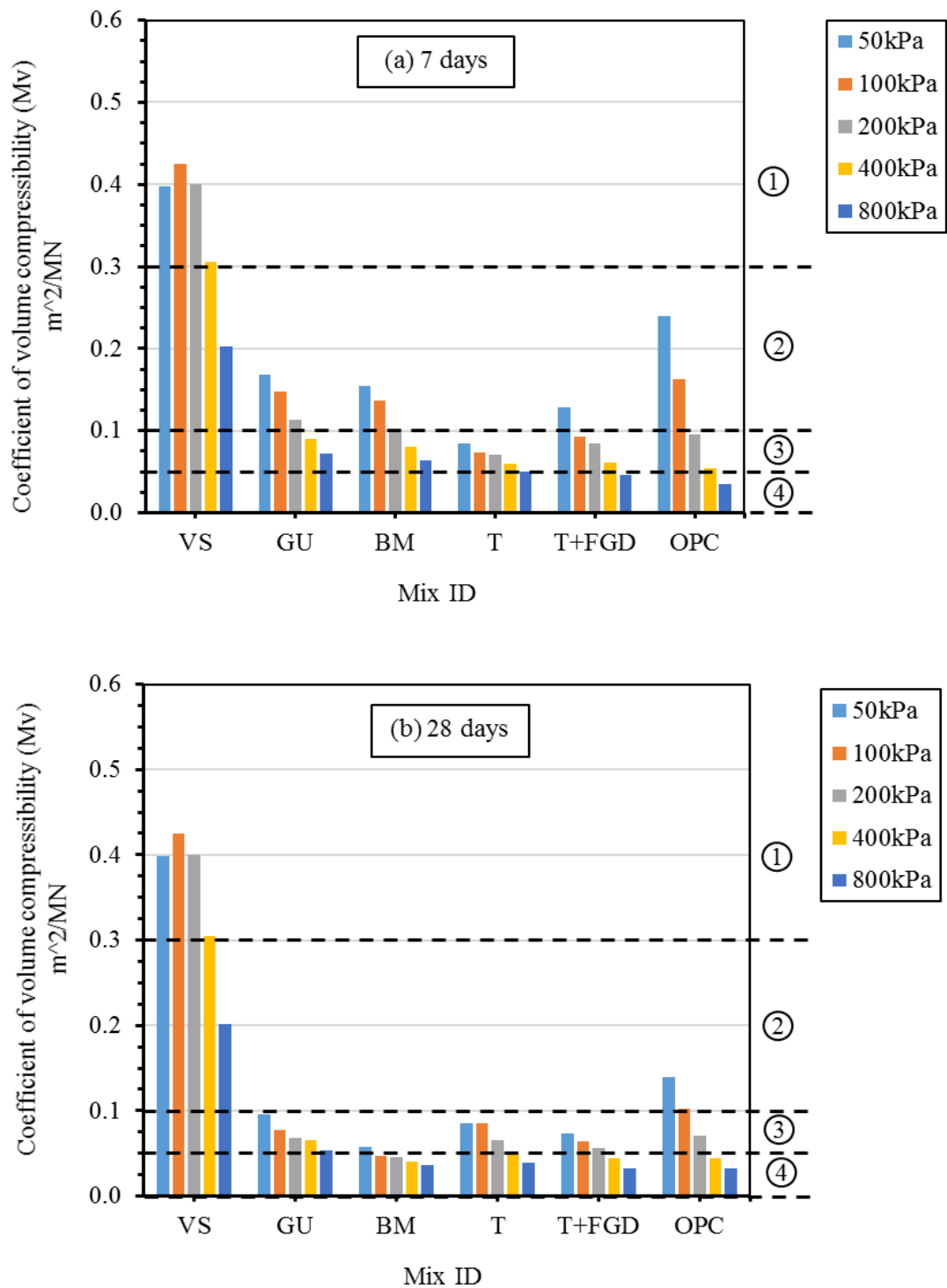


Figure 6.11 Comparative values of M_v calculated from the Oedometer tests on the stabilised soil after (a) 7 days and (b) 28 days of curing.

With respect to the reference samples and for the consolidation effective pressures of 50kPa and 100kPa, the calculated values of M_v were higher than those for the soil samples treated with the other mixtures. The values were ranged between 0.24 and 0.163m²/MN, and between 0.14 and 0.102m²/MN for the samples subjected to 7 and 28 days of curing correspondingly. Thus, the samples treated with OPC are considered as medium and low compressible at this case. Similar findings were reported by Sargent *et al.* (2013) after treating a soft alluvial soil which has a similar properties to the soft soil used in this research. Different waste binders that contained GGBS, PFA and red gypsum (RG) were mixed with different proportions; along with alkaline activation using sodium hydroxide (NaOH). The soft soil compressibility was improved significantly by the decrease in both C_c , C_s and M_v . They reported that the alkali activated GGBS-PFA binder containing 50% GGBS and 50% PFA was the most effect binder in reducing the soil compressibility. This improvement was attributed to the hydration and pozzolanic reaction for the cured samples up to 28 days, while for the non-cured samples the improvement referred to the flocculation reaction that occurred between the cations of the clay minerals and the ions of the hydrated lime produced from the binder.

A significant development in the pre-consolidation pressure (P_c) was achieved for the treated soil as shown in Figure 6.12. The P_c results complement the unconfined compressive strength (UCS) results presented earlier in this chapter (see Figure 7.3); whereby all of the mixture types increased the P_c of the soft soil significantly through the time of curing. The P_c value was increased from 150kPa for the untreated soil to the higher values of P_c that were obtained from the samples treated with T+FGD which were 1010kPa and 1180kPa after 7 and 28 days respectively. Moreover, the FGD was found very effective in activating the ternary mixture T, resulting in increasing P_c by 100kPa after 28 days of curing. Additionally, T+FGD indicated comparable values of P_c to the reference binder in which they exhibited 97.11% and 96.72% of those obtained from the reference mixture samples subjected to 7 and 28 days curing respectively. Additionally, the consolidation settlement (S_c) shown in Figure 6.13 was reduced noticeably for all mixtures. The results of the Oedometer tests indicated that S_c decreased with the increase in the curing time. The S_c value obtained from the consolidation test for the untreated soil was 5.325mm. Whereas for the soil treated

with different optimal mixtures, impressive reductions in S_c were observed. The results revealed that the use of GU decreased the S_c to 2.82mm and 2.31mm after 7 and 28 days of curing respectively. Further reductions were achieved in S_c from the samples treated with the binary and ternary mixtures as shown in Figure 6.13. The lowest values of S_c (2.133mm and 1.418mm for the samples of 7 and 28 days) were achieved by using T+FGD which indicated similar values to those obtained from the reference mixture especially after 28 days of curing, which was 1.416mm. Once again, the FGD was found very effective to decrease the consolidation settlement after it was used as an activator and grinding aid for the T mixture, whereby S_c decreased from 1.992mm for T treated samples to 1.418mm for the samples treated with T+FGD after 28 days of curing. Overall, with the use of T+FGD the S_c was decreased by about 60% to 73.4% of that for the non-stabilised soil.

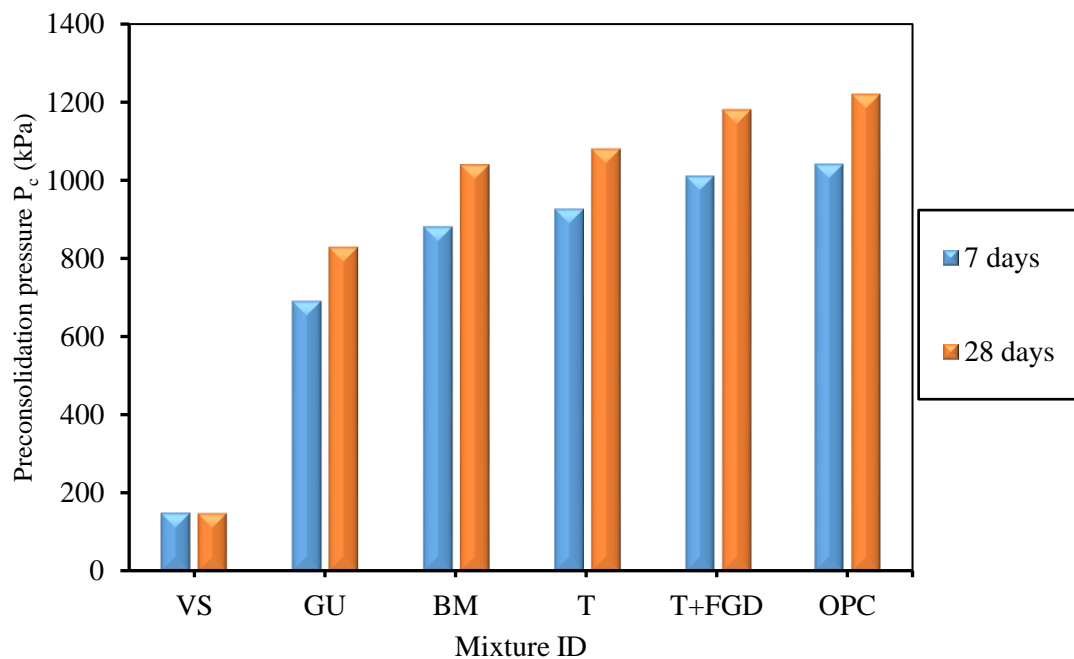


Figure 6.12 Comparative pre-consolidation pressure for the soil treated with different binder types.

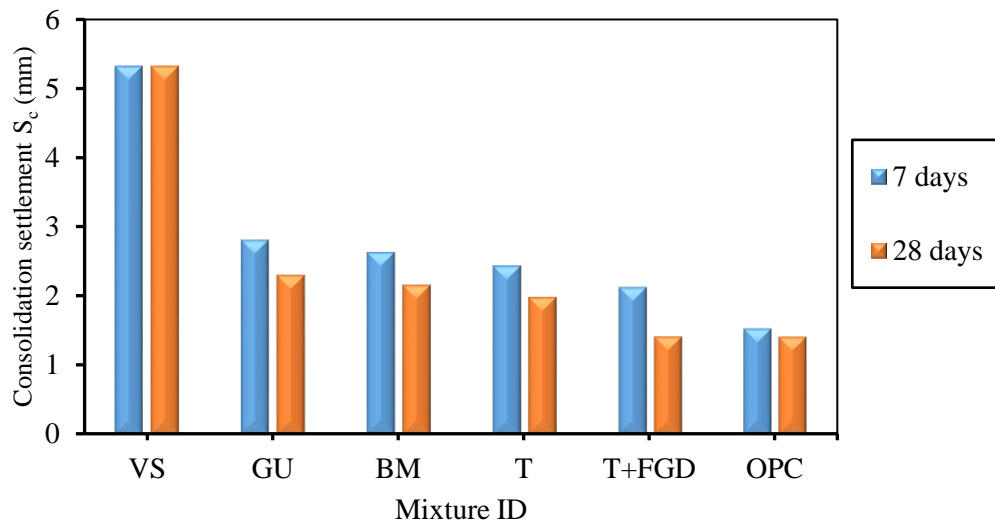


Figure 6.13 Summary of consolidation settlement S_c for the soil stabilised with different mixtures.

6.6 EFFECT OF WETTING-DRYING CYCLES

The wetting-drying testing was conducted to assess the durable performance of the optimum mixtures under severe circumstances. Specimens cured at 28 days for soil treated with different types of binder were subjected to a series of wetting and drying cycles (1, 3, 5, 7 and 12 cycles) in accordance with the American Standard D 559-03 (ASTM International, 2003); along with the virgin soil and the soil treated with OPC. The residual unconfined compressive strength, volume changes and soil-binder mass losses due to the wetting-drying cycles were determined. The results of the residual UCS after wetting and drying cycles shown in Figure 6.14 indicated that there were continuous reductions in the UCS with the increase in the number of wetting and drying cycles. Generally, all specimens of the treated soil showed acceptable resistances against the wetting-drying cycles but to different extents. Additionally, the untreated soil approached a zero strength before the completion of the first cycle along with the samples of the stabilised soil which failed to survive all the twelve cycles as shown in Figure 6.14. Interestingly, the specimens treated with T+FGD continued to survive to the highest number of wetting-drying cycles as well as exhibiting better resistance than the other types of mixtures. However, the soil treated with OPC showed a performance superior to that for the soil treated with the other binders. Only minor reductions in UCS for all binders after the first cycle of wetting and drying were

observed; while the effect of wetting and drying was clearly apparent at the end of the third cycle, which was the most harmful to all samples. This behaviour agrees with the findings of previous researchers (Yazdandoust and Yasrobi, 2010; Sargent *et al.*, 2013; Aldaood *et al.*, 2016). The samples treated with GU discontinued after the fifth cycle. At this cycle the samples exhibited residual strengths as percentages from their natural UCS of 41.66%, 52.16%, 59.43% and 64.35% for the soil samples treated with GU, BM, T and T+FGD respectively. The other samples disintegrated after the sixth and tenth cycles for BM and T, and T+FGD respectively. Therefore, the 5% of FGD that was used as a grinding aid as well as sulphate activator was found very beneficial to enhance the stabilised soil resistance against severe conditions such as the wetting drying cycles. This can be attributed to the reaction of the sulphate ions released from the FGD with the alumina phases of the soil and fly ashes which increased the hydration rate resulting in the formation of C-S-H, C-A-H and ettringite, which are responsible for the increase in the soil strength and resistance to the wetting and drying cycles (Aldaood *et al.*, 2014).

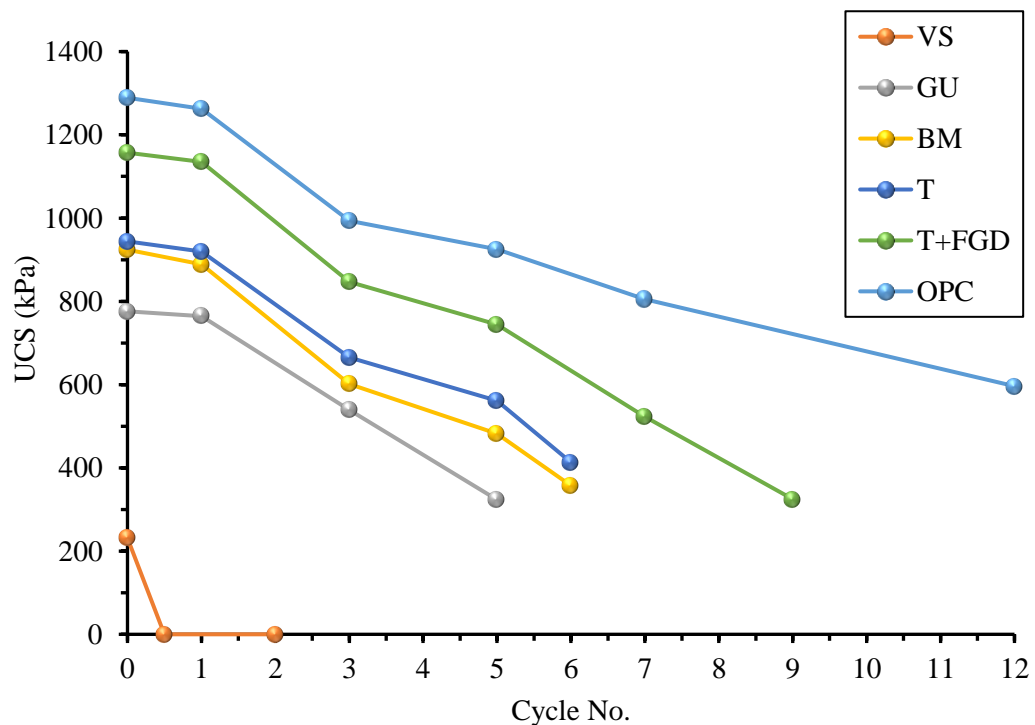
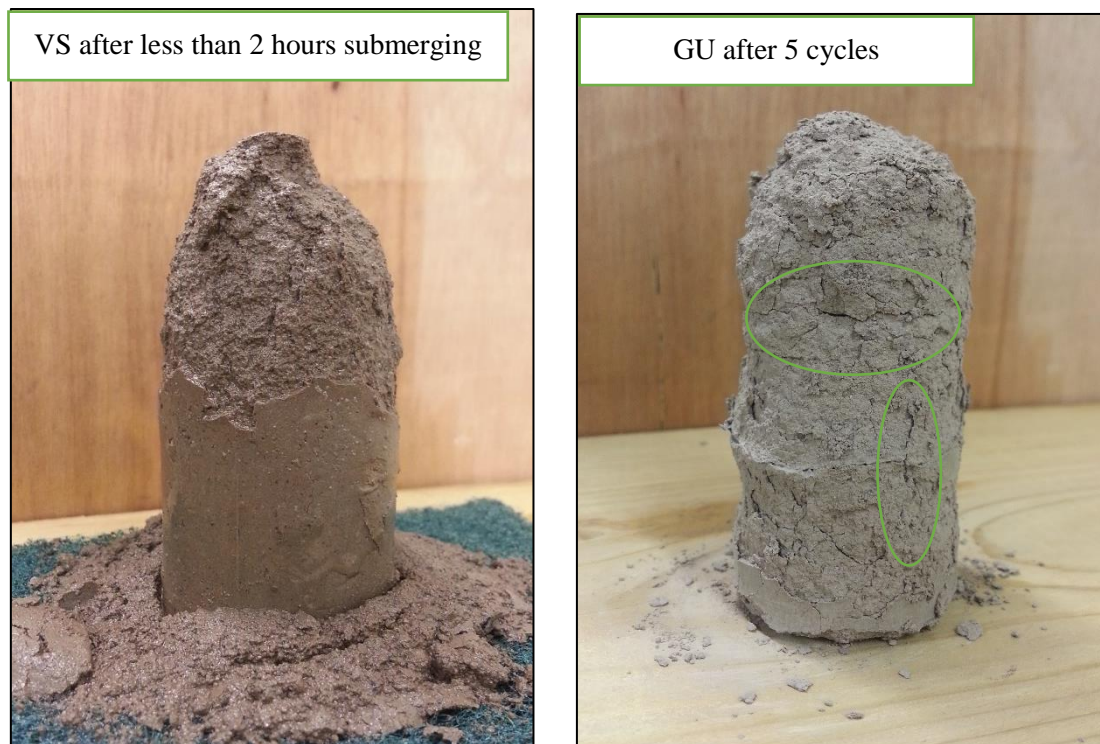


Figure 6.14 Residual UCS of the soil treated with different binders after wetting-drying cycles.

Figure 6.15 shows the crack propagation of the damaged samples after being exposed to different numbers of wetting drying cycles. This figure also shows that some samples collapsed from the top side in which the UCS test was very difficult or impossible to conduct. The reduction in the soil resistance against the wetting and drying cycles is attributed to the cracks formed in the samples due to the swelling and the shrinkage behaviour that occurred as a result of the wetting and drying (Wang *et al.*, 2015). These cracks create weak planes and lead to strength loss and thereafter accelerate the disintegration of the samples with water absorption (Aldood *et al.*, 2014). According to Aldood *et al.* (2014), due to the drying of the samples after they are submerged in water for 5hrs, the moisture content decreases dramatically. Consequently, suction forces increase until the internal tensile stresses are equal to the cohesion forces. More shrinkage occurs at this stage due to the formation of cracks. These cracks grow along with new crack formation with further water loss. Moreover, the external surfaces of the samples are more affected by drying as a result of faster water loss in comparison to that for inside the samples. During the start of the next cycle (wetting stage), the cracks are not completely closed especially on the surface in which the cracking is not fully reversible. Thus, for the following drying stage the cracks would most probably occur in the same place as the previous cycles leading to the creation of the weak planes.



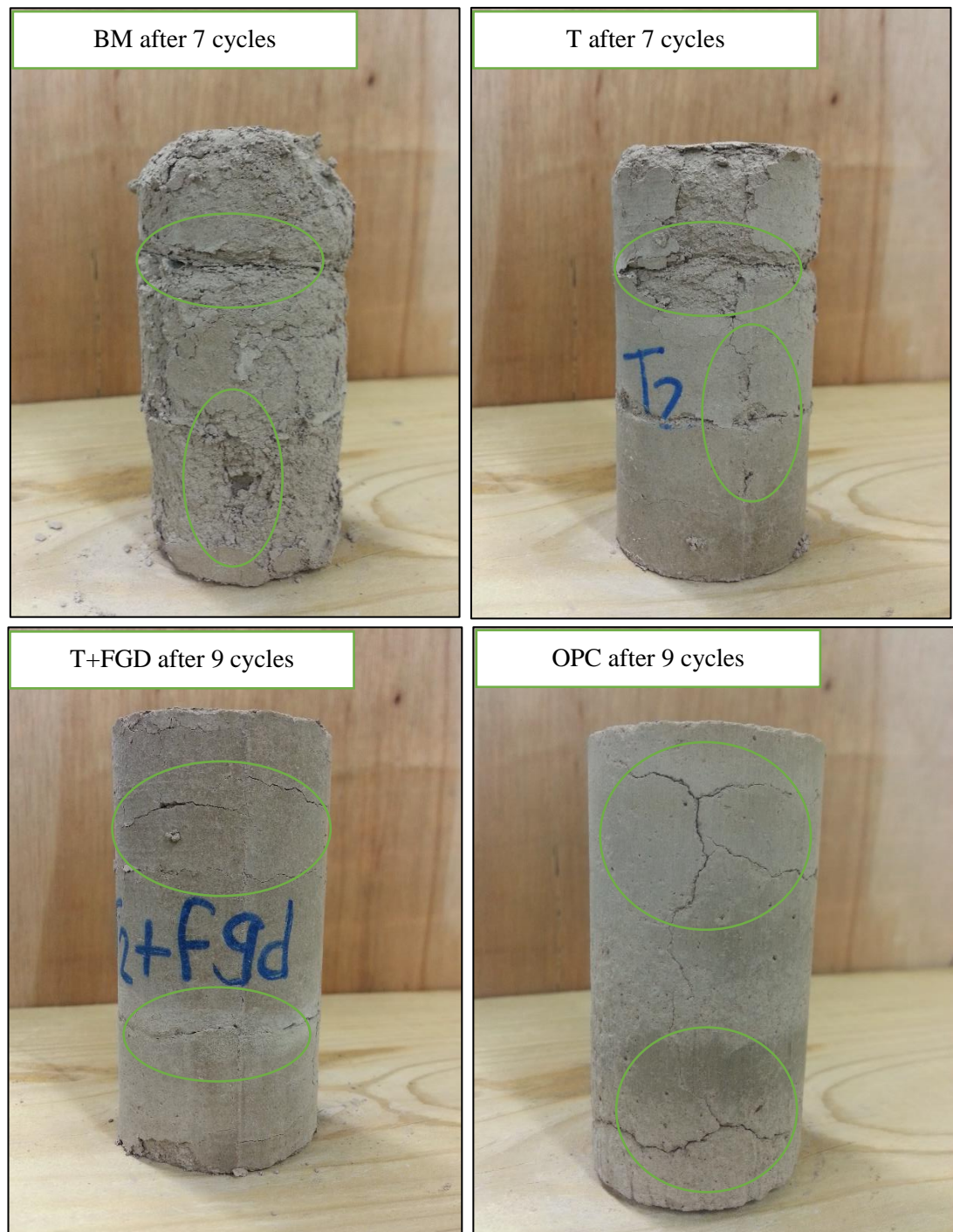


Figure 6.15 Crack propagation and sample damage of the soil treated with different binders after wetting-drying testing.

The variations in volume as percentages of the origin volume of the soil treated with different binders according to different numbers of wetting and drying cycles are plotted on Figure 6.16 in which each pair of days in this figure represents a completed

cycle of wetting and drying. For all types of binder excluding the reference cement, the greatest volume changes due to swelling and shrinking were observed after the first and second cycles. It was observed that the reductions in volume of the samples treated with GU and OPC were irreversible for the earlier cycles, even after wetting. At the fourth cycle, the samples treated with GU indicated a significant increase in the sample volume after wetting; while the samples treated with cement rebounded from the reduction in volume to reach their origin volume at the seventh cycle. Similar behaviour of samples treated with lime was reported by Stoltz *et al.* (2014). Interestingly, the samples treated with T+FGD showed the best volume stability against swelling and shrinkage in comparison with that for the samples treated with the other mixtures. The samples treated with GU and T displayed the highest volume change amongst all mixtures. Overall, the significant volume changes displayed by the samples treated with GU, BM and T can be attributed to the low densities that were adopted to prepare these samples which resulted in more permeable specimens than those for T+FGD and OPC. This enabled the water to permeate through the samples and consequently caused swelling; thereby making the samples prone to disintegration (Sargent *et al.*, 2013).

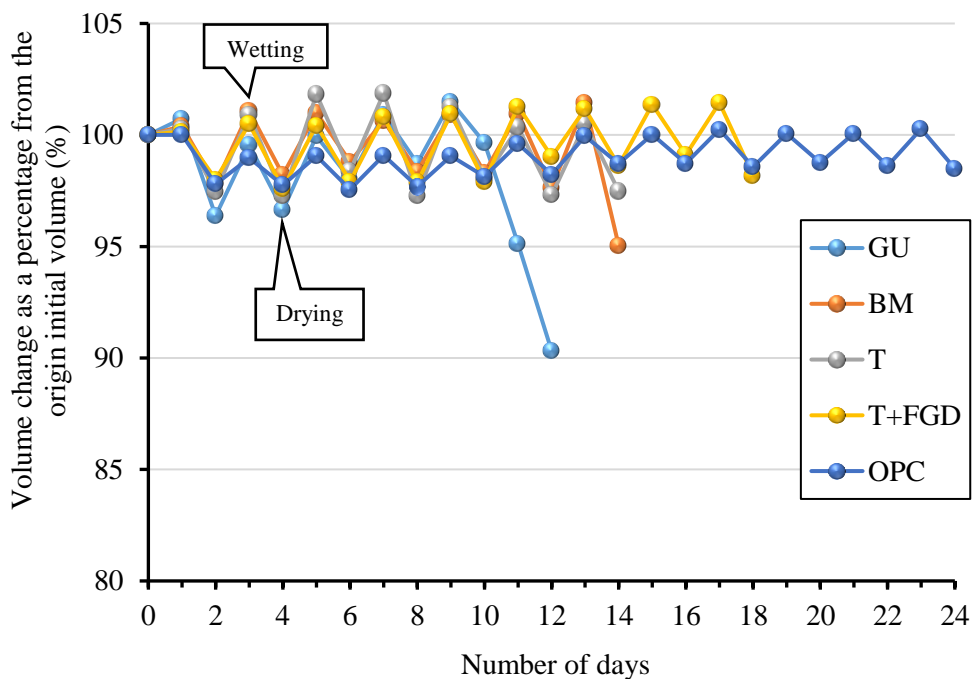


Figure 6.16 Volume changes of the soil samples treated with different binders experienced during wetting-drying cycles testing.

The soil-binder mass losses expressed as percentages of the initial dry mass of each of the corresponding specimens are displayed in Figure 6.17. Overall, the percentages of mass loss increased with the increase in wetting-drying cycles for all mixture types. However, with the exception of the untreated soil, no loss in samples mass was observed after the first cycle and the virgin soil sample collapsed completely before the required period of soaking ended (5 hours). The fifth cycle indicated significant mass losses for all mixtures except the samples treated with T+FGD which indicated a very low mass loss percentage (3.1%). This percentage was comparable to that for the samples treated with OPC which indicated 2.1%. Further cycles of wetting and drying indicated the discontinuity of the samples treated with GU, at the tenth cycle, with more than 50% mass loss for the samples treated with BM and T. At this stage, a very acceptable mass loss was indicated for the samples treated with T+FGD (20.65%); but it demonstrated approximately 5 times the mass loss obtained for the samples treated with OPC. Interestingly, amongst all the mixtures developed in this study, only the samples treated with T+FGD succeeded to survive all the twelve wetting-drying cycles with a recorded mass loss of 57.19%. The samples mass losses that occurred due to wetting-drying cycles can be attributed to the same reasons described in previous paragraphs regarding the strength losses and volume changes.

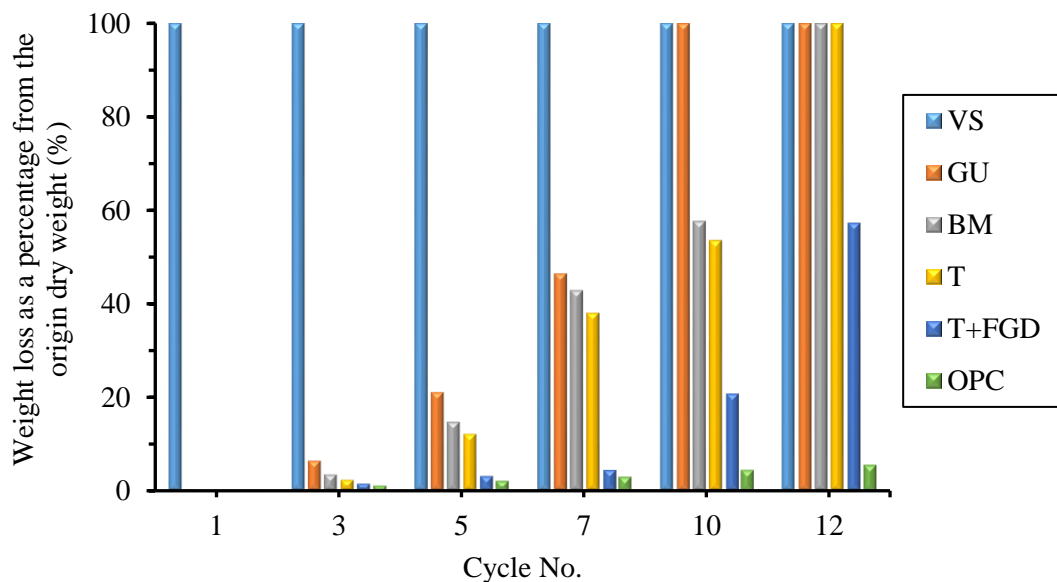


Figure 6.17 Effect of wetting-drying cycles on the soil-binder weight loss of the soil samples treated with different binders.

6.7 SUMMARY

Further to the results and conclusions drawn from the previous chapter on the stage of optimisation testing for the different types of blending; along with the grinding and FGD activation, a comparative study was conducted to compare the engineering performance of the most promising mixtures with that for OPC. The suitability of the binders for use in stabilising the Hightown silty clay soil was assessed dependent on the geotechnical properties of the stabilised soil. Results from a comprehensive suite of Atterberg limits, compaction parameters, UCS, compressibility and durability tests revealed that all binder mixtures showed acceptable results and improved the geotechnical properties of the stabilised soil. Moreover, the results indicated that among the optimum mixtures, the binder T+FGD at an optimum dosage of 12% by the dry mass, produced the most impressive engineering performance. This binder type had performance comparable to the reference binder (OPC). Based on the results obtained from the experiments in this chapter, the following points can be drawn:

- For all mixtures, the development of the Atterberg limits surpassed that achieved from the OPC in which the PI values achieved from the soil treated with all types of binder were lower than that achieved from the soil-OPC mixture. T+FGD indicated the lowest PI which was 11.74. BM indicated the second best value of PI which was 12.78. However, the other binders indicated PI between 13 and 13.5.
- The results of compaction tests indicated that different increments in MDD accompanied with different reductions in OMC were observed with the treatment using blended binders in comparison with the soil treated with GU. The highest increment in MDD with greatest reduction in OMC were achieved using T+FGD. However, all binders gave lower MDDs and higher OMCs than those for the soil treated with OPC. The increment achieved in MDD and the decline in OMC can be beneficial to increase the soil strength and enhance the workability of the soil-binder mixture.
- The strength development was found to increase with the increase of MDD and reduction in OMC in this study. This development was found to be linked with the amount of water content in which the soil-binder mixtures that had relatively higher OMC, demonstrated slower development in the soil strength. Additionally, significant strength developments were achieved from all binder types when they

were compared to that for the VS. The achieved strengths from the samples of treated soil comfortably met the requirement of the engineering performance stated by EuroSoilStab (2002). Interestingly, the UCS of the soil treated with T+FGD surpassed that for the soil treated with OPC after 180 days of curing. The UCS values at this age were 1464kPa and 1450kPa for the soil treated with T+FGD and OPC respectively. Whereas, the 180 days UCS for the soil treated with GU was 991kPa which was less even than that at 3 days curing of the reference samples. This gives an indication of the impressive enhancement of the pozzolanic reaction of the ternary binder for the longer curing periods by using FGD.

- Significant improvements in the stabilised soil stiffness as well as the compressibility were achieved from the soil samples treated with all the mixtures after consolidation testing. Soil compressibility was found to decrease impressively using the various binders over the curing times. Once again, T+FGD binder produced higher stiffness behaviour than the other binders and its performance was comparable to the OPC. By using the binder T+FGD at 28 days of curing and in comparison to the untreated soil, the initial void ratio was decreased from 0.904 to 0.806, C_c from 0.28 to 0.107, C_s from 0.075 to 0.012 and S_c from 5.325mm to 1.418mm. Moreover, the pre-consolidation pressure was increased significantly from 150kPa for the VS to 1180kPa for the soil treated with T+FGD. The coefficient of volume compressibility, M_v was found to decrease significantly with the increase in the applied effective pressure by using all binder types, especially with the use of T+FGD. For the effective stress of 400kPa, M_v was decreased from 0.305m²/MN for the VS to 0.061m²/MN for the soil treated with T+FGD, which was very close to that of the soil treated with OPC (0.055m²/MN). By this reduction in M_v the stabilised soil was transformed from the zone of a high compressible soil to very low compressible soil according to the criteria of Tomlinson (2001).
- All binders showed acceptable resistance against durability testing by wetting and drying cycles. However, with the exception of T+FGD and OPC, all binders failed to survive for all the twelve cycles. This was attributed to the lower densities for the samples treated with the binders in comparison to that for OPC. Consequently, the water suction of the samples treated with the binders was higher than that for

OPC. Thus, more cracks developed by the following wetting and drying cycles resulting in weak planes. Thus, the soil strength decreased significantly and some of the samples disintegrated before the completion of all cycles. The result of durability testing indicated that T+FGD demonstrated better durable performance amongst the other mixtures and this binder survived to the highest number of wetting drying cycles (9 cycles for the residual strength and volume change, and 12 cycles for the soil-binder loss testing).

Finally, it would be prudent to investigate the mineralogy and morphology of the soft soil used in this study in both its virgin and treated states to elucidate the improvements gained in the geotechnical properties of the stabilised soil. The soil and the most promising binder (T+FGD) mineralogy and microstructural development over the curing time are addressed in the next chapter as the final experimental works in this research.

CHAPTER 7

MINERALOGICAL AND MICROSTRUCTURAL ANALYSIS

7.1 INTRODUCTION

Based on the findings of the previous chapters, using T+FGD at a binder content of 12% by the dry mass has been determined as the optimum binder mixture, amongst all the other mixtures tested, for the use for Hightown silty clay stabilisation. With the use of this mixture as a binder, significant compressive strength and durability performances were observed over the curing periods. Therefore, in order to elucidate and understand the development in the soils compressive strength gained by using the most promising mixture (T+FGD) as a binder to stabilise the soft soil, an investigation of the changes in the mineralogy and microstructures of the stabilised soil and pastes of T+FGD was conducted.

This chapter presents a series of SEM micrographs, EDX and XRD patterns analyses for the binder pastes, the untreated soil and the soil treated with binder T+FGD after 3, 7, 28 and 180 days; along with the soil treated with OPC. The results are expected to provide insights into the mineralogical and microstructural changes within the soft soil after being stabilised with the aforementioned binders and the pastes of the binder materials without soil. It is also hoped that these findings will supply good visual insights into the detection of the cementitious products that occurred due to the hydration reaction; along with the formation of new minerals within the materials. Spectra from SEM, EDX and XRD analyses are the suggested most useful techniques for the investigation of the chemical and morphological reaction upon hydration (Li *et al.*, 2014; Jha and Sivapullaiah, 2016). These tests were utilised to provide useful information in determining the mineralogy of the pastes of binders and stabilised soil to understand the physico-chemical reactions occurring within the microstructures of the pastes of the binders and soil-binders over the curing period. The results achieved are anticipated to ultimately elucidate the vision of improved geotechnical performance presented in previous chapters.

7.2 X-RAY DIFFRACTOMETRY ANALYSES

XRD analyses were carried out on the dry and paste states of the binder T+FGD exposed to different curing periods ranging from 3 to 180 days; along with dry and hydrated paste of OPC for comparison purposes. These tests were carried out to detect the formation and development of cementitious products such as the cementitious gel (C-S-H and/or C-A-H), ettringite in both its phases, alumina-ferric oxide-trisulphate (AFt) and alumina-ferric oxide-monosulphate (AFm) and Portlandite (CH), over the curing period. Figure 7.1 shows the diffraction patterns of the T and T+FGD mixtures identifying the effect of the proportion of the fly ashes used to produce the ternary mixture on the crystalline and amorphous phases of T+FGD binder along with the effect of using FGD as a grinding agent (GA). No remarkable changes were detected in the XRD patterns of these mixtures except slight reductions in intensities of the crystal peaks of the quartz after the assistance of GA. Sadique *et al.* (2013) reported a similar phenomenon during dry grinding of a high calcium fly ash mixed with high alkaline fly ash and silica fume using FGD as a grinding aid. The phase compositions of T+FGD identified by XRD analysis were C: calcite, L: lime, G: gehlenite, A: arcanite, Mr: merwinite, M: mayenite and Q: quartz as labelled in Figure 7.1.

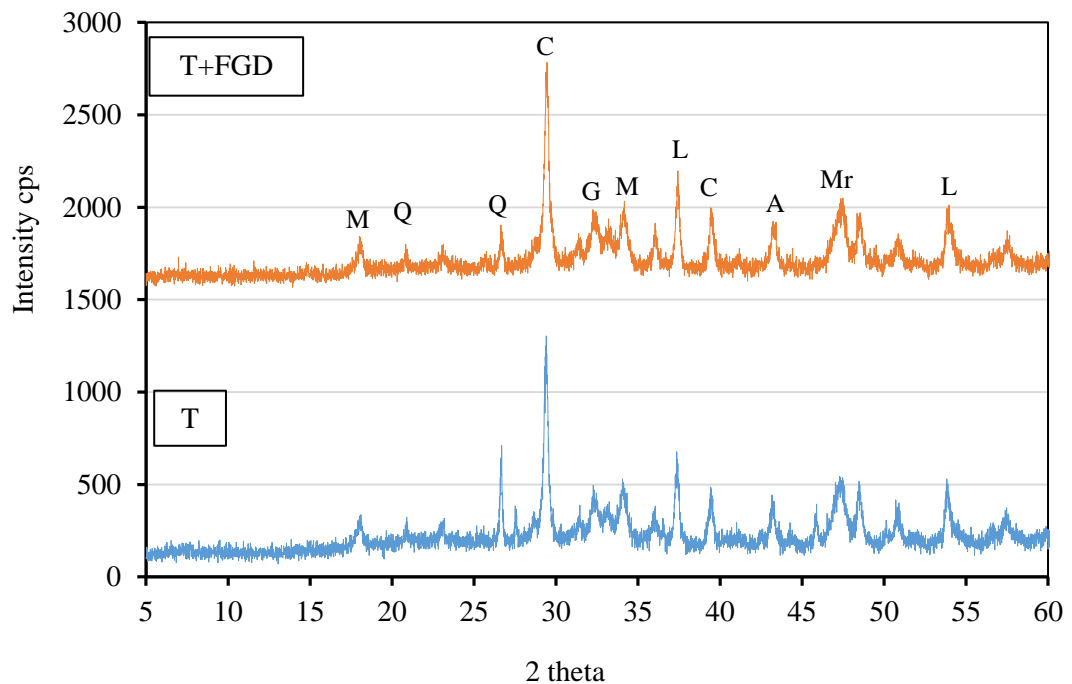


Figure 7.1 Powder XRD patterns of T and T+FGD binders.

Figure 7.2 and Figure 7.3 display the comparative diffraction patterns of the dry state and the hydrated pastes, exposed to different curing periods, for the binder T+FGD and OPC respectively. The identified phase composition of both hydrated binders (T+FGD and OPC) were mainly calcium silicate hydrated (C-S-H), Portlandite (CH) Ca(OH)_2 and ettringite ($\text{Ca}_6\text{Al}_2(\text{SO}_4)_3(\text{OH})_{12}\cdot 26\text{H}_2\text{O}$). As for the reference cement, clear changes could be distinguished in the intensities of the XRD peaks for T+FGD from the early stage of hydration (3 days), specifically for lime (Figure 7.2). With the increases in hydration time, the formation of C-S-H, C-A-H, C-S-A-H, ettringite and the Portlandite (CH) compounds was very clear, especially so after 28 days of curing. The production of C-S-H, CAH and CASH gels and CH is attributed to the chemical reaction that occurred between the lime (L) of WPSA and the amorphous silica produced from RHA in addition to the silicates and aluminates of POFA. As shown at 180 days of curing in Figure 7.2, these compounds are expected to be formed continuously as curing time progresses because the pozzolanic reaction of silica requires a longer period to activate the lime of WPSA forming more cementitious gel (Calligaris *et al.*, 2015; Jiang *et al.*, 2016).

At the early ages of curing, some peaks of CH developed then decreased or disappeared at 28 days curing. This indicates that CH was activated with pozzolanic materials represented by silicates and/or aluminates of POFA and RHA, and transferred to C-S-H and/or C-A-H and C-A-S-H compounds. Similar findings were reported by Sadique *et al.* (2013) after using a rich-calcium fly ash activated with a high alkali sulphate fly ash. XRD analysis results also showed peaks of calcite transformed to cementitious products represented by either C-S-H and/or C/K-S-H. They were identified as sharp peaks in crystalline phases as shown at 180 days age (Figure 7.2). In recent research, C-S-H has been identified in either amorphous or semi crystalline and crystalline phases according the hydration period, it is was reported that the crystalline phase of C-S-H has a lower calcium to silica ratio (Ca/Si) which is represented by C-S-H type I (Tajuelo Rodriguez *et al.*, 2017; Singh *et al.*, 2017).

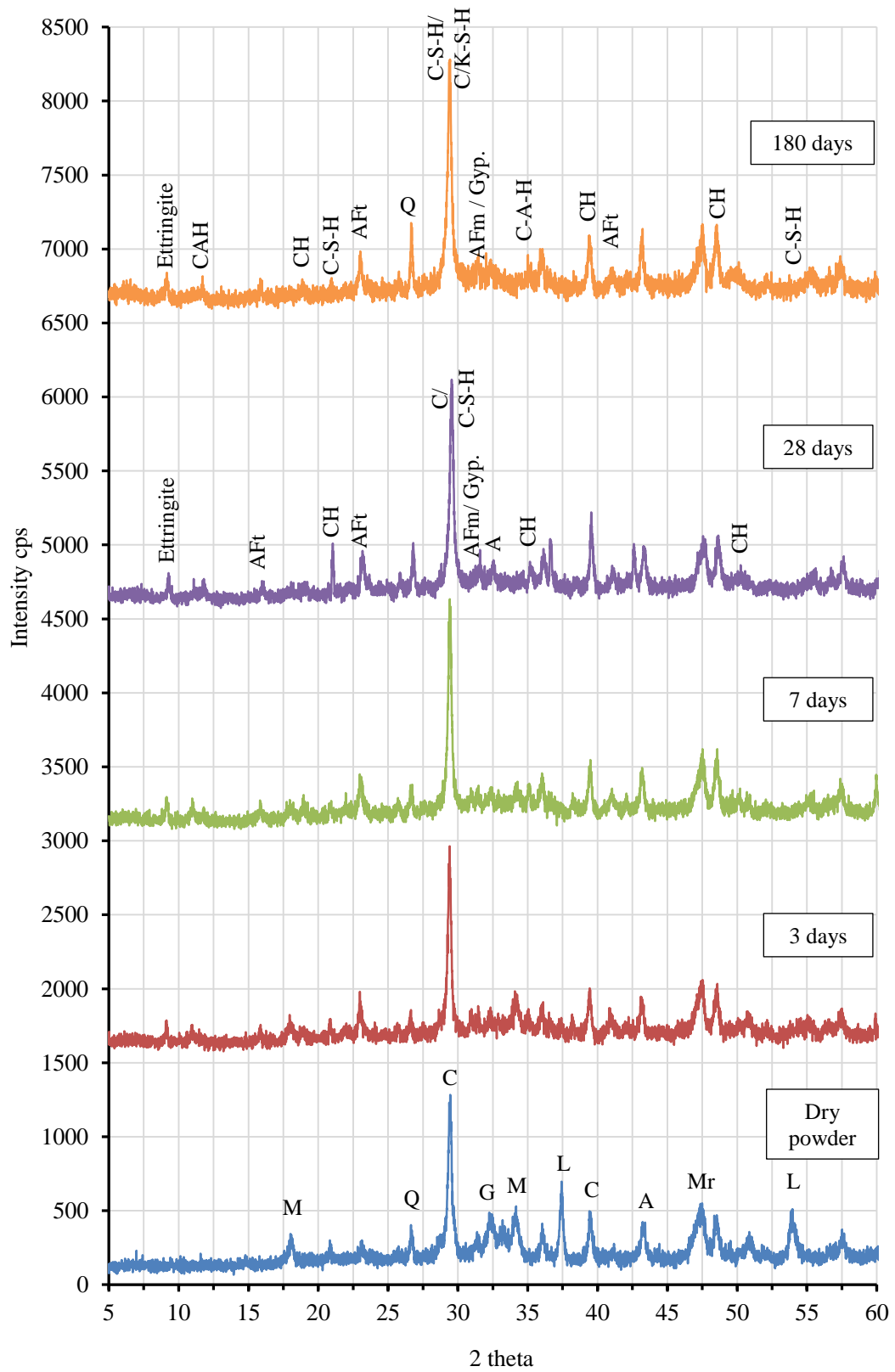


Figure 7.2 XRD analysis of T+FGD binder paste subjected to different curing periods; along with the dry powder state.

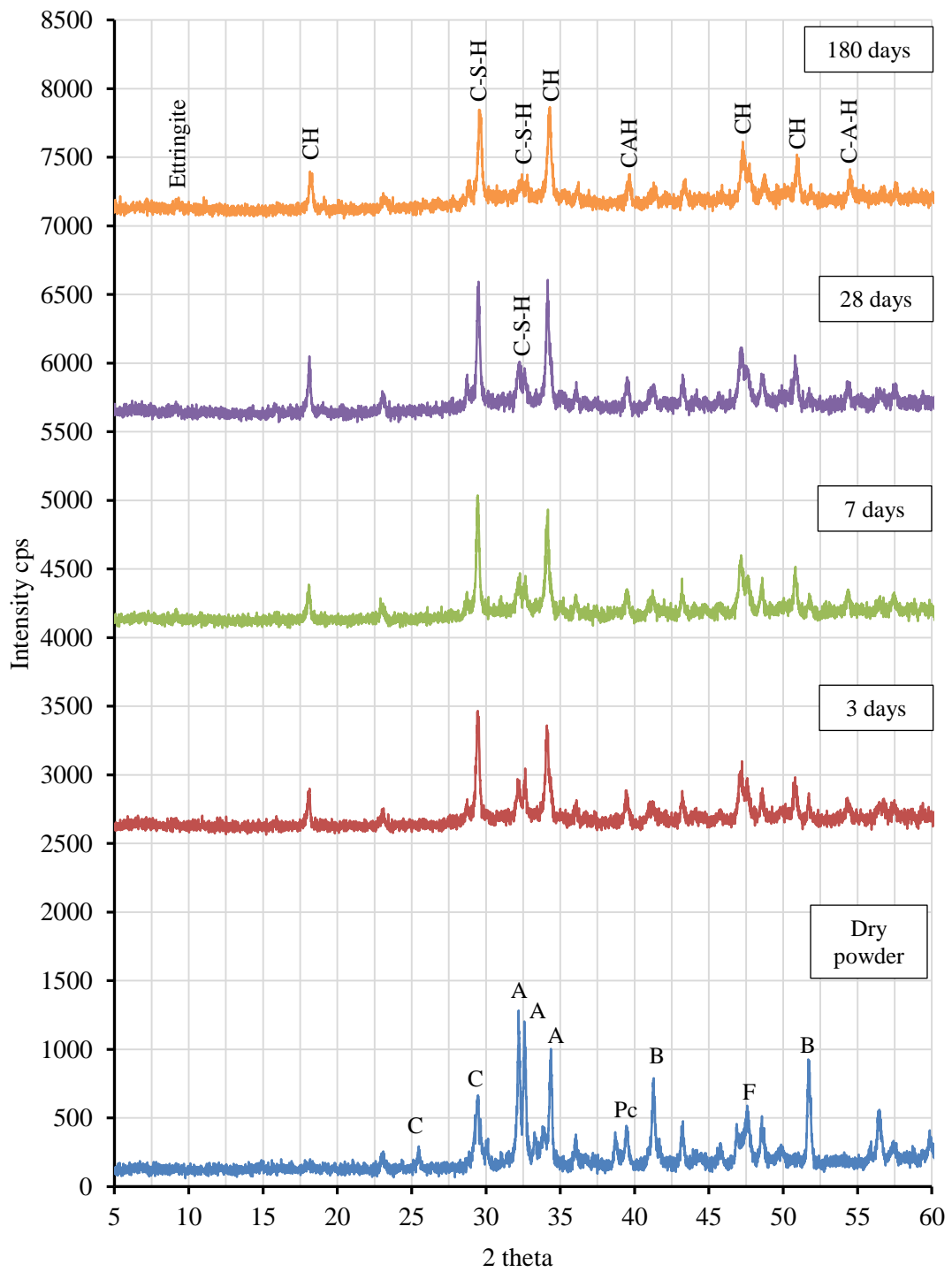


Figure 7.3 XRD analysis of reference cement paste subjected to different curing periods; along with the dry powder state.

T+FGD contains a sufficient content of K_2SO_4 , produced from POFA, to activate WPSA particles forming anhydrites, while potassium ions K^+ may also played an important role in the formation of the cementitious gel by increasing the pH value and accelerating the hydration reaction, and it will be expected to be balanced by SO_4^{2-} provided from FGD. Sadique and Al-Nageim (2012) stated that upon the interaction of the developed cementitious material, containing high calcium and high alkaline rich sulphate fly ashes called HSC-3, with water, ionic species from alkali sulphate (K^+ , Na^+ and SO_4^{2-}) dissolve immediately in the liquid phase forming hydrates. FGD as a GA along with WPSA contribute to Ca^{++} and additional SO_4^{2-} ions until saturation. Additionally, the aluminium oxides of WPSA and POFA dissolve in this stage and react with Ca^{++} and SO_4^{2-} and then precipitate as ettringite or AFt phases as shown in Figure 8.2 at 28 days of age. After a few hours of hydration, the concentration of the hydrated lime reaches its maximum. In the meantime, the concentration of SO_4^{2-} remains constant, even after the formation of ettringite, because it is replaced by the dissolution of additional $CaSO_4$. Consequently, the formation of C-S-H is initiated at this stage (Sadique and Al-Nageim, 2012).

Zhang *et al.* (2016b) conducted a study on the performance of a composite cementitious system containing FGD gypsum in dried and thermal activated states using heating of $80^\circ C$ and $800^\circ C$ respectively. They stated that, for the samples containing the dried FGD, hydration products such as AFt and C-A-H existed at the same time from the first day of hydration up to 1 year. However, unreacted gypsum was identified even after 1 year of hydration due to the excessive amount of FGD gypsum used. This behaviour agrees with the diffraction patterns of the T+FGD mixture shown in Figure 7.2 in which peaks for ettringite, AFt and AFm compounds were identified from 3 days to 180 days of curing.

Similar changes in the diffraction patterns were observed from the XRD analysis of the reference binder (OPC) as shown in Figure 7.3, but due to the rapid consumption of the mineral phases of cement, a faster reduction of crystalline peaks occurred since the early age of curing resulted in the appearance of new peaks identified as ettringite and CH.

7.3 ANALYSIS OF SEM AND SEM/EDX TESTING

SEM imaging testing has been increasingly used in cement and soil stabilisation research, especially for microstructural investigation purposes. It helps to understand the development in the geotechnical properties of the treated material by providing high-resolution micrograph images. Such images help to distinguish the changes in the microstructure over curing time (Li *et al.*, 2014; Jha and Sivapullaiah, 2016). Additionally, a combination of SEM and EDX analysis is also used to get information about the morphology, surface texture and elemental composition of the hydrated phases of binders and/or treated soils (Jha and Sivapullaiah, 2015; Rossen and Scrivener, 2017). In this research project, two types of pastes were prepared for this technique; untreated soil and soil-binder pastes which were subjected to SEM only and binder pastes which were investigated by SEM and SEM/EDX testing. All pastes were cured for different curing periods, 3, 7, 28 and 180 days, prior to the SEM and SEM/EDX testing. Two binders were involved in this analysis; T+FGD and the reference binder OPC.

7.3.1 SEM Analysis of Untreated Soil.

Based on the XRD analysis of the virgin soil presented in section 4.2.2, quartz was the dominant mineral phase of the soft soil used in this study with moderate content of kaolinite. The presence of these compounds was confirmed by the observations from SEM testing which revealed smaller lightly coloured particles (kaolin clay) less than 5µm in size which can be found in the microstructure of the compacted untreated soil shown in Figure 7.4. It can be seen that the small particles of kaolin clay can be recognised partially coating the surfaces of some larger lumps of the compacted sample (encircled areas on Figure 7.4); along with flaky and platy shaped particles of other minerals of clay. Regarding the surface and larger particles, they appear to be relatively clean and well defined in which there is no evidence of chemical bonding. This observation will prove useful when the particle morphology and overall specimen microstructure, after binder is introduced to the soil, are compared later in this chapter.

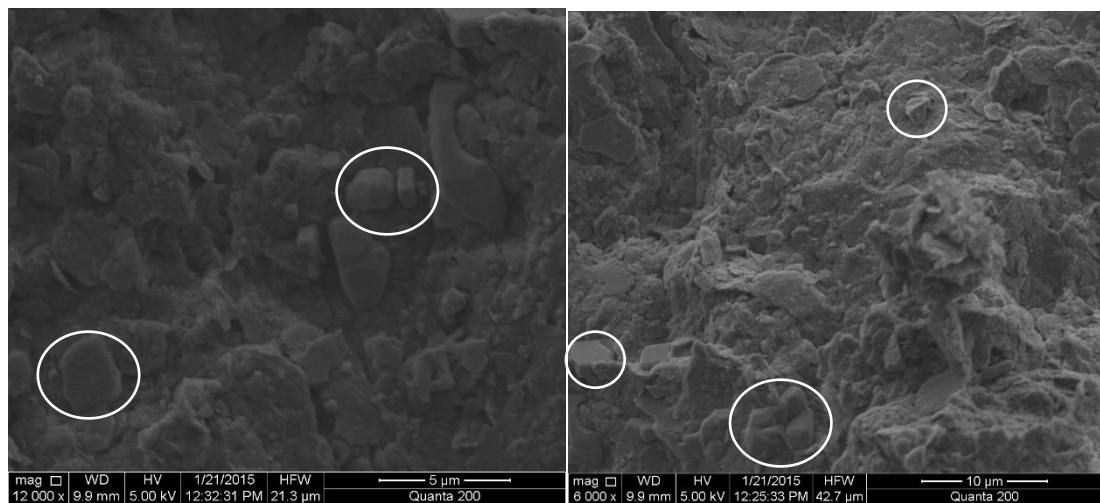


Figure 7.4 SEM images of compacted virgin soil with different magnifications.

7.3.2 SEM Analysis of Hydrated Soil-Binder

The sequence of changes that occurred over the curing time in the microstructure and morphology of the paste of soil treated with T+FGD are displayed in Figures 7.5 to 7.8. Upon inspecting the cured stabilised soil, the materials higher level of complexity compared with the untreated soil state became apparent in these figures. It is evident that the formation of cementitious products, such as C-S-H, CH and ettringite, occurred during the early age of curing (3 days) as shown in Figure 7.5. From Figure 7.5a, the needle-like crystals (ettringite) can be easily recognised, while C-S-H gel and flake-like particles of Portlandite (CH) appear clearly in Figure 7.5b. The formation of these products increased with the progression of curing time as shown in Figure 7.6 and Figure 7.7 at 7 and 28 days of curing respectively. Additionally, the pore space aperture between the particles became narrower or negligible and dense packing of the binder and soil particles was observed. Pore spaces were filled by either the clay particles of the treated soil or by the growth of cementitious products (Sargent, 2015). At the age of 28 days (Figure 7.7a), the ettringite became thicker and distributed widely to cover most of the surface area of the tested sample with the increase in the area coated by C-S-H gel. The CH particles also increased clearly at this age of curing. The microstructure of the stabilised soil became denser and its surface was completely coated by the hydration products. Similar microstructure changes was reported by Jha and Sivapullaiah (2016) for soil stabilised with lime and different dosages of gypsum.

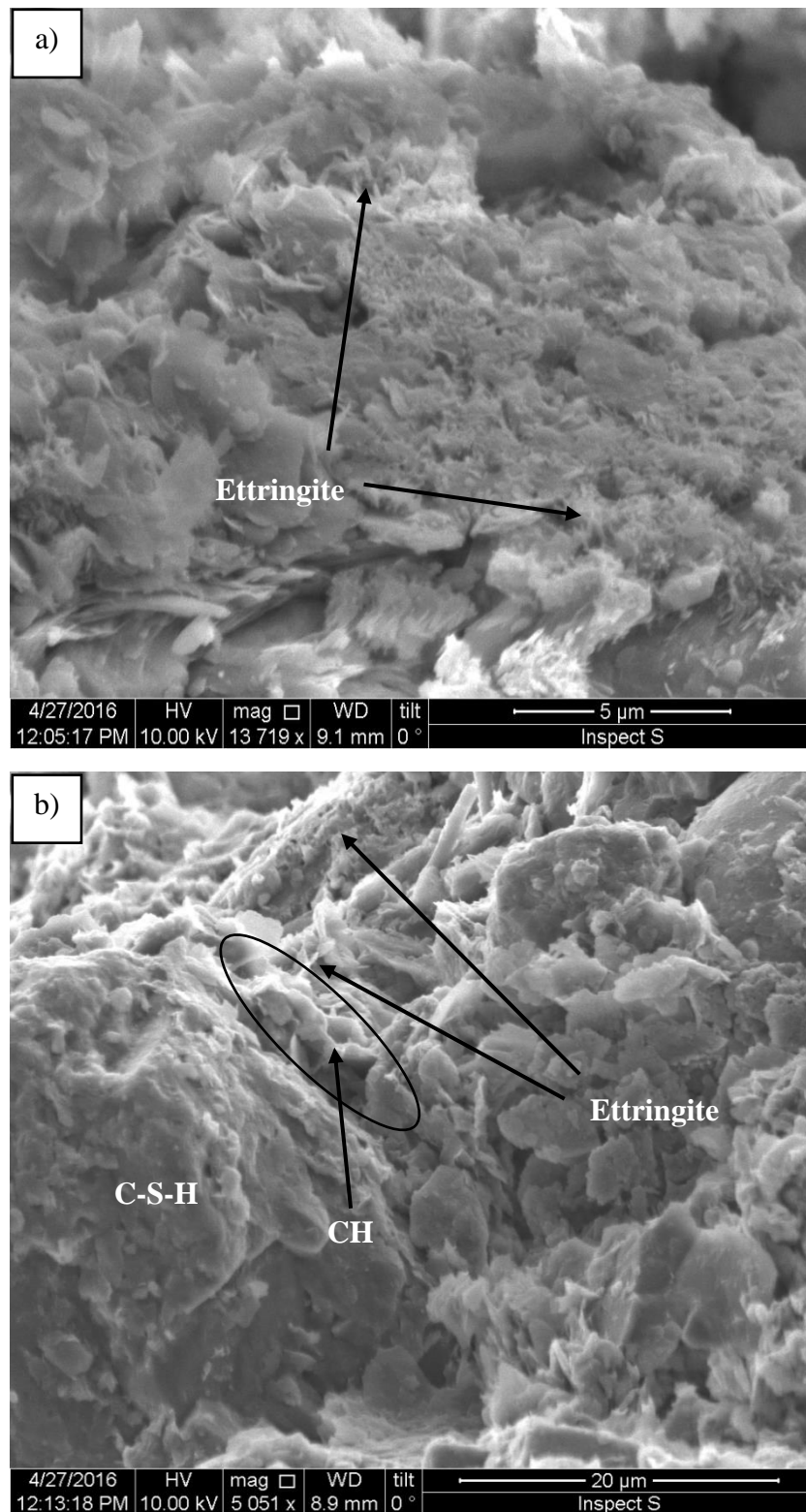


Figure 7.5 Hydrated paste of stabilised soil at 3 days curing; (a) 13719x and (b) 5051x.

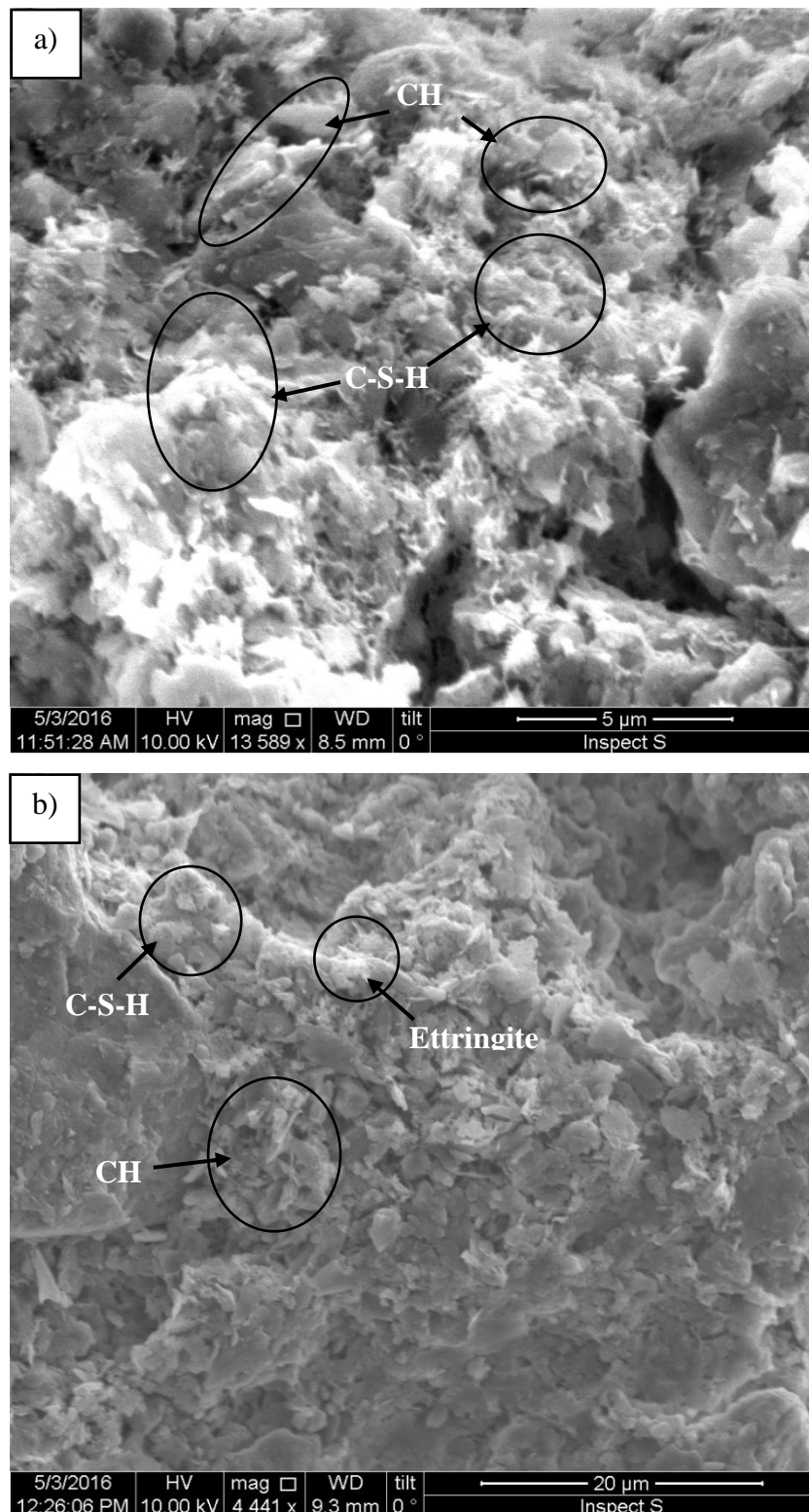


Figure 7.6 Hydrated paste of stabilised soil at 7 days curing; (a) 13589x and (b) 4441x.

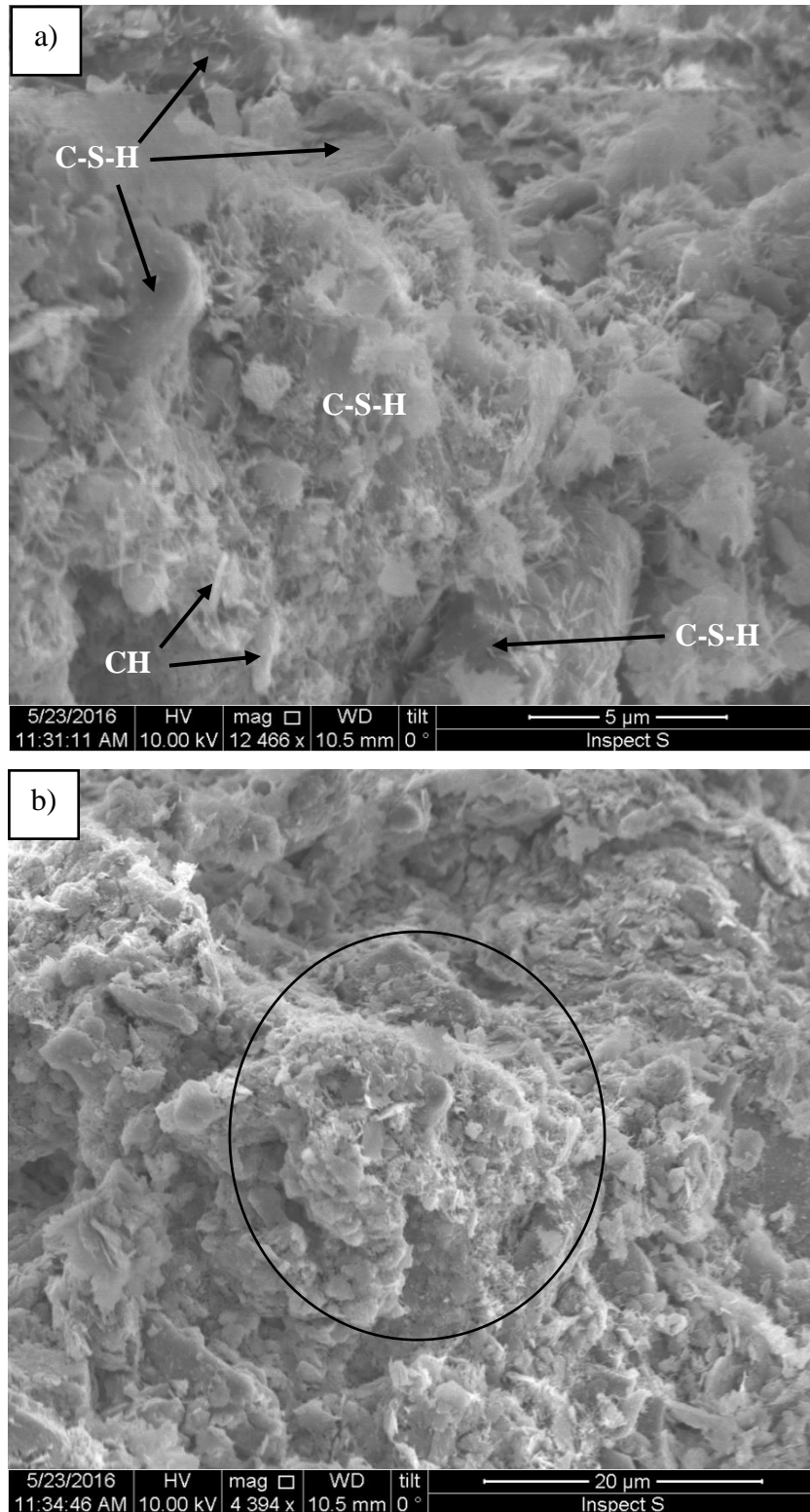


Figure 7.7 Hydrated paste of stabilised soil at 28 days curing; (a) 12466x and (b) 4394x.

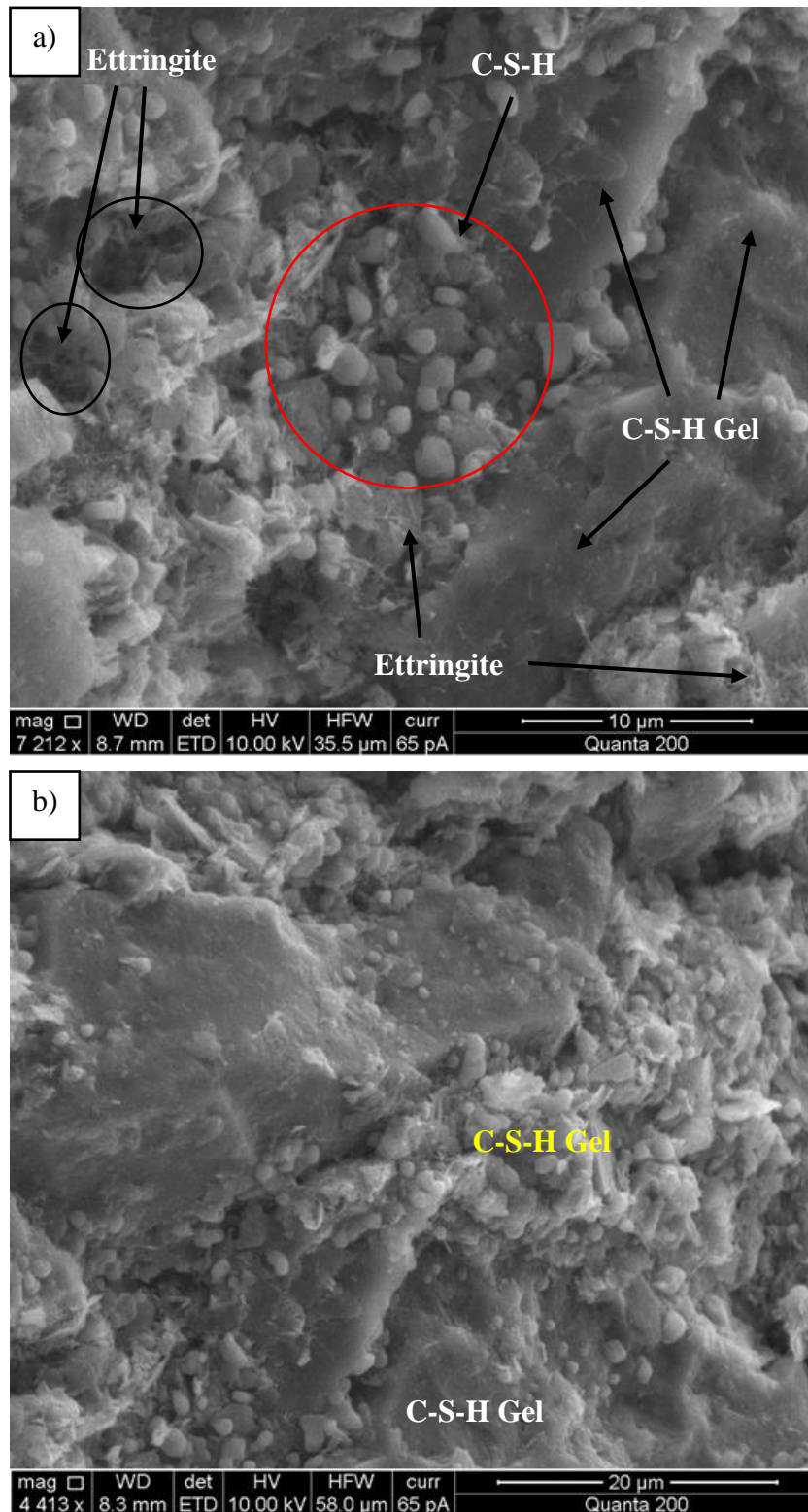


Figure 7.8 Hydrated paste of stabilised soil at 180 days curing; (a) 7212x and (b) 4413x.

The prolonged period of hydration (180 days) of the soil treated with T+FGD is shown in Figure 7.8. A very dense structure was observed and the void spaces within the stabilised material had become filled due to the development of cementitious products growths resulting in materials with lower permeability compared with that after 28 days of hydration reaction. There was a substantial increase in the area coated with C-S-H gel over that observed at 28 days age. Due to the extensive growth of the cementitious gel and hydration products occurring over the age of curing, the clay particles of the treated soil cannot be clearly seen as displayed in Figure 7.8. In contrast to the nature of cementitious products within the 28 days sample when observed in the gel phase, small lighter colour crystals appeared clearly in the 180 days sample as encircled with red line on Figure 7.8a which represent C-S-H crystals. This was in agreement with the XRD analysis presented previously in section 7.2, in which C-S-H could be detected as a crystalline phase, especially where the ratio of calcium to silica decreases (Tajuelo Rodriguez *et al.*, 2017). CH crystals no longer significantly appear at this age, while the formation of ettringite in the AFt phase is still detected, but in amounts less than those for the earlier ages of curing. This may be due to the existence of FGD within the binder used. A stronger and compacted soil matrix, after treatment with lime and different contents of gypsum, was reported by Jha and Sivapullaiah (2016) which was attributed to the formation of ettringite and cementitious products over the curing period. The formation of needle-like ettringite crystals was reported to increase with the increase in the percentage of gypsum mixed with lime. However, it was reported that, after 28 days of curing, there was a sufficient amount of cementitious gel formed which coated the ettringite crystals. Ettringite crystals were reported to gradually disappear with the continuous formation of the cementitious compound with the increase in the hydration period (Jha and Sivapullaiah, 2016). Similar findings regarding the microstructural changes for the stabilised clay soil with existence of sulphate materials were presented by Cheshomi *et al.* (2017).

7.3.3 SEM and SEM/EDX Analyses of Hydrated Binder Paste

The SEM micrographs of fractured fragments of T+FGD paste at different ages of hydration reaction are presented in Figure 7.9 to Figure 7.12. There are four main phases of ordinary Portland cement (OPC) which contribute to strength development of cement pastes and concrete; these phases are C_3S , C_2S , C_3A and C_4AF . These aforementioned compounds have different reactions during the cement hydration resulting in different hydrates or so called hydration products (Aïtcin, 2016a). According to Aïtcin (2016a) and Marchon and Flatt (2016a), the morphology of these hydrates can be summarised as follows:

- Portlandite (CH) which is formed due to the lime hydration of C_3S and C_2S during the early stage of hydration reaction. CH morphology are crystalline with hexagonal like crystals.
- Cementitious gel (C-S-H) is the more preferable product as it contributes to the strength development. This product formation occurs due to the pozzolanic reaction of the silicates of C_3S and C_2S with CH which is initiated in the first few hours of the hydration reaction and continues up to several months producing more C-S-H. The continuity of pozzolanic reaction depends on the availability of sufficient amounts of silicates and water.
- Ettringite (calcium-sulpho-aluminates) AFt appears in needle-like crystals in pore spaces during the early hydration.
- Monosulfoaluminoferrite (AFm) forms in platy crystals.

Both AFt and AFm result from the chemical reaction between the calcium sulphates and C_3A and C_4AF . AFt forms at the early stage of hydration due to the fast dissolution of C_3A . In contrast to the AFt, AFm results at the period of low activity due to the slow diffusion of species in the hardened materials which experience a chemical reaction between ettringite and C_3A (Marchon and Flatt, 2016a).

Similar changes were observed in the microstructure and morphology of the soil-binder paste over the curing time from the SEM testing of T+FGD paste. However, the hydration products were more clearly detected in the case of the binder paste alone. The dominant crystals observed at 3 days of hydration were Portlandite and ettringite

with small areas covered by the cementitious gel C-S-H as shown in Figure 7.9a and b. With the increase in the hydration time, most of the CH crystals reacted chemically with the pozzolanic minerals (silicates and aluminates) to form more C-S-H gel that appeared as clusters at 7 days of age as shown in Figure 7.10. At 28 days of curing, the sample surface was almost completely coated by C-S-H gel as shown in Figure 7.11. At this age, ettringite is still detected but in reduced amounts that were originally observed in the samples tested at 3 and 7 days. The transformation of AFt to AFm phase was revealed as shown in Figure 7.11b, in which it appeared in lath-like crystals (Jha and Sivapullaiah, 2016). Interestingly, a very dense and compacted microstructure with very low voids was achieved at 180 days of hydration as shown in Figure 7.12. Figure 8.12a shows that CH and ettringite crystals disappeared and C-S-H gel covered all the surface of the sample. C-S-H gel can be easily seen coating spherical particles of POFA and contributing to a less permeable microstructure as marked in Figure 7.12b. Jha and Sivapullaiah (2016) reported that ettringite crystals disappear with the increase in the hydration period, resulting in more cementitious gel.

For the C-S-H contribution, the SEM/EDX analyses of the T+FGD paste at 28 and 180 days of hydration reaction are shown in Figure 7.13 and Figure 7.14 respectively. The corresponding SEM/EDX analyses of the reference binder (OPC), at the same ages, is presented in Figure 7.15 and Figure 7.16 respectively. The EDX spectrum of C-S-H paste in the T+FGD mixture at 28 days of hydration, shown in Figure 8.13, revealed that the principal peaks consisted of calcium and silicon with trace amounts of Al, K, Mg and S. This phase is in accordance with the characteristic EDX spectrum of the C-S-H phase suggested by Peethamparan *et al.* (2008) as shown in Figure 7.17. However, a significant amount of sulphur was observed as the test paste contained a high proportion of cement kiln dust which is associated with high sulphate content. Moreover, a similar phase of C-S-H obtained from T+FGD paste in this study was reported by Harbec *et al.* (2016). Hence, the C-S-H phases identified as C-S-H and C/K-S-H in the XRD analysis displayed in Figure 7.2 was consistent with EDX analysis. A similar EDX spectrum of C-S-H phase was obtained from the reference cement paste as shown in Figure 8.15 at the same age of curing.

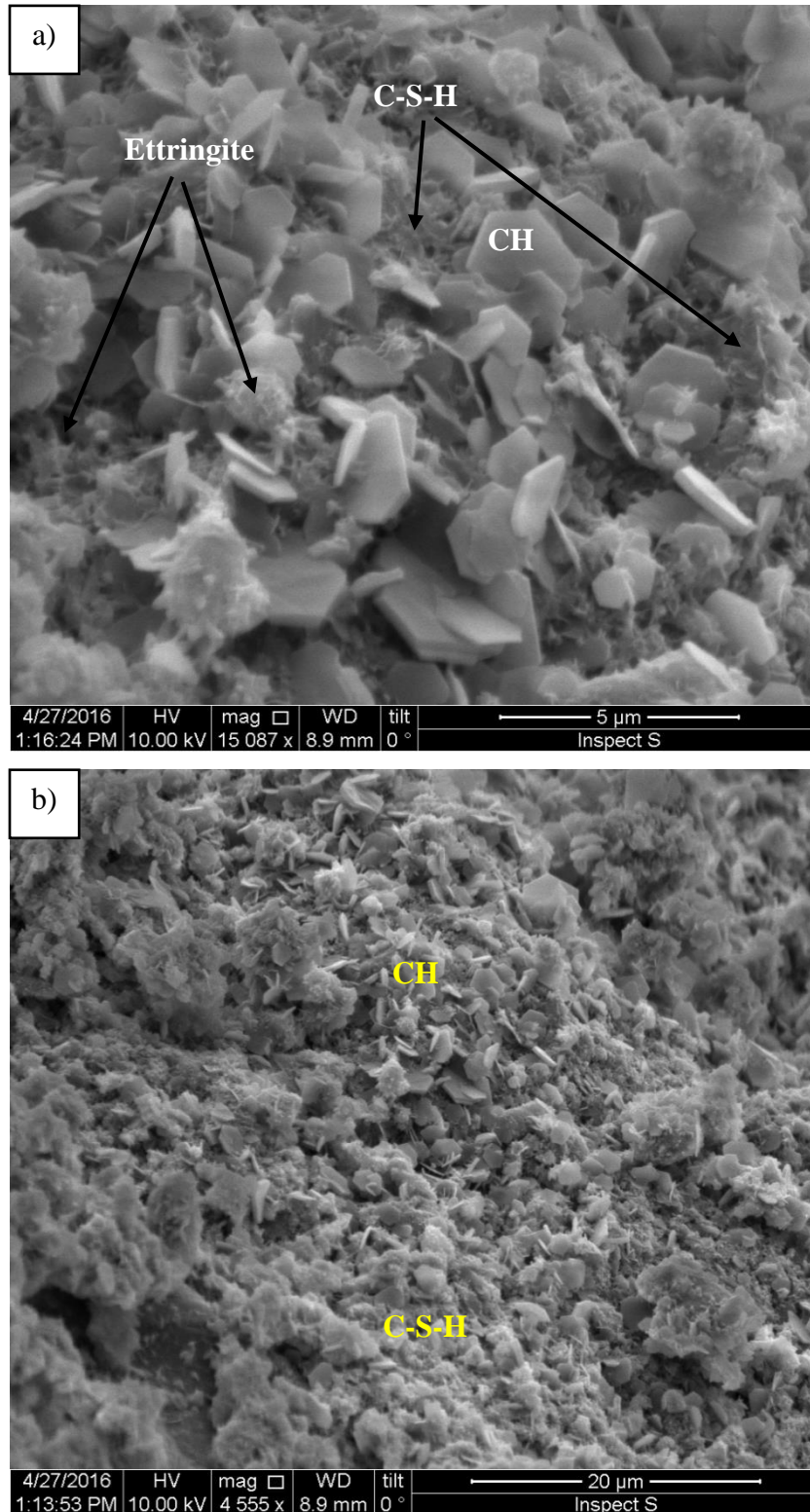


Figure 7.9 Hydrated paste of T+FGD at 3 days curing; (a) 15087x and (b) 4555x.

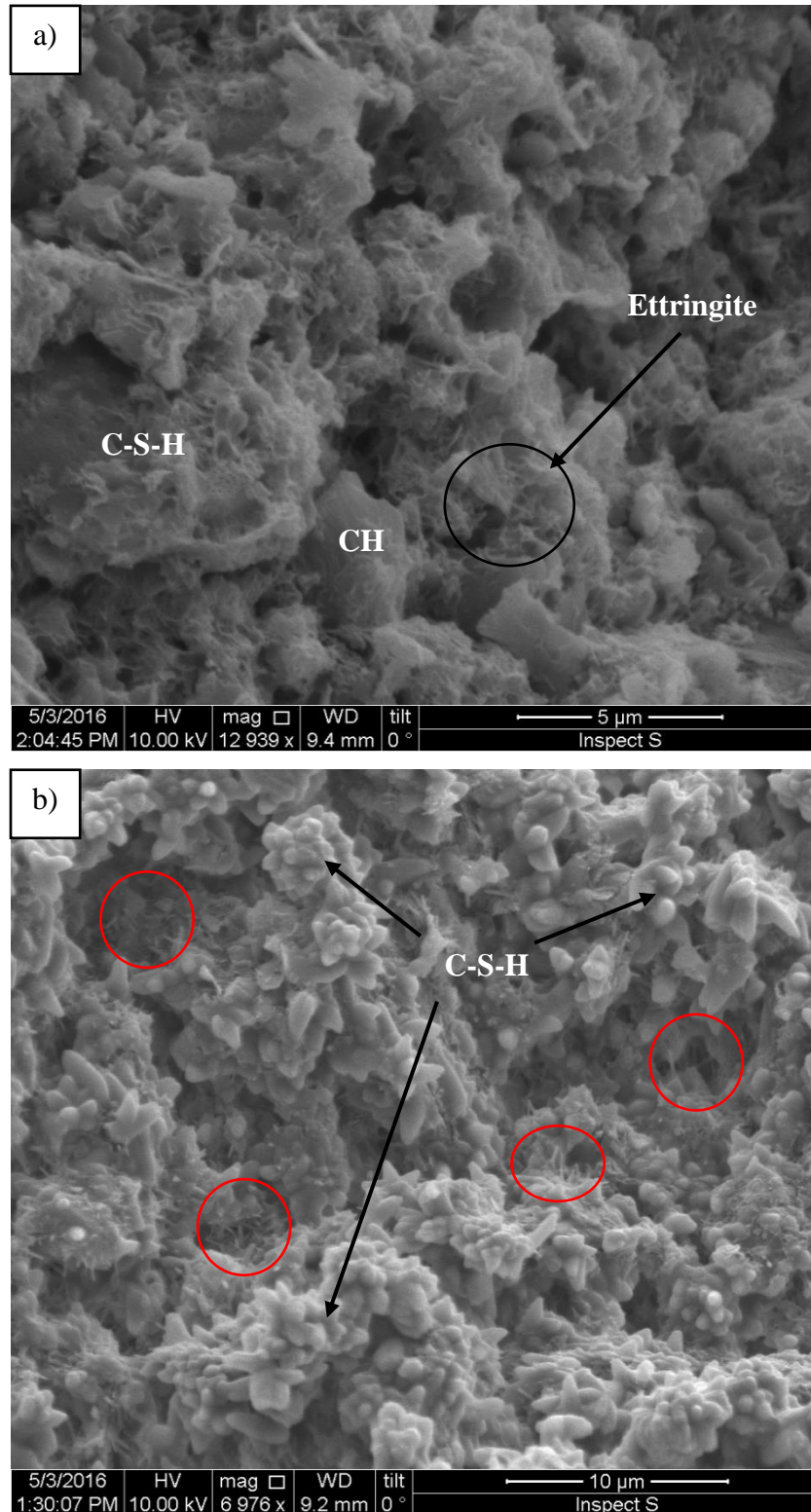


Figure 7.10 Hydrated paste of T+FGD at 7 days curing; (a) 12939x and (b) 6976x.

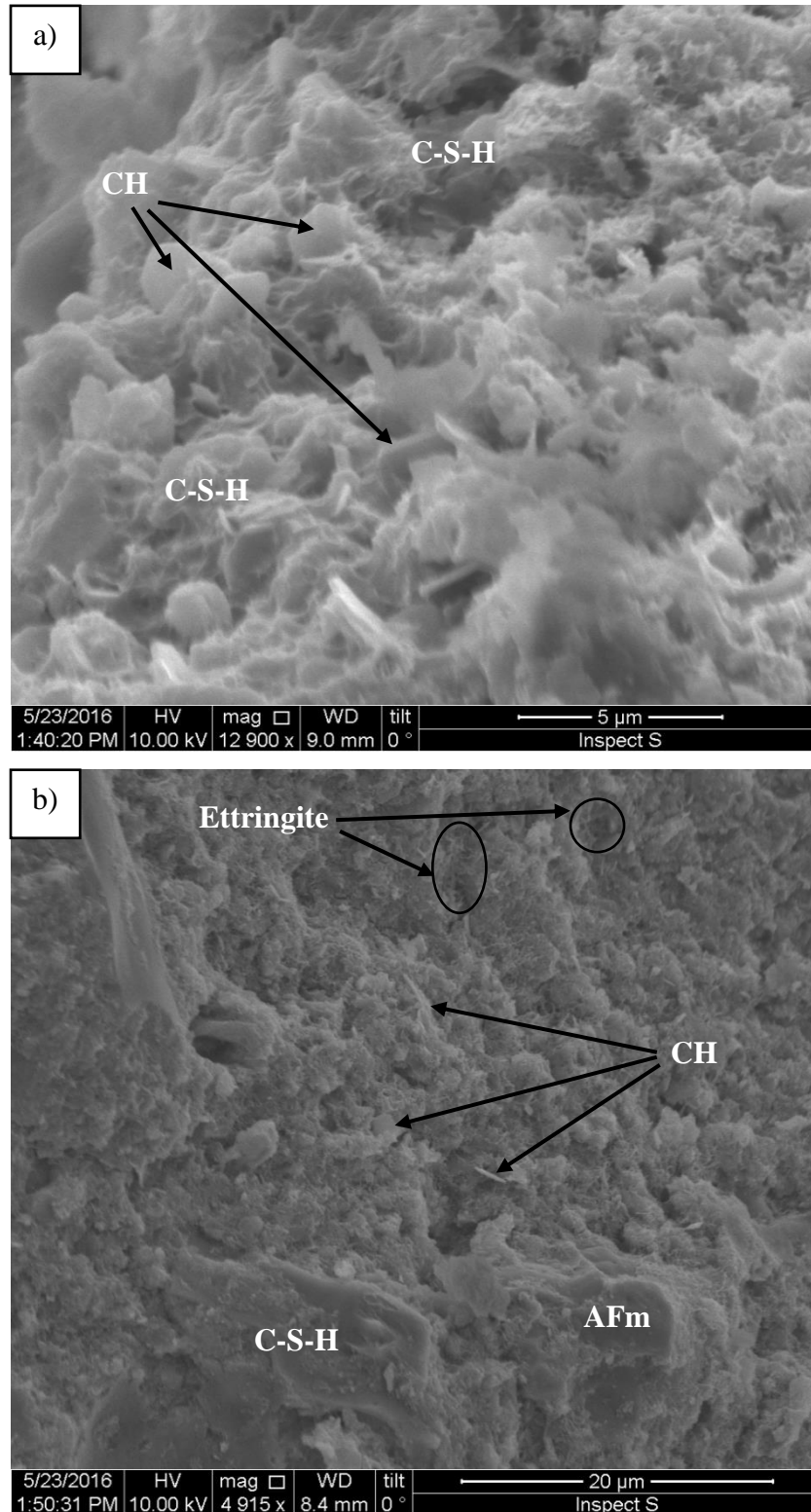


Figure 7.11 Hydrated paste of T+FGD at 28 days curing; (a) 12900x and (b) 4915x.

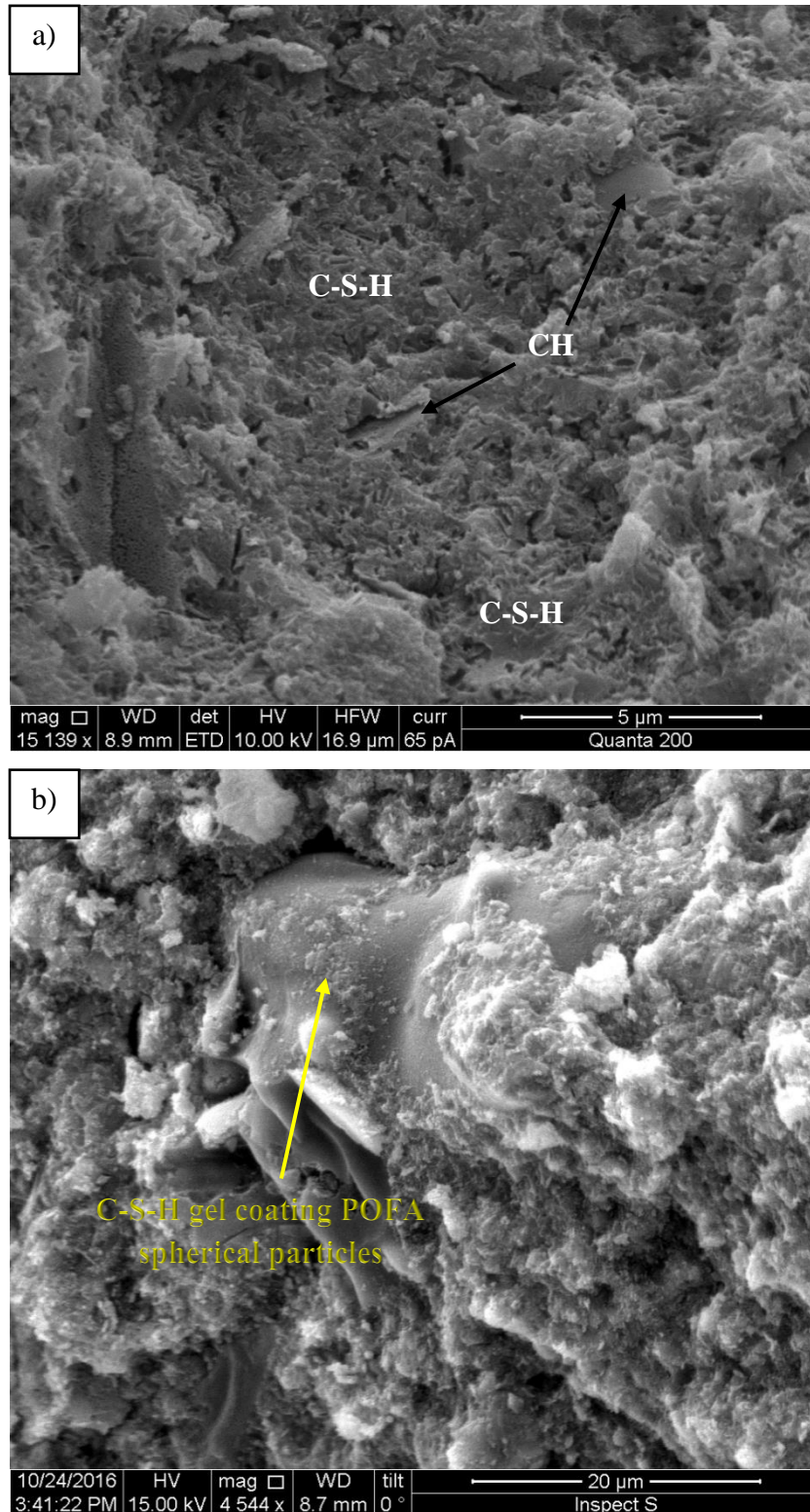


Figure 7.12 Hydrated paste of T+FGD at 180 days curing; (a) 15139x and (b) 4544x.

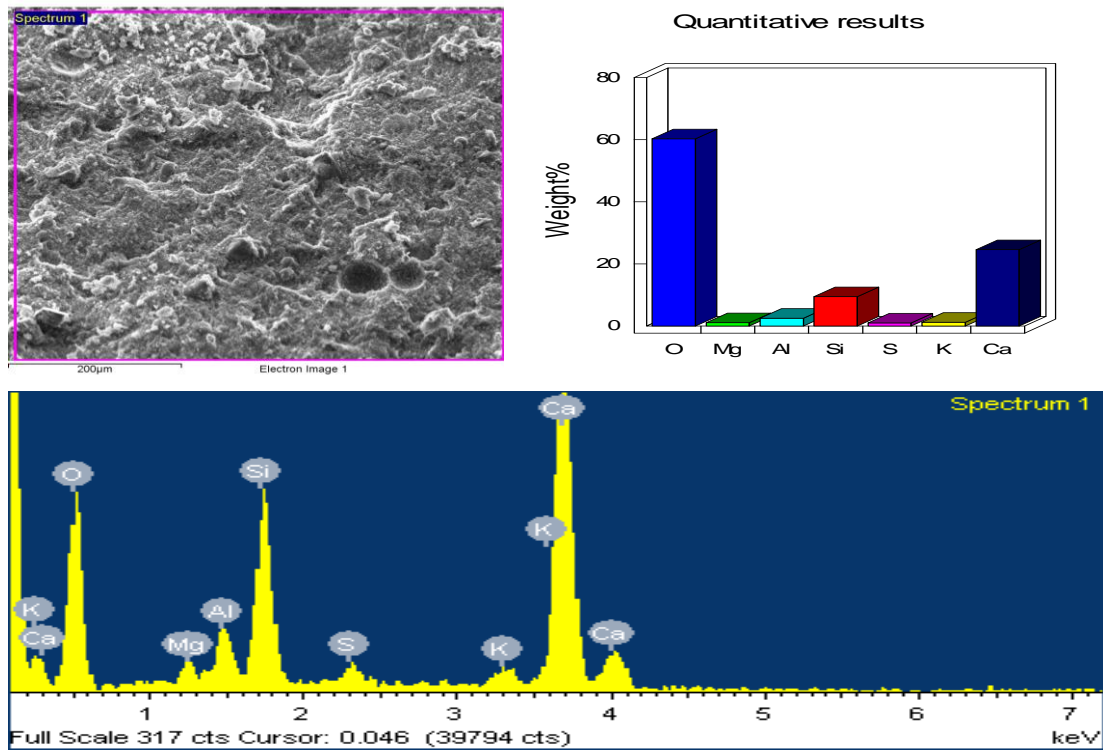


Figure 7.13 EDX spectrum of C-S-H in T+FGD paste at 28 days curing.

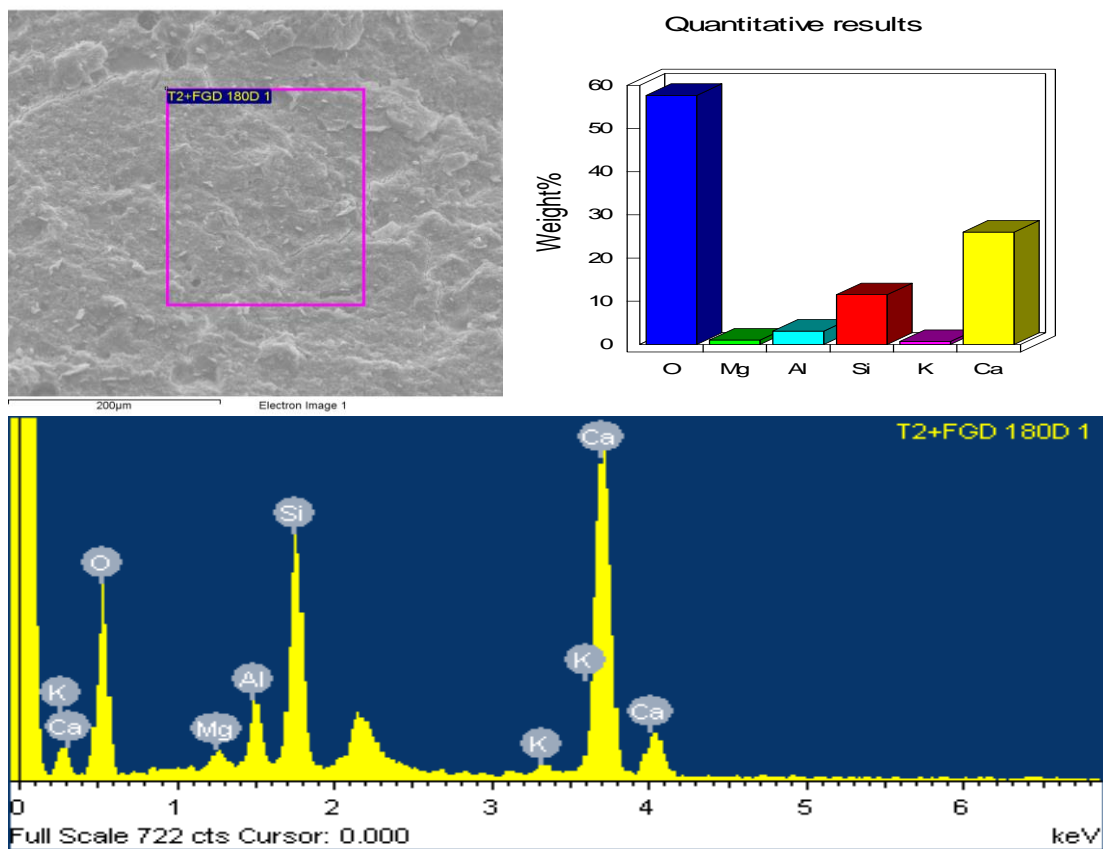


Figure 7.14 EDX spectrum of C-S-H in T+FGD paste at 180 days curing.

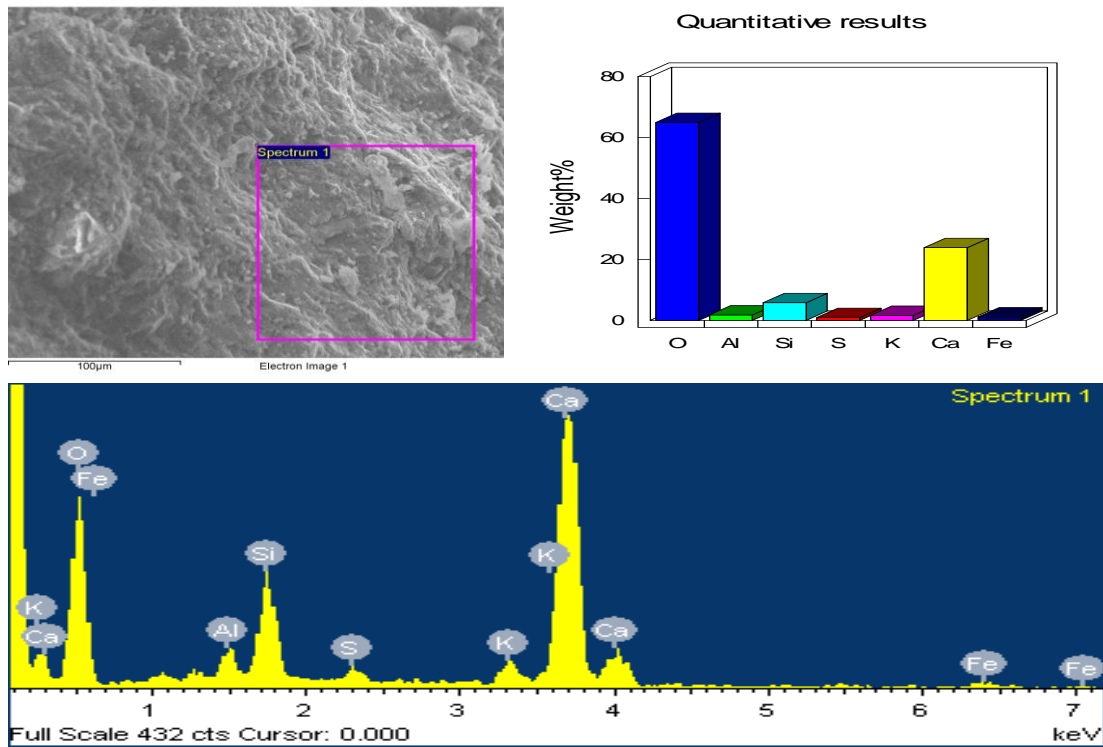


Figure 7.15 EDX spectrum of C-S-H in control cement paste at 28 days of curing.

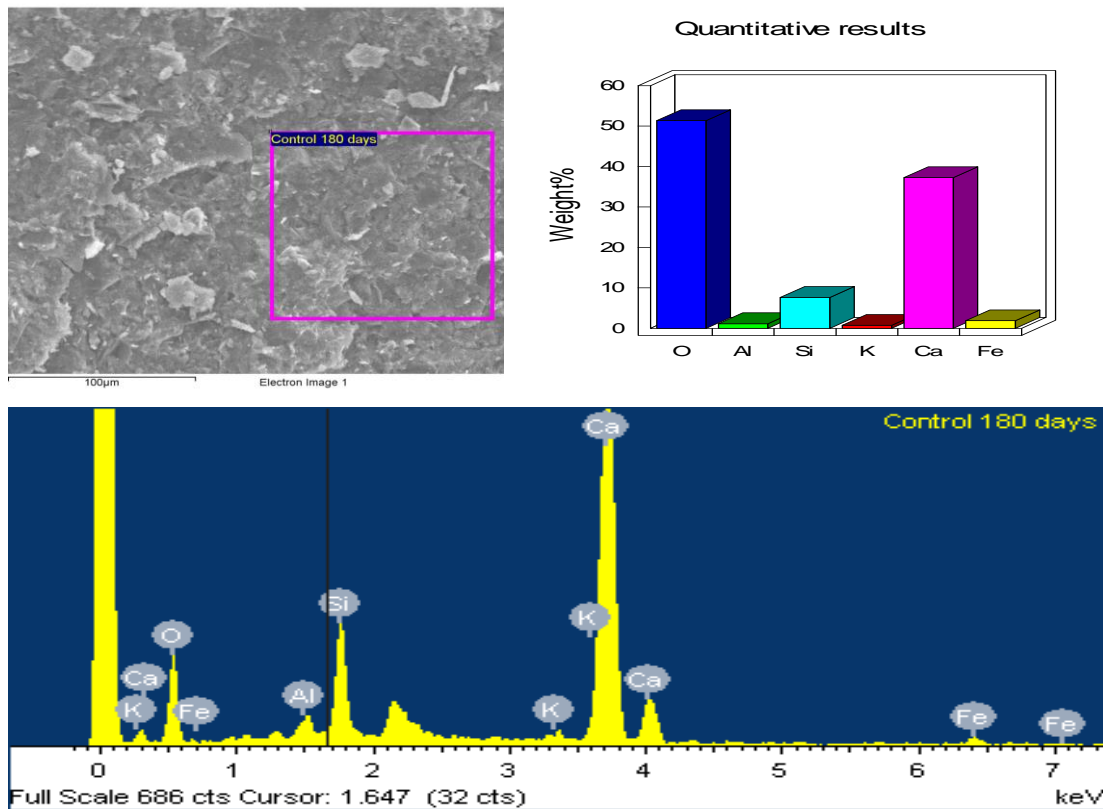


Figure 7.16 EDX spectrum of C-S-H in control cement paste at 180 days of curing.

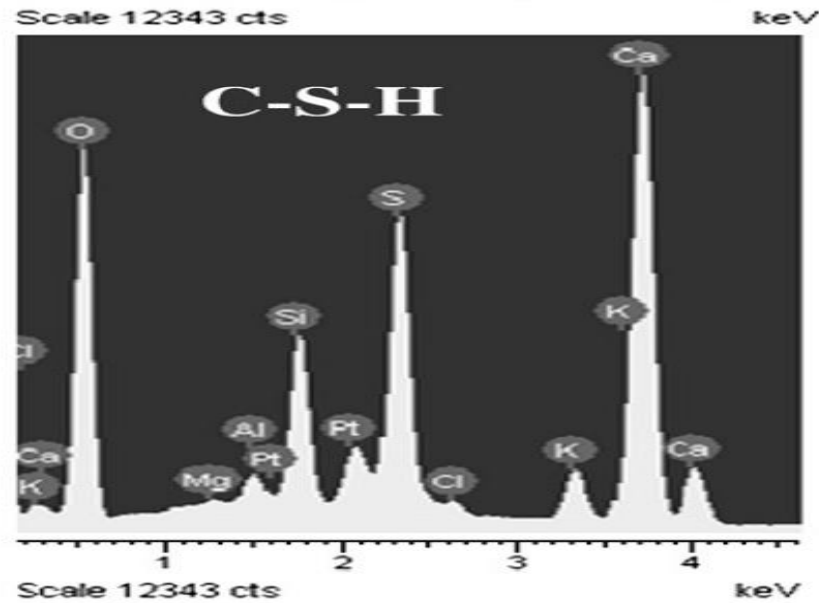


Figure 7.17 EDX spectrum of C-S-H reported by Peethamparan *et al.* (2008)
Permission to reproduce this figure has been granted by Elsevier.

The major elemental composition of the hydrated paste of T+FGD at 180 days was comprised of calcium, silicon, aluminium and potassium with a trace amount of magnesium as shown in Figure 7.14. The corresponding peaks of the control paste after 180 days of curing were mainly represented by calcium, silicon, iron and aluminium with a trace amount of potassium as shown in Figure 7.16. Furthermore, the compositional analysis of the hydrated pastes of T+FGD and the reference cement at different curing periods are listed in Table 7.1 and Table 7.2 respectively. The calcium concentration in the C-S-H gel reflects the stability and density of the cementitious product in which the higher the Ca and lower Na or K contents, the more stable gel and less deleterious expansion (Sadique and Al-Nageim, 2012). From Table 7.1 and Table 7.2 it can be observed that the concentration of Ca in T+FGD is very similar to that in the reference cement at all ages of curing. Moreover, a low Ca/Si molar ratio (1.58) at 180 days of curing was observed in T+FGD, which was much less than that for OPC (3.41), with an acceptable Si/Al ratio (3.57). This gives an indication about the availability of the sufficient amounts of silica that is required for the continuity of the pozzolanic reaction which contributes to the formation of more C-S-H gel and subsequent increases the compressive strength. This confirms that the compressive strength values obtained from the samples treated with T+FGD after 180 days of curing was greater than those obtained from the samples treated with reference

cement as shown in Figure 6.3 in the previous chapter. C-S-H with low CaO/SiO₂ was found to create more substitutions such as alkalis and aluminium and 1.7 was recommended as the typical ratio to insure the utilisation of most CH and formation of C-S-H gel during the hydration reaction (Gartner *et al.*, 2017). Singh *et al.* (2017) attributed the acceleration of the hydration rate of C₃S to the low concentration of Ca²⁺ in the pore solution which resulted in C-S-H gel exhibiting a low C/S ratio. It is expected that the rate of C-S-H formation in T+FGD may be faster than that for the reference cement. This can be attributed to the balance in the chemical composition of T+FGD represented by the high Ca of WPSA, high pH of WPSA and POFA and significant amorphous silica of RHA along with the aid of FGD as a grinding aid and a retarder for C₃A. Sadique and Al-Nageim (2012) referred to the importance of ensuring sufficient alkalis (Na₂O and/or K₂O) and sulphate in FA2 which are essential for the solubility of the silicates of SF to obtain higher compressive strength of the mortars. The mortars were prepared using ternary binder produced from a high calcium fly ash, alkaline sulphate waste material and SF using a combination of 60:20:20 respectively.

Table 7.1 EDX analysis of T+FGD paste after different periods of hydration reaction

Element	Hydration period (days)							
	3		7		28		180	
	Weight %	Atomic %	Weight %	Atomic %	Weight %	Atomic %	Weight %	Atomic %
O	14.29	27.81	55.73	73.96	65	80.61	57.66	74.51
Na	-	-	-	-	-	-	-	-
Mg	1.76	2.25	0.88	0.77	0.49	0.4	1.02	0.87
Al	2.22	2.56	2.16	1.7	1.85	1.36	3.09	2.37
Si	11.37	12.61	6.97	5.27	6.1	4.31	11.51	8.47
S	-	-	1.02	0.68	1.18	0.73	-	-
K	3.66	2.91	1.5	0.82	1.47	0.75	0.7	0.37
Ca	66.71	51.85	31.74	16.81	23.9	11.83	26.02	13.42
Fe	-	-	-	-	-	-	-	-
Ca/Si	4.11		3.19		2.74		1.58	
Si/Al	4.93		3.1		3.17		3.57	

Table 7.2 EDX analysis of the paste of reference cement after different periods of hydration reaction

Element	Hydration period (days)							
	3		7		28		180	
	Weight %	Atomic %	Weight %	Atomic %	Weight %	Atomic %	Weight %	Atomic %
O	44.08	64.09	43.17	64.68	64.95	80.93	51.34	71.22
Na	1.74	1.76	-	-	-	-	-	-
Mg	-	-	-	-	-	-	-	-
Al	3.34	2.88	0.99	0.88	1.79	1.33	1.14	0.94
Si	5.07	4.2	4.9	4.18	5.79	4.11	7.66	6.05
S	2.96	2.15	1.46	1.09	0.88	0.55	-	-
K	5.33	3.17	0.6	0.37	1.64	0.84	0.75	0.43
Ca	37.48	21.75	46.33	27.71	23.85	11.86	37.25	20.62
Fe	-	-	2.54	1.09	1.1	0.39	1.86	0.74
Ca/Si	5.18		6.63		2.88		3.41	
Si/Al	1.46		4.75		3.09		6.44	

7.4 SUMMARY

Following the successful improvements achieved in the geotechnical properties of the stabilised soft soil using T+FGD; along with the enhancement of the durability and long term performance as presented in previous chapters, the reasons for achieving such improvements were elucidated in this chapter by utilising the XRD analyses,

SEM imaging and SEM/EDX analyses. The results were compared with those obtained from the samples prepared from reference cement. Pastes of soil-T+FGD mixture and T+FGD and OPC were subjected to SEM testing at different ages of curing for microstructural and morphological investigation. Whereas, T+FGD and OPC pastes were subjected to further analyses which were XRD and SEM/EDX analyses at different hydration periods for mineralogical investigation.

XRD analyses revealed substantial changes in the mineral phases of T+FGD paste over the curing time. The formation of ettringite, Portlandite (CH) and C-S-H phases were evidenced from the early age of curing (3 days). Beyond this age, the utilisation of CH transferred to C-S-H was observed, especially after 28 days along with the transforming of ettringite from AFt to AFm phase. The mineral phases of T+FGD were found very similar to those observed for OPC paste over the curing period. The formation of these cementitious products was confirmed clearly by SEM testing conducted on both T+FGD and soil-T+FGD pastes subjected to various curing times. The results obtained from SEM testing strongly complied with those of XRD analyses. Moreover, a very dense and compacted microstructure was achieved, especially after 28 days of curing using the T+FGD mixture as a binder for the treated soil. SEM/EDX analyses were found to be in very good agreement with the results obtained from XRD analysis and SEM testing for each corresponding period of hydration. Moreover, the elemental composition of the T+FGD paste obtained from EDX analysis was found to be very akin to that for the OPC paste with slight differences, especially beyond 28 days of curing. A lower C/S atomic ratio, than that for OPC, was found in the elemental composition of T+FGD at 180 days which indicates a fast rate of hydration and more C-S-H gel would be formed resulting in higher compressive strength. This confirms the higher UCS of the soil treated with T+FGD at 180 days age in comparison to the soil-OPC samples.

Finally, the techniques utilised in this chapter clearly helped to understand and realise the improvement in the engineering and geotechnical properties of the stabilised soil using T+FGD. In addition, the results obtained from each individual test were consistent with those obtained from the others.

CHAPTER 8

CONCLUSIONS AND RECOMMENDATIONS

8.1 LIMITATIONS OF THE STUDY

The findings of this study are restricted to the specific type of the stabilised soil, the specific types of the waste materials used to develop the new cementitious binder and the investigated geotechnical properties that have been involved in this study. Additionally, the results of liquid limit and plastic limit testing in this study should be considered as a limitation in this study because performing this test is mainly dependent on the skills and experience of the person performing the test.

Many soil types have entirely different chemical and geotechnical properties that make their behaviour after treatment with the chemical additive vary according to the properties of a particular soil. Regarding the additives used in soil stabilisation, the performance and the effect of each type of binder could be different and influenced by various factors such as the production condition, the degree of the temperature of calcination, the period of burning and the composition of the raw materials used in the production processes. These factors affect the chemical properties and the reactivity of the produced wastes which in turn leads to different performances when they are used as additives. Moreover, due to the extensive experiments of optimisation that were carried out in this study, not all the geotechnical properties of the soil used in this study were investigated. There is a potential that the developed binder could exhibit a different effect on the other geotechnical properties of the treated soil.

8.2 CONCLUSIONS

This research project aimed to develop a new cementitious binder produced from ternary blending of different waste materials fly ashes along with the effect of FGD as a sulphate activator and grinding agent for the use as a 100% cement replacement in soft soil stabilisation. The physical and chemical properties of different types of waste

material fly ashes were investigated to evaluate their potential to contribute to the development of the new cementitious binder. The performance of the final form of the new binder was assessed in comparison to that for a traditional cement (OPC type 32-N) in terms of the Atterberg limits, unconfined compressive strength (UCS) and compressibility along with the durability performance under the effect of different numbers of wetting and drying cycles. The mineralogical and microstructural changes within the treated soil and the new binder structures were identified for a better understanding of the improvements in the engineering performance of the stabilised soil. Based on the results presented in this research, the following key conclusions can be drawn:

- A novel cementitious binder was developed produced from completely cement-free blended waste materials (T+FGD). This binder can be used in soft soil stabilisation resulting in successful improvements in the engineering and geotechnical properties. This newly developed binder is eco-friendly; contributes significantly in reducing the negative environmental footprint of cement manufacturing and offers sustainable economic advantages. These findings satisfy the aim of this research and represent a novel contribution to knowledge in the field of soft soil stabilisation with the application of waste materials as cement-free binders.
- The unary optimisation revealed that 12% was the optimum percentage of WPSA which indicated the higher compressive strength (offered 3.4 times the compressive strength of the untreated soil after 28 days of curing). This percentage of WPSA contributed in decreasing the PI from 20.22 for the virgin soil to 13.45.
- Grinding activation was found effective to increase the fineness and pozzolanic reactivity of WPSA. A period of ten minutes was the optimum grinding time which contributed to increasing the UCS from 690kPa to 776kPa using 12% of ground WPSA (GU) at 28 days of curing. However, longer periods of grinding caused reductions in the compressive strengths of the treated soil due to the agglomeration that occurred in WPSA particles which affected its pozzolanic reactivity.

- The results of binary treatment revealed that the optimum binary mixture (BM2) was comprised of 9% WPSA + 3% POFA by the dry mass of the treated soil. This mixture contributed to decreasing the PI to 12.78 and increasing the UCS by 4.57 times the UCS of the untreated soil.
- The optimisation of the ternary blended binder indicated that the amorphous silica of RHA participated in the increase of UCS, especially when used with the same amount of POFA. The balance between the alkalinity of POFA and amorphous silica of RHA played an important role to accelerate the rate of silica dissolution and the reaction with the hydrated lime $\text{Ca}(\text{OH})_2$ of WPSA resulting in the formation of more cementitious gel.
- FGD gypsum significantly contributed to the development of the performance of the newly developed cementitious binder (T+FGD). All examined geotechnical properties of the stabilised soil were enhanced significantly after grinding activation with the aid of FGD.
- In some tests T+FGD exhibited results even better than those obtained from samples treated with OPC. For example, the lowest PI was achieved by using T+FGD which was 12.6; this value is less than the PI for the soil treated with OPC (14.1).
- The best performance was achieved from T+FGD which had a performance comparable to the OPC. The 3 days UCS was above 900kPa for the soil treated with T+FGD. This improvement can facilitate the provision of a strong enough soil base for labour and equipment at building sites within a very short time. At 180 days UCS developed interestingly to be equal to 1464kPa which exceeded that for the reference cement at the same age (1450kPa).
- It was shown experimentally that all promising mixtures impressively improved the soil compressibility. The performance of T+FGD was the most comparable to that of the reference cement indicating the higher stiffness and lowest compressibility amongst the other binders. T+FGD impressively improved the soil compressibility

and showed a comparable performance to the OPC. The Initial e , C_c , C_s and S_c were significantly decreased. For example, S_c decreased from 5.325mm to 1.418mm after 28 days of curing.

- For the effective stress of 400kPa, the coefficient of volume compressibility M_v was decreased from $0.305\text{m}^2/\text{MN}$ for the VS to $0.061\text{m}^2/\text{MN}$ for the soil treated with T+FGD which was close to that of the soil treated with OPC ($0.055\text{m}^2/\text{MN}$). By this reduction in M_v the stabilised soil was transformed from the zone of a high compressible soil to very low compressible soil according to the criteria of Tomlinson (2001).
- In terms of durability performance, the ternary blended binder activated by FGD (T+FGD) showed a durable performance close to that of OPC. Samples treated with T+FGD survived for the highest number of wetting-drying cycles; 9 cycles for the residual strength and volume changes and 12 cycles for the soil-binder mass loss testing.
- XRD, SEM and EDX analysis for the newly developed binder (T+FGD) confirmed the improvement gained in the mechanical and engineering properties of the stabilised soil. Different hydration products were observed to be formed with the time of curing such as ettringite, portlandite and C-S-H gel.

8.3 RECOMMENDATIONS

Despite the comprehensive research investigation that was conducted into the use of waste or by-product materials as sustainable binders in soft soil stabilisation, several possible future studies can be recommended as stated below:

1. Although it has been proven that T+FGD was a very successful binder for the stabilisation of Hightown soft soil in Liverpool, further studies should be carried out involving the use of this binder at different dosages for other problematic soils in the UK such as very fine sands, high organic and peat soils. Moreover, it is recommended that this study should be repeated using alternative soil types.

2. As it was highlighted in the limitations, not all the geotechnical properties of the stabilised soil have been covered in this study. Therefore, it is recommended to investigate the effect of the developed binder (T+FGD) on the other geotechnical properties of the stabilised soil such as the hydraulic conductivity, California bearing ratio (CBR) and the resilient modulus of elasticity.
3. It is recommended to study the concept of adding other supplementary cementitious materials (SCMs), for better pozzolanic activation of WPSA. Biomass fly ashes can be promising for developing sustainable and eco-friendly binders such as Bagasse ash, wood waste ash, bamboo leaf ash, etc.
4. Investigate using another alkali sulphate activator instead of FGD for one of the unary, binary and ternary mixtures developed in this study. Poultry litter fly ash is recommended as its chemical properties were reported as a natural sulphate alkaline activator in scientific articles.
5. A financial costs analysis should be conducted in terms of the production and transportation of waste materials from the developed binder prior to be introduced commercially. The embodied carbon should also be considered as an additional barrier.
6. There are worries regarding the potential for any contamination and pollution that may occur in local environment system and watercourses due to the reproduction of waste materials. Therefore, the leaching test is suggested to be carried out on the individual candidates and the different mixtures developed on this study. The aggregate test stated in BS EN 1744-3 (British Standard, 2002b) would be suitable as a method for leaching measurement.

REFERNCES

- Abd El-Aziz, M. A., Abo-Hashema, M. A. & El-Shourbagy, M. 2006. The effect of lime-silica fume stabilizer on engineering properties of clayey subgrade. *Fourth Monsoura International Engineering Conference (4th IEC)*. Faculty of Engineering University, Egypt.
- Ahmad, J., Abdul Rahman, A. S., Mohd Ali, M. R. & Abd. Rahman, K. F. 2011. Peat soil treatment using pofa. *IEEE Colloquium on Humanities, Science and Engineering Research*. Malaysia, Penang.
- Aitcin, P. C. 2016a. 3 - portland cement. *Science and technology of concrete admixtures*. Woodhead Publishing. Available: <http://www.sciencedirect.com/science/article/pii/B9780081006931000035>
- Aitcin, P. C. 2016b. 4 - supplementary cementitious materials and blended cements. *Science and technology of concrete admixtures*. Woodhead Publishing. Available: <http://www.sciencedirect.com/science/article/pii/B9780081006931000047>
- Al-Amoudi, O. S. B. 2002. Attack on plain and blended cements exposed to aggressive sulfate environments. *Cement and Concrete Composites*, 24, 305 - 316.
- Al-Hdabi, A., Al Nageim, H. & Seton, L. 2014. Superior cold rolled asphalt mixtures using supplementary cementations materials. *Construction and Building Materials*, 64, 95-102.
- Al-Rawas, A. A., Hago, A. W. & Al-Sarmi, H. 2005. Effect of lime, cement and sarooj (artificial pozzolan) on the swelling potential of an expansive soil from oman. *Building and Environment*, 40, 681-687.
- Aldahdooh, M. A. A., Muhamad Bunnori, N. & Megat Johari, M. A. 2013. Development of green ultra-high performance fiber reinforced concrete containing ultrafine palm oil fuel ash. *Construction and Building Materials*, 48, 379-389.
- Aldaood, A., Bouasker, M. & Al-Mukhtar, M. 2014. Impact of wetting–drying cycles on the microstructure and mechanical properties of lime-stabilized gypseous soils. *Engineering Geology*, 174, 11-21.
- Aldaood, A., Bouasker, M. & Al-Mukhtar, M. 2016. Effect of water during freeze–thaw cycles on the performance and durability of lime-treated gypseous soil. *Cold Regions Science and Technology*, 123, 155-163.
- Alex, J., Dhanalakshmi, J. & Ambedkar, B. 2016. Experimental investigation on rice husk ash as cement replacement on concrete production. *Construction and Building Materials*, 127, 353-362.
- Alrubaye, A. J., Hasan, M. & Fattah, M. Y. 2016. Stabilization of soft kaolin clay with silica fume and lime. *International Journal of Geotechnical Engineering*, 11, 90-96.
- Anderson, T. R., Hawkins, E. & Jones, P. D. 2016. Co₂, the greenhouse effect and global warming: From the pioneering work of arrhenius and callendar to today's earth system models. *Endeavour*.
- Aylesford Newsprint Mill Limited (ANML). 2015. *Secondary products › what are they?* [Online]. UK: Available: http://aylesford-newsprint.co.uk/what_are_secondary_products.php [Accessed: 28-01-2015].
- Antiohos, S. K., Papadakis, V. G., Chaniotakis, E. & Tsimas, S. 2007. Improving the performance of ternary blended cements by mixing different types of fly ashes. *Cement and Concrete Research*, 37, 877-885.
- Aprianti, E., Shafiqh, P., Bahri, S. & Farahani, J. N. 2015. Supplementary cementitious materials origin from agricultural wastes – a review. *Construction and Building Materials*, 74, 176-187.
- Arabani, M., Hagh, A. K., Mohammadzade Sani, A. & Kamboozia, N. 2012. Use of nanoclay for improvement the microstructure and mechanical properties of soil stabilized by cement. *4th International Conference on Nanostructures (ICNS4)*. Kish Island, I.R. Iran.

- Areprasert, C., Zhao, P., Ma, D., Shen, Y. & Yoshikawa, K. 2014. Alternative solid fuel production from paper sludge employing hydrothermal treatment. *Energy & Fuels*, 28, 1198-1206.
- Arena, W., Attanasio, A., Marseglia, A., Pascale, S., Ristatore, E., Rocco, B., Saracino, S. & Urbano, G. 2016. Geo-clustering-market availability and mapping of waste streams across the eu-27
- Arenas-Piedrahita, J. C., Montes-García, P., Mendoza-Rangel, J. M., López Calvo, H. Z., Valdez-Tamez, P. L. & Martínez-Reyes, J. 2016. Mechanical and durability properties of mortars prepared with untreated sugarcane bagasse ash and untreated fly ash. *Construction and Building Materials*, 105, 69-81.
- Ashango, A. A. & Patra, N. R. 2014. Static and cyclic properties of clay subgrade stabilised with rice husk ash and portland slag cement. *International Journal of Pavement Engineering*, 15, 906-916.
- ASTM, I. 1996. Standard test method for unconfined compressive strength of compacted soil-lime mixtures. *D 5102*. United States: ASTM International.
- ASTM International 2003. Standard test methods for wetting and drying compacted soil-cement mixtures. *D 559-03*. USA: ASTM International.
- Awal, A. S. M. A. & Shehu, I. A. 2013. Evaluation of heat of hydration of concrete containing high volume palm oil fuel ash. *Fuel*, 105, 728-731.
- Axelsson, K., Johansson, S.-E. & Andersson, R. 2002. Stabilization of organic soils by cement and pozzolanic reactions - feasibility study. Swedish Deep Stabilization Research Centre.
- Aydın, S., Karatay, Ç. & Baradan, B. 2010. The effect of grinding process on mechanical properties and alkali-silica reaction resistance of fly ash incorporated cement mortars. *Powder Technology*, 197, 68-72.
- Baghini, M. S., Ismail, A. & Bin Karim, M. R. 2015. Evaluation of cement-treated mixtures with slow setting bitumen emulsion as base course material for road pavements. *Construction and Building Materials*, 94, 323-336.
- Bahmani, S. H., Farzadnia, N., Asadi, A. & Huat, B. B. K. 2016. The effect of size and replacement content of nanosilica on strength development of cement treated residual soil. *Construction and Building Materials*, 118, 294-306.
- Bahmani, S. H., Huat, B. B. K., Asadi, A. & Farzadnia, N. 2014. Stabilization of residual soil using SiO_2 nanoparticles and cement. *Construction and Building Materials*, 64, 350-359.
- Baran, B., Ertürk, T., Sarıkaya, Y. & Alemdaroglu, T. 2001. Workability test method for metals applied to examine a workability measure (plastic limit) for clays. *Applied Clay Science*, 20, 53 - 63.
- Baščarević, Z. 2015. The resistance of alkali-activated cement-based binders to chemical attack. 373-396.
- Basha, E. A., Hashim, R., Mahmud, H. B. & Muntohar, A. S. 2005. Stabilization of residual soil with rice husk ash and cement. *Construction and Building Materials*, 19, 448-453.
- Beckman Coulter, Inc. 2009. *Meeting and exceeding the standard for laser diffraction particle size analysis: Ls 13 320 particle size analyzer* [Online]. USA: Available: <https://www.beckmancoulter.com/wsrportal/bibliography?docname=BR-9809B.pdf> [Accessed: 18-10-2016].
- Bergaya, F., Lagaly, G. & Vayer, M. 2013. Cation and anion exchange. 5, 333-359.
- Bhattacharja, S. & Bhatta, J. I. 2003. Comparative performance of portland cement and lime stabilization of moderate to high plasticity clay soils. USA: Portland Cement Association.
- Bhuria, N. R. & Sachan, A. 2014. Shear strength and constant rate of strain consolidation behaviour of cement-treated slurry-consolidated soft soil. *Current Science*, 106, 972 - 979.
- Black, L. 2016. Low clinker cement as a sustainable construction material. 415-457.
- Blanco, F., Garcia, M. P., Ayala, J., Mayoral, G. & Garcia, M. A. 2006. The effect of mechanically and chemically activated fly ashes on mortar properties. *Fuel*, 85, 2018-2026.
- Bowles, J. E. 1997. *Foundation analysis and design*, The McGraw-Hill Companies, Inc.

- British Geological survey 2005. Cement raw materials. United Kingdom: Natural Environment Research Council.
- British Standard 1998a. Bs 1377-2, methods of test for soils for civil engineering purposes - part 2: Classification tests. London: UK: British Standard Institution.
- British Standard 1998b. Bs 1377-5, methods of test for soils for civil engineering purposes — part 5: Compressibility, permeability and durability tests. London, UK: British Standard Institution.
- British Standard 1999a. Bs 1377-3, methods of test for soils for civil engineering purposes — part 3: Chemical and electro-chemical tests. London, UK: British Standard.
- British Standard 1999b. Bs 1377-7, methods of test for soils for civil engineering purposes - part 7: Shear strength tests (total stress). London: UK: British Standard Institute
- British Standard 1999c. Bs en 450:1995 - fly ash for concrete - definitions, requirements and quality control. London, UK: British Standard Institution.
- British Standard 2002a. Bs 1377-4, methods of test for soils for civil engineering purposes - part 4: Compaction-related tests. London: UK: British Standard Institute.
- British Standard 2002b. Bs en 1744-3- test for chemical properties of aggregates - part 3: Preparation of eluates by leaching of aggregates. London: UK: The European Standard EN.
- British Standard 2005. Bs iso 10390: Soil quality — determination of ph. London, UK: British Standard.
- Brooks, R. M. 2010. Soil stabilization with lime and rice husk ash. *International Journal of Applied Engineering Research*, 5, 1077–1086.
- BS-5930:2015, T. B. s. 2015. Code of practice for ground investigation. *Section 6: Description of soils and rocks*. The British Standards Institution.
- Budhu, M. 2011. *Soil mechanics and foundations*, United States of America, JOHN WILEY & SONS, INC.
- Bujulu, P. M. S., Sorta, A. R., Priol, G. & Emdal, A. J. 2007. Potential of wastepaper sludge ash to replace cement in deep stabilization of quick clay. *Annual Conference of the Transportation Association of Canada*. Saskatoon, Saskatchewan.
- Bunga, E., Saleh Pallu, H. M., Selintung, M. & Thaha, M. A. 2011. Stabilization of sandy clay loam with emulsified asphalt. *International Journal of Civil & Environmental Engineering*, 11, 52 - 58.
- Bushra, I. & Robinson, R. G. 2009. Consolidation behaviour of a cement stabilised marine soil. *Indian Geotechnical Society IGS, IGC 2009*, 431-434.
- Buttress, A. J. 2013. *Physicochemical behaviour of artificial lime stabilised sulfate bearing cohesive soils*. PhD, University of Nottingham.
- Calligaris, G. A., Franco, M. K. K. D., Aldrige, L. P., Rodrigues, M. S., Beraldo, A. L., Yokaichiya, F., Turrillas, X. & Cardoso, L. P. 2015. Assessing the pozzolanic activity of cements with added sugar cane straw ash by synchrotron x-ray diffraction and rietveld analysis. *Construction and Building Materials*, 98, 44-50.
- Cao, Z., Shen, L., Zhao, J., Liu, L., Zhong, S., Sun, Y. & Yang, Y. 2016. Toward a better practice for estimating the CO₂ emission factors of cement production: An experience from China. *Journal of Cleaner Production*, 139, 527-539.
- Cardell, C. & Guerra, I. 2016. An overview of emerging hyphenated SEM-EDX and Raman spectroscopy systems: Applications in life, environmental and materials sciences. *TrAC Trends in Analytical Chemistry*, 77, 156-166.
- CEM-Bureau. 2015. *Key fact & figures* [Online]. The European Cement Association. Available: <http://www.cembureau.be/about-cement/key-facts-figures> [Accessed 19-08-2016].
- CEMBUREAU 2009. Co-processing of alternative fuels and raw materials in the European cement industry. *Sustainable Cement Production* Brussels, Belgium: The European Cement Association.

- Chaibeddra, S. & Kharchi, F. 2014. Study of sulphate attack on earth stabilized blocks. *International Journal of Application or Innovation in Engineering & Management*, 3, 184 - 187.
- Chen, H. & Wang, Q. 2006. The behaviour of organic matter in the process of soft soil stabilization using cement. *Bulletin of Engineering Geology and the Environment*, 65, 445-448.
- Cheshomi, A., Eshaghi, A. & Hassanpour, J. 2017. Effect of lime and fly ash on swelling percentage and atterberg limits of sulfate-bearing clay. *Applied Clay Science*, 135, 190-198.
- Chindaprasirt, P., Sinsiri, T., Kroehong, W. & Jaturapitakkul, C. 2014. Role of filler effect and pozzolanic reaction of biomass ashes on hydrated phase and pore size distribution of blended cement paste. *Journal of Materials in Civil Engineering*, 26, 04014057.
- Choobasti, A. J., Ghodrat, H., Vahdatirad, M. J., Firouzian, S., Barari, A., Torabi, M. & Bagherian, A. 2010. Influence of using rice husk ash in soil stabilization method with lime. *Frontiers of Earth Science in China*, 4, 471-480.
- Consoli, N. C., Winter, D., Rilho, A. S., Festugato, L. & Teixeira, B. d. S. 2015. A testing procedure for predicting strength in artificially cemented soft soils. *Engineering Geology*, 195, 327-334.
- Corinaldesi, V., Fava, G. & Ruello, M. L. 2010. Paper mill sludge ash as supplementary cementitious material. *Second International Conference on Sustainable Construction Materials and Technologies*. University of Politecnica delle Marche, Ancona, Italy.
- Correia, A. A. S., Venda, O. P. J. & Lemos, L. J. L. 2013. Prediction of the unconfined compressive strength in soft soil chemically stabilized. *18th International Conference on Soil Mechanics and Geotechnical Engineering*. Paris.
- Cristelo, N., Glendinning, S., Fernandes, L. & Pinto, A. T. 2013. Effects of alkaline-activated fly ash and portland cement on soft soil stabilisation. *Acta Geotechnica*, 8, 395-405.
- Croft, J. B. 1967. The influence of soil mineralogical composition on cement stabilization. *Geotechnique*, 17, 119 - 135.
- Dang, L. C., Fatahi, B. & Khabbaz, H. 2016. Behaviour of expansive soils stabilized with hydrated lime and bagasse fibres. *Procedia Engineering*, 143, 658-665.
- Daoudi, L., Knidiri, A., El Boudour El Idrissi, H., Rhouta, B. & Fagel, N. 2015. Role of the texture of fibrous clay minerals in the plasticity behavior of host materials (plateau du kik, western high atlas, morocco). *Applied Clay Science*, 118, 283-289.
- Das, B. M. 2010. *Principles of geotechnical engineering*, United States of America, CENGAGE Learning.
- Dave, N., Misra, A. K., Srivastava, A. & Kaushik, S. K. 2016. Experimental analysis of strength and durability properties of quaternary cement binder and mortar. *Construction and Building Materials*, 107, 117-124.
- Della, V. P., Ku'hn, I. & Hotza, D. 2002. Rice husk ash as an alternate source for active silica production. *Materials Letters*, 57, 818 - 821.
- Dhanao, N. S. 2013. *Effect of soil stabilizers on the structural design of flexible pavements*. MSc, Thapar University.
- Diego, M. E., Arias, B. & Abanades, J. C. 2016. Analysis of a double calcium loop process configuration for co2 capture in cement plants. *Journal of Cleaner Production*, 117, 110-121.
- Dri, M., Sanna, A. & Maroto-Valer, M. M. 2014. Mineral carbonation from metal wastes: Effect of solid to liquid ratio on the efficiency and characterization of carbonated products. *Applied Energy*, 113, 515-523.
- Dunster, A. M. 2007. Paper sludge and paper sludge ash in portland cement manufacture. UK: University of Leeds.
- Duxson, P., Fernández-Jiménez, A., Provis, J. L., Lukey, G. C., Palomo, A. & van Deventer, J. S. J. 2006. Geopolymer technology: The current state of the art. *Journal of Materials Science*, 42, 2917-2933.

- Edeh, J. E., Agbede, I. O. & Tyoyila, A. 2014. Evaluation of sawdust ash–stabilized lateritic soil as highway pavement material. *Journal of Materials in Civil Engineering*, 26, 367 - 373.
- Edina Geology Digimap. 2017. *Maps & geospatial data for uk academia - geology roam* [Online]. UK: British Geological Survey - Natural Environment Research Council (NERC). Available: <http://digimap.edina.ac.uk/> [Accessed 10-10 2017].
- Eskisar, T. 2015. Influence of cement treatment on unconfined compressive strength and compressibility of lean clay with medium plasticity. *Arabian Journal for Science and Engineering*, 40, 763-772.
- Eskişar, T., Altun, S. & Kalıpcılar, İ. 2015. Assessment of strength development and freeze–thaw performance of cement treated clays at different water contents. *Cold Regions Science and Technology*, 111, 50-59.
- Estabragh, A. R., Moghadas, M. & Javadi, A. A. 2013. Effect of different types of wetting fluids on the behaviour of expansive soil during wetting and drying. *Soils and Foundations*, 53, 617-627.
- European Committee for Standardisation 2004. Bs en 197-1:2000, cement —part 1: Composition, specifications and conformity criteria for common cements. London: UK: British Standard Institution.
- European Committee for Standardization 2012. Bs en 450-1: Fly ash for concrete - part 1: Definition, specifications and conformity criteria. London, UK: British Standard Institution.
- European Committee for Standardization 2013. Bs en iso 14688-2:2004+a2013. Geotechnical investigation and testing - identification and classification of soil, part 2: Principles for a classification. London: UK: British Standard Institution.
- European Committee for Standardization 2014a. Bs en 17892-4. Geotechnical investigation and testing - laboratory testing of soil, part 4: Determination of particle size distribution. London, UK: British Standard Institution.
- European Committee for Standardization 2014b. Bs en iso 11508:2014. Soil quality-determination of particle density. London, UK: British Standard Institution.
- European Committee for Standardization 2014c. Bs en iso 17892-1. Geotechnical investigation and testing - laboratory testing of soil, part 1: Determination of water content. London, UK: British Standard Institution.
- EuroSoilStab 2002. Development of design and construction methods to stabilise soft organic soils: Design guide soft soil stabilisation: Ct97-0351. Project no.: Be 96-3177.
- Farouk, A. & Shahien, M. M. 2013. Ground improvement using soil–cement columns: Experimental investigation. *Alexandria Engineering Journal*, 52, 733-740.
- Fattah, M. Y., Al-Saidi, A. a. A. & Jaber, M. M. 2014. Consolidation properties of compacted soft soil stabilized with lime-silica fume mix. *International Journal of Scientific & Engineering Research*, 5, 1675 - 1682.
- Faubert, P., Barnabé, S., Bouchard, S., Côté, R. & Villeneuve, C. 2016. Pulp and paper mill sludge management practices: What are the challenges to assess the impacts on greenhouse gas emissions? *Resources, Conservation and Recycling*, 108, 107-133.
- Fava, G., Ruello, M. L. & Corinaldesi, V. 2011. Paper mill sludge ash as supplementary cementitious material. *Journal of Materials in Civil Engineering*, 23, 772-776.
- Frías, M., García, R., Vigil, R. & Ferreiro, S. 2008. Calcination of art paper sludge waste for the use as a supplementary cementing material. *Applied Clay Science*, 42, 189-193.
- Fujita, Y. & Kobayashi, M. 2016. Transport of colloidal silica in unsaturated sand: Effect of charging properties of sand and silica particles. *Chemosphere*, 154, 179-86.
- Gadpalliwar, S. K., Deotale, R. S. & Narde, A. R. 2014. To study the partial replacement of cement by ggbs & rha and natural sand by quarry sand in concrete. *Journal of Mechanical and Civil Engineering*, 11, 69-77.
- Ganesan, K., Rajagopal, K. & Thangavel, K. 2008. Rice husk ash blended cement: Assessment of optimal level of replacement for strength and permeability properties of concrete. *Construction and Building Materials*, 22, 1675-1683.

- García-Gusano, D., Garraín, D., Herrera, I., Cabal, H. & Lechón, Y. 2015. Life cycle assessment of applying co₂ post-combustion capture to the spanish cement production. *Journal of Cleaner Production*, 104, 328-338.
- Gartner, E., Maruyama, I. & Chen, J. 2017. A new model for the c-s-h phase formed during the hydration of portland cements. *Cement and Concrete Research*, 97, 95-106.
- Garzón, E., Cano, M., O'Kelly, B. C. & Sánchez-Soto, P. J. 2016. Effect of lime on stabilization of phyllite clays. *Applied Clay Science*, 123, 329-334.
- Gluth, G. J. G., Lehmann, C., Rübner, K. & Kühne, H.-C. 2014. Reaction products and strength development of wastepaper sludge ash and the influence of alkalis. *Cement and Concrete Composites*, 45, 82-88.
- Goodarzi, A. R., Akbari, H. R. & Salimi, M. 2016. Enhanced stabilization of highly expansive clays by mixing cement and silica fume. *Applied Clay Science*.
- Goodarzi, A. R. & Salimi, M. 2015. Stabilization treatment of a dispersive clayey soil using granulated blast furnace slag and basic oxygen furnace slag. *Applied Clay Science*, 108, 61-69.
- Gourley, C. S. & Greening, P. A. K. 1999. Performance of chemically stabilized roadbase: Results and recommendations from studies in southern africa. Berkshire, United Kingdom: Transport Research Laboratory.
- Guney, Y., Sari, D., Cetin, M. & Tuncan, M. 2007. Impact of cyclic wetting–drying on swelling behavior of lime-stabilized soil. *Building and Environment*, 42, 681-688.
- Gutt, W. H. & Smith, M. A. 1976. Aspects of waste materials and their potential for use in concrete. *Resource Recovery and Conservation*, 1, 345 - 367.
- Habert, G. 2013. Environmental impact of portland cement production. 3-25.
- Habert, G. 2014. Assessing the environmental impact of conventional and 'green' cement production. 199-238.
- Hanson. 2016. *Regen ggbs* [Online]. Available: <http://www.hanson.co.uk/en/products/regen-ggbs> [Accessed 10-10-2016 2016].
- Harbec, D., Tagnit-Hamou, A. & Gitzhofer, F. 2016. Waste-glass fume synthesized using plasma spheroidization technology: Reactivity in cement pastes and mortars. *Construction and Building Materials*, 107, 272-286.
- Harichane, K., Ghrici, M. & Kenai, S. 2011. Effect of curing time on shear strength of cohesive soils stabilized with combination of lime and natural pozzolana. *International Journal of Civil Engineering*, 9, 90 - 96.
- Hartemink, A. E. 2015. The use of soil classification in journal papers between 1975 and 2014. *Geoderma Regional*, 5, 127-139.
- Hashad, A. & El-Mashad, M. 2014. Assessment of soil mixing with cement kiln dust to reduce soil lateral pressure compared to other soil improvement methods. *HBRC Journal*, 10, 169-175.
- Hassan, M. M. 2009. *Engineering characteristics of cement stabilized soft finnish clay - a laboratory study*. licentiate, Helsinki Uneversity of Technology.
- Heravi, G., Nafisi, T. & Mousavi, R. 2016. Evaluation of energy consumption during production and construction of concrete and steel frames of residential buildings. *Energy and Buildings*, 130, 244-252.
- Hermawan, Marzuki, P. F., Abduh, M. & Driejana, R. 2015. Identification of source factors of carbon dioxide (co₂) emissions in concreting of reinforced concrete. *Procedia Engineering*, 125, 692-698.
- HIE 2015. Sustainable construction policy and plan. Scotland, UK: Highlands and Islands Enterprise.
- Higgins, D. D. 2005. Soil stabilisation with ground granulated blastfurnace slag. UK: UK Cementitious Slag Makers Association (CSMA).
- Horpibulsuk, S., Phetchuay, C. & Chinkulkijniwat, A. 2012. Soil stabilization by calcium carbide residue and fly ash. *Journal of Materials in Civil Engineering*, 24, 184-193.

- Horpibulsuk, S., Phetchuay, C., Chinkulkijniwat, A. & Cholaphatsorn, A. 2013. Strength development in silty clay stabilized with calcium carbide residue and fly ash. *Soils and Foundations*, 53, 477-486.
- Horpibulsuk, S., Rachan, R., Chinkulkijniwat, A., Raksachon, Y. & Suddeepong, A. 2010. Analysis of strength development in cement-stabilized silty clay from microstructural considerations. *Construction and Building Materials*, 24, 2011-2021.
- Horsley, C., Emmert, M. H. & Sakulich, A. 2016. Influence of alternative fuels on trace element content of ordinary portland cement. *Fuel*, 184, 481-489.
- Huang, L.-M., Zhang, X.-H., Shao, M.-A., Rossiter, D. & Zhang, G.-L. 2016. Pedogenesis significantly decreases the stability of water-dispersible soil colloids in a humid tropical region. *Geoderma*, 274, 45-53.
- Huat, B. B. K., Alias, A. & Abdul Aziz, A. 2008. Evaluation, selection and assessment of guidelines for chemical stabilization of tropical residual soils. *American Journal of Environmental Sciences*, 4, 303 - 309.
- Huntzinger, D. N. & Eatmon, T. D. 2009. A life-cycle assessment of portland cement manufacturing: Comparing the traditional process with alternative technologies. *Journal of Cleaner Production*, 17, 668-675.
- Hwang, C.-L. & Huynh, T.-P. 2015. Effect of alkali-activator and rice husk ash content on strength development of fly ash and residual rice husk ash-based geopolymers. *Construction and Building Materials*, 101, 1-9.
- Igwe, C. A., Akamigbo, F. O. R. & Mbagwu, J. S. C. 1999. Chemical and mineralogical properties of soils in southeastern Nigeria in relation to aggregate stability. *Geoderma*, 92, 111 - 123.
- Indraratna, B., Balasubramaniam, A. S. & Khan, M. J. 1995. Effect of fly ash with lime and cement on the behaviour of a soft clay. *Quarterly Journal of Engineering Geology*, 28, 131-142.
- Ingles, O. G. & Metcalf, J. B. 1972. *Soil stabilization, principles and practice*, Sydney : Butterworths.
- Iranpour, B. & Haddad, A. 2016. The influence of nanomaterials on collapsible soil treatment. *Engineering Geology*, 205, 40-53.
- Ismadji, S., Soetaredjo, F. E. & Ayucitra, A. 2015. Natural clay minerals as environmental cleaning agents. *Clay materials for environmental remediation*. Cham: Springer International Publishing. Available: https://doi.org/10.1007/978-3-319-16712-1_2
- Jafer, H. M., Hashim, K. S., Atherton, W. & Alattabi, A. W. 2016. A statistical model for the geotechnical parameters of cement-stabilised hightown's soft soil: A case study of Liverpool, UK. *International Journal of Civil, Environmental, Structural, Construction and Architectural Engineering*, 10, 892 - 897.
- James, J. & Pandian, P. K. 2016. Industrial wastes as auxiliary additives to cement/lime stabilization of soils. *Advances in Civil Engineering*, 2016, 1-17.
- James, J. & Sivakumar, V. 2014. Effect of lime on the index properties of rice husk ash stabilized soil. *International Journal of Applied Engineering Research*, 9, 4263-4272.
- Jaturapitakkul, C., Tangpagasit, J., Songmue, S. & Kiattikomol, K. 2011. Filler effect and pozzolanic reaction of ground palm oil fuel ash. *Construction and Building Materials*, 25, 4287-4293.
- Jaubertie, R., Rendell, F., Rangeard, D. & Molez, L. 2010. Stabilisation of estuarine silt with lime and/or cement. *Applied Clay Science*, 50, 395-400.
- Jefferson, I., Rogers, C., Evststiev, D. & Karastanev, D. 2015. Improvement of collapsible loess in eastern Europe. 215-261.
- Jha, A. K. & Sivapullaiah, P. V. 2015. Mechanism of improvement in the strength and volume change behavior of lime stabilized soil. *Engineering Geology*, 198, 53-64.
- Jha, A. K. & Sivapullaiah, P. V. 2016. Volume change behavior of lime treated gypseous soil — influence of mineralogy and microstructure. *Applied Clay Science*, 119, 202-212.

- Jiang, J., Lu, Z., Niu, Y., Li, J. & Zhang, Y. 2016. Investigation of the properties of high-porosity cement foams based on ternary portland cement–metakaolin–silica fume blends. *Construction and Building Materials*, 107, 181-190.
- Johnes, L. D. & Jefferson, I. 2012. Expansive soils. In: BURLAND, J. (ed.) *Ice manual of geotechnical engineering*. London, UK.
- Jones, M., McCarthy, A. & Booth, A. 2006. Characteristics of the ultrafine component of fly ash. *Fuel*, 85, 2250-2259.
- Juhász, Z. & Opoczky, L. 1990. *Mechanical activation of minerals by grinding : Pulverizing and morphology of particles* Akadémiai Kiadó.
- Kalkan, E. 2013. Preparation of scrap tire rubber fiber–silica fume mixtures for modification of clayey soils. *Applied Clay Science*, 80-81, 117-125.
- Kamruzzaman, A. H. M. 2002. *Physico-chemical and engineering behaviour of cement treated singapore marine clay*. PhD, National University of Singapore.
- Kanadasan, J., Fauzi, A., Razak, H., Selliah, P., Subramaniam, V. & Yusoff, S. 2015. Feasibility studies of palm oil mill waste aggregates for the construction industry. *Materials*, 8, 6508-6530.
- Kang, G., Tsuchida, T. & Athapaththu, A. M. R. G. 2016. Engineering behavior of cement-treated marine dredged clay during early and later stages of curing. *Engineering Geology*, 209, 163-174.
- Karim, M. R., Zain, M. F. M., Jamil, M. & Lai, F. C. 2013. Fabrication of a non-cement binder using slag, palm oil fuel ash and rice husk ash with sodium hydroxide. *Construction and Building Materials*, 49, 894-902.
- Karin Axelsson, Sven-Erik Johansson & Andersson, R. 2002. Stabilisation of organic soils by cement and puzzolanic reactions - feasibility study. Sweden: Swedish Deep Stabilization Research Centre - Swedish Geotechnical Institute.
- Khalid, N., Arshad, M. F., Mukri, M., Kamarudin, F. & Ghani, A. H. A. 2014. The california bearing ratio (cbr) value for banting soft soil subgrade stabilized using lime-pofa mixtures. *EJGE*, 19, 155 - 163.
- Khalid, N., Mukri, M., Kamarudin, F., Sidek, N. & Arshad, M. F. 2013. Experimental studies on fibrous peat stabilized using waste paper sludge ash (wpsa). *Electronic Journal of Geotechnical Engineering open access (EJGE)*, 13, 1613 - 1621.
- Khatib, J. M., Wright, L. & Mangat, P. S. 2013. Effect of fly ash–gypsum blend on porosity and pore size distribution of cement pastes. *Advances in Applied Ceramics*, 112, 197-201.
- Kinuthia, J. M. 2016. Unfired clay materials and construction.
- Knappett, J. A. & Craig, R. F. 2012. *Craig's soil mechanics*, London and New York, Spon Press
- Kolias, S., Kasselouri-Rigopoulou, V. & Karahalios, A. 2005. Stabilisation of clayey soils with high calcium fly ash and cement. *Cement and Concrete Composites*, 27, 301-313.
- Kumar, A., Walia, B. S. & Bajaj, A. 2007. Influence of fly ash, lime, and polyester fibers on compaction and strength properties of expansive soil. *JOURNAL OF MATERIALS IN CIVIL ENGINEERING*, 19, 242–248.
- Kumar, S., Kumar, R., Bandopadhyay, A., Alex, T. C., Ravi Kumar, B., Das, S. K. & Mehrotra, S. P. 2008. Mechanical activation of granulated blast furnace slag and its effect on the properties and structure of portland slag cement. *Cement and Concrete Composites*, 30, 679-685.
- Li, P., Vanapalli, S. & Li, T. 2016. Review of collapse triggering mechanism of collapsible soils due to wetting. *Journal of Rock Mechanics and Geotechnical Engineering*, 8, 256-274.
- Li, Q., Chen, J., Shi, Q. & Zhao, S. 2014. Macroscopic and microscopic mechanisms of cement-stabilized soft clay mixed with seawater by adding ultrafine silica fume. *Advances in Materials Science and Engineering*, 2014, 1-12.
- Lin, D.-F., Lin, K.-L. & Luo, H.-L. 2007. A comparison between sludge ash and fly ash on the improvement in soft soil. *Air & Waste Management Association*, 57, 59-64.

- Lisbona, A., Vegas, I., Ainchil, J. & Ríos, C. 2012. Soil stabilization with calcined paper sludge: Laboratory and field tests. *Journal of Materials in Civil Engineering*, 24, 666-673.
- Little, D. N. & Nair, S. 2009. Recommended practice for stabilization of subgrade soils and base materials. Texas A&M University, College Station, Texas: Texas Transportation Institute.
- Liu, Z., Wang, Z., Yuan, M. Z. & Yu, H. B. 2015. Thermal efficiency modelling of the cement clinker manufacturing process. *Journal of the Energy Institute*, 88, 76-86.
- López-Querol, S., Peco, J. & Arias-Trujillo, J. 2014. Numerical modeling on vibroflotation soil improvement techniques using a densification constitutive law. *Soil Dynamics and Earthquake Engineering*, 65, 1-10.
- Ma, C., Chen, B. & Chen, L. 2016. Effect of organic matter on strength development of self-compacting earth-based construction stabilized with cement-based composites. *Construction and Building Materials*, 123, 414-423.
- Majeed, Z. H. 2014. *Treatment and improvement of the geotechnical properties of soft soils using nanomaterials*. DOCTOR OF PHILOSOPHY, UNIVERSITY KEBANGSAAN MALAYSIA.
- Makusa, G. P. 2012. Soil stabilization methods and materials in engineering practice. Luleå, Sweden: Luleå University of Technology.
- Malagavelli, V. & Rao, P. N. 2010. High performance concrete with ggbs and robo sand. *International Journal of Engineering Science and Technology*, 2, 5107-5113.
- Malhotra, V. M. & Mehta, P. K. 2012. *High-performance, high-volume fly ash concrete for building durable and sustainable structures*, Ottawa, Canada., Supplementary Cementing Materials for Sustainable Development Inc.
- Marchon, D. & Flatt, R. J. 2016a. 8 - mechanisms of cement hydration. *Science and technology of concrete admixtures*. Woodhead Publishing. Available: <http://www.sciencedirect.com/science/article/pii/B9780081006931000084>
- Marchon, D. & Flatt, R. J. 2016b. Mechanisms of cement hydration. 129-145.
- Marsland, T. & Whiteley, B. 2015. Rapid evidence assessment: Paper sludge ash. In: AGENCY, E. (ed.). Bristol, UK: Environment Agency, Horizon House.
- Martinez-Lage, I., Velay-Lizancos, M., Vazquez-Burgo, P., Rivas-Fernandez, M., Vazquez-Herrero, C., Ramirez-Rodriguez, A. & Martin-Cano, M. 2016. Concretes and mortars with waste paper industry: Biomass ash and dregs. *J Environ Manage*, 181, 863-73.
- Marto, A., Hasan, M., Hyodo, M. & Makhtar, A. M. 2014. Shear strength parameters and consolidation of clay reinforced with single and group bottom ash columns. *Arabian Journal for Science and Engineering*, 39, 2641-2654.
- Matakhah, F., Soroushian, P., Ul Abideen, S. & Peyvandi, A. 2016. Use of non-wood biomass combustion ash in development of alkali-activated concrete. *Construction and Building Materials*, 121, 491-500.
- McPhee, C., Reed, J. & Zubizarreta, I. 2015. Core sample preparation. 64, 135-179.
- Mikulčić, H., Cabezas, H., Vujanović, M. & Duić, N. 2016. Environmental assessment of different cement manufacturing processes based on energy and ecological footprint analysis. *Journal of Cleaner Production*, 130, 213-221.
- Mitchell, J. K. & Soga, K. 2005. *Fundamentals of soil behavior*, Canada, John Wiley and Sons.
- Miura, N., Horpibulsuk, S. & Nagaraj, T. S. 2001. Engineering behavior of cement stabilized clay at high water content. *Soils and Foundations*, 41, 33-45.
- Modarres, A. & Nosoudy, Y. M. 2015. Clay stabilization using coal waste and lime — technical and environmental impacts. *Applied Clay Science*, 116-117, 281-288.
- Moghal, A. A. B., Kareem Obaid, A. A., Al-Refeai, T. O. & Al-Shamrani, M. A. 2015. Compressibility and durability characteristics of lime treated expansive semiarid soils. *Journal of Testing and Evaluation*, 43, 20140060.
- Monte, M. C., Fuente, E., Blanco, A. & Negro, C. 2009. Waste management from pulp and paper production in the european union. *Waste Manag*, 29, 293-308.

- Montgomery, D. E. 1998. How does cement stabilisation work? *Stabilised Soil Research Progress Report SSRPR2*. Coventry, UK: Development Technology Unit, School of Engineering - University of Warwick.
- Morandea, A., Thiéry, M. & Dangla, P. 2014. Investigation of the carbonation mechanism of ch and c-s-h in terms of kinetics, microstructure changes and moisture properties. *Cement and Concrete Research*, 56, 153-170.
- Merchant Research & consulting ltd (MR&CL). 2013. *World production structure, by country, 2012* [Online]. Available: <https://mcgroup.co.uk/> [Accessed: 19-01-2015].
- Mu'azu, M. A. 2007. Evaluation of plasticity and particle size distribution characteristics of bagasse ash on cement treated lateritic soil. *Leonardo Journal of Sciences*, 10, 137 - 152.
- Muhunthan, B. & Sariosseiri, F. 2008. Interpretation of geotechnical properties of cement treated soils. Washington State University Department of Civil & Environmental Engineering.
- Murthy, V. N. S. 2003. *Geotechnical engineering : Principles and practices of soil mechanics and foundation engineering* New York, Marcel Dekker.
- Neramitkornburi, A., Horpibulsuk, S., Shen, S. L., Chinkulkijniwat, A., Arulrajah, A. & Disfani, M. M. 2015. Durability against wetting–drying cycles of sustainable lightweight cellular cemented construction material comprising clay and fly ash wastes. *Construction and Building Materials*, 77, 41-49.
- National Environmental Research Council - NERC. 2017. *Viw maps - geology of britain* [Online]. UK: Available: <http://www.bgs.ac.uk/data/mapViewers/home.html?src=topNav> [Accessed: 10-10-2017].
- Nicholson, P. G. 2015. Chapter 11 - admixture soil improvement. *Soil improvement and ground modification methods*. Boston: Butterworth-Heinemann. Available: <http://www.sciencedirect.com/science/article/pii/B978012408076800011X>
- O'Flaherty, C. A. 2002. Soil-stabilized pavements. *Highways the location, design, construction and maintenance of road pavements*. Fourth Edition ed.: Taylor & Francis
- O'Rourke, B., McNally, C. & Richardson, M. G. 2009. Development of calcium sulfate–ggbS–portland cement binders. *Construction and Building Materials*, 23, 340-346.
- Okyay, U. S. & Dias, D. 2010. Use of lime and cement treated soils as pile supported load transfer platform. *Engineering Geology*, 114, 34-44.
- Ola, S. A. 1978. Geotechnical properties and behaviour of some stabilized nigerian lateritic soils. *Q. JI Engng Geol.*, 11, 145 - 160.
- Önal, O. 2014. Lime stabilization of soils underlying a salt evaporation pond: A laboratory study. *Marine Georesources & Geotechnology*, 33, 391-402.
- Ornek, M., Laman, M., Demir, A. & Yildiz, A. 2012. Prediction of bearing capacity of circular footings on soft clay stabilized with granular soil. *Soils and Foundations*, 52, 69-80.
- Ouf, M. E.-S. A. R. 2001. *Stabilisation of clay subgrades soils using ground granulated blastfurnace slag*. Ph.D., University of Leeds.
- Ouhadi, V. R., Yong, R. N., Amiri, M. & Ouhadi, M. H. 2014. Pozzolanic consolidation of stabilized soft clays. *Applied Clay Science*, 95, 111-118.
- Oyediran, I. A. & Kalejaiye, M. 2011. Effect of increasing cement content on strength and compaction parameters of some lateritic soils from southwestern nigeria. *EJGE*, 16, 1501 - 1514.
- Pacheco-Torgal, F., Abdollahnejad, Z., Camões, A. F., Jamshidi, M. & Ding, Y. 2012. Durability of alkali-activated binders: A clear advantage over portland cement or an unproven issue? *Construction and Building Materials*, 30, 400-405.
- Pakbaz, M. S. & Alipour, R. 2012. Influence of cement addition on the geotechnical properties of an iranian clay. *Applied Clay Science*, 67-68, 1-4.
- Peethamparan, S., Olek, J. & Lovell, J. 2008. Influence of chemical and physical characteristics of cement kiln dusts (ckds) on their hydration behavior and potential suitability for soil stabilization. *Cement and Concrete Research*, 38, 803-815.

- Pontikes, Y. & Snellings, R. 2014. Cementitious binders incorporating residues. 219-229.
- Pourakbar, S., Asadi, A., Huat, B. B. K. & Fasihnikoutalab, M. H. 2015. Stabilization of clayey soil using ultrafine palm oil fuel ash (pofa) and cement. *Transportation Geotechnics*, 3, 24-35.
- Prabakar, J. & Sridhar, R. S. 2002. Effect of random inclusion of sisal fibre on strength behaviour of soil. *Construction and Building Materials*, 16, 123 - 131.
- Provis, J. L., Palomo, A. & Shi, C. 2015. Advances in understanding alkali-activated materials. *Cement and Concrete Research*, 78, 110-125.
- Puppala, A. J., Pedarla, A. & Bheemasetti, T. 2015. Soil modification by admixtures. 291-309.
- Pustovgar, E., D'Espinose, J.-B., Palacios, M., Andreev, A., Mishra, R. & Flatt, R. J. 2016. Impact of aluminates on silicates hydration. *II international Conference on Concrete Sustainability ICCS16, Barcelona, Spain*. Madrid, Spain: International Center for Numerical Methods in Engineering (CIMNE).
- Qiao, X. C., Poon, C. S. & Cheeseman, C. 2006. Use of flue gas desulphurisation (fgd) waste and rejected fly ash in waste stabilization/solidification systems. *Waste Manag*, 26, 141-9.
- Rahman, A., Rasul, M. G., Khan, M. M. K. & Sharma, S. 2015. Recent development on the uses of alternative fuels in cement manufacturing process. *Fuel*, 145, 84-99.
- Rahmat, M. N. & Kinuthia, J. M. 2011. Effects of mellowing sulfate-bearing clay soil stabilized with wastepaper sludge ash for road construction. *Engineering Geology*, 117, 170-179.
- Ramachandran, V. S. & Beaudoin, J. J. 2001. *Handbook of analytical techniques in concrete science and technology: Principles, techniques, and applications*, Ottawa, Ontario, Canada, Noyes Publications / William Andrew Publishing.
- Ranjbar, N., Mehrali, M., Behnia, A., Alengaram, U. J. & Jumaat, M. Z. 2014. Compressive strength and microstructural analysis of fly ash/palm oil fuel ash based geopolymer mortar. *Materials & Design*, 59, 532-539.
- Reeves, G. M., Sims, I. & Cripps, J. C. 2006. Clay materials used in construction. Geological society engineering geology special publication.
- Rêgo, J. H. S., Nepomuceno, A. A., Figueiredo, E. P. & Hasparyk, N. P. 2015. Microstructure of cement pastes with residual rice husk ash of low amorphous silica content. *Construction and Building Materials*, 80, 56-68.
- Rezaei, M., Ajalloeian, R. & Ghafoori, M. 2012. Geotechnical properties of problematic soils emphasis on collapsible cases. *International Journal of Geosciences*, 03, 105-110.
- Rice Husk Ash. 2008. *About rice husk ash* [Online]. Available: <http://www.ricehuskash.com/product.htm> [Accessed 29-01-2015 2015].
- Rios, S., Cristelo, N., Viana da Fonseca, A. & Ferreira, C. 2016. Structural performance of alkali-activated soil ash versus soil cement. *Journal of Materials in Civil Engineering*, 28, 04015125.
- Rollings, M. P. 1999. Sulfate attack on cement-stabilized sand. *Journal of Geotechnical and Geoenvironmental Engineering*, 125, 364-372.
- Rossen, J. E. & Scrivener, K. L. 2017. Optimization of sem-eds to determine the c-a-s-h composition in matured cement paste samples. *Materials Characterization*, 123, 294-306.
- Roy, T. K. 2013. Evaluation of strength of clayey soil by usc test with addition of rice husk ash and lime. *the 7th International Conference on Case Histories Geotechnical Engineering*. Chicago, USA: Missouri University of Science and Technology.
- Rozière, E., Loukili, A., El Hachem, R. & Grondin, F. 2009. Durability of concrete exposed to leaching and external sulphate attacks. *Cement and Concrete Research*, 39, 1188-1198.
- Sadique, M. & Al-Nageim, H. 2012. Hydration kinetics of a low carbon cementitious material produced by physico-chemical activation of high calcium fly ash. *Journal of Advanced Concrete Technology*, 10, 254-263.
- Sadique, M., Al-Nageim, H., Atherton, W., Seton, L. & Dempster, N. 2012a. A laboratory study for full cement replacement by fly ash and silica fume. *Magazine of Concrete Research*, 64, 1135-1142.

- Sadique, M., Al-Nageim, H., Atherton, W., Seton, L. & Dempster, N. 2013. Mechano-chemical activation of high-ca fly ash by cement free blending and gypsum aided grinding. *Construction and Building Materials*, 43, 480-489.
- Sadique, M., Al Nageim, H., Atherton, W., Seton, L. & Dempster, N. 2012b. A new composite cementitious material for construction. *Construction and Building Materials*, 35, 846-855.
- Salas, A., Delvasto, S., de Gutierrez, R. M. & Lange, D. 2009. Comparison of two processes for treating rice husk ash for use in high performance concrete. *Cement and Concrete Research*, 39, 773-778.
- Sanjuán, M. Á., Argiz, C., Gálvez, J. C. & Moragues, A. 2015. Effect of silica fume fineness on the improvement of portland cement strength performance. *Construction and Building Materials*, 96, 55-64.
- Sargent, P. 2015. The development of alkali-activated mixtures for soil stabilisation. 555-604.
- Sargent, P., Hughes, P. N., Rouainia, M. & White, M. L. 2013. The use of alkali activated waste binders in enhancing the mechanical properties and durability of soft alluvial soils. *Engineering Geology*, 152, 96-108.
- Saride, S., Puppala, A. J. & Chikyala, S. R. 2013. Swell-shrink and strength behaviors of lime and cement stabilized expansive organic clays. *Applied Clay Science*, 85, 39-45.
- Sariosseiri, F. & Muhunthan, B. 2009. Effect of cement treatment on geotechnical properties of some washington state soils. *Engineering Geology*, 104, 119-125.
- Sarkar, G., Rafiqul Islam, M., Alamgir, M. & Rokouzzaman, M. 2012. Study on the geotechnical properties of cement based composite fine-grained soil. *International Journal of Advanced Structure and Geotechnical Engineering*, 1, 42 - 49.
- Schumacher, G. & Juniper, L. 2013. Coal utilisation in the cement and concrete industries. 387-426.
- Seco, A., Ramírez, F., Miqueleiz, L. & García, B. 2011. Stabilization of expansive soils for use in construction. *Applied Clay Science*, 51, 348-352.
- Segui, P., Aubert, J. E., Husson, B. & Measson, M. 2012. Characterization of wastepaper sludge ash for its valorization as a component of hydraulic binders. *Applied Clay Science*, 57, 79-85.
- Sekulić, Ž., Popov, S., Đuričić, M. & Rosić, A. 1999. Mechanical activation of cement with addition of fly ash. *Materials Letters*, 39, 115-121.
- Sequaris, J. M. 2010. Modeling the effects of ca²⁺ and clay-associated organic carbon on the stability of colloids from topsoils. *J Colloid Interface Sci*, 343, 408-14.
- Silica Fume Association. 2016. *What is silica fume?* [Online]. USA: Available: <http://www.silicafume.org/general-silicafume.html> [Accessed 11-10-2016].
- Sherwood, P. T. 1993. *Soil stabilization with cement and lime*, London, Stationery Office Books (TSO).
- Shibi, T. & Kamei, T. 2014. Effect of freeze–thaw cycles on the strength and physical properties of cement-stabilised soil containing recycled bassanite and coal ash. *Cold Regions Science and Technology*, 106-107, 36-45.
- Shimadzu. 2016. *Shimadzu's edx-720 energy dispersive x-ray fluorescence spectrometer* [Online]. Available: <http://search1.shimadzu.co.jp/search?query=Shimadzu%E2%80%99s+EDX-720+Energy+Dispersive+X-Ray+Fluorescence+Spectrometer+&submit=search&site=EM0AJRZ6&charset=UTF-8&design=1&submit.x=30&submit.y=12> [Accessed 10-10-2016 2016].
- Shojaei Baghini, M., Ismail, A., Karim, M. R., Shokri, F. & Firoozi, A. A. 2014. Effect of styrene–butadiene copolymer latex on properties and durability of road base stabilized with portland cement additive. *Construction and Building Materials*, 68, 740-749.
- Singh, L. P., Zhu, W., Howind, T. & Sharma, U. 2017. Quantification and characterization of c-s-h in silica nanoparticles incorporated cementitious system. *Cement and Concrete Composites*, 79, 106-116.

- Singhania, N. P. 2004. Rice husk ash. *The Institute of Concrete Technology News Letter*, Autumn 2004.
- Sinsiri, T., Kroehong, W., Jaturapitakkul, C. & Chindaprasirt, P. 2012. Assessing the effect of biomass ashes with different finenesses on the compressive strength of blended cement paste. *Materials & Design*, 42, 424-433.
- Sivrikaya, O., Kiyıldı, K. R. & Karaca, Z. 2014. Recycling waste from natural stone processing plants to stabilise clayey soil. *Environmental Earth Sciences*, 71, 4397-4407.
- Soares, L. W. O., Braga, R. M., Freitas, J. C. O., Ventura, R. A., Pereira, D. S. S. & Melo, D. M. A. 2015. The effect of rice husk ash as pozzolan in addition to cement portland class g for oil well cementing. *Journal of Petroleum Science and Engineering*, 131, 80-85.
- Sobolev, K., Lin, Z., Cao, Y., Sun, H., Flores-Vivian, I., Rushing, T., Cummins, T. & Weiss, W. J. 2016. The influence of mechanical activation by vibro-milling on the early-age hydration and strength development of cement. *Cement and Concrete Composites*, 71, 53-62.
- Sol-Sánchez, M., Castro, J., Ureña, C. G. & Azañón, J. M. 2016. Stabilisation of clayey and marly soils using industrial wastes: Ph and laser granulometry indicators. *Engineering Geology*, 200, 10-17.
- Song, D. & Chen, B. 2016. Extended exergy accounting for energy consumption and co2 emissions of cement industry—a basic framework. *Energy Procedia*, 88, 305-308.
- Soriano, L., Payá, J., Monzó, J., Borrachero, M. V. & Tashima, M. M. 2016. High strength mortars using ordinary portland cement–fly ash–fluid catalytic cracking catalyst residue ternary system (opc/fa/fcc). *Construction and Building Materials*, 106, 228-235.
- Spathi, C., Vandeperre, L. J. & Cheeseman, C. R. 2015. Production of lightweight fillers from waste glass and paper sludge ash. *Waste and Biomass Valorization*, 6, 875-881.
- Specht, E., Redemann, T. & Lorenz, N. 2016. Simplified mathematical model for calculating global warming through anthropogenic co2. *International Journal of Thermal Sciences*, 102, 1-8.
- Sposito, G. 2008. *The chemistry of soils*, New York, Oxford University Press, Inc.
- Stoltz, G., Cuisinier, O. & Masroui, F. 2014. Weathering of a lime-treated clayey soil by drying and wetting cycles. *Engineering Geology*, 181, 281-289.
- Stubbs, B. 2008. Plain english guide to sustainable construction. UK: Constructing Excellence in The Built Environment.
- Sua-iam, G., Sokrai, P. & Makul, N. 2016. Novel ternary blends of type 1 portland cement, residual rice husk ash, and limestone powder to improve the properties of self-compacting concrete. *Construction and Building Materials*, 125, 1028-1034.
- Sun, H., Li, Z., Bai, J., Memon, S., Dong, B., Fang, Y., Xu, W. & Xing, F. 2015. Properties of chemically combusted calcium carbide residue and its influence on cement properties. *Materials*, 8, 638-651.
- Tajuelo Rodriguez, E., Garbev, K., Merz, D., Black, L. & Richardson, I. G. 2017. Thermal stability of c-s-h phases and applicability of richardson and groves' and richardson c-(a)-s-h(i) models to synthetic c-s-h. *Cement and Concrete Research*, 93, 45-56.
- Tasong, W. A., Wild, S. & Tilley, R. J. D. 1999. Mechanisms by which ground granulated blastfurnace slag prevents sulphate attack of lime-stabilised kaolinite. *Cement and Concrete Research*, 29, 975 - 982.
- The National Archive. 2012. *Paper sludge ash* [Online]. UK Government Web Archive. [Accessed 04-10-2016 2016].
- Thomas, M. 2007. Optimizing the use of fly ash in concrete. *PCA*.
- Tingle, J., Newman, J., Larson, S., Weiss, C. & Rushing, J. 2007. Stabilization mechanisms of nontraditional additives. *Transportation Research Record: Journal of the Transportation Research Board*, 1989, 59-67.
- Tomlinson, M., J. 2001. *Foundation design and construction*, Pearson Education, Prentice Hall.

- Tremblay, H., Duchesne, J., Locat, J. & Leroueil, S. 2002. Influence of the nature of organic compounds on fine soil stabilization with cement. *Canadian Geotechnical Journal*, 39, 535-546.
- Tripura, D. D. & Singh, K. D. 2015. Characteristic properties of cement-stabilized rammed earth blocks. *Journal of Materials in Civil Engineering*, 27, 04014214.
- Tyrer, M. J. 1987. *Stabilisation of clay type soils with cementitious material*. PhD, Cleveland University.
- UK Quality Ash Association. 2016. *Ukqaa ash availability report* [Online]. United Kingdom: Available: <http://www.ukqaa.org.uk/wp-content/uploads/2016/01/UKQAA-Ash-Availability-Report-Jan-2016.pdf> [Accessed: 10-10-2016].
- Vakili, M. V., Chegenizadeh, A., Nikraz, H. & Keramatikerman, M. 2016. Investigation on shear strength of stabilised clay using cement, sodium silicate and slag. *Applied Clay Science*, 124-125, 243-251.
- Van den Heede, P., Ringoot, N., Beirnaert, A., Van Brecht, A., Van den Brande, E., De Schutter, G. & De Belie, N. 2016. Sustainable high quality recycling of aggregates from waste-to-energy, treated in a wet bottom ash processing installation, for use in concrete products. *Materials*, 9, 9.
- van Ruijven, B. J., van Vuuren, D. P., Boskaljon, W., Neelis, M. L., Saygin, D. & Patel, M. K. 2016. Long-term model-based projections of energy use and co2 emissions from the global steel and cement industries. *Resources, Conservation and Recycling*, 112, 15-36.
- Vegas, I., Gaitero, J. J., Urreta, J., García, R. & Frías, M. 2014. Aging and durability of ternary cements containing fly ash and activated paper sludge. *Construction and Building Materials*, 52, 253-260.
- Veith, G. H. 2000. *Engineering properties of sulphatebearing clay soils stabilised with lime-activated ground granulated blast furnace slag (ggbs)*. Doctor of Philosophy, University of Glamorgan
- Velandia, D. F., Lynsdale, C. J., Provis, J. L., Ramirez, F. & Gomez, A. C. 2016. Evaluation of activated high volume fly ash systems using na2so4, lime and quicklime in mortars with high loss on ignition fly ashes. *Construction and Building Materials*, 128, 248-255.
- Venda Oliveira, P. J., Correia, A. A. S. & Garcia, M. R. 2011. Effect of organic matter content and curing conditions on the creep behavior of an artificially stabilized soil. *JOURNAL OF MATERIALS IN CIVIL ENGINEERING*, 24, 868-875.
- Vichan, S., Rachan, R. & Horpibulsuk, S. 2013. Strength and microstructure development in bangkok clay stabilized with calcium carbide residue and biomass ash. *ScienceAsia*, 39, 186.
- Vieira, C. M. F., Pinheiro, R. M., Rodriguez, R. J. S., Candido, V. S. & Monteiro, S. N. 2016. Clay bricks added with effluent sludge from paper industry: Technical, economical and environmental benefits. *Applied Clay Science*, 132-133, 753-759.
- Wagner, J. F. 2013. Mechanical properties of clays and clay minerals. 5, 347-381.
- Wang, B.-t., Zhang, C.-h., Qiu, X.-l., Ji, E.-y. & Zhang, W.-h. 2015. Research on wetting-drying cycles' effect on the physical and mechanical properties of expansive soil improved by otac-kcl. *Advances in Materials Science and Engineering*, 2015, 1-7.
- Wang, D., Zentar, R., Abriak, N. E. & Di, S. 2017. Long-term mechanical performance of marine sediments solidified with cement, lime, and fly ash. *Marine Georesources & Geotechnology*, 1-8.
- Wang, Y., Jing, H., Han, L., Yu, L. & Zhang, Q. 2014. Risk analysis on swell-shrink capacity of expansive soils with efficacy coefficient method and entropy coefficient method. *Applied Clay Science*, 99, 275-281.
- Wild, S., Kinuthia, J. M., Jones, G. I. & Higgins, D. D. 1998. Effect of partial substitution of lime with ground granulated blast furnace slag (ggbs) on the strength properties of lime-stabilised sulphate-bearing clay soils. *Engineering Geology*, 51, 37 - 53.
- Wong, H. S., Barakat, R., Alhilali, A., Saleh, M. & Cheeseman, C. R. 2015. Hydrophobic concrete using waste paper sludge ash. *Cement and Concrete Research*, 70, 9-20.

- Wright, L. & Khatib, J. M. 2016. 26 - sustainability of desulphurised (fgd) waste in construction. *Sustainability of construction materials (second edition)*. Woodhead Publishing. Available: <http://www.sciencedirect.com/science/article/pii/B9780081003701000263>
- Wu, Z.,Deng, Y.,Liu, S.,Liu, Q.,Chen, Y. & Zha, F. 2016. Strength and micro-structure evolution of compacted soils modified by admixtures of cement and metakaolin. *Applied Clay Science*, 127-128, 44-51.
- Yadu, L. & Tripathi, R. K. 2013. Stabilization of soft soil with granulated blast furnace slag and fly ash. *IJRET / FEB*, 2, 115 - 119
- Yazdandoust, F. & Yasrobi, S. S. 2010. Effect of cyclic wetting and drying on swelling behavior of polymer-stabilized expansive clays. *Applied Clay Science*, 50, 461-468.
- Yi, Y.,Zheng, X.,Liu, S. & Al-Tabbaa, A. 2015. Comparison of reactive magnesia- and carbide slag-activated ground granulated blastfurnace slag and portland cement for stabilisation of a natural soil. *Applied Clay Science*, 111, 21-26.
- Yilmaz, A. & Degirmenci, N. 2009. Possibility of using waste tire rubber and fly ash with portland cement as construction materials. *Waste Manag*, 29, 1541-6.
- Yilmaz, Y. & Ozaydin, V. 2013. Compaction and shear strength characteristics of colemanite ore waste modified active belite cement stabilized high plasticity soils. *Engineering Geology*, 155, 45-53.
- Yoder, E. J. & Witczak, M. W. 1975. *Principles of pavement design*, Canada, John Wiley & Sons, Inc.
- Yong, R. & Ouhadi, V. 2007. Experimental study on instability of bases on natural and lime/cement-stabilized clayey soils. *Applied Clay Science*, 35, 238-249.
- Yu, Y.,Zhang, Y. X. & Khennane, A. 2015. Numerical modelling of degradation of cement-based materials under leaching and external sulfate attack. *Computers & Structures*, 158, 1-14.
- Zhang, T.,Yue, X.,Deng, Y.,Zhang, D. & Liu, S. 2014. Mechanical behaviour and micro-structure of cement-stabilised marine clay with a metakaolin agent. *Construction and Building Materials*, 73, 51-57.
- Zhang, X.,Shen, J.,Wang, Y.,Qi, Y.,Liao, W.,Shui, W.,Li, L.,Qi, H. & Yu, X. 2017a. An environmental sustainability assessment of china's cement industry based on emergy. *Ecological Indicators*, 72, 452-458.
- Zhang, X.,Wang, J.,Wu, J.,Jia, X.-J.,Du, Y.,Li, H. & Zhao, B. 2016a. Phase- and morphology-controlled crystallization of gypsum by using flue-gas-desulfurization gypsum solid waste. *Journal of Alloys and Compounds*, 674, 200-206.
- Zhang, Y.,Pan, F. & Wu, R. 2016b. Study on the performance of fgd gypsum-metakaolin-cement composite cementitious system. *Construction and Building Materials*, 128, 1-11.
- Zhang, Z. & Tao, M. 2008. Durability of cement stabilized low plasticity soils. *Journal of Geotechnical and Geoenvironmental Engineering*, 134, 203-213.
- Zhang, Z.,Yang, T. & Wang, H. 2017b. Alkali-activated cement (aac) from fly ash and high-magnesium nickel slag. 357-374.
- Zhao, J.,Wang, D.,Yan, P.,Zhao, S. & Zhang, D. 2016. Particle characteristics and hydration activity of ground granulated blast furnace slag powder containing industrial crude glycerol-based grinding aids. *Construction and Building Materials*, 104, 134-141.
- Zheng, J. & Qin, W. 2003. Performance characteristics of soil-cement fro industry waste binder. *Journal of Materials in Civil Engineering*, 15, 616 - 618.

APPENDICES

Appendix A: Results of the soil treated with the coarse grade of WPSA

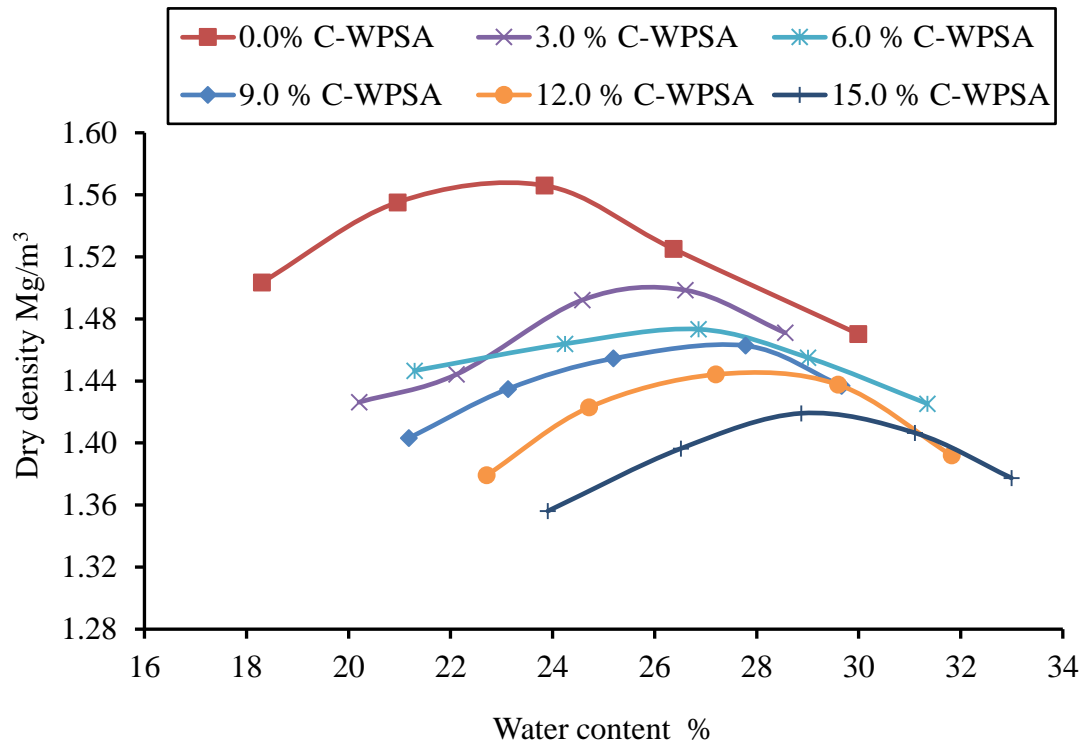


Figure AA-1 Dry density – water content relationship of the soil treated with different C-WPSA content.

Table AA-1 MDDs and OMCs of the soil treated with C-WPSA

C-WPSA content (%)	MDD (Mg/m ³)	OMC (%)
0	1.57	23.00
3	1.50	25.75
6	1.47	26.70
9	1.46	27.5
12	1.45	28.00
15	1.42	29.00

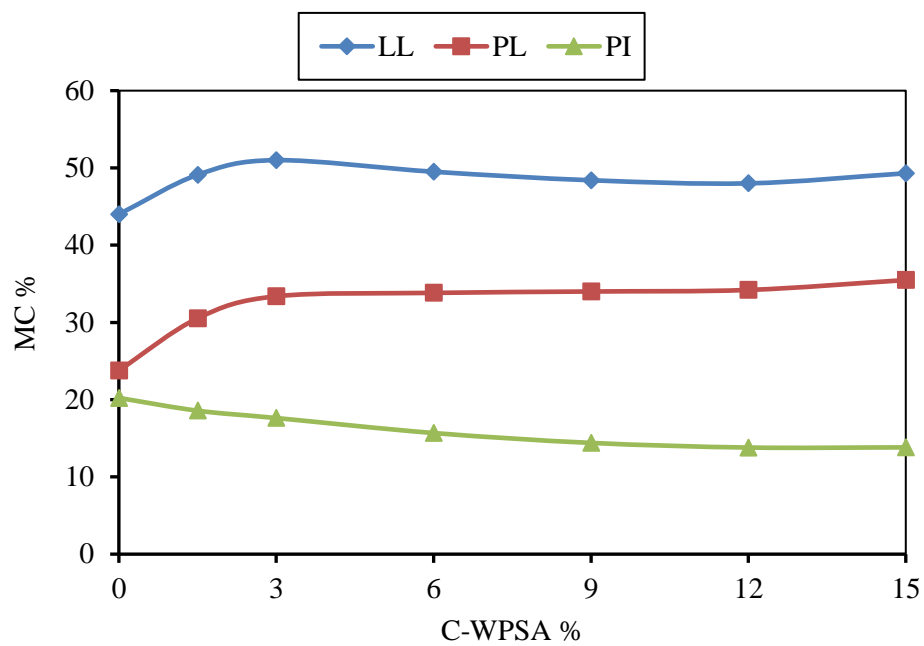


Figure AA-2 Atterberg limits of the soil treated with C-WPSA

Table AA-2 Atterberg limits of the soil treated with different C-WPSA contents

C-WPSA content (%)	LL (%)	PL (%)	PI
0	44.00	23.78	20.22
3	49.10	30.53	18.57
6	51.00	33.38	17.62
9	49.50	33.82	15.68
12	48.40	34.00	14.40
15	48.00	34.20	13.80

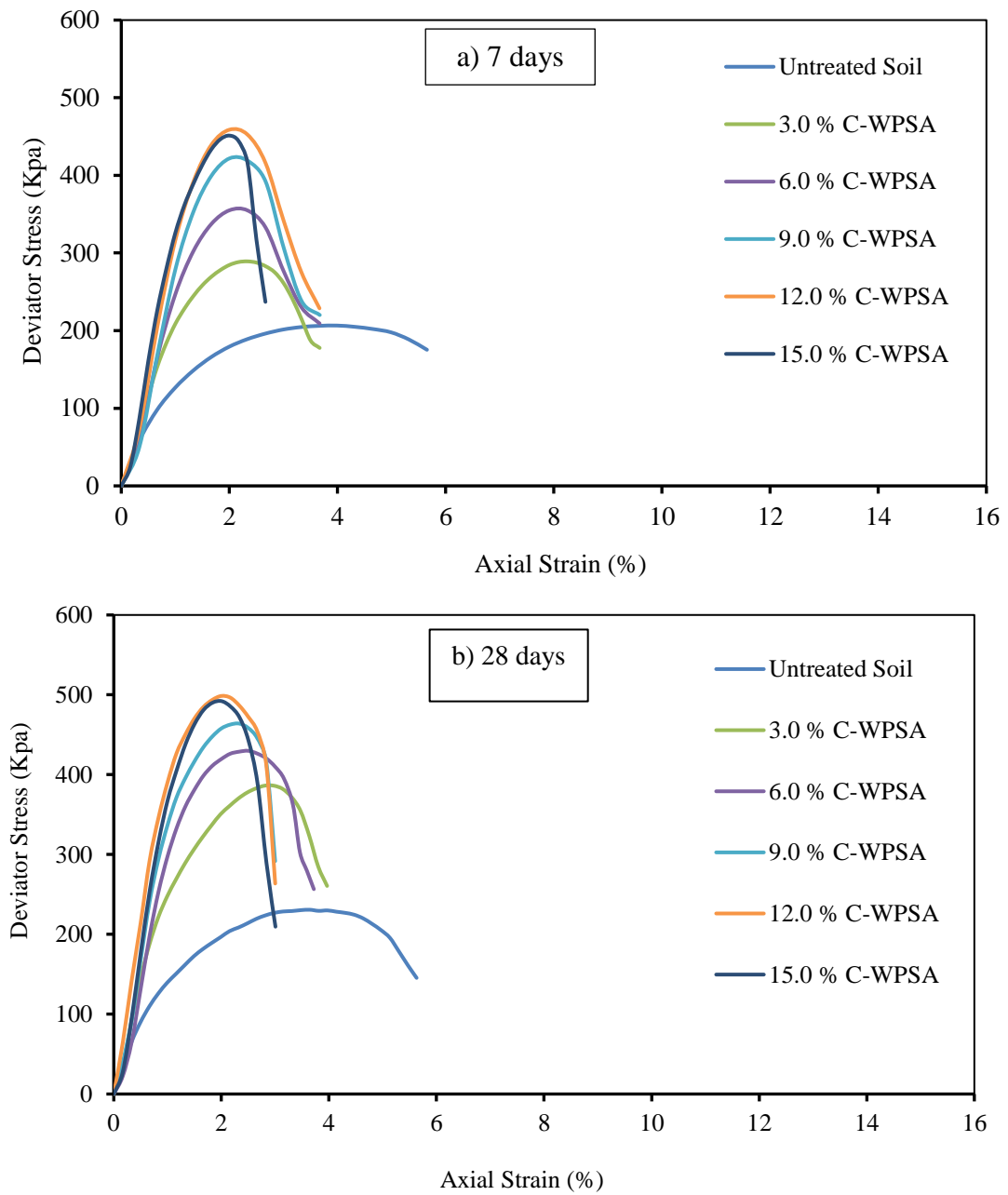


Figure AA-3 Stress – axial strain diagrams of the soil treated with C-WPSA; a) 7 days and b) 28 days of curing.

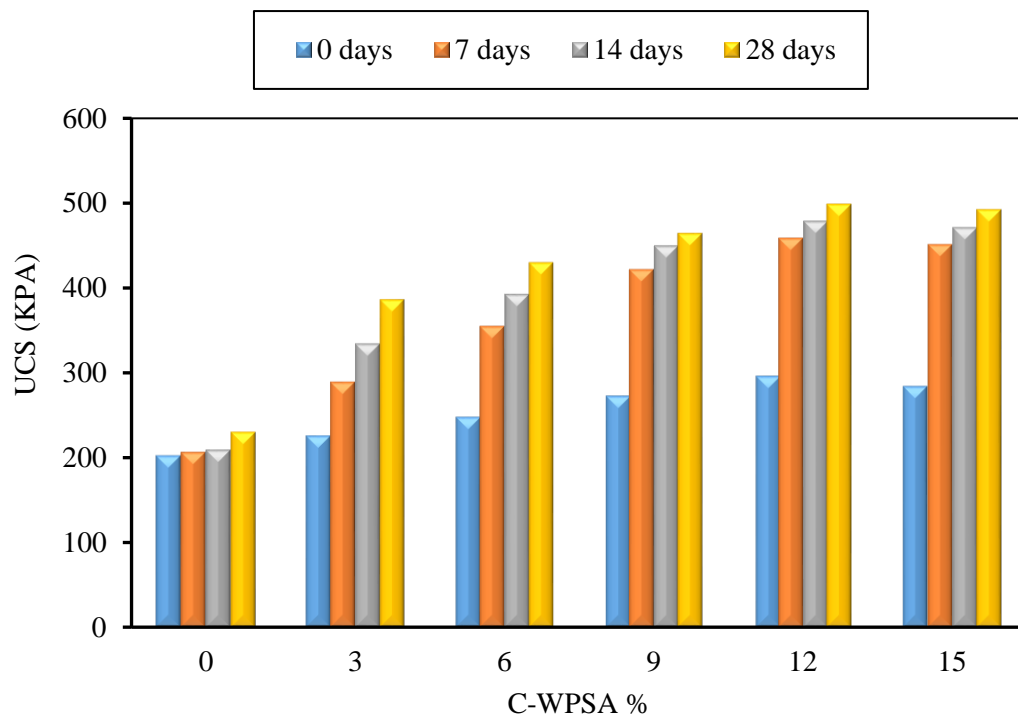


Figure AA-4 UCS of the soil treated with different C-WPSA content at different periods of curing

Table AA-3 UCS values of the soil treated with C-WPSA at different curing times

C-WPSA content (%)	Curing time (days)			
	0	7	14	28
0	202.0	206.5	209.8	225.8
3	220.0	246.5	278.6	338.1
6	225.5	289.2	334.6	386.3
9	247.6	355.0	392.6	429.9
12	272.2	421.9	449.9	464.0
15	295.7	458.8	478.8	498.6

Appendix B: Lis of journal and conference publications
Published journal papers:

1. Jafer, H., Atherton, W., Ruddock, F. and Loffill, E. "Development of a New Ternary Blended Cementitious Binder Produced from Waste Materials for use in Soft Soil Stabilisation", *Journal of Cleaner Production*, 172, 516-528.
2. Jafer, H., Atherton, W., Ruddock, F. and Loffill, E. (2015) "Assessing the Potential of a Waste Material for Cement Replacement and the Effect of Its Fineness in Soft Soil Stabilisation", *International Journal of Civil, Environmental, Structural, Construction and Architectural Engineering*, 9 (8), 894 – 900.
3. Jafer, H., Atherton, W., Ruddock, F. and Loffill, E. (2016) "The Utilisation of Two Types of Fly Ashes Used as Cement Replacement in Soft Soil Stabilisation". *International Journal of Civil, Environmental, Structural, Construction and Architectural Engineering*, 10 (7), 896 – 899.
4. Jafer, H., Hashim, K. and Atherton, W. (2016) "A Statistical Model for the Geotechnical Parameters of Cement-Stabilised Hightown's Soft Soil: A Case Study of Liverpool, UK". *International Journal of Civil, Environmental, Structural, Construction and Architectural Engineering*, 10 (7), 885-890.

Accepted journal papers (under production):

1. Jafer, H., Atherton, W., Sadique, M., Ruddock, F. and Loffill, E. "Stabilisation of Soft Soil Using Binary Blending of High Calcium Fly Ash and Palm Oil Fuel Ash", *Applied Clay Science*, ELSEVIER.

Journal papers under preparation:

1. Jafer, H., Atherton, W., Ruddock, F. and Loffill, E. "Strength and Compressibility Characterisation of Soft Soil Stabilised with a Novel Ternary Blended Binder Produced from Waste Materials Fly Ashes", *Applied Clay Science*, ELSEVIER.
2. Jafer, H., Atherton, W., Ruddock, F. and Loffill, E. "The Characterisation of Geotechnical Properties of a Soft Soil Stabilised with High Calcium Fly Ash" to be submitted in *Geotechnical and Geological Engineering* – Springer.
3. Jafer, H., Atherton, W., Ruddock, F. and Loffill, E. "Effect of Wetting – Drying Cycles on Geotechnical Properties of Soft Soil Stabilised with Waste Materials Fly Ashes" to be submitted to *Applied Clay Science* – ELSEVIER.

Conference papers with oral presentation:

1. Jafer, H., Atherton, W. and Ruddock, F. (2015) "Soft Soil Stabilisation Using High Calcium Waste Material Fly Ash". *12th International Post-Graduate Conference 2015*. Salford University, Manchester, UK.
2. Jafer, H., Atherton, W., Ruddock, F. and Loffill, E. (2015) "Comparative study of the performance of Ordinary Portland Cement and a waste material in soft soil stabilisation".

-
- Faculty of Engineering and Technology Research Week Conference 2015*. Liverpool John Moores University, Liverpool, UK.
3. Jafer, H., Atherton, W., Ruddock, F. and Loffill, E. (2015) "Assessing the Potential of a Waste Material for Cement Replacement and the Effect of Its Fineness in Soft Soil Stabilisation". *17th International Conference on Civil, Environmental and Geological Engineering*, Venice, Italy.
 4. Jafer, H., Atherton, W., Ruddock, F. and Loffill, E. (2016) "Mechanical Activation of a Waste Material Used as Cement Replacement in Soft Soil Stabilisation". *15th International Conference on Asphalt, Pavement Engineering and Infrastructures*. LJMU, Liverpool, UK.
 5. Jafer, H., Atherton, W., Ruddock, F. and Loffill, E. (2016) "Mechano-Chemical Activation of a Waste Fly Ash Used in Soft Soil Stabilisation". *Faculty of Engineering and Technology Research Week Conference 2016*. Liverpool John Moores University, Liverpool, UK.
 6. Jafer, H. and Atherton, W. (2016) "Characterisation of a Soft Soil Microstructure Stabilised With a Binary Blending Using Two Waste Fly Ashes". *The Second BUiD Doctoral Research Conference*, the British University in Dubai, UAE.
 7. Jafer, H., Atherton, W., Ruddock, F. and Loffill, E. (2016) "The Utilisation of Two Types of Fly Ashes Used as Cement Replacement in Soft Soil Stabilisation". *ICBMCE 2016: 18th International Conference on Building Materials and Civil Engineering*, Paris, France.
 8. Jafer, H., Hashim, K. and Atherton, W. (2016) "A Statistical Model for the Geotechnical Parameters of Cement-Stabilised Hightown's Soft Soil: A Case Study of Liverpool, UK". *ICBMCE 2016: 18th International Conference on Building Materials and Civil Engineering*, Paris, France.
 9. Jafer, H., Atherton, W. and Al-Dulaimi, A. (2017) "The Characterisation of the Strength Development of a Cement-Stabilised Soft Soil Treated with Two Different Types of Fly Ashes". *16th International Conference on Asphalt, Pavement Engineering and Infrastructures*. LJMU, Liverpool, UK.
 10. Jafer, H., Atherton, W., Ruddock, F. and Loffill, E. (2017) "The Stabilisation of a Soft Soil Subgrade Layer Using a New Sustainable Binder Produced from Free-Cement Blending of Waste Materials Fly Ashes". *BCRRA 2017: 10th International Conference on the Bearing Capacity of Roads, Railways and Airfields, 28-30 June 2017*. Athens, Greece.

Poster presentations:

1. Jafer, H. (2014) "Effect of organic matter on salt-nanomaterial stabilized soft soil". *Faculty of Engineering and Technology Bean Conference 2014*. Liverpool John Moores University, Liverpool, UK.
2. Jafer, H., Atherton, W., Ruddock, F. and Loffill, E. (2015) "Soft Soil Stabilisation Using Waste Material Fly Ash". *Faculty of Engineering and Technology Research Week Conference 2015*. Liverpool John Moores University, Liverpool, UK.
3. Jafer, H., Atherton, W., Ruddock, F., Loffill, E. and Hashim, K. (2017) "Physico-chemical Activation of a High Calcium Fly Ash Used as a Cement Replacement in The Stabilisation of Soft Soils". *The 9th MMU Postgraduate Research Conference*

'CHANGING LIVES' 22nd February 2017. Manchester Metropolitan University, Manchester, UK.

3 Minutes thesis and elevator pitch:

1. Jafer, H. and Atherton, W. (2016) "The Utilisation of Waste Materials in Soft Soil Stabilisation". *1st Graduate School Conference 2016*, LJMU, Liverpool, UK.
2. Jafer, H., Atherton, W., Ruddock, F. and Loffill, E. (2017) "The Development of a New Ternary Blended Cementitious Binder for the Use in the Soft Soil Stabilisation". *Faculty of Engineering and Technology Research Week Conference 2017*. Liverpool John Moores University, Liverpool, UK.

Contribution in Master Students Publications as a Co-supervisor:

1. Shubbar, A., Atherton, W., Jafer, H., Dulaimi, A. and Al-Faluji, D. (2017) "The Development of a New Cementitious Material Produced from Cement and GGBS". *BDRC 2017, The Third BUiD Doctoral Research Conference 13th May 2017*. The British University in Dubai, UAE.
2. Al-Faluji, D., Jafer, H., Dulaimi, A., Atherton, W. and Shubbar, A. (2017) "The Effect of CKD Content on the Geotechnical Properties of GGBS Stabilised Kaolin Clays". *BDRC 2017, The Third BUiD Doctoral Research Conference 13th May 2017*. The British University in Dubai, UAE.
3. Al-Khafaji, Z., Jafer, H., Dulaimi, A., Atherton, W. and Al-Masoodi, Z. (2017) "The Soft Soil Stabilisation Using Binary Blending of Ordinary Portland Cement and a High Alumina-Silica Waste Material". *BDRC 2017, The Third BUiD Doctoral Research Conference 13th May 2017*. The British University in Dubai, UAE.
4. Al-Masoodi, Z., Dulaimi, A., Jafer, H., Atherton, W. and Al-Khafaji, Z. (2017) "The Effect of a High Alumina-Silica Waste Material on the Engineering Properties of a Cement-Stabilised Soft Soil". *BDRC 2017, The Third BUiD Doctoral Research Conference 13th May 2017*. The British University in Dubai, UAE.
5. Al-Khafaji, R., Jafer, H., Dulaimi, A., Atherton, W. and Jwaida, Z. (2017) "Soft Soil Stabilisation Using Ground Granulated Blast Furnace Slag". *BDRC 2017, The Third BUiD Doctoral Research Conference 13th May 2017*. The British University in Dubai, UAE.
6. Jwaida, Z., Dulaimi, A., Jafer, H., Atherton, W. and Al-Khafaji, R. (2017) "Soft Subgrade Stabilisation Using Cement Kiln Dust and Ground Granulated Blast Furnace Slag". *BDRC 2017, The Third BUiD Doctoral Research Conference 13th May 2017*. The British University in Dubai, UAE.
7. Shubbar, A., Jafer, H., Dulaimi, A., Atherton, W., and Al-Rifaie, A. (2017) "The Development of a Low Carbon Cementitious Material Produced from Cement, Ground Granulated Blast Furnace Slag and High Calcium Fly Ash". *International Journal of Civil, Environmental, Structural, Construction and Architectural Engineering*, 11 (7), 893 – 896.

Appendix C: Awards and Recognitions

Table AC-1 List of awards and recognitions

No.	Award	Event and awarding body	Date
1	<i>Certificate of Appreciation and Recognition of Achievements while studying at LJMU</i>	Liverpool John Moores University, Faculty of Engineering and Technology Research Week.	26-05-2017
2	<i>Certificate of excellence for Academic Achievements</i>	The Iraqi embassy in London, awarded by the ambassador of the republic of Iraq to the United Kingdom.	05-03-2017
3	<i>Certificate of excellence for Academic Achievements</i>	The Iraqi embassy in London, awarded by the chair of Iraqi Student Society in the UK.	05-03-2017
4	<i>Medal of excellence</i>	The Iraqi embassy in London, awarded by the Iraqi Minister of Higher Education and Scientific Research	24-01-2017
5	<i>The second best Paper presentation</i>	Liverpool John Moores University, Faculty of Engineering and Technology.	13-05-2016
6	<i>Second Best Poster</i>	Bean Conference, Liverpool John Moores University, Faculty of Engineering and Technology	16-06-2014





